

**Identification of novel ubiquitin-proteasome
dependent pathways in *Arabidopsis thaliana***

Dissertation

der Fakultät für Biologie
der Eberhard Karls Universität Tübingen

zur Erlangung des Grades eines Doktors
der Naturwissenschaften

vorgelegt

von

Luz Irina Alejandro Calderón Villalobos
aus Bogotá, Kolumbien

2006

Tag der mündlichen Qualifikation:

3. Februar 2006

Dekan:

Prof. Dr. Friedrich Schöffl

1. Berichterstatter:

Prof. Dr. Gerd Jürgens

2. Berichterstatter:

Prof. Dr. Friedrich Schöffl

“Ideals and dreams are like stars: you will not succeed in touching them with your hands, but like the seafaring man on the ocean desert of waters, you choose them as your guides, and following them, you reach your destiny. “

Carl Shurz (1829-1906)

To My Parents

Acknowledgments

I would like sincerely to thank all members of the Department of Developmental Genetics in the ZMBP, especially Prof. Dr. Gerd Jürgens, who let me join his Department, and always encouraged me with positive words.

A special acknowledgement also goes to Prof. Dr. Friedrich Schöffl for his kind acceptance to be the second “Berichterstatter” of this work, for his readiness to help in the analysis of the heat induction of *AtFBP7*, and also for being three years ago one of those who allowed me to start my PhD.

Specially, I thank Dr. Claus Schwechheimer, my supervisor, my mentor, who gave me the opportunity to be his first apprentice. His valuable guidance and timely suggestions gave me the chance to be more critical. Claus also gave me a lot of his time and patience, and although there were difficulties he never lost his trust in me. Furthermore, he always helped me and opened doors for me and continues doing so.

My acknowledgments to Prof. Dr. Claudia Oecking for always being willing to help and listen.

I would also thank many essential people including Dieter Steinmetz, Felicity de Courcy, Sylvia Roecker, because they helped me unselfishly in all circumstances.

I would like to express my gratitude to many colleagues –present and past- of the Developmental Genetics Department for their invaluable advice and support not only during the preparation of this manuscript, but during the last years. In particular, I thank Nadine Anders, Ute Voß, Katharina Heß, Sandra Richter, Alexandra Schlereth, Hanno Wolters, as well as Anne Hermesdorf from the Plant Physiology Department. Despite of the “physical distance”, I felt always like it was also my “home lab”, they provided me energy, laughs and positivism, and I know that these are treasures. Thanks really to the rest of that wonderful group of mismatched colleagues.

Naturally, my thanks also to my colleagues in the protein degradation group: Melina, Andreas, Katja and Esther, who have shared continuously and intensively my journey. Besonders bedanke ich mich bei Carola Nil, meine Mitstreiterin, die mir das schönste Willkommen gegeben hat in diesem Schwabenland. Danke für deine Freundschaft, für deine Wärme. Also, my thanks to Stephan Knierer to let me experiment in being supervisor, and to Dr Hanbing Li, my favourite Chinese guy.

My thanks of course to all, who supported me in the last 5 years after my arrival to Germany, to the DeWitt, Krell, and Ottmann families, who welcomed me warmly when it was really necessary.

Specially thanks to my friends from a distance Martin, Diego and Miriam, as well as Roberto, because in several situations their invaluable presence comforted me.

My enormous thanks to my dear friend Dr. Karen Cornelis, who knew how to support me, how to listen to me, how to be with me, despite of the big distance. Thanks also to Isabel for not always agreeing with me, but also for sharing with me a bit of her interesting world and thought, for her friendship and warmth.

Gracias a mis padres que me enseñaron a trabajar, a ser paciente y a perseverar. También gracias le doy a Karen Larissa y a Gonzalo Ernesto, mis hermanos que compartieron mis sueños. A mi adorada familia le doy gracias por su amor, apoyo incondicional y por creer en mi siempre.

Thanks to Christian, who with enormous patience always supported me and made me see other ways...thanks to him, who teaches me what courage means.

Thanks to my Hope, my Faith.

Table of Contents

Acknowledgments

<i>I. Summary</i>	3
I.I. Introduction	3
I.II Aim of this work	13
I.III. Results	16
I.IV. Discussion	20
I.V. References	29

<i>II. Own Contribution to the Publications</i>	34
--	----

<i>III. Publications</i>	37
---------------------------------	----

III.I. Schwechheimer C. and Calderón Villalobos L.I.A. (2004). Cullin-containing E3 ubiquitin ligases in plant development (review article, published in <i>Current Opinion in Plant Biology</i>).	38
---	----

III.II. Calderón Villalobos L.I.A. <i>et al.</i> The evolutionarily conserved <i>Arabidopsis thaliana</i> F-box protein AtFBP7 is required for efficient translation during temperature stress (manuscript of a research article, submitted to <i>The Journal of Biological Chemistry</i>).	50
---	----

III.III. Schwager K. <i>et al.</i> Characterization of the <i>VIER F-BOX</i> <i>PROTEINE (VFB)</i> genes from <i>Arabidopsis</i> reveals their importance for	74
--	----

plant growth and development (manuscript of a research article, submitted to *Plant Cell*).

III.IV. Calderón Villalobos L.I.A. *et al.* (2005). The evolutionarily conserved TOUGH protein is required for proper development of *Arabidopsis thaliana* (research article, published in *Plant Cell*). 125

III.V. Calderón Villalobos L.I.A. *et al.* LucTrap Vectors – a versatile tool for the analysis of transcriptional and translational luciferase fusions (manuscript of a research article, under revision in *Plant Physiology*). 139

IV. Zusammenfassung 171

V. Curriculum vitae 173

I. Summary

I.I. Introduction

The controlled degradation of regulatory proteins such as transcription factors and cell cycle regulators via the ubiquitin-proteasome system is a major regulatory mechanism in eukaryotes. This study aims at contributing to the understanding of the role of the ubiquitin-proteasome system in plants. The main part of this thesis (chapter III) consists of a series of submitted and published manuscripts, which provide new insights into the role of protein degradation in *Arabidopsis thaliana*. The first part of this work is an introduction into the ubiquitin-proteasome system and presents in a concise manner the most relevant results of the manuscripts. Finally, the discussion alludes to how important it is to understand substrate recognition proteins, to find targets for degradation, but also to disclose the biological relevance of the mechanisms that control ubiquitin-proteasome mediated events in plants.

Ubiquitin-mediated proteolysis

Growth and development consist of a series of cellular and molecular events that require precise programming and control, otherwise the consequences may be disease and death. Cells develop, adapt and evolve to a large extent thanks to the proper functioning and regulation of their proteins. In fact, protein regulation contributes to growth and development and it can occur at multiple levels including changes in protein localization, changes in protein conformation and changes in the protein's activity state.

Selective proteolysis is another such sophisticated mechanism that permits precise regulation of proteins and their reactions.

In 2004, Avram Hershko, Aaron Ciechanover and Irwin Rose were awarded with the Nobel Prize in Chemistry, “who have made fundamental discoveries concerning how cells regulate the breakdown of intracellular proteins with extreme specificity as to target, time and space”. They discovered the ubiquitin-mediated proteolysis as an energy-dependent enzymatic mechanism that uses a type of “death label” called ubiquitin to tag unwanted proteins. Proteins so labelled are then degraded rapidly in a multisubunit protease complex called 26S proteasome. Through the discovery of controlled protein degradation, Avram Hershko, Aaron Ciechanover and Irwin Rose “explain, at molecular level, the function of a regulation system that is very central for the cell” (Nobel Prize Announcement, the Royal Swedish Academy of Sciences, December 10, 2004).

Ubiquitin-mediated proteolysis is the most relevant proteolytic pathway in eukaryotes and allows the cells to respond rapidly to intracellular signalling events and environmental changes by adjusting the level of key proteins (Hershko, 1998). It also provides an important post-translational mechanism, in which misfolded or unassembled proteins from the endoplasmic reticulum are recognized and then exported to the cytosol to be ubiquitylated and degraded. (Schubert et al., 2000; Meusser et al., 2005; Muller et al., 2005). Ubiquitin-mediated proteolysis is therefore an essential mechanism, which

regulates numerous important cellular processes, like the cell cycle, DNA repair, gene transcription, protein quality control and immune response (Figure 1) (Ciechanover, 1998).

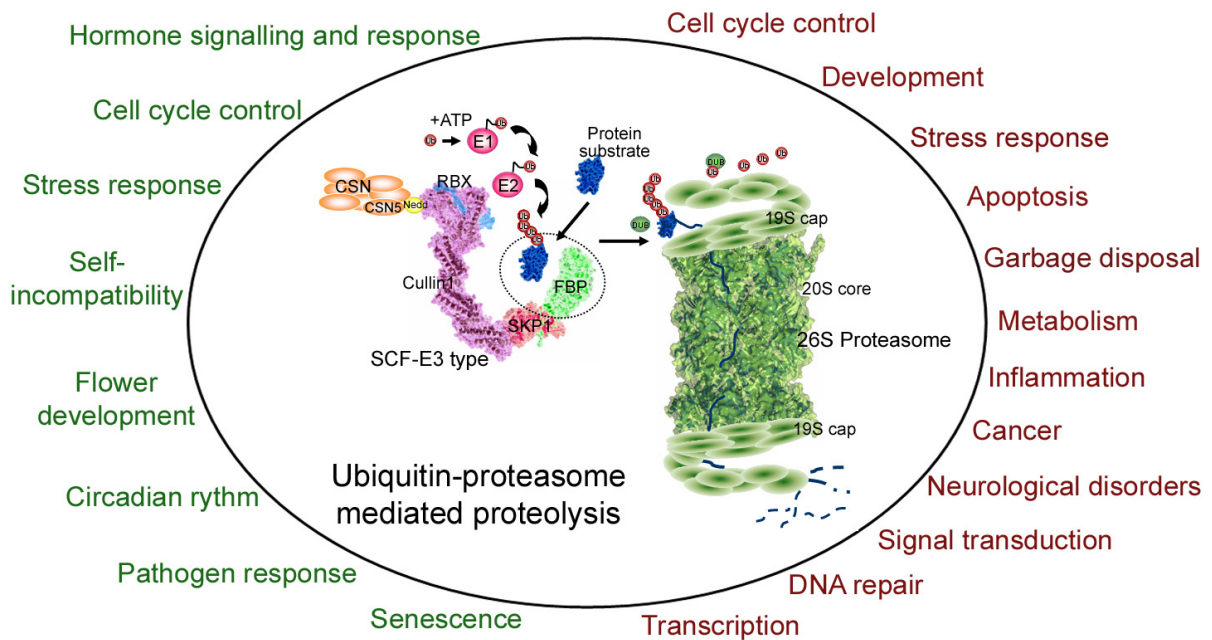


Figure 1. Ubiquitin-mediated proteolysis plays a crucial role in a large variety of essential cellular pathways in eukaryotes. Plant specific (in green) and mammalian specific (in red) processes regulated through the ubiquitin-proteasome pathway. Targeting of protein substrates with ubiquitin occurs by the coordinated activity of an E1 ubiquitin activating enzyme, an E2 ubiquitin conjugating enzyme and an E3 ubiquitin ligase. The SCF complex is one type of Cullin-containing E3. F-box proteins confer the specificity to the whole protein degradation process by specifically recognizing protein degradation targets. SCF activity is regulated by the attachment of NEDD8 to the Cullin subunit. CSN directly interacts with SCF-E3s and the CSN5 subunit mediates Cullin-deneddylation. Poly-ubiquitylated substrates are recognized by the 19S regulatory particle of the 26S proteasome. Substrates are finally degraded by the proteolytic activity of the 20S proteasome core, accompanied by the subsequent recycling of ubiquitin and amino acids.

The molecular components of the ubiquitin-proteasome system

Ubiquitin-dependent proteolysis is thought to occur in the cytoplasm and nucleus and involves the attachment of multiple ubiquitin residues to the degradation substrate, which is thereby targeted for degradation by the 26S

proteasome (Deshaies, 1995; Bates and Vierstra, 1999). This process requires the activities of an E1 ubiquitin activating enzyme, an E2 ubiquitin conjugating enzyme and an E3 ubiquitin ligase (E3), whereby the specificity of the whole process is conferred by the E3 ubiquitin ligase.

SKP1-Cullin-F-box protein (SCF) complexes are one type of the so-called Cullin-RING E3s. SCF complexes are a large family of Cullin-RING E3s and they have been shown to ubiquitylate a broad range of proteins involved in cell cycle progression, signal transduction, and transcription in eukaryotes (Deshaies, 1999). The Cullin (CDC53) and the RING-BOX 1 (RBX1 or ROC1/HRT1) subunits form the core of the complex, which recruits the E2 ubiquitin conjugating enzyme and the Suppressor of Kinetochores Protein 1 (SKP1) (Cardozo and Pagano, 2004). The SKP1 subunit binds to the F-box domain of the F-box proteins (FBPs), which in turn interact specifically with the degradation substrate (Figure 1). Different FBPs can associate in an interchangeable manner with SKP1 and this permits the formation of different SCF complexes with distinct substrate specificities (Schwechheimer and Calderón-Villalobos, 2004).

The SCF complex is regulated by the modification of the Cullin subunit by NEDD8, an ubiquitin-related protein (neddylation) (Hori et al., 1999). NEDD8 protein is detached from the Cullin by the activity of the COP9 signalosome (CSN), a multiprotein complex with similarity to the lid of the 26S proteasome (see below), in a process called deneddylation (Hori et al., 1999; Osaka et al., 2000). Although the role of neddylation and

deneddylation for E3 function is not fully understood, continuous rounds of neddylation and deneddylation seem to be essential for SCF assembly and activity (Lyapina et al., 2001; Schwechheimer and Deng, 2001; Schwechheimer, 2004).

The 26S proteasome is a multi-subunit complex responsible for the degradation of ubiquitin tagged proteins and consists of the 19S regulatory particle and the 20S core particle (Baumeister et al., 1998). The 19S regulatory particle executes an ATP-dependent function and is subdivided in a lid and a base. Polyubiquitylated substrates are not only recognized by 19S regulatory particle, but also unfolded, deubiquitylated and transmitted to the 20S core particle, which is in charge of the irreversible proteolysis of the targets (Figure 1).

The role of ubiquitin-mediated protein degradation in human disease

Because the regulation of biological events through ubiquitin-mediated proteolysis is a complex, highly selective and carefully regulated process, it is not surprising that alterations in its function has dramatic defects and causes cellular aberrations. In yeast, for instance, proper degradation of the cyclin-dependent kinase inhibitor Sic1 is essential for normal cell cycle progression (Schwob, 1994). In mammals, defects in ubiquitin-mediated protein degradation correlate with the onset of many diseases or malignancies, including a variety of cancers (Ciechanover and Schwartz, 2004). These pathological conditions can occur as result of loss of function of the ubiquitin

system or its components that lead to stabilization of the targets, as it occurs in certain brain disorders like in Parkinson's disease, Alzheimer's disease as well as in the Angelman syndrome and the Von Hippel-Lindau syndrome. On the other side, pathologies can also occur as a result of increased protein degradation, as has been observed for some types of cancer as well as for viral infections by human papillomavirus or cytomegalovirus (Table 1) (Ciechanover and Schwartz, 2004; Jiang and Beaudet, 2004). For instance, the levels of the tumor suppressor protein and transcription factor p53 are steadily controlled through ubiquitination and degradation in normal cells. p53 is involved in cell cycle control, DNA repair as well as apoptosis and alterations in ubiquitin-mediated proteolysis of p53 cause almost 50% of all human cancers, including cancer of the breast, colon, lung, liver, prostate, bladder and skin (Ciechanover and Schwartz, 2004). During cervical cancer, p53 protein levels are very low and this is highly correlated with human papilloma virus infection. The human papilloma virus E6 oncoprotein forms a complex with p53, resulting in the rapid ubiquitin-dependent degradation of p53 (Huibregtse et al., 1991). In consequence, infected cells cannot longer repair DNA damage in a normal manner. Some extensive stress conditions, in contrast, can block p53 ubiquitin-mediated degradation by inducing its modification and/or from its receptors, which induces irreversible growth arrest or apoptosis (Scheffner and Whitaker, 2003). Hence, regulated protein degradation is essential for human health, and general or specific defects in

the ubiquitin-proteasome system are the molecular cause for some major human diseases.

Table 1. Some diseases caused by disorders of the ubiquitin proteasome pathway (Modified according to Ciechanover, 2004 and Jiang, 2004).

Targets	Disorders
Stabilization of oncoproteins/growth factors	
c-Myc	Several Tumors, e.g. Burkitt's Lymphoma
c-Fos	Several Tumors
c-Jun	Several Tumors, e.g. Breast Tumors
Src	Several Colon, Liver, Lung, Breast, and Pancreas Tumors
Adenovirus E1A	Several Tumors, e.g. Ewing Tumors
Stabilization of membrane proteins	
ENaC	Liddle's Syndrome
CFTR	Cystic Fibrosis
Destabilization of tumor suppressors	
p53	Human Papillomavirus (Cervical Carcinoma)
p27	Colorectal Cancer Prostate Cancer Breast Cancer
β-catenin	Colorectal Tumor
Alterations of the ubiquitin-proteasome machinery/ oncoproteins	
pVHL E3	Von Hippel Lindau Syndrome Renal Cell Carcinoma Pheochromocytoma Cerebellar Hemangioblastomas Retinal Angiomas
c-Cbl and Hakai E3	Human Malignancies
BRCA1 and BARD1	Breast Carcinoma
PARKIN	Parkinson's Disease
Ubiquitin/Tau	Alzheimer's Disease
E6-AP	Angelman Syndrome

Ubiquitin-mediated proteolysis in plants

In Arabidopsis, around 1400 genes (~ 5% of the genome) encode components of the ubiquitin-proteasome pathway and previous analysis have shown that mutations in specific components of this pathway block many processes in plants ranging from embryogenesis to hormonal responses,

flower development, photomorphogenesis, circadian rhythms, senescence and pathogen invasion (Callis and Vierstra, 2000). F-Box Proteins (FBPs) represent a large protein family in Arabidopsis, comprising 694 members. Arabidopsis FBPs were identified based on the presence of the N-terminal F-box domain, which promotes association with the SCF core complex through SKP1 (Gagne et al., 2002). The carboxy terminal domains of FBPs capable of protein-protein interactions are in general variable and required for substrate binding and probably specify their diverse roles in different cellular pathways. The potential substrate recognition domains include leucine-rich (LRR), Kelch, WD-40, Armadillo (Arm), and tetratricopeptide (TPR) repeats, as well as Tubby (Tub), actin, DEAD-like helicase and jumonji (Jmj) domains, where LRR and Kelch repeats are the most common C-terminal domains in Arabidopsis FBPs (Gagne et al., 2002). This variety of FBPs substrate recognition domains evidences therefore the variety of targets that could be recognized and degraded through ubiquitin-mediated proteolysis and on the other way the relevance that such a pathway could play in the biology of the plant.

Table 2. List of F-box proteins from Arabidopsis with a known function

FBP	Pathway	Substrate	Subfamily	Conserved	Reference
AtSKP2;1 / AtSKP2;2	Cell cycle	E2Fc	C4	Yes	(del Pozo et al., 2002)
AtFBP7	Translation	Unknown	C4	Yes	This work
EBF1, EBF2	Ethylene signalling	EIN3	C4	No	(Guo and Ecker, 2003; Potuschak et al., 2003; Yanagisawa et al., 2003; Gagne et al., 2004)
EID1	Photomorphogenesis	Unknown	C4	No	(Dieterle, 2001)
TIR1, AFB1 / 2 / 3	Auxin perception and signalling	AUX/IAAs	C3	No	(Ruegger et al., 1998; Gray et al., 2001; Dharmasiri et al., 2005a; Kepinski and Leyser, 2005)
COI1	Jasmonic acid signalling and pathogen response	Unknown	C3	No	(Xie et al., 1998)
MAX2/ORE9	Shoot branching and senescence	Unknown	C3	No	(Woo et al., 2001; Stirnberg et al., 2002)
VFB1 / 2 / 3 / 4	Lateral root dev.	Unknown	C3	No	This work
UFO	Flower development	Unknown	C5	No	(Levin, 1995; Wang et al., 2003)
AFR1	Photomorphogenesis	Unknown	C5	No	(Harmon and Kay, 2003)
SLY	Giberellic acid signalling	GAI, RGA	C2	No	(Silverstone et al., 2001; McGinnis et al., 2003; Dill et al., 2004)
FKF/ ZTL	Circadian rhythm	CO, TOC1	E	No	(Nelson, 2000; Somers, 2000; Kim et al., 2003; Mas et al., 2003)
SON1	Pathogen response	NIM1	A1	No	(Kim and Delaney, 2002)
SLFs	Self incompatibility	Unknown	A	No	(Wang et al., 2004)

Using genetic approaches, it has been shown that FBPs play a role in crucial biological processes in plants (Table 2). In auxin signalling, for instance, TIR1, AFB1, AFB2 and AFB3, which belong to the C3 subfamily of the Arabidopsis FBP super family target AUX/IAA transcriptional repressors for degradation (Ruegger et al., 1998; Gray et al., 1999; Gray et al., 2001; Dharmasiri et al., 2005a; Dharmasiri et al., 2005b). Recently, it was also shown that the interaction between TIR1 and AUX/IAA proteins does not require stable modification of either protein as initially thought (Gray et al.,

2001; Ramos et al., 2001; Dharmasiri et al., 2003; Kepinski and Leyser, 2004). Instead, auxin promotes the interaction of AUX/IAA and the ubiquitin protein ligase SCF^{TIR1} by binding directly to the TIR1 F-box protein, thereby presumably promoting the ubiquitylation and degradation of these repressors (Dharmasiri et al., 2005a; Dharmasiri et al., 2005b; Kepinski and Leyser, 2005). The interaction between AUX/IAAs and SCF^{TIR1} plays a central role in the plant auxin biology. Mutations in AUX/IAAs that increase their stability by severely reducing their interaction with SCF^{TIR1}, as well as mutations that disrupt SCF^{TIR1} function confer defects in auxin-induced gene expression. This causes a wide range of auxin-related morphological phenotypes ranging from growth arrest during embryogenesis to impairment in hypocotyl elongation and root and shoot meristem formation (Dharmasiri et al., 2005a; Dharmasiri et al., 2005b; Kepinski and Leyser, 2005).

Collectively, these results together with investigations of the last years have shown that Arabidopsis has exploited the SCF complex and the ubiquitin-mediated degradation pathway as a major route for the regulation of plant specific cellular regulation and that a diverse array of as yet largely unknown FBPs targets must exist in plants (Table 2).

Although several lines of evidence have emerged concerning the function of ubiquitin-mediated proteolysis in plants, a number of important questions remain to be answered, which currently are the topic of investigations in several laboratories: (i) Why have FBPs evolved into such an extensive family in Arabidopsis? (ii) Are there evolutionarily conserved FBPs and have

they preserved their function and substrate specificity? or (iii) Have FBPs evolved to allow the regulation of other cellular processes? (iv) How is the activity of these FBPs regulated and how does this regulation influence distinct cellular pathways? (v) What are the specific degradation targets of plant FBPs? (vi) How relevant is the regulation by SCF mediated degradation of specific targets for plant survival? (vii) How redundant is FBP activity? (viii) Is there a combinatorial use of FBP in SCF complexes to allow the regulation of different cellular processes?

I.II. Aim of this work

To shed light onto how specific FBPs work and how plant signalling pathways are regulated through ubiquitin-mediated degradation, the main purpose of this dissertation was the investigation of previously uncharacterized FBPs from *Arabidopsis* as well as the elucidation of the biological mechanisms that they regulate.

Because selective targeting of various intracellular proteins by E3 ubiquitin ligases (E3s) plays an essential role in eukaryotic cell regulation in general, we focused initially on the identification of evolutionarily conserved FBPs. I conducted a systematic comparative analysis of *Arabidopsis*, human and yeast FBPs. Surprisingly, I found that only four FBPs are evolutionarily conserved between yeasts, animals and plants. One of these FBPs was a previously uncharacterized FBP with an atypical putative substrate recognition domain that we named *Arabidopsis thaliana* F-BOX PROTEIN 7

(AtFBP7). Further work consisted of the characterization of AtFBP7 and the analysis of its biological function. Results on AtFBP7 investigation will finally permit to determine whether Arabidopsis AtFBP7 has conserved their biological function through evolution by regulating the same targets and the same pathways of its eukaryotic counterparts, or whether AtFBP7 has specialized its degradation targets in plants.

Perhaps one of the most intriguing examples of the complex relationship between ubiquitin-mediated proteolysis and plant growth and development comes from auxin signalling in Arabidopsis. Different genetic analysis have revealed that loss-of-function mutations in SCF components confer auxin resistance phenotypes as, for instance, observed in *axr6*, *tir1* and *afb1*, *afb2* and *afb3* mutants (Gray et al., 2001; Hellmann et al., 2003; Dharmasiri et al., 2005b). The TIR1/AFB FBPs not only function redundantly by promoting the degradation of AUX/IAA proteins in an auxin-dependent manner, but they were also shown to be the auxin receptors *per se* (Dharmasiri et al., 2005b; Kepinski and Leyser, 2005). TIR1/AFBs belong to the C3 subfamily of the Arabidopsis FBP superfamily, which also includes COI1 required for jasmonic acid response and pathogen response (Table 2). In addition, the C3 subfamily contains four plant-specific FBPs, designated VIER F-BOX PROTEINE (VFB, German for FOUR F-BOX PROTEINS), which we characterized in the laboratory. Because of the high homology between VFBs and TIR1/AFBs, as well as COI1, we speculate that VFBs act in a similar way and mediate the targeting of key regulatory protein(s) in an

auxin or another hormone signalling pathway. Our studies on VFBs focus on the analysis of *vfb* mutants from Arabidopsis to evaluate our hypothesis and reveal VFB's specific biological function.

While components of the ubiquitin-proteasome system can be predicted based on sequence homologies to proteins from other eukaryotes with known function, it is at present impossible to predict the identity of unstable proteins based on sequence features. Proteins with a so-called PEST domain, thus a sequence stretch that is enriched in prolines, glutamic acids, serines and threonines, have been postulated to be unstable proteins (Rechsteiner and Rogers, 1996). One novel Arabidopsis protein with a PEST domain is TOUGH (TGH) and its biological characterization represents one part of the present dissertation. Furthermore, this dissertation also includes an introduction into the LucTrap vector series that allows to generate protein fusions with the luciferase reporter so that the dynamics and regulation of a protein of interest can be followed *in vivo*. It provides an efficient tool for the identification of regulated proteins and putative targets for degradation.

In general terms, the purpose of this work is the identification of the cellular processes in Arabidopsis that require ubiquitin-mediated degradation, through the specific characterization of a set of novel FBPs, as well as one putative target for degradation, and the presentation of a technology that should allow the identification of unstable ubiquitin-regulated proteins.

I.III. Results

Prior to the analysis of the Arabidopsis genome sequence, the relevance and amount of proteins considered to play a role in ubiquitin-mediated proteolysis was underestimated by the plant scientific community (Xiao, 2000). In the past five years, the number of reported processes that require control through proteolysis has been continuously increasing. This evidenced how important the regulation of regulatory proteins through ubiquitin-mediated proteolysis is and how many components could play a role in this pathway. This increase in novel information generated a need for reviews that provide an overview of the current knowledge of ubiquitin-mediated protein degradation in plants. For this reason the review article, which represents chapter II.I of this dissertation, was written. Rather than providing a list of pathways and components of the plant ubiquitin-proteasome system, this review focuses on selected examples from ethylene response, gibberellic acid response and photomorphogenesis. These examples underline the importance of the identification of new signal components and regulators of proteolysis-controlled pathways.

Chapter II.II describes the characterization of the novel evolutionarily conserved FBP from Arabidopsis, which was named AtFBP7. As mentioned before, AtFBP7 was one of only 4 FBPs, for which it was found evidence for conservation in all studied model organisms ranging from yeast to mammals, suggesting that AtFBP7 may control an evolutionarily conserved process. AtFBP7 is a unique gene in Arabidopsis and is

ubiquitously expressed in the plant. However, *fbp7* loss-of-function mutants do not exhibit any obvious phenotypes. In the yeast two-hybrid system, AtFBP7 interacts with Arabidopsis Skp1 homologues, confirming that it is also a component of SCF E3 complexes. The AtFBP7 yeast counterpart interacts not only with SKP1 for binding to the SCF complex, but also with the eukaryotic translation elongation factor eEF-2. In support of a functional relevance of this interaction, the experiments described in chapter II.II show that *fbp7* knock-out mutants have reduced translation efficiencies in cold and in heat stress conditions. Using promoter fusions to the reporter β -glucuronidase as well as transcript analysis, it was also shown that AtFBP7 is transcriptionally up-regulated after cold and heat stresses. Based on these results, a model of AtFBP7 regulation is proposed, where AtFBP7 is required for the degradation of a translational inhibitor during temperature stresses.

The analysis of the plant specific VFBs Vier F-box Proteins (VFB) in chapter II.III pointed out their possible role in plant growth in general and lateral root formation in particular. VFB1 through VFB4 are four LRR-containing F-box proteins, which belong to the C3 FBP subfamily. To this group belong also the TIR1/AFB and COI1 FBPs, which are required for auxin perception and response and jasmonic acid signalling, respectively. My contribution to this study consisted of a micro-array based gene expression study, which revealed that the expression of a set of auxin induced genes is reduced in *vfb* mutants. This result together with the *vfb* mutant phenotype points a role for VFBs during auxin response, specifically in the root.

Furthermore, genes significantly misregulated in *vfb* mutants are also affected in *csn4-1*, a mutant allele for CSN subunit 4, providing evidence that VFB F-box proteins and CSN have common targets.

Proteins of the ubiquitin-proteasome system such as FBPs can be easily identified in plants based on their homology to ubiquitin-proteasome proteins from other organisms. In contrast, the identification of putative targets for degradation is not trivial, considering that there is not a characteristic domain present in unstable proteins. There is, however, a so-called PEST domain, which was shown to serve as proteolytic signal and a large number of proteins were predicted to be degraded by its presence (Rechsteiner and Rogers, 1996). TGH protein presented in chapter II.IV was initially thought to be an unstable plant protein and as such considered as a putative target for degradation during auxin signalling due to the *tgh* mutant phenotype. TGH is enriched at its C-terminus in glutamic acid, and serine residues (KRDES domain) and therefore shares similarity with the PEST domain. The hypothesis that TGH is a target for degradation could, however, as yet not be confirmed. TGH protein colocalizes with the splicing regulator SRp34 in subnuclear particles, is an evolutionarily conserved and has two additional protein domains, a G-patch and a SWAP domain, which are exclusively found in RNA binding and processing proteins. TGH exhibits transcriptional activation activity and TGH was shown to interact with TATA-box binding protein (TBP) in yeast two-hybrid assays. Genetic evidence points towards a role of TGH protein as regulator of plant growth and

vascular development in *Arabidopsis*. *tgh* mutants exhibit pleiotropic developmental defects, which include dwarfism, reduced fertility, multiple cotyledons, lanceolated leaves and distortion of vascular patterning. Although a number of mutants defective in auxin transport and response show similar phenotypes, no evidence for a role of TGH in such pathways could be provided.

The last publication in Chapter II.V describes a set of LucTrap vectors that should allow to evaluate gene expression and protein degradation *in vivo*. These LucTrap plant transformation vectors are based on the quantifiable activity of luciferase as a reporter and they permit to generate transcriptional and translational luciferase reporter fusions. Another set of LucTrap vectors allows promoter and gene trap fusions. A collection of own generated LucTrap lines harbouring gene trap fusions was analyzed and this revealed how useful and versatile these vectors can be to follow gene expression and protein dynamics *in vivo*.

I.IV. Discussion

In eukaryotes, ubiquitin-mediated proteolysis participates in the control of signal transduction events by the selective elimination of proteins. Arabidopsis contains a surprisingly large number of FBPs, which are the substrate receptors of SCF-type E3 ubiquitin ligases, and they confer the specificity to the degradation process. This suggests that SCF-type E3s are required for many cellular and developmental processes in plants. To contribute to the understanding of FBP-mediated proteolysis in plants, this work has focused not only on the characterization of novel FBPs substrate receptors itself but also on the investigation of the biological pathways in which they play a role. The results presented in this work are new and significant with respect to aspects of regulation of plant biology through proteolysis, thus providing relevant understanding of the plant as a whole organism.

My sequence analysis revealed that only four FBPs are seemingly conserved among all eukaryotic model organisms. AtFBP7 is one of them and may have preserved its original function as a regulator of an evolutionarily conserved process. AtFBP7 was shown to form an SCF^{AtFBP7} complex and to be ubiquitously expressed in the plant. Although a direct target for degradation could not be found, AtFBP7 may function as a degradation receptor during translation in temperature stress and possibly also in other as yet unidentified conditions. It is therefore possible that apart from the specificity of AtFBP7 in terms of its degradation target, the AtBP7

field of action is extremely restricted, which would explain the absence of an obvious phenotype of *fbp7* mutant plants in normal or during stress growth conditions. One could speculate that during temperature stresses, AtFBP7 promotes the degradation of a repressor of protein synthesis, which would explain the impairment of translation efficiency observed in *fbp7* mutants in such conditions. Presumably, regulation of translation by proteolysis provides the cell with a rapid response mechanism that is necessary to overcome stresses, hence AtFBP7 is a positive regulator of this process. In mammals, it was shown that one way of translational control by the ubiquitin-proteasome pathway is the degradation of miss-folded polypeptides, so called DRIPs (small defective ribosomal products) following protein neosynthesis (Yewdell et al., 1996; Schubert et al., 2000) DRIPs constitute circa 30% of newly synthesized proteins as determined in a variety of mammalian cell types and are polypeptides that never attain native structure owing to errors in translation or posttranslational processes necessary for proper protein folding (Schubert et al., 2000). Presumably, DRIP formation is enhanced by temperature stress and its accumulation potentially interferes with protein synthesis. It is therefore possible to hypothesize that AtFBP7 fulfills its conserved function by regulating the degradation of these newly synthesized proteins, produced by errors in translation during temperature stresses. That way, AtFBP7 would function as a “quality control officer” of polypeptides, which would otherwise block or disturb the translational machinery. Essentially, the investigation on AtFBP7

hints towards a role of protein degradation in an event that is required for protein synthesis during temperature stresses, which still needs to be confirmed or re-evaluated for its eukaryotic counterparts. This could be conducted in yeast, for instance, where a viable mutant is available and would confirm that AtFBP7 has conserved its function. Furthermore, the identification of AtFBP7 specific degradation substrates should be a priority.

From the evolutionarily conserved AtFBP7 from Arabidopsis, we shift to a plant specific subfamily of FBPs, namely VFBs. VIER F-BOX PROTEINS (VFBs) all share a high degree of homology with TIR1/AFBs and COI1. Do these four closely related VFBs fulfill similar functions as their homologues during auxin and/or other hormone responses or in another pathway during plant development? Auxin response requires the degradation of AUX/IAA inhibitors, which promotes the ARF dependent transcriptional activation of auxin target genes (Weijers and Jürgens, 2004). Arabidopsis contains 29 AUX/IAA and 23 ARF proteins, which homo- and heterodimerize (Reed, 2001). A set of studies suggests that cell-specific combinations of AUX/IAAs and ARFs may determine auxin responses and also that specific AUX/IAAs are probably targeted by specific FBPs for degradation. This is supported by the fact that single mutants of TIR1 or AFBs exhibit only a mild phenotype, while gain-of-function mutants of AUX/IAAs, in which the repressors are stabilized, show stronger phenotypes (Weijers et al., 2005). It has been suggested that there is not only a degree of functional redundancy in FBP function, but also that there are other

FBPs, which target specific AUX/IAAs for degradation (Weijers and Jürgens, 2004). VFBs were characterized in this study and although they do not seem to be functional orthologues of TIR1/AFBs, they appear to mediate auxin responses. This was evidenced by the reduced expression of auxin responsive genes, a reduction of DR5:GUS expression and the lack of lateral roots in *vfb* mutants. Interestingly, loss of *VFB* function causes the repression of a significant number of auxin-induced genes, which are also repressed in *csn* mutants. One could assume that VFBs role in auxin signalling is highly probable but other factors like the level of tissue-specific expression as well as the subcellular localization, would define their specificity. Further, it has to be considered that 29 AUX/IAAs could be targeted for degradation for distinct FBPs in specific pathways therefore supporting the fact that VFBs and TIR1/AFBs are simply functionally distinct during auxin signalling.

During this study, the attempt to identify VFBs degradation targets by yeast two-hybrid screens was not successful. Possibly, substrate modifications are required for VFB recognition, making their identification difficult. It remains, however, imperative to discover VFBs' substrates to be able to define their particular role in auxin signalling. Eventually, genetic analysis using specific candidate genes whose mutations give rise to a similar lateral root phenotype than that observed in *vfb* mutants could help to identify targets. If the block of VFB activity causes stabilization of their targets, similar lateral root phenotypes from *vfb* loss-of-function mutants are

expected to be observed in gain-of-function mutants of their substrates. SOLITARY ROOT 1 (SLR1) /IAA14 protein can be considered as candidate for VFB mediated degradation. SLR1/IAA4 is one of the central regulators of lateral root initiation due to the fact that *slr1* gain-of-function mutants develop a primary root but lack lateral roots (Fukaki et al., 2002). Moreover, there are other AUX/IAAs with a proven role in lateral root formation such as AUXIN RESISTANT 5 (AXR5) /IAA1 or MASSUGU 2 (MSG2)/IAA19 (Park et al., 2002; Tatematsu et al., 2004) that could be targeted by VFBs. To confirm the role of VFBs in the regulation of SLR1/IAA14, AXR5/IAA1, MSG2/IAA19, one could evaluate the effect of loss-of-function mutations of these AUX/IAAs in the *vfb* mutant background. In an ideal case, a rescue of the mutant *vfb* lateral root phenotype could be expected. However, not only the instability of the *vfb* mutant phenotype but also functional redundancy with other AUX/IAAs makes this experiment difficult. Furthermore, AUX/IAAs gene expression is subject to a complex feedback regulation, which would not only affect the transcription of the primary AUX/IAA effectors but also this of others AUX/IAAs. Therefore a simple model of VFB action targeting AUX/IAAs for degradation cannot yet be proposed.

Because the initiation of lateral roots is marked by specific cell divisions in the pericycle (Casimiro et al., 2001), cell cycle activation is inherently connected with lateral root initiation, meaning that the expression or activity of some cell cycle regulators has to be regulated for proper lateral root initiation (Fukaki et al., 2002). It is also possible to hypothesize that

VFBs mediate between auxin signalling and cell cycle activation during lateral root formation. To assess this hypothesis, cell cycle activity was examined in *vfb* mutants using a CycB:GUS transgene. At least this experiment did not show any marked defects in the cell cycle activity in the *vfb* mutants. Therefore, the hypothetical role for VFBs in auxin signalling or cell cycle regulation requires additional work and this is the purpose of one ongoing thesis project in the laboratory.

This work also aimed to investigate protein degradation during plant growth and development from another point of view, namely from the degradation substrates. TOUGH (TGH) was presumed to be a target of the degradation machinery during auxin signalling due to the *tgh* mutant phenotype and the presence of a putative PEST domain in TGH protein. In our studies, however, TGH does not appear to be an unstable protein targeted for ubiquitin-mediated degradation. Some reasons can be hypothesized: the first and most trivial explanation is that the prediction of a PEST domain in the TGH protein was wrong, and that TGH is a stable protein. Second, TGH could require a type of modification for its subsequent recognition and degradation. And finally, it is possible that our experiments were not conducted in the specific conditions in which TGH levels are regulated. Further analyses are therefore necessary to evaluate TGH stability.

A very intriguing issue concerning TGH is its presumed biological function. *tgh* loss-of-function mutants show some vascularization and

growth defects that could be interpreted as misregulation of auxin transport or auxin signalling pathways. However, no evidence for a role of TGH in these processes could be found. It is also possible, that our analysis was not detailed enough to substantiate this hypothesis and that TGH is involved in auxin signalling. Additionally, genetic analysis revealed that *TGH* expression seems to be correlated with increased cell cycle activity. Taken together, it is very difficult to point out a role for TGH in hormone signalling or response. On the other side, TGH domain structure and TGH localization let to postulate that TGH functions probably in RNA binding or processing in close proximity to the spliceosome machinery. Development and differentiation processes require the selective control of gene expression, which can be regulated at a number of steps, including the availability of DNA for transcription, the transcription process itself, splicing, transport and stability of mRNA, translation, and post-translational transport or modification of the protein product (Maniatis and Reed, 2002). Although TGH or its orthologues have not been identified in previous searches for components of the RNA metabolic machinery (Rappsilber et al., 2002; Zhou et al., 2002), it is not possible to rule out that TGH functions in this process. One could speculate that TGH acts as a regulator of gene expression in a co- or posttranscriptional process, in which TGH binds to RNA and regulates gene expression of its targets in a specific developmental process. Although the elucidation of TGH targets is relevant for the understanding of TGH function, this is at present out of our interest.

One point that became evident throughout the analysis of Arabidopsis FBPs was the fact that the knowledge about the identity of their degradation targets will help to understand their biological function. However, to date only a few unstable proteins are known. To provide a new tool to identify and study putative degradation targets, this work also introduced the LucTrap vectors that serve to generate translational fusions. This approach can be used to follow changes in gene expression but also to monitor protein dynamics and stability *in vivo*, for instance after hormone treatments, and thus to reveal new protein degradation-dependent signal transduction cascades.

From this work, it is clear that multiple efforts must be oriented to the development of additional technologies to identify processes that are potentially controlled by protein degradation. The characterization of more F-box proteins, the mechanisms of target regulation, but most importantly, the identity of the targets themselves requires further investigation. Some methods like comparative proteomics or yeast two-hybrid screens have been used for these purposes (Potuschak et al., 2003). However, an inherent feature of unstable proteins is their fast turnover, and this fact considerably hinders their detection.

Gene expression and therefore protein regulation are triggered by environmental signals as well as by changes in the concentration of endogenous hormones, making the elucidation of putative targets for degradation and their biological function more complex. Also it has to be

considered that there is a “developmental program” required for the activation and repression of sets of genes/proteins necessary for specific plant developmental processes.

A major challenge remains the understanding of the whole ubiquitin degradation signalling event: what SCF complexes are really possible in plants and what is their function in Arabidopsis, which substrates can be recognized by a specific F-box protein, what are the substrate modifications required for its instability, how is the regulation of F-box proteins itself, etc, etc. Only parts of the answers are currently known, but research into these questions will improve our understanding of development and growth in plants and in eukaryotes.

I.V. References

- Bates, P.W., and Vierstra, R.D.** (1999). UPL1 and 2, two 450 kDa ubiquitin-protein ligases from *Arabidopsis thaliana* related to the HECT-domain protein family. *Plant J* **20**, 183 - 195.
- Baumeister, W., Walz, J., Zühl, F., and Seemüller, E.** (1998). The proteasome: paradigm of a self-compartmentalizing protease. *Cell* **92**, 367-380.
- Callis, J., and Vierstra, R.D.** (2000). Protein degradation in signaling. *Curr Opin Plant Biol* **3**, 381-386.
- Cardozo, T., and Pagano, M.** (2004). The SCF ubiquitin ligase: insights into a molecular machine. *Nat Rev Mol Cell Biol* **5**, 739-751.
- Casimiro, I., Marchant, A., Bhalerao, R.P., Beeckman, T., Dhooge, S., Swarup, R., Graham, N., Inze, D., Sandberg, G., Casero, P.J., and Bennett, M.** (2001). Auxin transport promotes *Arabidopsis* lateral root initiation. *Plant Cell* **13**, 843-852.
- Ciechanover, A.** (1998). The ubiquitin-proteasome pathway: on protein death and cell life. *EMBO J.* **17**, 7151-7160.
- Ciechanover, A., and Schwartz, A.L.** (2004). The ubiquitin system: pathogenesis of human diseases and drug targeting. *Biochim Biophys Acta* **1695**, 3-17.
- del Pozo, J.C., Boniotti, M.B., and Gutierrez, C.** (2002). *Arabidopsis* E2Fc functions in cell division and is degraded by the ubiquitin-SCF(AtSKP2) pathway in response to light. *Plant Cell* **2002**, 3057 - 3071.
- Deshaies, R.J.** (1995). Make it or break it: the role of ubiquitin-dependent proteolysis in cellular regulation. *Trends Cell Biol* **5**, 428-434.
- Deshaies, R.J.** (1999). SCF and Cullin/RING H2-based ubiquitin ligases. *Annu Rev Cell Dev Biol* **15**, 435 - 467.
- Dharmasiri, N., Dharmasiri, S., and Estelle, M.** (2005a). The F-box protein TIR1 is an auxin receptor. *Nature* **435**, 441-445.
- Dharmasiri, N., Dharmasiri, S., Jones, A.M., and Estelle, M.** (2003). Auxin action in a cell free system. *Curr Biol* **13**, 1418 - 1422.
- Dharmasiri, N., Dharmasiri, S., Weijers, D., Lechner, E., Yamada, M., Hobbie, L., Ehrismann, J.S., Jürgens, G., and Estelle, M.** (2005b). Plant development is regulated by a family of auxin receptor F box proteins. *Dev Cell* **9**, 109-119.
- Dieterle, M., Zhou, Y.-C., Schäfer, E., Funk, M., Kretsch, T.** (2001). EID1, an F-box protein involved in phytochrome A-specific light signaling. *Genes Dev* **15**, 939 - 944.
- Dill, A., Thomas, S.G., Hu, J., Steber, C.M., and Sun, T.-p.** (2004). The *Arabidopsis* F-box protein SLEEPY1 targets gibberellin signaling repressors for gibberellin-induced degradation. *Plant Cell* **16**, 1392 - 1405.

- Fukaki, H., Tameda, S., Masuda, H., and Tasaka, M.** (2002). Lateral root formation is blocked by a gain-of-function mutation in the SOLITARY-ROOT/IAA14 gene of *Arabidopsis*. *Plant J* **29**, 153 - 168.
- Gagne, J.M., Downes, B.P., Shiu, S.H., Durski, A.M., and Vierstra, R.D.** (2002). The F-box subunit of the SCF E3 complex is encoded by a diverse superfamily of genes in *Arabidopsis*. *Proc Natl Acad Sci U S A* **99**, 11519 - 11524.
- Gagne, J.M., Smalle, J., Gingerich, D.J., Walker, J.M., Yoo, S.D., Yanagisawa, S., and Vierstra, R.D.** (2004). *Arabidopsis* EIN3-binding F-box 1 and 2 form ubiquitin-protein ligases that repress ethylene action and promote growth by directing EIN3 degradation. *Proc Natl Acad Sci U S A* **101**, 6803-6808.
- Gray, W.M., Kepinski, S., Rouse, D., Leyser, O., and Estelle, M.** (2001). Auxin regulates SCF^{TIR1}-dependent degradation of AUX/IAA proteins. *Nature* **414**, 271 - 276.
- Gray, W.M., del Pozo, J.C., Walker, L., Hobbie, L., Risseuw, E., Banks, T., Crosby, W.L., Yang, M., and Estelle, M.** (1999). Identification of an SCF ubiquitin-ligase complex required for auxin response in *Arabidopsis thaliana*. *Genes Dev* **13**, 1678 - 1687.
- Guo, H., and Ecker, J.R.** (2003). Plant responses to ethylene gas are mediated by SCF(EBF1/EBF2)-dependent proteolysis of EIN3 transcription factor. *Cell* **115**, 667 - 677.
- Harmon, F.G., and Kay, S.A.** (2003). The F box protein AFR is a positive regulator of phytochrome A-mediated light signaling. *Curr Biol* **13**, 2091 - 2096.
- Hellmann, H., Hobbie, L., Chapman, A., Dharmasiri, S., Dharmasiri, N., del Pozo, c., Reinhardt, D., and Estelle, M.** (2003). *Arabidopsis* AXR6 encodes CUL1 implicating SCF E3 ligases in auxin regulation of embryogenesis. *EMBO J.* **22**, 3314 - 3325.
- Hershko, A., Ciechanover, A.** (1998). The ubiquitin system. *Annu Rev Biochem* **67**, 425-479.
- Hori, T., Osaka, F., Chiba, T., Miyamoto, C., Okabayashi, K., Shimbara, N., Kato, S., and Tanaka, K.** (1999). Covalent modification of all members of human cullin family proteins by NEDD8. *Oncogene* **18**, 6829-6834.
- Huibregtse, J.M., Scheffner, M., and Howley, P.M.** (1991). A cellular protein mediates association of p53 with the E6 oncoprotein of human papillomavirus types 16 or 18. *EMBO J* **10**, 4129-4135.
- Jiang, Y.H., and Beaudet, A.L.** (2004). Human disorders of ubiquitination and proteasomal degradation. *Curr Opin Pediatr* **16**, 419-426.
- Kepinski, S., and Leyser, O.** (2004). Auxin-induced SCFTIR1-Aux/IAA interaction involves stable modification of the SCFTIR1 complex. *Proc Natl Acad Sci U S A* **101**, 12381-12386.
- Kepinski, S., and Leyser, O.** (2005). The *Arabidopsis* F-box protein TIR1 is an auxin receptor. *Nature* **435**, 446-451.

- Kim, H.S., and Delaney, T.P.** (2002). Arabidopsis SON1 is an F-Box protein that regulates a novel induced defense response independent of both salicylic acid and systemic acquired resistance. *Plant Cell* **14**, 1469 - 1482.
- Kim, W.-Y., Geng, R., and Somers, D.E.** (2003). Circadian phase-specific degradation of the F-box protein ZTL is mediated by the proteasome. *Proc Natl Acad Sci U S A* **100**, 4933 - 4938.
- Levin, J.Z., Meyerowitz, E.M.** (1995). UFO: an Arabidopsis gene involved in both floral meristem and floral organ development. *Plant Cell Physiol* **7**, 529 - 548.
- Lyapina, S., Cope, G., Shevchenko, A., Serino, G., Zhou, C., Wolf, D.A., Wei, N., Shevchenko, A., and Deshaies, R.J.** (2001). COP9 Signalosome promotes cleavage of NEDD8-CUL1 conjugates. *Science* **292**, 1382 - 1385.
- Maniatis, T., and Reed, R.** (2002). An extensive network of coupling among gene expression machines. *Nature* **416**, 499-506.
- Mas, P., Kim, W.-Y., Somers, D.E., and Kay, S.A.** (2003). Targeted degradation of TOC1 by ZTL modulates circadian function in Arabidopsis thaliana. *Nature* **426**, 567 - 570.
- McGinnis, K.M., Thomas, S.G., Soule, J.D., Strader, L.C., Zale, J.M., Sun, T.-p., and Steber, C.M.** (2003). The Arabidopsis *SLEEPY1* gene encodes a putative F-box subunit of an SCF E3 ubiquitin ligase. *Plant Cell* **15**, 1120 - 1130.
- Meusser, B., Hirsch, C., Jarosch, E., and Sommer, T.** (2005). ERAD: the long road to destruction. *Nat Cell Biol* **7**, 766-772.
- Muller, J., Piffanelli, P., Devoto, A., Miklis, M., Elliott, C., Ortmann, B., Schulze-Lefert, P., and Panstruga, R.** (2005). Conserved ERAD-like quality control of a plant polytopic membrane protein. *Plant Cell* **17**, 149-163.
- Nelson, D.C., Lasswell, J., Rogg, L.E., Cohen, M.A., Bartel, B.** (2000). FKF1, a clock-controlled gene that regulates the transition to flowering in Arabidopsis. *Cell* **101**, 331 - 340.
- Osaka, F., Saeki, M., Katayama, S., Aida, N., Toh-e, A., Kominami, K., Toda, T., Suzuki, T., Chiba, T., Tanaka, K., and Kato, S.** (2000). Covalent modifier NEDD8 is essential for SCF ubiquitin-ligase in fission yeast. *EMBO J.* **19**, 3475 - 3484.
- Park, J.-Y., Kim, H.-J., and Kim, J.** (2002). Mutation in domain II of IAA1 confers diverse auxin-related phenotypes and represses auxin-activated expression of Aux/IAA genes in steroid regulator inducible system. *Plant J* **32**, 669 - 683.
- Potuschak, T., Lechner, E., Parmentier, Y., Yanagisawa, S., Grava, S., Koncz, C., and Genschik, P.** (2003). EIN3-dependent regulation of plant ethylene hormone signaling by two arabidopsis F box proteins: EBF1 and EBF2. *Cell* **115**, 679 - 689.
- Ramos, J.A., Zenser, N., Leyser, O., and Callis, J.** (2001). Rapid degradation of auxin/indoleacetic acid proteins requires conserved

- amino acids of domain II and is proteasome dependent. *Plant Cell* **13**, 2349-2360.
- Rappsilber, J., Ryder, U., Lamond, A.I., and Mann, M.** (2002). Large-scale proteomic analysis of the human spliceosome. *Genome Res* **12**, 1231-1245.
- Rechsteiner, M., and Rogers, S.W.** (1996). PEST sequences and regulation by proteolysis. *Trends Biochem Sci* **21**, 267-271.
- Reed, J.** (2001). Roles and activities of Aux/IAA proteins in Arabidopsis. *Trends Plant Sci* **6**, 420 - 425.
- Ruegger, M., Dewey, E., Gray, W.M., Hobbie, L., Turner, J., and Estelle, M.** (1998). The TIR protein of Arabidopsis function in auxin response and is related to human SKP2 and yeast Grr1p. *Genes Dev* **12**, 198-207.
- Scheffner, M., and Whitaker, N.J.** (2003). Human papillomavirus-induced carcinogenesis and the ubiquitin-proteasome system. *Semin Cancer Biol* **13**, 59-67.
- Schubert, U., Anton, L.C., Gibbs, J., Norbury, C.C., Yewdell, J.W., and Bennink, J.R.** (2000). Rapid degradation of a large fraction of newly synthesized proteins by proteasomes. *Nature* **404**, 770-774.
- Schwechheimer, C.** (2004). The COP9 signalosome (CSN): an evolutionary conserved proteolysis regulator in eukaryotic development. *Biochim Biophys Acta* **1695**, 45-54.
- Schwechheimer, C., and Deng, X.-W.** (2001). COP9 signalosome revisited: a novel mediator of protein degradation. *Trends Cell Biol* **11**, 420 - 426.
- Schwechheimer, C., and Calderón-Villalobos, L.I.A.** (2004). Cullin-containing E3 ubiquitin ligases in plant development. *Curr Opin Plant Biol* **7**, 677-686.
- Schwechheimer, C., Serino, G., Callis, J., Crosby, W.L., Lyapina, S., Deshaies, R.J., Gray, W.M., Estelle, M., and Deng, X.-W.** (2001). Interactions of the COP9 signalosome with the E3 ubiquitin ligase SCF^{TIR1} in mediating auxin response. *Science* **292**, 1379 - 1382.
- Schwob, E., Boehm, T., Mendenhall, M., and Nasmyth, K.** (1994). The B-type cyclin kinase inhibitor p40SIC1 controls the G1 to S transition in *S. cerevisiae*. *Cell* **79**, 233-244.
- Silverstone, A.L., Jung, H.-S., Dill, A., Kawaide, H., Kamiya, Y., and Sun, T.-p.** (2001). Repressing a repressor: gibberellin-induced rapid reduction of the RGA protein in Arabidopsis. *Plant Cell* **13**, 1555 - 1565.
- Somers, D.E., Schultz, T.F., Milnamow, M., Kay, S.A.** (2000). *ZEITLUPE* encodes a novel clock-associate PAS protein from Arabidopsis. *Cell* **101**, 319 - 329.
- Tatematsu, K., Kumagai, S., Muto, H., Sato, A., Watahiki, M.K., Harper, R.M., Liscum, E., and Yamamoto, K.T.** (2004). MASSUGU2 encodes Aux/IAA19, an auxin-regulated protein that functions together with the transcriptional activator NPH4/ARF7 to regulate differential growth

- responses of hypocotyl and formation of lateral roots in *Arabidopsis thaliana*. *Plant Cell* **16**, 379 - 393.
- Wang, L., Dong, L., Zhang, Y., Zhang, Y., Wu, W., Deng, X., and Xue, Y.** (2004). Genome-wide analysis of S-locus F-box like genes in *Arabidopsis thaliana*. *Plant Mol Biol* **56**, 929-945.
- Wang, X., Feng, S., Nakayama, N., Crosby, W.L., Irish, V.F., Deng, X.W., and Wei, N.** (2003). The COP9 Signalosome interacts with SCF^{UFO} and participates in *Arabidopsis* flower development. *Plant Cell* **15**, 1071 - 1082.
- Weijers, D., and Jürgens, G.** (2004). Funneling auxin action: specificity in signal transduction. *Curr Opin Plant Biol* **7**, 687-693.
- Weijers, D., Benkova, E., Jager, K.E., Schlereth, A., Hamann, T., Kientz, M., Wilmoth, J.C., Reed, J.W., and Jürgens, G.** (2005). Developmental specificity of auxin response by pairs of ARF and Aux/IAA transcriptional regulators. *EMBO J.* **24**, 1874-1885.
- Xiao, W., Jang, J.-C.** (2000). F-box proteins in *Arabidopsis*. *Trends Plant Sci* **5**, 454 - 457.
- Xie, D.-X., Feys, B.F., James, S., Nieto-Rostro, M., and Turner, J.G.** (1998). COI1: An *Arabidopsis* gene required for jasmonate-regulated defense and fertility. *Science* **280**, 1091 - 1094.
- Yanagisawa, S., Yoo, S.-D., and Sheen, J.** (2003). Differential regulation of EIN3 stability by glucose and ethylene signalling in plants. *Nature* **425**, 521 - 525.
- Yewdell, J.W., Anton, L.C., and Bennink, J.R.** (1996). Defective ribosomal products (DRiPs): a major source of antigenic peptides for MHC class I molecules? *J Immunol* **157**, 1823-1826.
- Zhou, Z., Licklider, L.J., Gygi, S.P., and Reed, R.** (2002). Comprehensive proteomic analysis of the human spliceosome. *Nature* **419**, 182-185.

II. Own contribution to the Publications

Chapter III.I

Cullin-containing E3 ubiquitin ligases in plant development.

Published in *Curr Opin Plant Biol* (2004) Dec; 7(6):677-86. Review article.

Claus Schwechheimer and Luz Irina A. Calderón Villalobos

- Written together with Claus Schwechheimer. Specific elaboration of the ethylene hormone synthesis and response topic.

Chapter III.II

The evolutionarily conserved *Arabidopsis thaliana* F-box protein AtFBP7 is required for efficient translation during temperature stress.

Submitted to the *Journal of Biological Chemistry*.

Luz Irina A. Calderón Villalobos, Carola Kuhnle, Katia Marrocco, Thomas Kretsch, and Claus Schwechheimer

- Main PhD project. All the general scientific and experimental work was done by myself, with the exception of: (i) the yeast two hybrid interaction studies against 19 SKPs (Figure 1C, collaboration with T. Kretsch, Freiburg) and (ii) the identification of the *fbp7-5* allele and GUS promoter constructs (carried out by C. Schwechheimer when at Yale University).

Chapter III.III

Characterization of the *VIER-F-BOX PROTEINE (VFB)* genes from *Arabidopsis* reveals their importance for plant growth and development

Submitted for publication to *Plant Cell*

Katja M. Schwager, Luz Irina A. Calderón Villalobos, Esther M.N. Dohmann, Stephan Knierer, Carola Kuhnle, and Claus Schwechheimer

- Initial knock out screens for *VFB1* - *VFB4* in the T-DNA collections of Burkhard Schulz and in the Wisconsin lines.
- Partial supervision of the Diploma thesis of Stephan Knierer, who initiated gene expression studies for the VFBs and conducted yeast two-hybrid experiments to find VFB interactors.
- Gene expression analysis of *vfb* mutants using Affymetrix GeneChips (Tables 1, 2 and Supplemental data Tables 1-4)

Chapter III.IV

The evolutionarily conserved TOUGH protein is required for proper development of *Arabidopsis thaliana*.

Published in *Plant Cell* (2005) 17(9):2473-85.

Luz Irina A. Calderón Villalobos, Carola Kuhnle, Esther M. N. Dohmann, Hanbing Li, Mike Bevan, and Claus Schwechheimer

- Yeast two-hybrid experiments dedicated to prove the interaction of TGH with the general transcription factor TATA-box binding protein (Figure 1E).

- Phenotypic analysis of *tgh* mutant plants (Figure 2C-H).
- Analysis of rescued *tgh* mutant plants expressing 35S:TGH:GFP and TGH:TGH:GFP (Supplemental Data).
- Examination of *TGH* expression in TGH:GUS transgenic plants as well as vascularization defects in *tgh1-1* mutant plants (Figure 4).
- Analysis of auxin-induced gene expression to elucidate the role of TGH in auxin response (Figure 5A-B and Figure 7).
- Investigation of the genetic interaction between *TGH* and *AMP1* through gene expression analysis and morphological examination (Figure 6).

Chapter III.V

LucTrap Vectors – a versatile tool for the analysis of transcriptional and translational luciferase fusions

Under revision in *Plant Physiology*

Luz Irina A. Calderón Villalobos, Carola Kuhnle, Hanbing Li, Mario Rosso, Bernd Weisshaar, and Claus Schwechheimer

- Evaluation of the auxin-induced *GH3-2* expression through RT-PCR analysis (Figure 1D-E).
- Analysis of around 400 LucTrap lines by ligation-mediated PCR followed by sequencing to determine the insertion sites of LucTrap2 lines (Table 1 or 2).

III. Publications

III.I. Schwechheimer C. and Calderón Villalobos L.I.A. , 2004
(review article)

Cullin-containing E3 ubiquitin ligases in plant development

Current Opinion in Plant Biology, 7,677-686.

(2004)



ELSEVIER

Cullin-containing E3 ubiquitin ligases in plant development

Claus Schwechheimer¹ and Luz Irina A Calderón Villalobos

In eukaryotes, the ubiquitin–proteasome system participates in the control of signal transduction events by selectively eliminating regulatory proteins. E3 ubiquitin ligases specifically bind degradation substrates and mediate their poly-ubiquitylation, a prerequisite for their degradation by the 26S proteasome. On the basis of the analysis of the *Arabidopsis* genome sequence, it is predicted that there are more than 1000 E3 ubiquitin ligases in plants. Several types of E3 ubiquitin ligases have already been characterized in eukaryotes. Recently, some of these E3 enzymes have been implicated in specific plant signaling pathways.

Addresses

Centre for Plant Molecular Biology, Developmental Genetics, Auf der Morgenstelle 5, 72076 Tübingen, Germany

¹e-mail: claus.schwechheimer@zmbp.uni-tuebingen.de

Current Opinion in Plant Biology 2004, 7:677–686

This review comes from a themed issue on

Cell biology

Edited by Martin Hülskamp and Yasunori Machida

Available online 27th September 2004

1369-5266/\$ – see front matter

© 2004 Elsevier Ltd. All rights reserved.

DOI 10.1016/j.pbi.2004.09.009

Abbreviations

ACS	1-aminocyclopropane-1-carboxylic acid synthase
APC/C	anaphase-promoting complex/cyclosome
BTB/POZ	Bric-a-Brac Tramtrack and Broad Complex/Pox virus and Zinc finger
CAND1	CULLIN-ASSOCIATED NEDDYLATION DISSOCIATED1
COP9	CONSTITUTIVELY PHOTOMORPHOGENIC9
CSN	COP9 signalosome
DCX	DDB1/cullin 4A/X-box
DDB1	DAMAGED DNA-BINDING PROTEIN1
DET1	DEETIOLATED1
E1	ubiquitin-activating enzyme
E2	ubiquitin-conjugating enzyme
E3	ubiquitin ligase
EBF	EIN3-BINDING F-BOX
EIN3	ETHYLENE INSENSITIVE3
EIL1	ETHYLENE INSENSITIVE3-LIKE1
eto2	<i>ethylene overproducer2</i>
GA	gibberellic acid
GAI	GIBBERELIC ACID INSENSITIVE
HY5	LONG HYPOCOTYL5
HYH	LONG HYPOCOTYL5-LIKE
LAF1	LONG AFTER FAR-RED LIGHT1
NEDD8/RUB1	NEURAL PRECURSOR CELL EXPRESSED, DEVELOPMENTALLY DOWNREGULATED 8/ RELATED TO UBIQUITIN1
phyA	phytochrome A
RBX1	RING-BOX1

RGA
SCF
SKP1
SLY1
SPA1

REPRESSOR OF *ga1-3*
SKP1/Cullin1/F-box protein
SUPPRESSOR OF KINETOCHORE PROTEIN1
SLEEPY1
SUPPRESSOR OF PHYTOCHROME A1

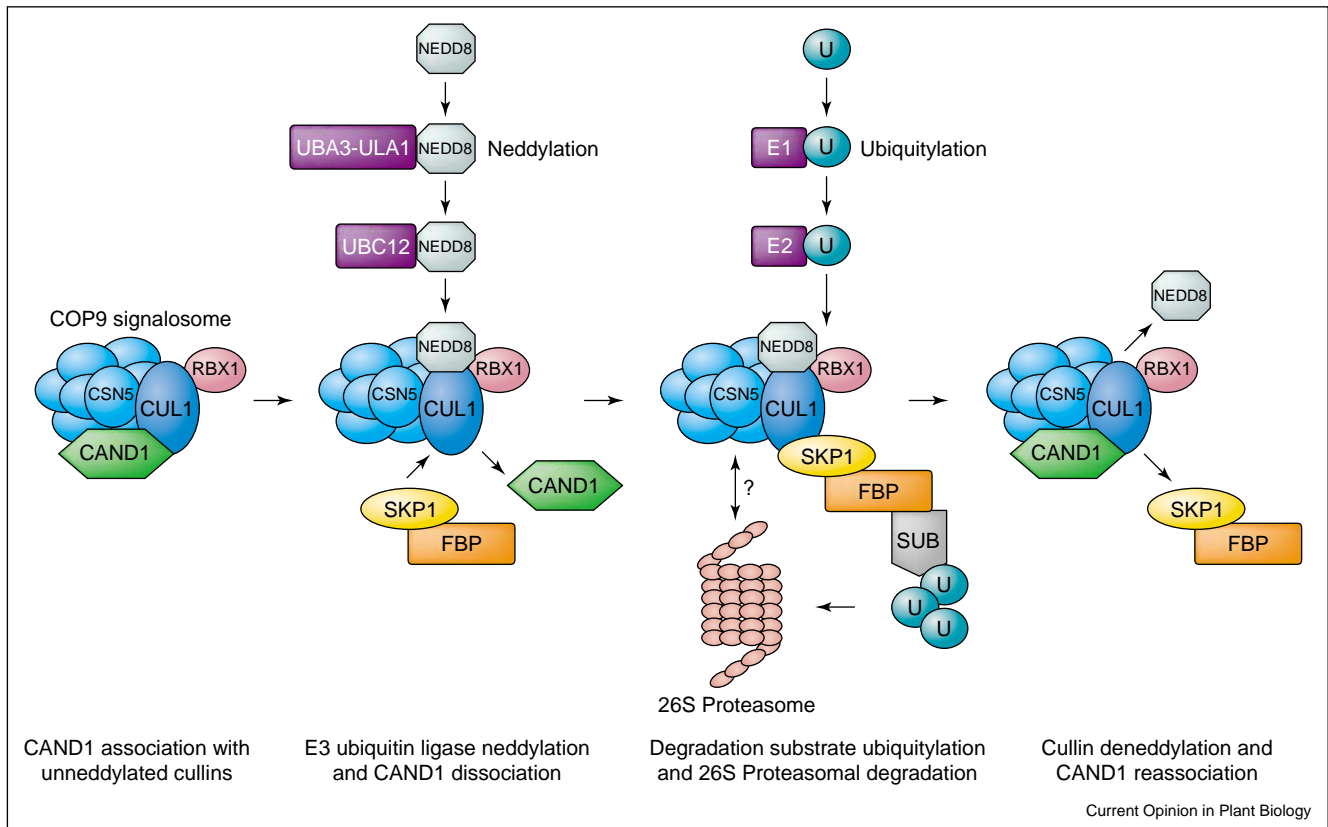
Introduction

The ubiquitin–proteasome-mediated degradation of regulatory proteins, such as transcription factors and cell-cycle regulators, plays an important role in controlling eukaryotic growth and development. The ubiquitin–proteasome system requires enzymatic activities for poly-ubiquitylation and for proteolysis of degradation substrates (Figure 1; [1]). The 2 MDa 26S proteasome is the proteolytic component of the ubiquitin–proteasome system. It consists of the proteolytic 20S core particle (CP), which is capped on either side by the 19S regulatory particle (RP) [2]. The 19S RP recognizes and unfolds poly-ubiquitylated proteolysis substrates before their degradation in the 20S CP. Poly-ubiquitylation of degradation targets is achieved by the consecutive activities of an E1 ubiquitin-activating enzyme, an E2 ubiquitin-conjugating enzyme and an E3 ubiquitin ligase. E1 and E2 enzymes serve to activate free ubiquitin for ubiquitylation at the same time as E3 enzymes promote ubiquitylation by mediating the interaction between E2 enzymes and the degradation substrate [3].

E3 ubiquitin ligases interact with specific degradation substrates and thereby confer specificity to the degradation process. To date, several evolutionary conserved multiprotein complexes with E3 activity have been identified (Figure 2). Four of these E3 complexes are composed of a specific member of the cullin protein family and the RING-domain protein RBX1. This E3 core complex can associate with a degradation substrate receptor subunit, either via a separate adaptor subunit or via an integral adaptor domain. This modular architecture allows the formation of a large array of substrate-specific E3 complexes through the association of distinct substrate receptor subunits with a given E3 core. The E3 anaphase-promoting complex/cyclosome (APC/C) also contains a cullin-related subunit (APC2) and a RBX1-related RING domain protein (APC11), indicating that there is an evolutionary relationship between APC/C and other E3 complexes.

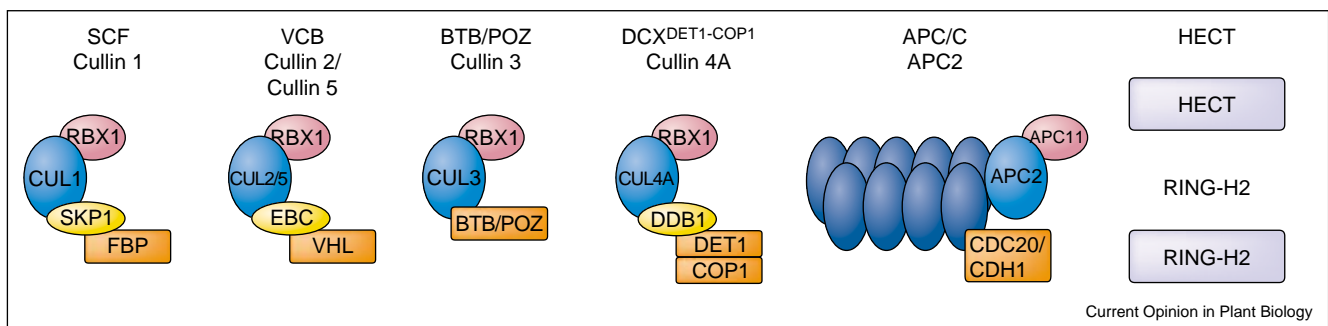
Protein degradation can be controlled at various levels. First, the most obvious level of control is the presence or absence of proteolysis components [4*]. Second, the accessibility of E3 enzymes to their substrates can be regulated by their compartmentalization [5]. Third, the

Figure 1



General overview of the eukaryotic ubiquitin–proteasome system. Proteolysis substrates (SUB) are recognized by E3 ubiquitin (U) ligases (E3), exemplified here by an SCF-type E3 complex. Poly-ubiquitylation of the bound substrate also requires the activities of E1 ubiquitin-activating enzymes (E1) and E2 ubiquitin-conjugating enzymes (E2). Following poly-ubiquitylation, substrates are degraded in the 26S proteasome [1,3]. The E3 subunit cullin can be modified by NEDD8 conjugation (neddylation) [12]. At the biochemical level, ubiquitylation and neddylation are highly related processes. Cullin neddylation results in the dissociation of the cullin-interacting protein CAND1 [13,14,15*]. This process may allow the cullin–RBX1 complex to associate with specificity components of the E3, such as SKP1–F-box protein (FBP) heterodimers. The COP9 signalosome (CSN) is associated with unneddylated and neddylated cullins [16,17]. Its CSN5 subunit mediates cullin deneddylation and may therefore play a role in controlling E3 complex formation [16–18]. There is some evidence that CSN interacts with subunits of the 26S proteasome [25,74].

Figure 2



Proteins and protein complexes that have reported E3 ubiquitin ligase activity. Many of these complexes share a common architecture. They are composed of a cullin subunit that associates with the RING-domain protein RBX1 and a receptor subunit. The E3 APC/C also contains a cullin-related subunit, APC2, and a RBX1-related RING-domain protein APC11. There is no evidence for a conservation of a VCB complex in plants.

binding between E3 enzymes and their substrate can be controlled by post-translational modifications such as phosphorylation, modification by prolyl hydroxylation or the addition of sugars [6–9]. Finally, de-ubiquitylation can re-stabilize poly-ubiquitylated targets that were already destined for degradation by the E1, E2, E3 system [10].

In this review, we highlight recent advances in understanding the role of neddylation in the ubiquitin-proteasome system. We then give an overview of the role of proteolysis in plant development by using selected examples from gibberellic acid (GA) response, ethylene response, and photomorphogenesis.

Neddylation, deneddylation and the COP9 signalosome

NEDD8/RUB1 (NEDD8) is an 8 kDa protein that is closely related to ubiquitin. Just like ubiquitin, NEDD8 can be conjugated to proteins (neddylation). Unlike ubiquitin, however, NEDD8 does not form chains and does not target proteins for degradation [11]. The proteins that mediate neddylation are closely related to the E1 and E2 enzymes of the ubiquitylation pathway [11]. Although it is anticipated that other proteins are also subject to NEDD8 modification, the cullin subunits of E3 ligases are the only neddylated proteins known to date [12]. Cullin neddylation is required for proper protein degradation, and neddylated as well as unneddylated or deneddylated cullins are found in eukaryotic protein extracts.

The role of neddylation in E3 ubiquitin ligase function and protein degradation was enigmatic for a long time. The recent discovery of the CULLIN-ASSOCIATED NEDDYLATION DISSOCIATED1 (CAND1) protein suggests, however, that neddylation is required for proper assembly of the E3 complex ([13,14,15[•]]; Figure 1). CAND1 associates specifically with unneddylated cullins, and CAND1 dissociates from the cullins after NEDD8 conjugation. In the case of SCF-type E3 enzymes, cullin neddylation and CAND1 dissociation are followed by the association of a SKP1–F-box protein heterodimer (Figure 1). As the F-box proteins are interchangeable substrate receptor subunits within SCF-type E3 enzymes, neddylation might permit the formation of substrate-specific E3 complexes.

Deneddylation is a biochemical activity of subunit 5 (CSN5) of the CONSTITUTIVELY PHOTOMORPHOGENIC9 (COP9) signalosome (CSN) ([16–18]; Figure 1). CSN is an evolutionary conserved multiprotein complex that shares significant homologies with the lid substructure of the 26S proteasome [19–22]. CSN physically interacts with E3 enzymes that contain cullin and is required for substrate degradation [16,17,23^{••}]. Although the role of CSN in degradation is unclear, two functions have been proposed for CSN. First, it might function as

an assembly platform for cullin-containing E3 enzymes [24]. Second, CSN might be part of an alternative proteasome, and its direct association with E3 enzymes could serve to facilitate or accelerate the degradation of ubiquitylated targets [17,25].

The ubiquitin–proteasome system in plant development

Analysis of the *Arabidopsis* genome sequence has revealed that the ubiquitin–proteasome system is conserved in plants [26^{••},27]. Interestingly, some E3 families seem to have expanded significantly during plant evolution. The *Arabidopsis* genome encodes more than 500 RING-domain proteins and almost 700 F-box proteins [28,29]. As RING-domain proteins are characterized predominantly and F-box proteins exclusively as E3 enzymes or as E3 subunits, these findings imply that plants could contain over a thousand E3 enzymes that have distinct substrate specificities.

Many mutants that are impaired in general and specific components of the ubiquitin–proteasome system have been characterized to date. These findings indicate that ubiquitin–proteasome-mediated proteolysis plays a role in almost every aspect of plant development (Table 1). However, the number of known proteolysis-dependent processes is still relatively small when compared with the large number of E3 enzymes estimated for *Arabidopsis*. In the past year, considerable progress has been achieved in understanding the role of protein degradation in GA response, ethylene response, and photomorphogenesis.

GA-induced degradation of RGA and GAI is mediated by SCF^{SLY1}

The phytohormone GA controls specific events during plant growth, such as germination, stem elongation, and the onset of flowering. In the absence of GA, the elongation growth of hypocotyls and stems in the wildtype is repressed by REPRESSOR OF *ga1-3* (RGA) and GIBBERELIC ACID INSENSITIVE (GAI), two members of the DELLA protein family [30–35]. Consequently, loss-of-function mutants of *RGA* and *GAI* are taller than wildtype plants [33,34]. Furthermore, loss of *RGA* or *GAI* function can partially suppress the severe dwarfism observed in the GA biosynthesis mutant *ga1-3* [33,34]. Conversely, gain-of-function mutants of the *GAI* gene are severely dwarfed [36,37].

An explanation for the genetics of *RGA* and *GAI* was provided by the finding that *RGA* and *GAI* are degraded in response to GA by the 26S proteasome ([30,38,39, 40^{••},41^{••}]; Figure 3a). In the GA-biosynthesis mutant *ga1-3*, the destabilizing GA signal is absent and both *RGA* and *GAI* can accumulate [40^{••}]. Therefore, the dwarfism of the *ga1-3* mutant can be explained by the accumulation of the *RGA* and *GAI* growth repressors. *RGA*- and *GAI*-controlled repression of elongation

Table 1

Summary of proteolysis components with known biological function.

E3 specificity component	Biochemical function	Pathway	Proteolysis substrate	Biochemical function	Reference(s)
PRT1	RING-domain protein		N-end rule substrates		[75]
AFP		Abscisic acid	ABI5	Transcription factor	[76]
TIR1	F-box protein	Auxin	AUX/IAAs	Transcription repressors	[77–79]
SINAT5	RING-domain protein	Auxin	NAC1	Putative transcription factor	[80]
		Auxin transport	EIR1/PIN2	Putative auxin efflux carrier	[81]
		Brassinosteroid	BZR1/BZR2		[82]
SKP2	F-box protein	Cell cycle	E2Fc	Transcription factor	[83]
APC/C	APC/C	Cell cycle	Cyclin B1, Cyclin A3	Cyclin	[84]
APC/C	APC/C	Cell cycle	CDC6		[85]
		Cell cycle	ICK1	Cell-cycle inhibitor	[86]
		Circadian rhythm	CO	Transcription factor	[87]
		Circadian rhythm	ZTL	F-box protein	[4*,88]
FKF	F-box protein	Circadian rhythm			[89]
ZTL	F-box protein	Circadian rhythm	TOC1		[4*,88,90]
AtCHIP	U-box protein	Denatured proteins			[91]
EBF1, EBF2	F-box protein	Ethylene	EIN3	Transcription factor	[50**–53**]
ETO1	BTB/POZ-domain protein	Ethylene	ACS5, ACS9	Biosynthetic enzyme	[56**]
UFO	F-box protein	Floral development			[92,93]
SLY1	F-box protein	Gibberellic acid	GAI, RGA	Putative transcription factors	[38,39,40**,41**,43]
COI1	F-box protein	Jasmonic acid			[94]
SON1	F-box protein	Pathogen response	NIM1		[95]
COP1	RING-domain protein	Photomorphogenesis	HY5, HYH, LAF1, phyA	Transcription factors, photoreceptor	[63–65,70,71]
DET1		Photomorphogenesis	HY5, HYH	Transcription factor	[63,64]
EID1	F-box protein	Photomorphogenesis			[96]
AFR1	F-box protein	Photomorphogenesis			[97]
ORE9/MAX2	F-box protein	Shoot branching/senescence			[98,99]
UPL3/KAK	HECT-domain protein	Trichome development			[100,101]
CER3	RING-domain protein	Wax biosynthesis			[102]

ABI, ABSCISIC ACID INSENSITIVE; AFP, ABI FIVE INTERACTING PROTEIN; AFR, ATTENUATED FAR-RED RESPONSE; AtCHIP, *ARABIDOPSIS THALIANA* Hsc70-INTERACTING PROTEIN; AUX/IAA, AUXIN/INDOLEACETIC ACID; BZR, BRASSINAZOLE RESISTANT; CDC, CELL DIVISION CYCLE; CER, ECERIFERUM; CO, CONSTANS; COI, CORONATINE INSENSITIVE; EID, EMPFINDLICHER IM DUNKELROTEN LICHT; EIR, ETHYLENE INSENSITIVE ROOT; FKF, FLAVIN-BINDING/KELCH-REPEAT/F-BOX; ICK, INHIBITOR OF CYCLIN-DEPENDENT KINASE; KAK, KAKTUS; MAX, MORE AXILLIARY GROWTH; NAC, NO-APICAL-MERISTEM/CUP-SHAPED COTYLEDON; NIM, NON-INDUCIBLE IMMUNITY; ORE, ORESARA; PIN, PINFORM; PRT, PROTEOLYSIS; SINAT, SEVEN-IN-ABSENTIA OF *ARABIDOPSIS THALIANA*; SON, SUPPRESSOR OF *nim1-1*; TIR, TRANSPORT INHIBITOR RESISTANT; TOC, TIMING OF CAB EXPRESSION; UFO, UNUSUAL FLORAL ORGANS; UPL, UBIQUITIN PROTEIN LIGASE; ZTL, ZEITLUPE.

growth is genetically suppressed in the loss-of-function mutants of *RGA* and *GAI*. This suppression results in increased elongation growth of the *rga gai* loss-of-function mutant in otherwise wildtype or *gai-3* mutant plants [33,34]. The *gai* protein that is expressed in the *gai* gain-of-function mutant is resistant to GA-induced proteolysis, and the resulting accumulation of GAI repressor provides a molecular cause for the dwarfism of this mutant [41**].

Arabidopsis sleepy1 (sly1) and rice *gid2* mutants are GA-insensitive dwarf mutants. *SLY1* and *GID2* have been found to encode orthologous F-box proteins, that is, the substrate receptor subunits of SCF-type E3 ubiquitin ligases [40**,41**,42,43,44**,45]. DELLA proteins directly interact with *SLY1* and accumulate in *sly1* and *gid2* mutants, indicating that DELLA proteins are direct degradation targets for *SLY1* and *GID2*. Furthermore, DELLA proteins accumulate in a phosphorylated form in

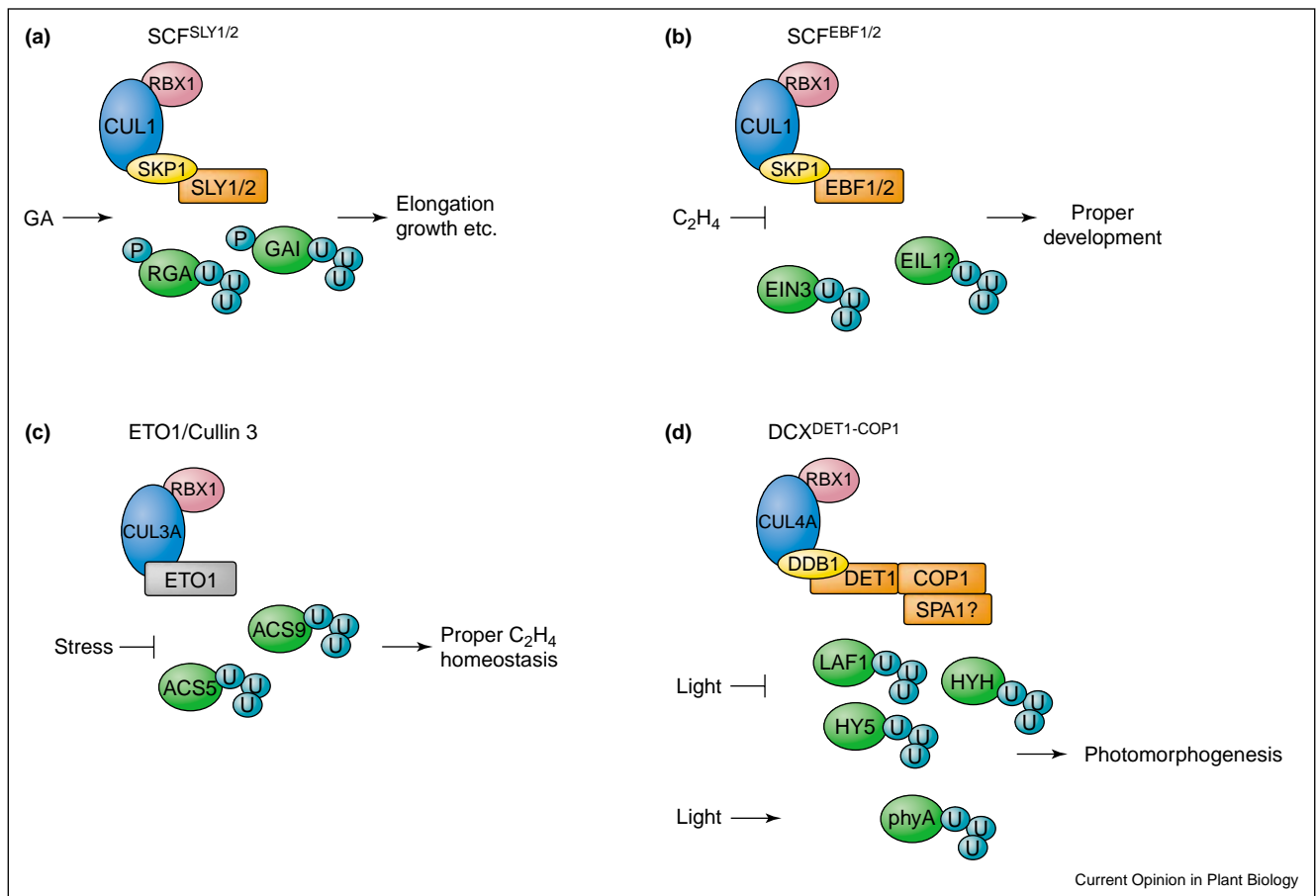
these mutants, opening the possibility that phosphorylation precedes the degradation of the DELLA protein [40**,41**,43].

The recent cloning of *gar2-1* is an interesting development [40**,41**,46]. *gar2-1* is a dominant allele of *SLY1* with a point mutation in the protein–protein interaction domain of *SLY1*. The resulting mutant *SLY1* protein has increased affinity for RGA and GAI protein. Consequently, the *gar2-1* mutant might have increased GAI and RGA protein turnover; a hypothesis that is supported by several genetic interaction studies.

Ethylene response is regulated by SCF-dependent degradation of the transcription factor EIN3

The gaseous phytohormone ethylene is involved in proper seedling development, cell elongation, pathogen response, senescence and fruit ripening [47]. Ethylene-

Figure 3



(a) The SCF^{SLY1/2} E3 ubiquitin ligase mediates the degradation of the putative transcription factors RGA and GAI in response to gibberellic acid (GA) [40**,41**,43,45]. Mutants that are deficient in RGA and GAI degradation accumulate phosphorylated forms of RGA and GAI. Therefore, phosphorylation might precede degradation. SLY2, a close homolog of SLY1, also participates in mediating GAI and RGA degradation. **(b)** The SCF^{EBF1/2} mediates the degradation of EIN3 and possibly that of the related EIL1 [51**,53**]. In the presence of ethylene (C₂H₄), EIN3 is stabilized. **(c)** The BTB/POZ domain-containing ETO1 protein is part of a CULLIN3-containing E3 complex that regulates the abundance of the ethylene biosynthetic enzymes ACS5 and ACS9 [55,56**]. **(d)** In plants, COP1, DET1, and DDB1 mediate the degradation of HY5, HYH, and LAF1 in the dark [63,64,67,70]. Furthermore, COP1 mediates the light-induced degradation of phyA [71]. The human orthologs of COP1, DET1, and DDB1 are part of a CULLIN4A-containing E3 complex, DCX^{hDET1-hCOP1} [23**]. It has been hypothesized that an orthologous DCX^{hDET1-hCOP1} regulates the degradation of the COP1 targets in plants. However, the existence of such a complex has not been demonstrated as yet. The ubiquitylation of E3 substrates, as shown in this figure, has not been experimentally proven for each individual degradation substrate.

treated dark-grown seedlings react with the so-called triple response, which is characterized by the inhibition of root elongation, shortening and swelling of the hypocotyl, and exaggeration of apical hook curvature. ETHYLENE INSENSITIVE3 (EIN3) is a transcription factor that regulates the expression of downstream genes of the ethylene response pathway [48,49]. Mutants that are defective in EIN3 function do not exhibit the triple response after ethylene treatment. Conversely, the overexpression of EIN3 or that of its closest homolog EIL1 produces a constitutive triple-response phenotype [49]. These results indicate that the intensity of the triple-response phenotype correlates with EIN3 or EIL1 accumulation.

The finding that EIN3 protein accumulates after treatment with ethylene as well as after treatment with 26S proteasome inhibitors gave a primary indication of a role for protein degradation in ethylene response [50**]. In a two-hybrid screen, EIN3 and its homolog EIL1 were found to interact with an F-box protein, subsequently termed EIN3-BINDING F-BOX (EBF1) ([51**–53**]; Figure 3b). Consistent with the postulated role for EBF1 in EIN3 degradation, the *ebf1* loss-of-function mutant displays a mild constitutive triple-response phenotype. Furthermore, loss of *EBF1* and the closest *EBF1* homolog *EBF2* causes a strong constitutive triple-response phenotype that resembles that of transgenic lines that overexpress EIN3. Consistent with the genetic data,

EIN3 protein levels are elevated in *ebf1 ebf2* double mutants. The phenotype of the *ebf1 ebf2* double mutant is only partially suppressed when EIN3 function is missing, indicating that these F-box proteins may also target other proteins, such as EIL1, for degradation.

Interestingly, EBF1 and EBF2 seem to associate with unmodified EIN3 [51^{••}–53^{••}]. Multiple protein kinases have been placed upstream of EIN3 in the ethylene-signaling pathway [47]. It is therefore possible that EIN3 phosphorylation prevents its association with EBF1 and EBF2, resulting in EIN3 stabilization.

A CULLIN3-containing E3 ubiquitin ligase controls ethylene hormone synthesis

Protein degradation has also been implicated in ethylene biosynthesis. Two *Arabidopsis* mutants that have gain-of-function mutations in two genes encoding 1-aminocyclopropane-1-carboxylic acid (ACS) synthase proteins, *ethylene overproducer2* (*eto2*; which has mutated ACS5) and *eto3* (which has mutated ACS9), show exaggerated ethylene responses that are caused by increased ethylene production [54,55]. Similar phenotypes have been reported for the recessive *eto1* mutant, which affects a gene that encodes a member of the BTB/POZ protein family [55,56^{••}]. The recent characterization of a new type of E3 enzyme that contains CULLIN3 and BTB/POZ domain proteins suggested that ETO1 may be part of an E3 complex in plants ([57]; Figure 2). Indeed, the ETO1 BTB/POZ adaptor domain interacts with *Arabidopsis* CULLIN3A ([56^{••}]; Figure 3c). This raised the hypothesis that ETO1 could regulate the stability of ACS5 and ACS9. Consistent with this hypothesis, ETO1 was found to interact with ACS5 *in vitro* and *in vivo*, and ACS5 protein was found to accumulate in the *eto1* mutant [55,56^{••}]. Conversely, overexpression of ETO1 reduced ACS5 protein levels and enzymatic activity [56^{••}].

As *eto1*, *eto2*, and *eto3* mutants have similar phenotypes, it was speculated that the *eto2* and *eto3* gain-of-function mutants might express stabilized variants of ACS5 and ACS9 [56^{••}]. In fact, posttranslational control of ACS protein turnover by phosphorylation and dephosphorylation had already been postulated for tomato ACS [58]. Subsequently, the *eto2* mutant was found to have a frame-shift mutation that prevents the resulting truncated ACS5 protein from interacting with ETO1 [54,56^{••}]. Mutant ACS9 protein in the *eto3* mutant is characterized by a single amino-acid exchange from valine to aspartate at position 457 [55]. This mutation is located near a serine residue that had been reported to be a target of a calcium-dependent protein kinase in *LeACS2* and *LeACS3* [59]. The ACS9 protein produced in the *eto3* mutant might therefore be a phosphorylation mimic mutant of ACS9 that fails to interact with ETO1.

The photomorphogenesis regulators COP1 and DET1 may be part of a CULLIN4-containing E3

The bZIP transcription factors LONG HYPOCOTYL5 (HY5) and LONG HYPOCOTYL5-LIKE (HYH) are positive regulators of photomorphogenic development and activate the expression of several light-regulated genes [9,60–63]. The developmental switch from skotomorphogenic growth of the dark-grown etiolated *Arabidopsis* seedling to photomorphogenic growth of the light-grown de-etiolated seedling is accompanied by HY5 and HYH accumulation [63,64]. Although HY5 and HYH transcription occurs in the dark as well as in the light, HY5 and HYH proteins that are produced in the dark are constitutively degraded by the ubiquitin–proteasome system.

Loss of HY5 and HYH function results in seedlings that have elongated hypocotyls in the light, a phenotype that can be interpreted as the result of incomplete de-etiolation [63,64]. Conversely, mutants that fail to degrade HY5 and HYH de-etiolate even in the dark. Degradation of HY5 and HYH in the dark requires COP1 function [63,64]. COP1 has a RING-domain, a coiled-coil domain and WD40 repeats. On the basis of the fact that HY5 degradation is blocked in dark-grown *cop1* mutant seedlings, it was thought for a long time that COP1 might act as a RING-domain E3 enzyme for HY5 degradation ([64]; Figure 3d). In support of this hypothesis, HY5 was found to interact physically with the WD40 repeat domain of COP1; however, it was only recently that COP1's E3 activity on the HY5 substrate could be demonstrated *in vitro* [63–65].

HY5 degradation in the dark also requires the activity of DEETIOLATED1 (DET1) [64,66]. As DET1 was devoid of any recognizable functional domains, the link between DET1 and HY5 as well as that between DET1 and COP1 had remained mysterious for a long time. Interestingly, the biochemical purification of DET1 from plant extracts indicated that DET1 interacts with a protein that in humans is known as DAMAGED DNA-BINDING PROTEIN1 (DDB1) [67]. The biochemical interaction between DET1 and DDB1 is supported by the synergistic genetic interaction between *Arabidopsis* *ddb1* and *det1* mutants. The full impact of this interaction only became clear when the human orthologs of COP1, DET1, and DDB1 were found to be subunits of a novel E3 complex, designated DCX^{hDET1hCOP1}, that also contains CULLIN4A and RBX1 [68^{••},69^{••}]. On the basis of these results, it is now expected that an orthologous DCX^{DET1COP1} complex mediates the degradation of HY5 and HYH in plants (Figure 3d). With regard to the postulated DCX^{DET1COP1} E3 complex, it is surprising that recombinant monomeric COP1 can function as an E3 enzyme *in vitro*. Therefore, whether or not COP1 requires the DCX^{DET1COP1} complex to exert proper E3 activity *in vivo* needs to be reassessed [65].

In addition to HY5 and HYH, the MYB transcription factor LONG AFTER FAR-RED LIGHT1 (LAF1) and the far-red light receptor phytochrome A (phyA) have been reported to require COP1 function for their proper degradation [70,71]. LAF1 degradation may require the activity of SUPPRESSOR OF PHYTOCHROME A1 (SPA1) in addition to COP1 [70,72]. SPA1 can interact with COP1 *in vitro* and *in vivo*, and both proteins share a high degree of sequence homology in their WD40 repeat domains [72,73]. This invites the hypothesis that SPA1 and COP1 might control partially overlapping processes. Indeed, the coiled-coil domain of SPA1 was found to stimulate the ubiquitylation activity of COP1 on its LAF1 substrate when COP1 is present at low concentrations [70]. Although the effect of SPA1 on COP1-mediated ubiquitylation and degradation could explain the physiological observations, these data are somewhat controversial because experiments with full-length SPA1 fail to detect a significant influence of SPA1 on the ubiquitylation activity of COP1 [65].

When light is perceived by the (etiolated) seedling, HY5 and HYH degradation is turned off and these proteins accumulate readily [63,64]. Two regulatory mechanisms have been proposed that might control this switch. First, HY5 was found to be phosphorylated by a casein kinase II in a region of the protein that is essential for HY5 and HYH interaction with COP1 [9]. Second, COP1 is excluded from the nucleus after light perception, thus preventing its interaction with cognate nuclear substrates by differential compartmentalization [5]. HY5 phosphorylation occurs rapidly after light perception, whereas exclusion of COP1 from the nucleus is relatively slow. COP1 redistribution is therefore not sufficient to explain the immediate accumulation of HY5. It could, however, be envisioned that phosphorylation and COP1 redistribution are two complementary mechanisms that are both required to prevent HY5 (and HYH) degradation.

Conclusions

Several E3 ubiquitin ligase complexes have been implicated in a variety of plant signaling pathways. However, the number of proteolysis components that are understood at the biological level is still relatively small when compared to the postulated number of E3 complexes and E3-controlled pathways in plants. Besides the limited data that are currently available on proteolysis-controlled pathways in plants, information on the upstream regulators that induce protein degradation is even more limited. Therefore, besides identifying more and more proteolysis-dependent signaling pathways, future research should be actively committed to identifying the components that control proteolysis.

Acknowledgements

We would like to thank D Weijers for his insightful comments on this review. Research in our laboratory is supported by the Deutsche

Forschungsgemeinschaft and the Centre for Plant Molecular Biology at Tübingen University.

References and recommended reading

Papers of particular interest, published within the annual period of review, have been highlighted as:

- of special interest
- of outstanding interest

1. Hershko A, Ciechanover A: **The ubiquitin system.** *Annu Rev Biochem* 1998, **67**:425-479.
2. Baumeister W, Walz J, Zühl F, Seemüller E: **The proteasome: paradigm of a self-compartmentalizing protease.** *Cell* 1998, **92**:367-380.
3. Deshaies RJ: **SCF and Cullin/RING H2-based ubiquitin ligases.** *Annu Rev Cell Dev Biol* 1999, **15**:435-467.
4. Kim W-Y, Geng R, Somers DE: **Circadian phase-specific degradation of the F-box protein ZTL is mediated by the proteasome.** *Proc Natl Acad Sci USA* 2003, **100**:4933-4938.
5. von Arnim AG, Deng X-W: **Light inactivation of *Arabidopsis* photomorphogenic repressor COP1 involves a cell-specific regulation of its nucleocytoplasmic partitioning.** *Cell* 1994, **79**:1035-1045.
6. Yoshida Y, Chiba T, Tokunaga F, Kawasaki H, Iwai K, Suzuki T, Ito Y, Matsuoka K, Yoshida M, Tanaka K *et al.*: **E3 ubiquitin ligase that recognizes sugar chains.** *Nature* 2002, **418**:438-442.
7. Chung KKK, Thomas B, Li X, Pletnikova O, Troncoso JC, Marsh L, Dawson VL, Dawson TM: **S-nitrosylation of parkin regulates ubiquitination and compromises parkin's protective function.** *Science* 2004, **304**:1328-1331.
8. Jaakkola P, Mole DR, Tian Y-M, Wilson MI, Gielbert J, Gaskell SJ, von Kriegsheim A, Hebestreit HF, Mukheri M, Schofield CJ *et al.*: **Targeting of HIF- α to the von Hippel-Lindau ubiquitylation complex by O₂-regulated prolyl hydroxylation.** *Science* 2001, **292**:468-472.
9. Hardtke CS, Gohda K, Osterlund MT, Oyama T, Okada K, Deng XW: **HY5 stability and activity in *Arabidopsis* is regulated by phosphorylation in its COP1 binding domain.** *EMBO J* 2000, **19**:4997-5006.
10. Wilkinson KD, Hochstrasser M: **The deubiquitinating enzymes.** In *Ubiquitin and the Biology of the Cell*. Edited by Peters J-M, Harris JR, Finley D. New York: Plenum Press; 1998:99-126.
11. Hochstrasser M: **Biochemistry. All in the ubiquitin family.** *Science* 2000, **289**:563-564.
12. Hori T, Osaka F, Chiba T, Miyamoto C, Okabayashi K, Shimbara N, Kato S, Tanaka K: **Covalent modification of all members of human cullin family proteins by NEDD8.** *Oncogene* 1999, **18**:6829-6834.
13. Liu J, Furukawa M, Matsumoto T, Xiong Y: **NEDD8 modification of CUL1 dissociates p120^{Cand1}, an inhibitor of CUL1-SKP1 binding and SCF ligases.** *Mol Cell* 2002, **10**:1511-1518.
14. Zheng J, Yang X, Harrell JM, Ryzhikov S, Shim E-H, Lykke-Andersen K, Wei N, Sun H, Kobayashi R, Zhang H: **CAND1 binds to unneddylated CUL1 and regulates the formation of SCF ubiquitin E3 ligase complex.** *Mol Cell* 2002, **10**:1519-1526.
15. Min K-W, Hwang J-W, Lee J-S, Park Y, Tamura T-A, Yoon J-B: **TIP120A associates with cullins and modulates ubiquitin ligase activity.** *J Biol Chem* 2003, **278**:15905-15910.
16. Lyapina S, Cope G, Shevchenko A, Serino G, Zhou C, Wolf DA, Wei N, Shevchenko A, Deshaies RJ: **COP9 signalosome promotes cleavage of NEDD8-CUL1 conjugates.** *Science* 2001, **292**:1382-1385.
17. Schwechheimer C, Serino G, Callis J, Crosby WL, Lyapina S, Deshaies RJ, Gray WM, Estelle M, Deng X-W: **Interactions of the**

- COP9 signalosome with the E3 ubiquitin ligase SCF^{TIR1} in mediating auxin response.** *Science* 2001, **292**:1379-1382.
18. Cope GA, Suh GSB, Aravind L, Schwarz SE, Zipursky SL, Koonin EV, Deshaies RJ: **Role for predicted metalloprotease motif of JAB1/Csn5 in cleavage of NEDD8 from CUL1.** *Science* 2002, **298**:608-611.
 19. Glickman MH, Rubin DM, Coux O, Wefes I, Pfeifer G, Cjeka Z, Baumeister W, Fried VA, Finley D: **A subcomplex of the proteasome regulatory particle required for ubiquitin-conjugate degradation and related to the COP9-signalosome and eIF3.** *Cell* 1998, **94**:615-623.
 20. Schwechheimer C, Deng X-W: **COP9 signalosome revisited: a novel mediator of protein degradation.** *Trends Cell Biol* 2001, **11**:420-426.
 21. Wei N, Deng XW: **The COP9 signalosome.** *Annu Rev Cell Dev Biol* 2003, **19**:261-286.
 22. Wei N, Chamovitz DA, Deng X-W: **Arabidopsis COP9 is a component of a novel signaling complex mediating light control of development.** *Cell* 1994, **78**:117-124.
 23. Groisman R, Polanowska J, Kuraoka I, Sawada J-I, Sijao M, Tanaka K, Nakatani Y: **The ubiquitin ligase activity in the DDB2 and CSA complexes is differentially regulated by the COP9 signalosome in response to DNA damage.** *Cell* 2003, **113**:357-367.
- This report describes, for the first time, an E3 enzyme that contains CULLIN4 and its association with the COP9 signalosome.
24. Wolf DA, Zhou C, Wee S: **The COP9 signalosome: an assembly and maintenance platform for cullin ubiquitin ligases?** *Nat Cell Biol* 2003, **5**:1029-1033.
 25. Peng Z, Shen Y, Feng S, Wang X, Chittetei BN, Vierstra RD, Deng XW: **Evidence for a physical association of the COP9 signalosome, the proteasome, and specific SCF E3 ligases in vivo.** *Curr Biol* 2003, **13**:R504-R505.
 26. Smalle J, Vierstra R: **The ubiquitin 26S proteasome proteolytic pathway.** *Annu Rev Plant Physiol Plant Mol Biol* 2004, **55**:555-590.
- A comprehensive review of the plant ubiquitin-proteasome system.
27. Bachmair A, Novatchkova M, Potuschak T, Eisenhaber F: **Ubiquitylation in plants: a post-genomic look at a post-translational modification.** *Trends Plant Sci* 2001, **6**:463-470.
 28. Kosarev P, Mayer KFX, Hardtke CS: **Evaluation and classification of RING-finger domains encoded by the Arabidopsis genome.** *Genome Biol* 2002, **3**:0016.0011-0016.0012.
 29. Gagne JM, Downes BP, Shiu SH, Durski AM, Vierstra RD: **The F-box subunit of the SCF E3 complex is encoded by a diverse superfamily of genes in Arabidopsis.** *Proc Natl Acad Sci USA* 2002, **99**:11519-11524.
 30. Richards DE, King KE, Ait-ali T, Harberd NP: **How gibberellin regulates plant growth and development: a molecular genetic analysis of gibberellin signaling.** *Annu Rev Plant Physiol Plant Mol Biol* 2001, **52**:67-88.
 31. Silverstone AL, Mak PYA, Martinez EC, Sun T-p: **The new RGA locus encodes a negative regulator of gibberellin response in Arabidopsis thaliana.** *Genetics* 1997, **146**:1087-1099.
 32. Yu H, Ito T, Zhao Y, Peng J, Kumar P, Meyerowitz EM: **Floral homeotic genes are targets of gibberellin signaling in flower development.** *Proc Natl Acad Sci USA* 2004, **101**:7827-7832.
 33. King KE, Moritz T, Harberd NP: **Gibberellins are not required for normal stem growth in Arabidopsis thaliana in the absence of GAI and RGA.** *Genetics* 2001, **159**:767-776.
 34. Dill A, Sun T-p: **Synergistic derepression of gibberellin signaling by removing RGA and GAI function in Arabidopsis thaliana.** *Genetics* 2001, **159**:777-785.
 35. Lee S, Cheng H, King KE, Wang W, He Y, Hussain A, Lo J, Harberd NP, Peng J: **Gibberellin regulates Arabidopsis seed germination via RGL2, a GAI/RGA-like gene whose expression is up-regulated following imbibition.** *Genes Dev* 2002, **16**:646-658.
 36. Peng J, Carol P, Richards DE, King KE, Cowling RJ, Murphy GP, Harberd NP: **The Arabidopsis GAI gene defines a signaling pathway that negatively regulates gibberellin responses.** *Genes Dev* 1997, **11**:3194-3205.
 37. Peng J, Richards DE, Hartley NM, Murphy GP, Devos KM, Flinham JE, Beales J, Fish L, Worland AJ, Pelica F et al.: **'Green revolution' genes encode mutant gibberellin response modulators.** *Nature* 1999, **400**:256-261.
 38. Dill A, Jung H-S, Sun T-p: **The DELLA motif is essential for gibberellin-induced degradation of RGA.** *Proc Natl Acad Sci USA* 2001, **98**:14162-14167.
 39. Silverstone AL, Jung H-S, Dill A, Kawaide H, Kamiya Y, Sun T-p: **Repressing a repressor: gibberellin-induced rapid reduction of the RGA protein in Arabidopsis.** *Plant Cell* 2001, **13**:1555-1565.
 40. Dill A, Thomas SG, Hu J, Steber CM, Sun T-p: **The Arabidopsis F-box protein SLEEPY1 targets gibberellin signaling repressors for gibberellin-induced degradation.** *Plant Cell* 2004, **16**:1392-1405.
- See annotation [41**].
41. Fu X, Richards DE, Fleck B, Xie D, Burton N, Harberd NP: **The Arabidopsis mutant sleepy1^{gar2-1} protein promotes plant growth by increasing the affinity of the SCF^{Sly1} E3 ubiquitin ligase for DELLA protein substrates.** *Plant Cell* 2004, **16**:1406-1418.
- These two largely complementary reports [40**,41**] describe the gain-of-function SLY1 allele *gar2-1*, a mutant with increased RGA and GAI turnover.
42. Steber CM, Cooney SE, McCourt P: **Isolation of the GA-response mutant *sly1* as a suppressor of ABI1-1 in Arabidopsis thaliana.** *Genetics* 1998, **149**:509-521.
 43. McGinnis KM, Thomas SG, Soule JD, Strader LC, Zale JM, Sun T-p, Steber CM: **The Arabidopsis SLEEPY1 gene encodes a putative F-box subunit of an SCF E3 ubiquitin ligase.** *Plant Cell* 2003, **15**:1120-1130.
 44. Sasaki A, Itoh H, Gomi K, Ueguchi-Tanaka M, Ishiyama K, Kobayashi M, Jeong D-H, An G, Kitano H, Ashikari M et al.: **Accumulation of phosphorylated repressor for gibberellin signaling in an F-box mutant.** *Science* 2003, **299**:1896-1898.
- The first report of the SLY1 ortholog from rice. The authors provide the first evidence that phosphorylation might precede DELLA protein degradation.
45. Gomi K, Sasaki A, Itoh H, Ueguchi-Tanaka M, Ashikari M, Kitano H, Matsuoka M: **GID2, an F-box subunit of the SCF E3 complex, specifically interacts with phosphorylated SLR1 protein and regulates the gibberellin-dependent degradation of SLR1 in rice.** *Plant J* 2004, **37**:626-634.
 46. Wilson RN, Somerville CR: **Phenotypic suppression of the gibberellin-insensitive mutant (*gai*) of Arabidopsis.** *Plant Physiol* 1995, **108**:495-502.
 47. Guo H, Ecker JR: **The ethylene signaling pathway: new insights.** *Curr Opin Plant Biol* 2004, **7**:40-49.
 48. Solano R, Stepanova A, Chao Q, Ecker JR: **Nuclear events in ethylene signaling: a transcriptional cascade mediated by ETHYLENE-INSENSITIVE3 and ETHYLENE-RESPONSE-FACTOR1.** *Genes Dev* 1998, **12**:3703-3714.
 49. Chao Q, Rothenberg M, Solano R, Roman G, Terzaghi W, Ecker JR: **Activation of the ethylene gas response pathway in Arabidopsis by the nuclear proteins ETHYLENE-INSENSITIVE3 and related genes.** *Cell* 1997, **89**:1133-1144.
 50. Yanagisawa S, Yoo S-D, Sheen J: **Differential regulation of EIN3 stability by glucose and ethylene signalling in plants.** *Nature* 2003, **425**:521-525.
- First evidence of EIN3 degradation by the 26S proteasome.
51. Potuschak T, Lechner E, Parmentier Y, Yanagisawa S, Grava S, Koncz C, Genschik P: **EIN3-dependent regulation of plant ethylene hormone signaling by two Arabidopsis F-box proteins: EBF1 and EBF2.** *Cell* 2003, **115**:679-689.
- See annotation [53**].

52. Gagne JM, Smalle J, Gingerich DJ, Walker JM, Yoo S-D,
 ● Yanagisawa S, Vierstra R: **Arabidopsis EIN3-binding F-box 1 and 2 form ubiquitin-protein ligases that repress ethylene action and promote growth by directing EIN3 degradation.** *Proc Natl Acad Sci USA* 2004, **101**:6803-6808.
 See annotation [53**].
53. Guo H, Ecker JR: **Plant responses to ethylene gas are mediated by SCF(EBF1/EBF2)-dependent proteolysis of EIN3 transcription factor.** *Cell* 2003, **115**:667-677.
 These three reports [51**–53**] describe the independent isolation of EBF1 and EBF2 as cognate E3 ubiquitin ligases of EIN3.
54. Vogel JP, Woeste KE, Theologis A, Kieber JJ: **Recessive and dominant mutations in the ethylene biosynthetic gene ACS5 of Arabidopsis confer cytokinin insensitivity and ethylene overproduction, respectively.** *Proc Natl Acad Sci USA* 1998, **95**:4766-4771.
55. Chae HS, Faure F, Keiber JJ: **The eto1, eto2, and eto3 mutations and cytokinin treatment increase ethylene biosynthesis in Arabidopsis by increasing the stability of ACS protein.** *Plant Cell* 2003, **15**:545-559.
56. Wang KL-C, Yoshida H, Lurin C, Ecker JR: **Regulation of ethylene gas biosynthesis by the Arabidopsis ETO1 protein.** *Nature* 2004, **428**:945-950.
 First report of an E3 enzyme that contains CULLIN3 from Arabidopsis.
57. Xu L, Wei Y, Reboul J, Vaglio P, Shin T-H, Vidal M, Elledge SJ, Harper JW: **BTB proteins are substrate-specific adaptors in an SCF-like modular ubiquitin ligase containing Cul-3.** *Nature* 2003, **425**:316-321.
58. Spanu P, Grosskopf DG, Felix G, Boller T: **The apparent turnover of 1-aminocyclopropane-1-carboxylate synthase in tomato cells is regulated by protein phosphorylation and dephosphorylation.** *Plant Physiol* 1994, **106**:529-535.
59. Tatsuki M, Mori H: **Phosphorylation of tomato 1-aminocyclopropane-1-carboxylic acid synthase, Le-ACS2, at the C-terminal region.** *J Biol Chem* 2001, **276**:28051-28057.
60. Oyama T, Shimura Y, Okada K: **The Arabidopsis HY5 gene encodes a bZIP protein that regulates stimulus-induced development of root and hypocotyl.** *Genes Dev* 1997, **11**:2983-2995.
61. Chattopadhyay S, Ang L-H, Puente P, Deng X-W, Wei N: **Arabidopsis bZIP protein HY5 directly interacts with light-responsive promoters in mediating light control of gene expression.** *Plant Cell* 1998, **10**:673-683.
62. Ang L-H, Chattopadhyay S, Wei N, Oyama T, Okada K, Batschauer A, Deng X-W: **Molecular interaction between COP1 and HY5 defines a regulatory switch for light control of Arabidopsis development.** *Mol Cell* 1998, **1**:213-222.
63. Holm M, Ma L, Qu L-J, Deng XW: **Two interacting bZIP proteins are direct targets of COP1-mediated control of light-dependent gene expression in Arabidopsis.** *Genes Dev* 2002, **16**:1247-1259.
64. Osterlund MT, Hardtke CS, Wei N, Deng XW: **Targeted destabilization of HY5 during light-regulated development of Arabidopsis.** *Nature* 2000, **405**:462-466.
65. Saijo Y, Sullivan JA, Wang H, Yang J-Y, Shen Y, Rubia V, Ma L, Hoecker U, Deng XW: **The COP1-SPA1 interaction defines a critical step in phytochrome A-mediated regulation of HY5 activity.** *Genes Dev* 2003, **17**:2642-2647.
66. Pepper A, Delaney T, Wahsburn T, Poole D, Chory J: **DET1, a negative regulator of light-mediated development and gene expression in Arabidopsis, encodes a novel nuclear-localized protein.** *Cell* 1994, **78**:109-116.
67. Schroeder DF, Gahrz M, Maxwell BB, Cook RK, Kan JM, Alonso JM, Ecker JR, Chory J: **De-etiolated 1 and Damaged DNA Binding Protein 1 interact to regulate Arabidopsis photomorphogenesis.** *Curr Biol* 2002, **12**:1462-1472.
68. Dornan D, Wertz I, Shimizu H, Arnott D, Frantz GD, Dowd P,
 ● O'Rourke KM, Koeppen H, Dixit VM: **The ubiquitin ligase COP1 is a critical negative regulator of p53.** *Nature* 2004, **429**:86-92.
 See annotation [69**].
69. Wertz IE, O'Rourke KM, Zhang Z, Dornan D, Arnott D,
 ● Deshaies RJ, Dixit VM: **Human De-Etiolated-1 Regulates c-Jun by assembling a CUL4A ubiquitin ligase.** *Science* 2004, **303**:1371-1374.
 These two reports [68**,69**] together helped to identify the novel CUL-LIN4-containing DCX-complexes. These complexes regulate the degradation of c-JUN and p53 in humans, and possibly the degradation of HY5, HYH, LAF1 and phyA in plants.
70. Seo HS, Yang J-Y, Ishikawa M, Bolle C, Ballesteros ML, Chua N-H: **LAF1 ubiquitination by COP1 controls photomorphogenesis and is stimulated by SPA1.** *Nature* 2003, **423**:995-999.
71. Seo HS, Watanabe E, Tokutomi S, Nagatani A, Chua N-H: **Photoreceptor ubiquitination by COP1 E3 ligase desensitizes phytochrome A signaling.** *Genes Dev* 2004, **18**:617-622.
72. Hoecker U, Tepperman JM, Quail PH: **SPA1, a WD-repeat protein specific to phytochrome A signal transduction.** *Science* 1999, **284**:496-499.
73. Hoecker U, Quail P: **The phytochrome A-specific signaling intermediate SPA1 interacts directly with COP1, a constitutive repressor of light signaling in Arabidopsis.** *J Biol Chem* 2001, **276**:38173-38178.
74. Kwok SF, Staub JM, Deng X-W: **Characterization of two subunits of Arabidopsis 19S proteasome regulatory complex and its possible interaction with the COP9 complex.** *J Mol Biol* 1999, **285**:85-95.
75. Potuschak T, Stary S, Schlögelhofer P, Becker F, Nehjnskaia V, Bachmair A: **PRT1 of Arabidopsis thaliana encodes a component of the plant N-end rule pathway.** *Proc Natl Acad Sci USA* 1998, **95**:7904-7908.
76. Lopez-Molina L, Mongrand S, Kinoshita N, Chua N-H: **AFP is a novel negative regulator of ABA signaling that promotes ABI5 protein degradation.** *Genes Dev* 2003, **17**:410-418.
77. Ruegger M, Dewey E, Gray WM, Hobbie L, Turner J, Estelle M: **The TIR protein of Arabidopsis function in auxin response and is related to human SKP2 and yeast Grr1p.** *Genes Dev* 1998, **12**:198-207.
78. Gray WM, del Pozo JC, Walker L, Hobbie L, Risseeuw E, Banks T, Crosby WL, Yang M, Estelle M: **Identification of an SCF ubiquitin-ligase complex required for auxin response in Arabidopsis thaliana.** *Genes Dev* 1999, **13**:1678-1687.
79. Gray WM, Kepinski S, Rouse D, Leyser O, Estelle M: **Auxin regulates SCF^{TIR1}-dependent degradation of AUX/IAA proteins.** *Nature* 2001, **414**:271-276.
80. Xie Q, Guo H-S, Dallman G, Fang S, Weissman AM, Chua N-H: **SINAT5 promotes ubiquitin-related degradation of NAC1 to attenuate auxin signals.** *Nature* 2002, **419**:167-170.
81. Sieberer T, Seifert GJ, Hauser M-T, Grisafi P, Fink GR, Luschnig C: **Post-transcriptional control of the Arabidopsis auxin efflux carrier EIR1 requires AXR1.** *Curr Biol* 2000, **10**:1595-1598.
82. He J-X, Gendron JM, Yang Y, Li J, Wang Z-Y: **The GSK3-like kinase BIN2 phosphorylates and destabilizes BZR1, a positive regulator of the brassinosteroid signaling pathway in Arabidopsis.** *Proc Natl Acad Sci USA* 2002, **99**:10185-10190.
83. del Pozo JC, Boniotti MB, Gutierrez C: **Arabidopsis E2Fc functions in cell division and is degraded by the ubiquitin-SCF(AtSKP2) pathway in response to light.** *Plant Cell* 2002, **14**:3057-3071.
84. Genschik P, Criqui MC, Parmentier Y, Derevier A, Fleck J: **Cell cycle-dependent proteolysis in plants: identification of the destruction box pathway and metaphase arrest produced by the proteasome inhibitor MG132.** *Plant Cell* 1998, **10**:2063-2075.
85. Castellano MM, del Pozo JC, Ramirez-Parra E, Brown S, Gutierrez C: **Expression and stability of Arabidopsis CDC6 are associated with endoreduplication.** *Plant Cell* 2001, **13**:2671-2686.
86. Zhou Y, Li G, Brandizzi F, Fowke LC, Wang H: **The plant cyclin-dependent kinase inhibitor ICK1 has distinct function domains for in vivo inhibition, protein instability and nuclear localization.** *Plant J* 2003, **35**:476-489.

87. Valverde F, Mouradov A, Soppe W, Ravenscroft D, Samach A, Coupland G: **Photoreceptor regulation of CONSTANS protein in photoperiodic flowering.** *Science* 2004, **303**:1003-1006.
88. Somers DE, Schultz TF, Milnamow M, Kay SA: **ZEITLUPE encodes a novel clock-associate PAS protein from Arabidopsis.** *Cell* 2000, **101**:319-329.
89. Nelson DC, Lasswell J, Rogg LE, Cohen MA, Bartel B: **FKF1, a clock-controlled gene that regulates the transition to flowering in Arabidopsis.** *Cell* 2000, **101**:331-340.
90. Mas P, Kim W-Y, Somers DE, Kay SA: **Targeted degradation of TOC1 by ZTL modulates circadian function in Arabidopsis thaliana.** *Nature* 2003, **426**:567-570.
91. Yan J, Wang J, Li Q, Hwang JR, Patterson C, Zhang H: **AtCHIP, a U-box containing E3 ubiquitin ligase, plays a critical role in temperature stress tolerance in Arabidopsis.** *Plant Physiol* 2003, **132**:861-869.
92. Wang X, Feng S, Nakayama N, Crosby WL, Irish VF, Deng XW, Wei N: **The COP9 signalosome interacts with SCF UFO and participates in Arabidopsis flower development.** *Plant Cell* 2003, **15**:1071-1082.
93. Levin JZ, Meyerowitz EM: **UFO: an Arabidopsis gene involved in both floral meristem and floral organ development.** *Plant Cell* 1995, **7**:529-548.
94. Xie D-X, Feys BF, James S, Nieto-Rostro M, Turner JG: **COI1: an Arabidopsis gene required for jasmonate-regulated defense and fertility.** *Science* 1998, **280**:1091-1094.
95. Kim HS, Delaney TP: **Arabidopsis SON1 is an F-box protein that regulates a novel induced defense response independent of both salicylic acid and systemic acquired resistance.** *Plant Cell* 2002, **14**:1469-1482.
96. Dielerle M, Zhou Y-C, Schäfer E, Funk M, Kretsch T: **EID1, an F-box protein involved in phytochrome A-specific light signaling.** *Genes Dev* 2001, **15**:939-944.
97. Harmon FG, Kay SA: **The F box protein AFR is a positive regulator of phytochrome A-mediated light signaling.** *Curr Biol* 2003, **13**:2091-2096.
98. Stirnberg P, van de Sande K, Leyser HMO: **MAX1 and MAX2 control shoot lateral branching in Arabidopsis.** *Development* 2002, **129**:1131-1141.
99. Woo HR, Chung KM, Park J-H, Oh SA, Ahn T, Hong SH, Jang SK, Nam HG: **ORE9, an F-box protein that regulates leaf senescence in Arabidopsis.** *Plant Cell* 2001, **13**:1779-1790.
100. El Refy A, Perazza D, Zekraoui L, Valay JG, Bechtold N, Brown S, Hülskamp M, Herzog M, Bonneville JM: **The Arabidopsis KAKTUS gene encodes a HECT protein and controls the number of endoreduplication cycles.** *Mol Genet Genomics* 2003, **270**:403-414.
101. Downes BP, Stupar RM, Gingerich DJ, Vierstra RD: **The HECT ubiquitin-protein ligase (UPL) family in Arabidopsis: UPL3 has a specific role in trichome development.** *Plant J* 2003, **35**:729-742.
102. Hannoufa A, Negruk V, Eisner G, Lemieux B: **The CER3 gene of Arabidopsis thaliana is expressed in leaves, stems, roots, flowers and apical meristems.** *Plant J* 1996, **10**:459-467.

III.II. Calderón Villalobos et al., (manuscript of a research article)

Luz Irina A. Calderón Villalobos, Carola Kuhnle, Katia Marroco,
Thomas Kretsch, and Claus Schwechheimer

The evolutionarily conserved *Arabidopsis thaliana* F-box protein AtFBP7 is required for efficient translation during temperature stress

(Submitted to *The Journal of Biological Chemistry*)

THE EVOLUTIONARILY CONSERVED *ARABIDOPSIS THALIANA* F-BOX PROTEIN AtFBP7 IS REQUIRED FOR EFFICIENT TRANSLATION DURING TEMPERATURE STRESS*

Luz Irina A. Calderón-Villalobos‡, Carola Kuhnle‡, Katia Marrocco¶, Thomas Kretsch¶, Claus Schwechheimer‡**

From the ‡Department of Developmental Genetics, Centre for Plant Molecular Biology, Tübingen University, Auf der Morgenstelle 5, 72076 Tübingen, Germany, and the ¶ Department of Plant Developmental Biology, Institut für Biologie II, Freiburg University, Schänzlestrasse 1, 79104 Freiburg, Germany.

Running title: The Evolutionarily Conserved F-box Protein AtFBP7.

** Address correspondence to: Department of Developmental Genetics, Centre for Plant Molecular Biology, Tübingen University, Auf der Morgenstelle 5, 72076 Tübingen, Germany. Tel.: ++49 7071 2976669; Fax: ++49 7071 295135; Email: claus.schwechheimer@zmbp.uni-tuebingen.de.

In eukaryotes, E3 ubiquitin ligases (E3s) mediate the ubiquitylation of proteins that are destined for degradation by the ubiquitin-proteasome system. In SKP1/CDC53/F-Box protein (SCF)-type E3 complexes, the interchangeable F-box protein confers specificity to the E3 subunit through direct physical interactions with the degradation substrate. The vast majority of the approximately 700 F-box proteins from the plant model organism *Arabidopsis thaliana* remain to be characterized. Here, we investigate the previously uncharacterized and evolutionarily conserved *Arabidopsis* F-box protein 7 (AtFBP7), which is encoded by a unique gene in *Arabidopsis* (At1g21760). Several apparent *fbp7* loss-of-function alleles do not have an obvious phenotype. AtFBP7 is ubiquitously expressed and its expression is induced after cold and heat stress. When we followed up on a reported co-purification of the eukaryotic elongation factor-2 (eEF-2) with YLR097c, the budding yeast orthologue of AtFBP7, we discovered a general defect in protein biosynthesis after cold and heat stress in *fbp7* mutants. Thus, our findings suggest that AtFBP7 is required for protein synthesis in temperature stress conditions. (166 words)

Eukaryotes use the ubiquitin-proteasome system for the selective degradation of regulatory proteins such as cell cycle regulators and transcription factors (1). Proteins that are destined for degradation by the ubiquitin-

proteasome system are polyubiquitylated, a result of the consecutive activities of an E1 ubiquitin activating enzyme (E1)¹, an E2 ubiquitin conjugating enzyme (E2) and an E3 ubiquitin ligase (E3) (1). Polyubiquitylated proteins can then be recognized and degraded by the 26S proteasome (2). E3s interact directly with the degradation substrate and they therefore function as degradation substrate receptors (1). Cullin-RING E3s represent an important class of E3 enzymes and these protein complexes are characterized by their RING box1 (RBX1) subunit and a Cullin (CUL) subunit, which is specific for one of the four known types of Cullin-RING E3s, namely Cul1 in SCF (SKP1, Cullin 1, F-Box protein), Cul2 or Cul5 in VCB (Von-Hippel-Lindau, Elongin C, Elongin B), Cul3 in BTB/POZ (Bric-a-Brac, Tramtrack and Broad Complex/Pox Virus and Zinc-Finger), and Cul4 in DCX (Damaged DNA binding protein1, Cullin 4A, X-Box) (3-8).

A common feature of Cullin-RING E3s is the ability to associate with specific degradation substrate receptor subunits to alter their substrate specificity (9). F-box proteins are the degradation substrate receptor subunits of SCF-type E3s (3,4,10). They associate with the CUL1-RBX1 core complex via functional orthologues of the adaptor protein Suppressor of Kinetochores (SKP) 1 (11). The finding that the plant model organism *Arabidopsis thaliana* may contain close to 700 different F-box proteins (approximately 3% of the *Arabidopsis* genome) was one of the unexpected results of the analysis

of the Arabidopsis genome sequence (12). In absolute as well as in relative terms, this number by far exceeds the number F-box proteins that have been identified in yeasts, fruit fly, and human (3,9,13). It therefore seems that plants use SCF-mediated protein degradation as a major mechanism for the regulation of plant growth and development.

Based on available mutants, it has so far only been possible to attribute specific biological functions to approximately 20 Arabidopsis F-box proteins (14,15). Many of these F-box proteins are closely related to the mammalian cell cycle regulator Suppressor of kinetochore protein2 (SKP2) (16). In mammals, SKP2 controls the ubiquitylation of E2F cell-cycle promoting transcription factors and the cell cycle inhibitors p21^{CIP1} and p27^{Kip1} (17-19). SKP2 as well as E2F proteins are conserved between mammals and plants, and experimental evidence suggests that the Arabidopsis SKP2 orthologues control the degradation of Arabidopsis E2F proteins (20). SKP2 is therefore an example for an F-box protein that has seemingly retained its substrate specificity and its biological function throughout animal and plant evolution. Interestingly, examples of evolutionarily conserved F-box protein functions or conserved substrate specificities are rare in the published literature.

We conducted a search for Arabidopsis proteins that share sequence homology with the 21 F-box proteins from *Saccharomyces cerevisiae* (3,9,21,22). Our search identified 19 Arabidopsis F-box proteins as the putative orthologues of 12 yeast F-box proteins (Supplemental Table 1). We also found that only 13 Arabidopsis F-box proteins that shared homology with only 4 yeast F-box proteins are also conserved in humans, fruit fly, and nematodes (Supplemental Table 1). Thus, the number of evolutionarily conserved F-box proteins appears to be very small.

Three of the four evolutionarily conserved F-box proteins have known biological functions in yeast where they have been implicated in the regulation of the cell cycle (Met30 and Cst13/Amn1) or the regulation of metabolism (Met30 and Grr1) (9). The remaining F-box protein, encoded by YLR097c in yeast,

has not been characterized as yet in any organism. A protein that we designated *Arabidopsis thaliana* F-box protein 7 (AtFBP7; At1g21760) is the apparent YLR097c orthologue in Arabidopsis (Fig. 1A). Here, we characterize AtFBP7 and demonstrate that AtFBP7 expression is induced in response to cold and heat stress. *fbp7* mutants are impaired in protein synthesis when cold or heat-stressed, and we therefore suggest that AtFBP7 is required for translation in temperature stress conditions.

EXPERIMENTAL PROCEDURES

Sequence alignments and phylogeny – Basic Local Alignment Sequence Tool (BLAST) protein searches were conducted at <http://www.ncbi.nlm.nih.gov/blast/> and at <http://www.arabidopsis.org/Blast/> with the 21 F-box proteins from *Saccharomyces cerevisiae* as query sequences (9,23). Unless otherwise stated, proteins that contained an F-box domain and shared at least 20% amino acid identity in the putative protein-protein interaction domain were classified as putative orthologues. Putative Arabidopsis orthologues were then compared with human F-box proteins to specify phylogenetic relationships (3). Protein sequences of the Met30 and the AtFBP7 families as shown in Fig. 1A, were aligned using ClustalW at <http://www.ebi.ac.uk/>. The unrooted phylogenetic tree was generated using TreeViewPPC.1 (22). The pretty box alignment was produced using the DNASTar MegAlign software.

Biological material - *Arabidopsis thaliana* Columbia (Col), Wassilewskija (Ws) and Nossen-0 (No-0) seed were obtained from the Nottingham Arabidopsis Stock Centre (NASC, UK) and used as wild type controls. Transposon-tagged lines *fbp7-1* (pst17753, No-0), *fbp7-2* (pst19185, No-0) and *fbp7-3* (pst18526, No-0) and the T-DNA-tagged line *fbp7-5* (SALK_144992, Col) were identified at <http://signal.salk.edu/cgi-bin/tdnaexpress> and obtained from the RIKEN Biological Resources Centre (Japan) and the NASC (UK), respectively (24,25). The *fbp7-4* mutant allele (Ws) was identified by PCR-based screening of the

Wisconsin T-DNA collection (26). Homozygous *fbp7-4* or *fbp7-5* mutants were identified by genotyping with the gene specific primers Primer1 5'-AAGACAGAGAAAGAGTCTCTGTTTCTAT-3' and Primer4 5'-AACCTCAAGCTAGCATCTGATCAAGTCC-3', and nested primers Primer2 5'-CAAATCGTCTCTCAGTTTCCATGACTTCA-3', Primer3 5'-GTAATCTCTGTAAACAAACAAAATCCCA-3', in combination with T-DNA insertion border primers JL202 5'-TTTTATAATAACGCTGCGGACATCTAC-3' (*fbp7-4*) or LBb1 5'-GCGTGGACCGCTTGCTGCAACT-3' (*fbp7-5*). For genotyping of transposon tagged alleles, Primer1 and Primer4 were used in combination with the Ds-element specific primers Ds5-1 5'-ACGGTCGGGAACTAGCTCTAC-3' or Ds3-1 5'-ACCCGACCGGATCGTATCGGT-3'. The temperature sensitive *los1-1* allele (a gift from Y. Guo, Beijing, China) was previously described (27). Unless otherwise stated, seedlings were germinated and grown at 22°C under constant light on standard growth medium supplemented with 1% sucrose (28).

Yeast two-hybrid analysis - The full-length and truncated *AtFBP7* gene fragments were obtained by PCR from expressed sequence tag (EST) 186N16T7 with the primers *AtFBP7* FW-cDNA 5'-CTCGAGATGACTTCAGATGCTCTC-3' or Δ N-FW 5'-CTCGAGATGTGGCAGACTGCT-3' and *AtFBP7* RV-cDNA 5'-GTCGACTTAGCAGTGACATAGTA-3'. PCR products were cloned into pCR2.1-TOPO™ (Invitrogen, UK), fully sequenced and subsequently subcloned as *XhoI/SalI* fragments into the pLexA and pAS2-1 'bait' vectors (29). The LexA-AD-ASK2 and the GAL4-AD-ASK prey constructs were previously reported (30,31). Yeast interaction assays and quantitative LacZ measurements were performed as previously described (29).

Subcellular localization studies - To generate *AtFBP7*:GFP for stable plant transformation, *AtFBP7* was amplified by PCR using attB1-FBP7 5'-attB1-TCATGACTTCAGATGCTCTC-3' and attB2-FBP7 5'-attB2-CTTAGCCAGTGACATAGTAATC-3'. The fragment was introduced into pDONR™201 and then transferred to 35S-GW-GFP (a gift from G. Coupland, Cologne, Germany). 15 transgenic

lines expressing the *AtFBP7*:GFP construct were generated in *Arabidopsis thaliana* ecotype Columbia. For transient expression in protoplasts, the 35S:*AtFBP7*:GFP construct was generated by cloning *AtFBP7* cDNA into pGEM-T™ (Promega), and subsequent transfer of a *SacI/BamHI* fragment into CF203 (a gift from K. Schumacher, Tübingen, Germany). This construct was introduced in tobacco protoplasts as previously described (32). Protein fluorescence was analyzed using a Leica TCS SP2 confocal microscope.

Gene expression analyses - Total RNA was extracted from 10 day-old *Arabidopsis* seedlings using the RNeasy™ kit (Qiagen, Hilden, Germany). Reverse transcription (RT) was performed with 1 µg of total RNA and an oligo (dT)₁₇-adaptor 5'-GACTCGAGTCGACATCGA(T)₁₇-3' (33). *AtFBP7* gene expression was evaluated with Primer1 and Primer4. Amplification of *ACTIN* (At3g18780) with the primers ACTIN-FW 5'-ATTCAGATGCCCA GAAGTCTTGTTTC-3' and ACTIN-RV 5'-GCAAGTGCTGTGATTTCTTTGCTCA-3' served as a normalization control. All RT-PCR reactions were repeated using independent RNA preparations and reverse transcription reactions. Transcripts were amplified using 28 or 30 amplification cycles as indicated in the Figure legends. To generate the *AtFBP7*:GUS reporter construct, a 1300 base pair *AtFBP7* promoter fragment was amplified with Promoter1 5'-TCTAGATGTGGACTGCCCCAAAAGCTTGC TCC-3' and Promoter2 5'-CCATGGGAGAGACGATTTGAAAATACAGCGA-3' and introduced into pGEM-T™. The resulting construct was fully sequenced and cloned into pCAMBIA1391Z. 18 *AtFBP7*:GUS transgenic *Arabidopsis* lines were obtained and 10 day-old T2 seedlings and 3 week-old T2 transgenic plants expressing *AtFBP7*:GUS were used for GUS staining following published procedures (28).

Microarray Analysis - Three replicate samples were harvested and prepared from 5 day-old light grown wild type and *fbp7-3* mutant seedlings. RNA for microarray analyses was extracted using the RNeasy™ kit (Qiagen, Hilden, Germany). Complementary RNA was prepared

from 6 μ g of total RNA as described in the Affymetrix Expression Analysis Technical Manual. In brief, double-stranded cDNA was synthesized using the SuperScript Choice System (Invitrogen, Carlsbad, CA). Biotin-labeled target cRNA was prepared by cDNA *in vitro* transcription using the GeneChip® Expression 3'-Amplification Reagents (Affymetrix, Santa Clara, CA) in the presence of biotinylated UTP and CTP. After purification with the GeneChip Sample Cleanup Module (Qiagen, Hilden, Germany), cRNA was fragmented and used for hybridization of the Arabidopsis ATH1 GeneChip (Affymetrix, Santa Clara, CA). Hybridization, washing, staining, scanning and data collection were performed in an Affymetrix GeneChip® Fluidics Station 450 and GeneArray® Scanner. The microarray computational analysis was performed on CHP data files and analyzed using the robust multi-array average (RMA) GC method of the GeneSpring XT software (SiliconGenetics). Differentially expressed genes (2 fold induced or two fold repressed) were identified using the LogiT algorithm. The microarray data files were submitted to the Gene Expression Omnibus at <http://www.ncbi.nlm.nih.gov/geo/> and are available under accession number GSE3864.

eEF-2 protein stability and translation assays – eEF-2 protein stability was determined from 10 day-old Arabidopsis wild type and mutant seedlings treated with 250 μ M cycloheximide (CHX) and 10 μ M MG132 as indicated. EF2 was detected using a polyclonal antibody raised against purified wheat eEF-2 protein (a gift from K. Browning, Austin, Texas). Translation assays were performed according to published protocols (34). 10 day-old wild type and mutant seedlings were incubated in liquid GM medium supplemented with 50 μ Ci/ml [³⁵S]Methionine for translation assays conducted at 22°C and 45°C (Amersham Biosciences). Seedlings that had been grown for 4 days at 4°C were used for the cold stress assays (0°C). At the indicated time points, protein extracts were prepared in 2x Laemmli buffer and analysed by SDS-PAGE (35). SDS-PAGE gels were dried and exposed to X-ray film or stained with Coomassie to verify equal sample loading.

RESULTS

In a search for evolutionarily conserved F-box proteins, we identified AtFBP7 (At1g21760) as an as yet uncharacterized F-box protein (Fig. 1A). AtFBP7 encodes a protein with 329 amino acids and a predicted molecular mass of 37.5 kDa. An alignment of AtFBP7 and its apparent orthologues from other eukaryotes suggests the presence of three conserved protein domains, the 40 amino acid F-box domain at the protein's N-terminus as well as two conserved domains located in the middle of the protein (Fig. 1, B - D).

The F-box domain serves as an adaptor domain for interactions with the SKP1 subunit of the SCF core complex (11). The Arabidopsis genome encodes 21 apparent SKP1 orthologues (Arabidopsis SKP1, ASK). ASK1 and ASK2 represent the two closest homologues of human and yeast SKP1 proteins in this species (30,36-38). To confirm the functionality of the AtFBP7 F-box domain, we tested the interaction between AtFBP7 and ASK2 using the yeast two-hybrid system. As expected, a strong interaction between both proteins was detected with the full-length protein but not with a variant lacking the N-terminal F-box domain (Fig. 2, A and B). To examine whether AtFBP7 interacts with specific ASK proteins, we tested its interaction with 19 members of the Arabidopsis ASK protein family (31). In this experiment, strong interactions were detected with ASK1 and ASK2, the predominant ASK family members, but also with ASK4, ASK11 and ASK14 (Fig. 2, A and C). In summary, this indicates that AtFBP7 is an F-box protein that may act together with different ASKs to form SCF^{AtFBP7} E3 ubiquitin ligase complexes.

The two conserved protein domains that are located in the middle of the protein are specific for the AtFBP7 protein family (Fig. 1, B and D). Sequence alignments reveal the presence of a total of five conserved tyrosines and of one conserved serine within these domains (Fig. 1D). These residues can potentially be modified by phosphorylation, and it may therefore be hypothesized that protein phosphorylation

regulates the activity of AtFBP7 or its specificity for degradation targets. Since the function of the two conserved domains remained unclear throughout our analyses, we named these domains ‘mystery domain 1’ (MD1) and MD2 (Fig. 1B).

To identify the subcellular localization of AtFBP7, we generated constructs that express the protein under control of the constitutive 35S cauliflower mosaic virus promoter (35S CaMV) as a translational fusion with the reporter green fluorescent protein (GFP). When examined in transiently transformed protoplasts and in transgenic Arabidopsis plants, AtFBP7:GFP was found to be enriched in the nucleus (Figure 3). A nuclear targeting sequence could however not be identified and we therefore speculate that AtFBP7 is transported to the nucleus together with an interacting nuclear-localized protein or protein complex (39).

When we examined AtFBP7 localization in transiently transformed protoplasts, we could also observe accumulation of the fusion protein in mitochondria (Fig. 3, A – C). In line with these findings, the PSORT algorithm (<http://psort.nibb.ac.jp/>) predicts the presence of a domain for mitochondrial targeting in MD1 and a 53.5% certainty for mitochondrial localization.

To examine the organ-specific expression of AtFBP7, we tested for transcript abundance in a range of plant organs using RT-PCR. In this analysis, we found strong expression of AtFBP7 in leaves, flowers, and stems of the adult plant and weaker expression in light-grown seedlings, roots, and siliques (Fig. 4A). To examine the tissue-specific expression of AtFBP7, we then generated 15 transgenic lines that express the β -glucuronidase reporter (GUS) under control of a 1.3 kb AtFBP7 promoter fragment. In five day old light-grown seedlings, strong GUS expression was detected in the hypocotyl, in the shoot meristem and in root tips (Fig. 4, B and C). In adult plants, GUS expression was strong in the vasculature, in pollen, pollen tubes, and trichomes (Fig. 4, D and E). Throughout leaf development, AtFBP7 was found to be strongest in senescing leaves (Fig. 4, F and G).

To elucidate the biological function of AtFBP7, we characterized five insertion alleles for AtFBP7 (Fig. 5). Three insertion lines with Ds transposon insertions immediately upstream of the ATG (*fbp7-1*), in the first intron (*fbp7-2*), and in the second exon (*fbp7-3*) were obtained from the RIKEN collection (Fig. 5A) (24). Two additional T-DNA insertion lines with insertions in intron 7 (*fbp7-4*) and intron 8 (*fbp7-5*), were identified in the SALK and Wisconsin collections, respectively (Fig. 5A) (25,26). The positions of all insertions were confirmed by PCR and homozygous insertion lines were generated. Using semi-quantitative RT-PCR, we then examined AtFBP7 expression in the five insertion lines. We found a clear down-regulation of the full-length transcript in the alleles *fbp7-2* through *fbp7-5*, which all carry in-gene-insertions. In contrast, AtFBP7 expression was seemingly unaltered in the *fbp7-1* allele (Fig. 6B). To examine whether truncated AtFBP7 transcripts are expressed in these lines, we further tested for the expression of partial AtFBP7 transcripts using primer combinations that amplify gene regions downstream of the insertion sites in *fbp7-2* and *fbp7-3* or upstream of the insertion sites in *fbp7-4* and *fbp7-5* (Fig. 5B). *fbp7-2*, *fbp7-3*, and *fbp7-4* expressed strongly reduced levels of the respective truncated transcripts, and we therefore consider these lines to be AtFBP7 knock-down or knock-out alleles (Fig. 5B). Since we were able to amplify a residual AtFBP7 transcript in the *fbp7-5* mutant that spans most of the open reading frame, we cannot be certain that gene function is lost in this mutant.

When we then analysed these *fbp7* mutant alleles for growth defects in a range of growth conditions and in a series of physiological assays (phytohormone responses, stress responses etc.), we failed to identify apparent growth defects in the mutants suggesting that AtFBP7 is not required for normal plant growth and development.

In the absence of an apparent mutant phenotype, we examined gene expression changes between 5 day-old *fbp7-3* mutant seedlings and the wild type using Affymetrix ATH1 GeneChips (40). This analysis identified

only 32 genes whose expression was induced and 24 genes whose expression was repressed in the mutant when compared to the wild type (Supplemental Table 2). The validity of the experiment was substantiated by the apparent absence (14 fold repression) of the *AtFBP7* transcript in the *fbp7-3* mutant. The list of misregulated genes includes several transcription factors and many enzymes. Overall, however, the identity of the misregulated genes does not point clearly at a specific *AtFBP7*-dependent pathway.

During the analysis of publicly available microarray data, we noticed that *AtFBP7* was reported to be induced after temperature stress (41). We addressed this point by examining *AtFBP7* expression using RT-PCR and *AtFBP7* promoter:GUS lines. In response to heat and cold stress, both approaches revealed a rapid, in the case of heat stress transient, upregulation of *AtFBP7* expression (Fig. 6, *A - D*). Taken together, these results suggest that *AtFBP7* expression can be induced by temperature stresses.

In search of a biological process that requires *AtFBP7* function, our attention was brought to the fact that an affinity purification of YLR097c, the yeast orthologue of *AtFBP7*, had resulted in the co-purification of the eukaryotic translation elongation factor-2 (eEF-2) ((42,43) and A. Shevchenko, personal communication). Based on these reports, we reasoned that eEF-2 may be a target of *AtFBP7* and the 26S proteasome. Using an eEF-2 antibody, we followed eEF-2 stability over time in seedlings following a block of protein neosynthesis with the inhibitor cycloheximide (CHX), or a block of protein degradation with the 26S proteasome inhibitor MG132 (Fig. 7*A*). Both experiments indicated that eEF-2 is a stable protein under the conditions tested. Next, we examined whether eEF-2 abundance is altered in *fbp7* mutants (Fig. 7*B*). This experiment revealed that eEF-2 levels are not altered in the mutant suggesting that eEF-2 is not targeted for degradation by *AtFBP7*.

Since eEF-2 is a central component of the protein translation, we tested next whether *AtFBP7* is required for protein synthesis. In *in vivo* translation assays, we measured the incorporation of radioactive methionine into

newly synthesized proteins. In these experiments, we could not detect a difference in protein synthesis between the wild type and the mutant at ambient temperature (Fig. 7*C*). However, translation assays conducted with cold and heat-treated seedlings showed a marked and general decrease in protein translation efficiency in the *fbp7-3* mutant when compared to the wild type (Fig.7, *D - F*). *los1-1*, a previously described cold and in our assays also heat-sensitive mutant allele of the Arabidopsis *eEF-2* gene served as a control for these experiments (27). While translation was completely abolished in assays with cold-treated *los1-1*, *fbp7-3* still retained some residual protein synthesis activity in these conditions (Fig.7 *B*). To examine whether the effect observed in the *fbp7-3* allele could also be observed in the other *fbp* mutant alleles, we examined translation efficiency of the four alleles with in-gene-insertions and found that all of them had reduced protein synthesis rates in the cold when compared to the respective wild types (Fig. 7*G*). We therefore concluded that the translation defect is linked to loss of *AtFBP7* gene function.

Next, we reasoned that the strong reduction in protein biosynthesis in the temperature-stressed *fbp7-3* mutants should also have an effect on plant growth and development when the mutants are grown in temperature stress. However, neither cold nor different heat stresses had a distinct effect on *fbp7* mutant growth. Furthermore, ion leakage assays did not reveal any differences in cell integrity indicating that the translation defects in the *fbp7* mutants do not have an affect on general plant growth. Taken together, we suggest that *AtFBP7* is required for efficient protein synthesis during temperature stress conditions but that *AtFBP7* function is not essential for plant survival.

DISCUSSION

Our search for F-box proteins that are conserved in yeasts, animals and the plant model organism *Arabidopsis thaliana* resulted in the identification of only four evolutionarily conserved F-box protein families. One of these families has not been characterized as yet. We characterized *AtFBP7* from Arabidopsis as the

first member of this previously uncharacterized F-box protein family. AtFBP7 interacts with Arabidopsis SKP1 orthologues and contains two additional conserved domains that may serve for interactions with the degradation substrate. Although there is precedence that such an approach can help to identify degradation substrates, our own attempts to identify AtFBP7 interacting proteins using the yeast two-hybrid system resulted only in the identification of ASK interactors (44,45). This may suggest that AtFBP7 or its interactors require specific posttranslational modifications for interaction. This hypothesis is further substantiated by the conservation of specific serine and tyrosine residues, thus amino acids that can be phosphorylated, in the conserved domains of all AtFBP7 family members.

The evolutionary conservation of AtFBP7 suggests that the AtFBP7 orthologous proteins may control a biological process that is conserved in all eukaryotes. We discovered that Arabidopsis *fbp7* mutants are deficient in protein translation, thus a biological process that is regulated and conserved, following cold and heat stress treatments. Our incentive to examine protein translation in temperature stress conditions in *fbp7* mutants was based on our own observations that *AtFBP7* expression is induced in cold and heat stressed samples and on the observations made by others that YLR097c, the putative *AtFBP7* orthologue from *Saccharomyces cerevisiae*, copurifies with eEF-2 after affinity purification ((42,43) and A. Shevchenko, personal communication). Interestingly, YLR097c expression in yeast is also induced after heat stress (46).

Since the eEF-2 interaction was identified in affinity purified samples, its interactions with SKP1 and YLR097c may not necessarily be direct. Our own attempts to show a direct interaction between AtFBP7 and eEF-2 using the yeast two-hybrid system as well as pull-downs and overlay assays using the purified recombinant proteins were unsuccessful (data not

shown). Furthermore, we could show that eEF-2 is a stable protein in different temperature conditions and that loss of AtFBP7 does not have an effect on eEF-2 protein levels. Based on our findings, we propose that AtFBP7 regulates translation by ubiquitylating and thereby inactivating a translational repressor that blocks eEF-2 activity or protein synthesis in general during temperature stress. Precedence for a role of protein degradation in translation comes from work on eEF-2 kinase, which regulates eEF-2 activity in mammals (47). In mammalian cells, eEF-2 kinase is targeted for degradation by the ubiquitin-proteasome system and eEF-2 kinase abundance has an effect on the translation rate (47,48). Thus, there is evidence for a role of the ubiquitin-proteasome system during protein synthesis in at least in some experimental systems.

It should however also be considered that AtFBP7-mediated ubiquitylation may not necessarily affect the protein's stability. Proteolysis independent regulation by ubiquitylation has for example been observed for Met4, the target of the F-box protein Met30 (49,50). In the case of Met4, Met30-mediated mono-ubiquitylation inactivates Met4 but does not destabilize the protein. If such a regulatory mechanism would apply to AtFBP7 then loss of *AtFBP7* function would not necessarily reflect on the abundance of its ubiquitylation target.

The identification of translation as an AtFBP7-dependent biological process is intriguing since it is a candidate mechanism that may be controlled by the AtFBP7 orthologues in other organisms. Future experiments on AtFBP7 orthologues in other model organisms will reveal whether the translational defects observed in the plant mutants can also be observed in other organisms, after temperature stress or other stress conditions. These future experiments may therefore help to provide a functional explanation for the evolutionary conservation of AtFBP7.

REFERENCES

1. Hershko, A., Ciechanover, A. (1998) *Annu. Rev. Biochem.* **67**, 425-479
2. Glickman, M. H., and Raveh, D. (2005) *FEBS* **579**, 3214-3223
3. Jin, J., Cardozo, T., Lovering, R. C., Elledge, S. J., Pagano, M., and Harper, J. W. (2004) *Genes Dev.* **18**, 2573-2580
4. Deshaies, R. J. (1999) *Annu. Rev. Cell Dev. Biol.* **15**, 435-467
5. Kamura, T., Koepp, D. M., Conrad, M. N., Skowyra, D., Moreland, R. J., Iliopoulos, O., Lane, W. S., Kaelin, W. G. J., Elledge, S. J., Conaway, R. C., Harper, J. W., and Conaway, J. W. (1999) *Science* **284**, 657-661
6. Xu, L., Wei, Y., Reboul, J., Vaglio, P., Shin, T.-H., Vidal, M., Elledge, S. J., and Harper, J. W. (2003) *Nature* **425**, 316-321
7. Wertz, I. E., O'Rourke, K. M., Zhang, Z., Dornan, D., Arnott, D., Deshaies, R. J., and Dixit, V. M. (2004) *Science* **303**, 1371-1374
8. Higa, L. A. A., Mihaylov, I. S., Banks, D. P., Zhneg, J., and Zhang, H. (2003) *Nature Cell Biol.* **5**, 1008-1015
9. Willems, A. R., Schwab, M., and Tyers, M. (2004) *Biochim. Biophys. Acta* **1695**, 133-170
10. Patton, E. E., Willems, A. R., and Tyers, M. (1998) *Trends Genet.* **14**, 236-243
11. Bai, C., Sen, P., Hofmann, K., Ma, L., Goebel, M., Harper, J. W., and Elledge, S. J. (1996) *Cell* **86**, 263-274
12. Gagne, J. M., Downes, B. P., Shiu, S. H., Durski, A. M., and Vierstra, R. D. (2002) *Proc. Natl. Acad. Sci. USA* **99**, 11519-11524
13. The Arabidopsis Genome Initiative. (2000) *Nature* **408**, 796 - 815
14. Schwechheimer, C., and Calderon-Villalobos, L. I. A. (2004) *Curr. Opin. Plant Biol.* **7**, 677-686
15. Schwechheimer, C., and Schwager, K. (2004) *Plant Cell Rep.* **23**, 353-364
16. Gstaiger, M., Marti, A., and Krek, W. (1999) *Exp. Cell Res.* **247**, 554-562
17. Marti, A., Wirbelauer, C., Scheffner, M., and Krek, W. (1999) *Nat. Cell Biol.* **1**, 14-19
18. Wang, W., Nacusi, L., Sheaff, R. J., and Liu, X. (2005) *Biochem.* **44**, 14553-14564
19. Ungermannova, D., Gao, Y., and Liu, X. (2005) *J. Biol. Chem.* **280**, 30301-30309
20. del Pozo, J. C., Boniotti, M. B., and Gutierrez, C. (2002) *Plant Cell* **2002**, 3057 - 3071
21. Altschul, S. F., Madden, T. L., Schaffer, A. A., Zhang, J., Zhang, Z., Miller, W., and Lipman, D. J. (1997) *Nucleic Acids Res.* **25**, 3389-3402
22. Thompson, J. D., Higgins, D. G., and Gibson, T. J. (1994) *Nucleic Acids Res.* **22**, 4673-4680
23. Altschul, S. F., Gish, W., Miller, W., Myers, E. W., and Lipman, D. J. (1990) *J. Mol. Biol.* **215**, 403-410
24. Kuromori, T., Hirayama, T., Kiyosue, Y., Takabe, H., Mizukado, S., Sakurai, T., Akiyama, K., Kamiya, A., Ito, T., and Shinozaki, K. (2004) *Plant J.* **37**, 897-905
25. Alonso, J. M., Stepanova, A. N., Leisse, T. J., Kim, C. J., Chen, H., Shinn, P., Stevenson, D. K., Zimmerman, J., Barajas, P., Cheuk, R., Gadrinab, C., Heller, C., Jeske, A., Koesema, E., Meyers, C. C., Parker, H., Prednis, L., Ansari, Y., Choy, N., Deen, H., Geralt, M., Hazari, N., Hom, E., Karnes, M., Mulholland, C., Ndubaku, R., Schmidt, I., Guzman, P., Aguilar-Henonin, L., Schmid, M., Weigel, D., Carter, D. E., Marchand, T., Risseuw, E., Brogden, D., Zeko, A., Crosby, W. L., Berry, C. C., and Ecker, J. R. (2003) *Science* **301**, 653-657
26. Krysan, P. J., Young, J. C., and Sussman, M. R. (1999) *Plant Cell* **11**, 2283-2290
27. Guo, Y., Xiong, L., Ishitani, M., and Zhu, J. K. (2002) *Proc. Natl. Acad. Sci. USA* **99**, 7786-7791
28. Weigel, D., and Glazebrook, J. (2002) *Arabidopsis: A laboratory manual.*, CSHL Press, Cold Spring Harbor, New York

29. Schwechheimer, C., and Deng, X.W. (2002) in *Molecular Plant Biology* (Gilmartin, P. M., and Bowler, C., eds) Vol. 2, pp. 173 - 198, Oxford University Press, Oxford
30. Risseuw, E. P., Daskalchuk, T. E., Banks, T. W., Liu, E., Cotelesage, J., Hellmann, H., Estelle, M., Somers, D. E., and Crosby, W. L. (2003) *Plant J.* **34**, 753-767
31. Marrocco, K., Zhou, Y., Bury, E., Dieterle, M., Zhou, Y.-C., Schäfer, E., Funk, M., Kretsch, T., Funk, M., Genschik, P., Krenz, M., Stolpe, T., and Kretsch, T. *Plant J.* In press.
32. Negrutiu, I., Shillito, R., Potrykus, I., and Sala, F. (1987) *Plant Mol. Biol.* **8**, 363-373
33. Frohman, M. A., Dush, M. K., and Martin, G. R. (1988) *Proc. Natl. Acad. Sci. USA* **85**, 8998-9002
34. Assaad, F. F., and Signer, E. R. (1990) *Mol. Gen. Genet.* **223**, 517-520
35. Laemmli, U. K. (1970) *Nature* **227**, 680-685
36. Liu, F., Ni, W., Griffith, M. E., Huang, Z., Chang, C., Peng, W., Ma, H., and Xie, D. (2004) *Plant Cell* **16**, 5 - 20
37. Zhao, D., Ni, W., Feng, B., Han, T., Petrasek, M. G., and Ma, H. (2003) *Plant Phys.* **133**, 203-217
38. Farrás, R., Ferrando, A., Jásik, J., Kleinow, T., Ökrész, L., Tiburcio, A., Salchert, K., del pozo, C., Schell, J., and Koncz, C. (2001) *EMBO J.* **20**, 2742-2756
39. Dingwall, C., and Laskey, R. A. (1991) *Trends Biochem. Sci.* **16**, 478-481
40. McGall, G. H., and Christians, F. C. (2002) *Adv. Biochem. Eng. Biotechnol.* **77**, 21-42
41. Zimmermann, P., Hirsch-Hoffmann, M., Hennig, L., and Gruissem, W. (2004) *Plant Phys.* **136**, 2621-2632
42. Seol, J. H., Shevchenko, A., and Deshaies, R. J. (2001) *Nat. Cell Biol.* **3**, 384-391
43. Willems, A. R., Goh, T., Taylor, L., Chernushevich, I., Shevchenko, A., and Tyers, M. (1999) *Philos. Trans. R. Soc. Lond. B. Biol. Sci.* **354**, 1533-1550
44. Guo, H., and Ecker, J. R. (2003) *Cell* **115**, 667 - 677
45. Potuschak, T., Lechner, E., Parmentier, Y., Yanagisawa, S., Grava, S., Koncz, C., and Genschik, P. (2003) *Cell* **115**, 679 - 689
46. Gasch, A. P., Spellman, P. T., Kao, C. M., Carmel-Harel, O., Eisen, M. B., Storz, G., Botstein, D., and Brown, P. O. (2000) *Mol. Biol. Cell* **11**, 4241-4257
47. Marin, P., Nastiuk, K. L., Daniel, N., Girault, J. A., Czernik, A. J., Glowinski, J., Nairn, A. C., and Premont, J. (1997) *J. Neurosci.* **17**, 3445-3454
48. Arora, S., Yang, J. M., and Hait, W. N. (2005) *Cancer Res.* **65**, 3806-3810
49. Kaiser, P., Flick, K., Wittenberg, C., and Reed, S. I. (2000) *Cell* **102**, 303-314
50. Flick, K., Ouni, I., Wohlschlegel, J. A., Capati, C., McDonald, W. H., Yates, J. R., and Kaiser, P. (2004) *Nat. Cell Biol.* **6**, 634-641

FOOTNOTES

- This work was supported by grants from the Arabidopsis Functional Genomics Network of the Deutsche Forschungsgemeinschaft (Schw751/4-1 and Schw751/4-2) to C.S. and a grant of the European Union to T.K. (HPRN-CT-2002-00333).

¹ The abbreviations used are: E1, E1 ubiquitin activating enzyme; E2, E2 ubiquitin conjugating enzyme; E3, E3 ubiquitin ligase; RING, Really interesting new gene; RBX, RING box; CUL, Cullin; SCF, SKP1/CDC53/F-Box; VCB, Von-Hippel-Lindau, Elongin C, Elongin B; BTB, Bric-a-Brac, Tramtrack, Broad Complex; POZ, Pox Virus and Zinc-Finger; DCX, Damaged DNA-Binding Protein1, Cullin 4A, X-Box; SKP, *Saccharomyces cerevisiae* Suppressor of Kinetochore; AtFBP7, *Arabidopsis thaliana* F-box protein 7; BLAST, Basic Local Alignment Sequence Tool; Col, Columbia; Ws, Wassilewskija; No-O, Nossen; NASC, Nottingham Arabidopsis Stock Centre; EST, expressed sequence tag; RT, reverse transcription; PCR, polymerase chain reaction; RMA, robust multi-array average; eEF-2, eukaryotic elongation factor-2; CHX, cycloheximide; MG132, N-carbobenzoxyl-Leu-Leu-leucinal; ASK, Arabidopsis SKP1; MD, mystery domain; 35S CaMV, 35S cauliflower mosaic virus; GFP, green fluorescent protein; GUS, β -glucuronidase; CaMV, cauliflower mosaic virus; DAE, days after emergence.

FIGURES AND LEGENDS

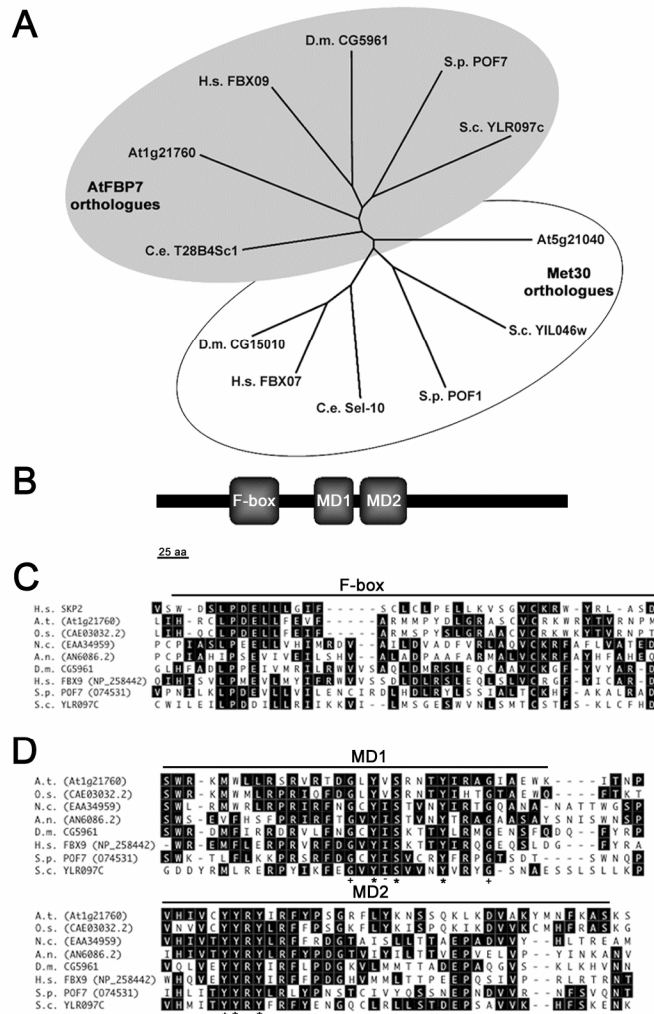


Figure 1

Fig. 1. AtFBP7 is an evolutionarily conserved F-box protein from *Arabidopsis thaliana*. **A.** Unrooted phylogenetic tree of Arabidopsis AtFBP7 (At1g21760) and the Arabidopsis Met30 orthologue (At5g21040) and their apparent orthologues from *Saccharomyces cerevisiae* (S.c.), *Schizosaccharomyces pombe* (S.p.), *Drosophila melanogaster* (D.m.), humans (H.s.), and *Caenorhabditis elegans* (C.e.). **B.** Schematic representation (drawn to scale) of the AtFBP7 protein. Boxes indicate the characteristic F-box domain (F-box), and the putative protein-protein interaction domains Mystery Domain (MD) 1 and MD2. **C.** Protein sequence alignment of the F-box domain of human SKP2 (H.s. NP005974, amino acids 107-145), Arabidopsis AtFBP7 (A.t. At1g21760, aa 59-97), rice (O.s. CAE03032.2, aa 59-97;), *Neurospora crassa* (N.c. EAA34959.1, aa 232-274), *Aspergillus nidulans* (A.n. AN6086.2, aa 203-245), *Drosophila melanogaster* (D.m. CG5961, aa 178-220), human FBX9 (H.s. NP258442, aa 187-229), *Schizosaccharomyces pombe* (S.p., POF7, aa 111-174), *Saccharomyces cerevisiae* (S.c. YLR097c, aa 99-140). **D.** Alignment of MD1 and MD2 from AtFBP7 (A.t., aa 126-201), rice (O.s., aa 121-196), *Neurospora crassa* (N.c., aa 384-460), *Aspergillus nidulans* (A.n., aa 301-378), *Drosophila melanogaster* (D.m., aa 252-327), human (H.s., aa 254-327), *Schizosaccharomyces pombe* (S.p., aa 188-261), *Saccharomyces cerevisiae* (S.c., aa 180-257). Amino acids underlined and marked indicate conserved residues. Accession number of the proteins in C and D are identical to those provided in A, unless otherwise stated.

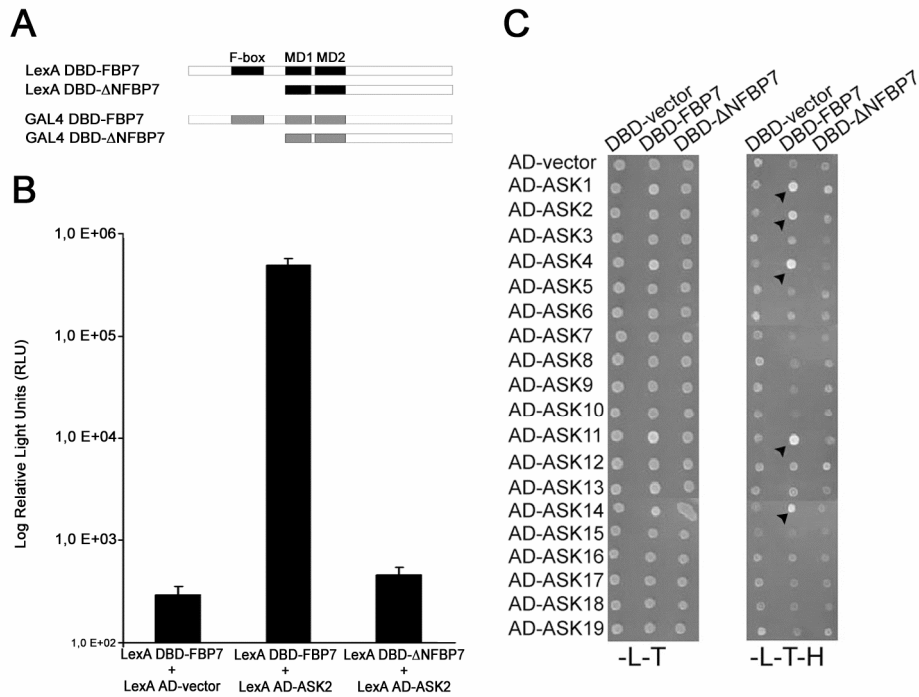


Figure 2

Fig. 2. AtFBP7 interacts with Arabidopsis SKP1 (ASK) proteins. *A.* Schematic representation of the AtFBP7 constructs used in the yeast two-hybrid interaction experiments shown in *B* (LexA DBD) and *C* (GAL4 DBD). *B.* Quantification of LacZ reporter activity in yeast cells expressing proteins as indicated. Average and standard deviation were calculated based on 8 replicate samples. *C.* Yeast two-hybrid interactions between AtFBP7 and 19 Arabidopsis SKP1-homologues (ASK). Yeast clones expressing GAL4 DBD-FBP7 or the F-box domain deletion construct GAL4 DBD-ΔNFBP7 and one of 19 AD-ASK clones were grown on media lacking leucine and tryptophane (-L-T, left panel, co-transformation control) or media lacking leucine, tryptophane, and histidine (-L-T-H, right panel, interaction experiment).

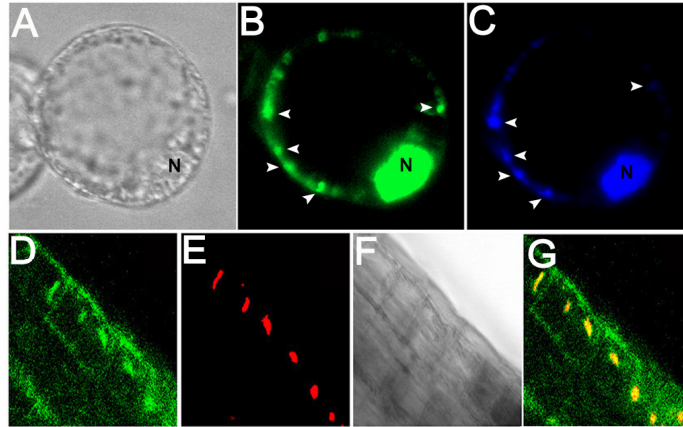


Figure 3

Fig. 3. Subcellular localization of AtFBP7:GFP. Transiently transformed tobacco protoplasts that express 35S:AtFBP7:GFP show enrichment of the protein in the nucleus (N) and in mitochondria (arrows). *A.* Nomarski, *B.* fluorescence, and *C.* DAPI staining. Root cells of transgenic Arabidopsis plants expressing 35S:AtFBP7:GFP also show nuclear enrichment of the fusion protein. *D.* GFP channel, *E.* propidium iodide staining, *F.* Nomarski, and *G.* overlay.

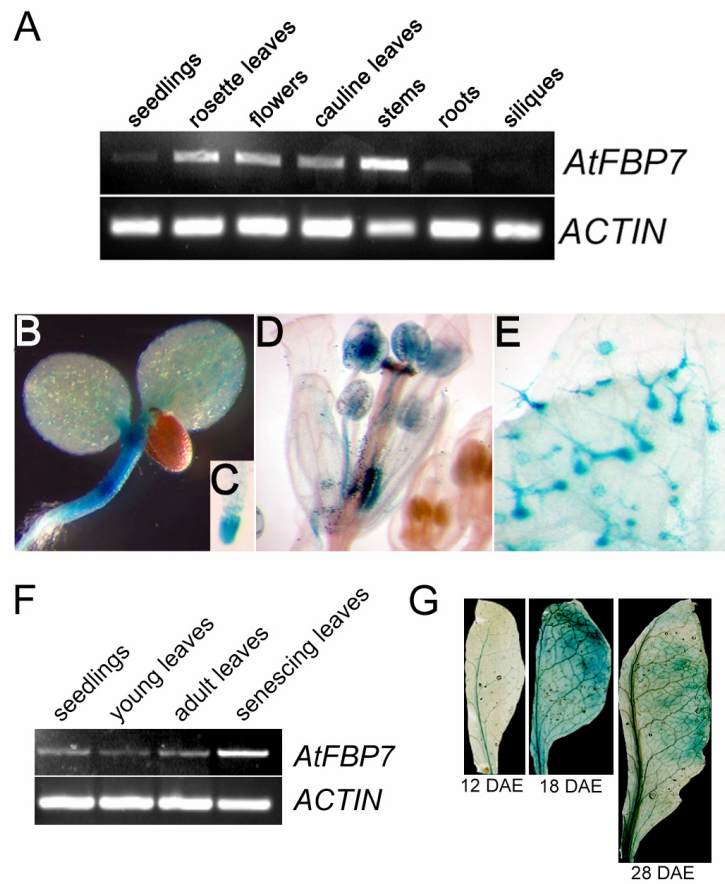


Figure 4

Fig. 4. Tissue-specific expression of *AtFBP7*. *A*, *AtFBP7* and *ACTIN* expression in different tissues. *B* to *E*, *AtFBP7*:GUS expression in 5-day-old transgenic seedlings (*B*), the root tip (*C*), flowers (*D*) and leaves (*E*) of 3 week-old transgenic plants. *F* and *G*, *AtFBP7* gene expression is increased in senescing leaves as determined by RT-PCR (*F*) and *AtFBP7*:GUS expression (*G*). DAE, days after emergence.

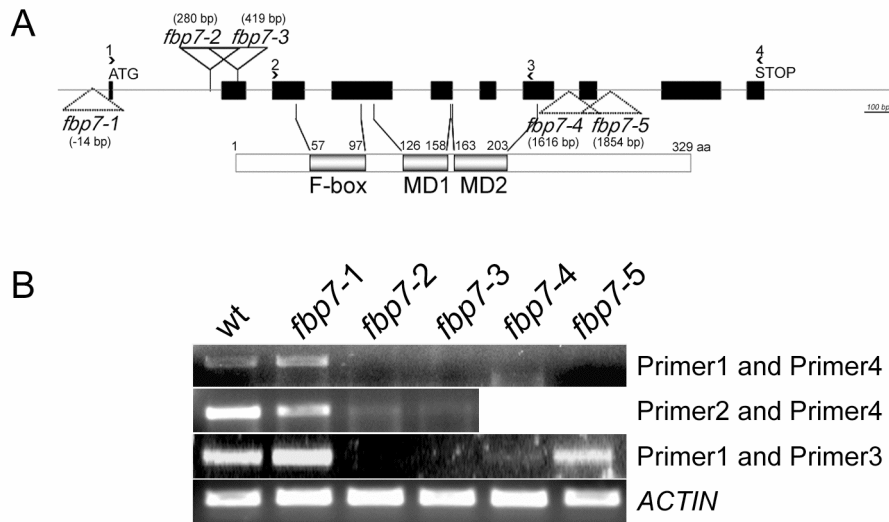


Figure 5

Fig. 5. Characterization of *AtFBP7* mutant alleles. *A*. Structure of the *AtFBP7* gene (exons, black bars; introns, lines) and insertion sites in the five *fbp* mutant alleles. The ATG start and STOP codons are indicated. The positions of the insertions are indicated in brackets with respect to the first base of the ATG start codon (+1 bp). Numbered arrows show the positions of Primer1 through Primer4 that were used for genotyping and RT-PCR expression analysis. *B*. Semi-quantitative RT-PCR for *AtFBP7* expression using primer combinations as indicated. *ACTIN* expression was used as a normalization control for cDNA amounts.

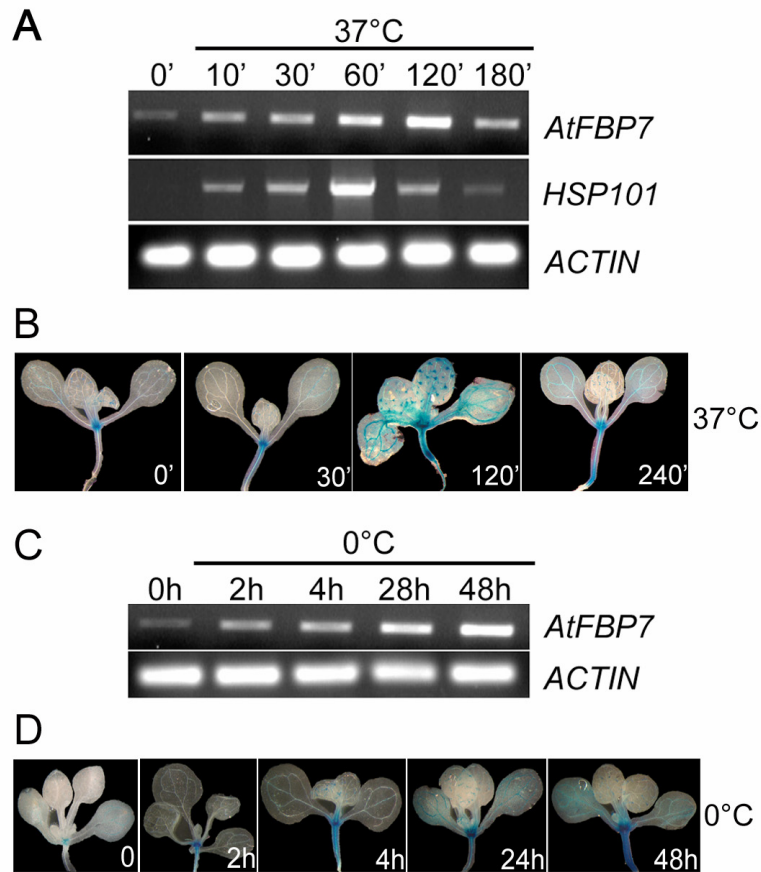


Figure 6

Fig. 6. *AtFBP7* expression is induced after heat and cold stress. *A.* Semi-quantitative RT-PCR analysis of *AtFBP7* expression after heat treatment (37°C). *HEAT SHOCK PROTEIN101* (*HSP101*) expression was used as a control for heat stress conditions. *ACTIN* expression was used as control for cDNA amounts. *B.* *AtFBP7*:GUS expression is induced in 10 day-old seedlings after heat stress (37°C). Samples were taken at the time points indicated. *C.* Semi-quantitative RT-PCR analysis of *AtFBP7* expression after cold treatment (0°C). *D.* *AtFBP7*:GUS expression in 10 day-old seedlings after cold treatment (0°C) for 0, 2, 4, 24 and 48 hours.

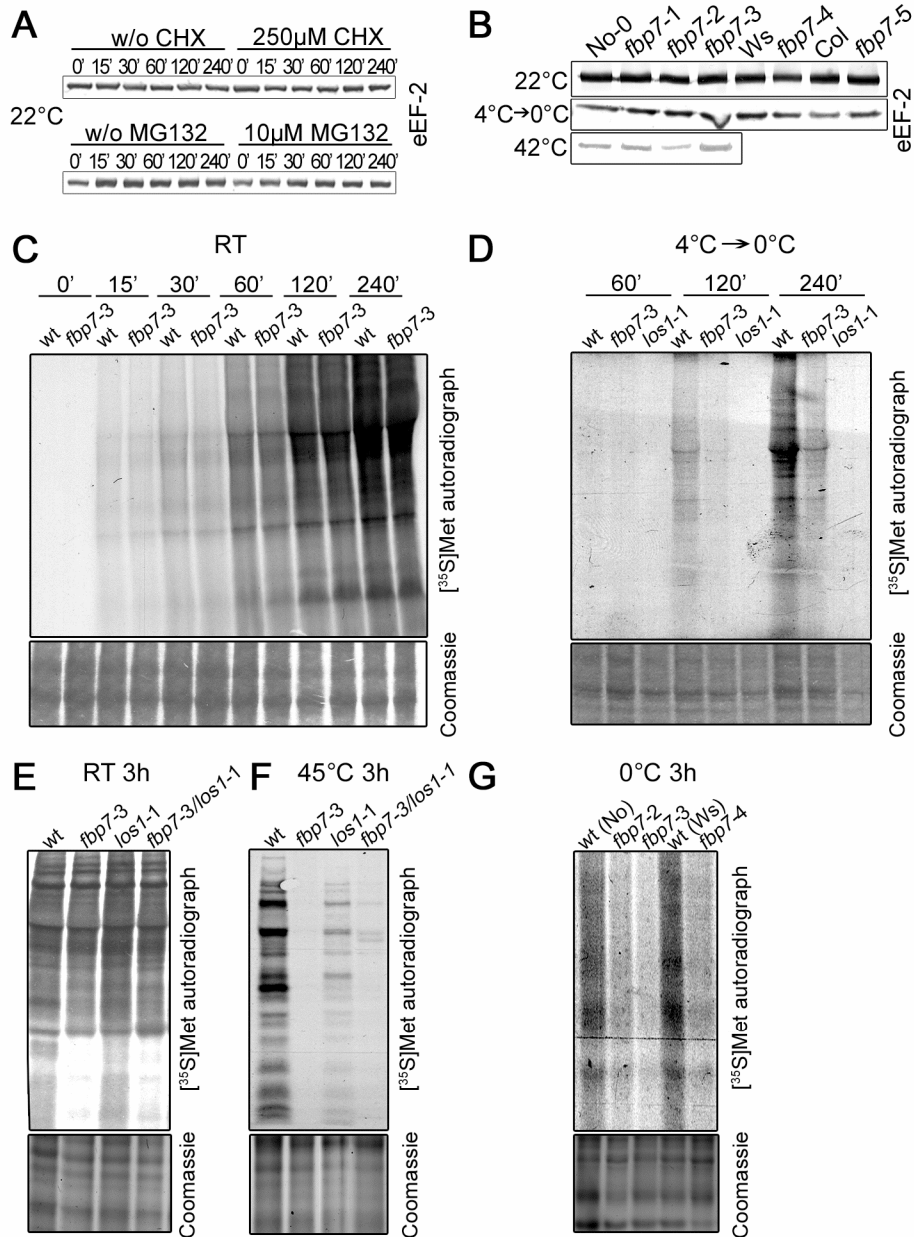


Figure 7

Fig. 7. AtFBP7 is required for protein translation after temperature stress. *A.* EF-2 is a stable protein at ambient temperature as determined by western blotting with an anti-EF2 antibody in protein extracts from untreated, cycloheximide treated and MG132 treated protein samples. *B.* The abundance of EF-2 is unaltered in *fbp7* mutants at room temperature as well as after temperature stress. *C.* *In vivo* translation assays reveal no difference in translation efficiency between the wild type and the *fbp7-3* mutant at room temperature. *D.* *fbp7* mutants are impaired in protein translation following cold treatment. The cold-sensitive *eEF-2* mutant *los1-1* was used as a control for the assay. *E.* Protein synthesis is not impaired at room temperature in *fbp7-3* and *los1-1* mutants. *F.* The *fbp7-3* mutant shows reduced translation efficiency after heat stress. *G.* *In vivo* translation assays reveal that all *fbp7* mutant alleles with in gene insertions are translation deficient. Samples used for translation assays were seedlings (*A*, *B*, and *G*) or 5 mm leaf discs (*C*, *D*, *E* and *F*).

SUPPLEMENTAL DATA

Supplemental Table 1. *Saccharomyces cerevisiae* F-box proteins and their apparent orthologues in eukaryotes (9). *S. cerevisiae*, *Saccharomyces cerevisiae*; *S. pombe*, *Schizosaccharomyces pombe*; *H. sapiens*, *Homo sapiens*; *A. thaliana*, *Arabidopsis thaliana*; *D. melanogaster*, *Drosophila melanogaster*; *C. elegans*, *Caenorhabditis elegans*.

F-box protein (FBP)	Synonyms	Organism	Identity	Region of identity (aa)
Ylr097c		<i>S. cerevisiae</i>	100%	
POF7	SPCC70.11c	<i>S. pombe</i>	28%	7-311
FBX09		<i>H. sapiens</i>	26%	7-258
At1g21760	<u>AtFBP7</u>	<i>A. thaliana</i>	30%	185-275
CG5961		<i>D. melanogaster</i>	24%	6-261
T28B4.1A¹		<i>C. elegans</i>	35%	62-100
Yil046w	Met30	<i>S. cerevisiae</i>	100%	
POF1	SPAC57A10.05c	<i>S. pombe</i>	38%	126-637
Fbw7		<i>H. sapiens</i>	31%	131-587
At5g21040	FBP	<i>A. thaliana</i>	22%	187-469
CG15010		<i>D. melanogaster</i>	27%	136-590
Sel-10	F55B12.3b	<i>C. elegans</i>	24%	61-582
Ybr158w	Cst13/Amn1	<i>S. cerevisiae</i>	100%	
POF2		<i>S. pombe</i>	23%	251-485
FBL2/FBL3		<i>H. sapiens</i>	27%	289-485
At2g25490 ³	FBL6	<i>A. thaliana</i>	26%	337-513
At5g01720 ³	FBL3		21%	306-513
At3g58530 ³			20%	238-485
CG9003-PA		<i>D. melanogaster</i>	28%	292-488
C02F5.7a		<i>C. elegans</i>	25%	311-485
Yjr090c	Grr1	<i>S. cerevisiae</i>	100%	
POF2	SPBC25B2.11	<i>S. pombe</i>	28%	320-785
FBL20		<i>H. sapiens</i>	25%	404-694
At5g01720 ³	FBL3	<i>A. thaliana</i>	25%	390-757
At4g15475	FBL4		22%	400-741
At5g27920 ³	like FBL3		22%	404-745
At1g21410 ³			20%	412-631
At1g77000 ³	like FBL5, FBL2		21%	412-631
At3g58530 ³			21%	414-678
At5g25350 ³	like FBL6		19%	316-741
At2g25490 ³			24%	411-734
CG9003-PA		<i>D. melanogaster</i>	27%	423-738
C02F5.7a		<i>C. elegans</i>	23%	415-738

Supplemental Table 1 (continued)

F-box protein (FBP)	Synonyms	Organism	Identity	Region of identity (aa)
Ylr352w		<i>S. cerevisiae</i>	100%	
(-)		<i>S. pombe</i>		
FBXL16		<i>H. sapiens</i>	28%	214-293
At5g27920 ³	FBP	<i>A. thaliana</i>	20%	99-278
At1g10780	FBP		27%	222-327
CG9952-PA		<i>D. melanogaster</i>	24%	89-282
(-)		<i>C. elegans</i>		
Ydr219c		<i>S. cerevisiae</i>	100%	
(-)		<i>S. pombe</i>		
(-)		<i>H. sapiens</i>		
At1g61340	FBP	<i>A. thaliana</i>	29%	13-72
EG:4E4.1		<i>D. melanogaster</i>	19%	93-433
C32E12.1		<i>C. elegans</i>	29%	255-338
Yor080w	Fcl1/Dia2	<i>S. cerevisiae</i>	100%	
POF3		<i>S. pombe</i>		
(-)		<i>H. sapiens</i>		
At5g44960	FBP	<i>A. thaliana</i>	25%	219-387
At4g07400	FBP		25%	164-251
CG40500		<i>D. melanogaster</i>	29%	495-670
T28B4.1c		<i>C. elegans</i>	30%	181-252
Ydr306c		<i>S. cerevisiae</i>	100%	
SPAC6F6.2c	POF5	<i>S. pombe</i>	33%	154-476
(-)		<i>H. sapiens</i>		
At1g77000 ³	AtFBL5	<i>A. thaliana</i>	30%	196-353
At1g21410 ³	sim. to SKP1		26%	150-343
(-)		<i>D. melanogaster</i>		
(-)		<i>C. elegans</i>		
Yjl149w		<i>S. cerevisiae</i>	100%	
(-)		<i>S. pombe</i>		
FBX11		<i>H. sapiens</i>	33%	39-93 F-box domain
At5g25860	FBP	<i>A. thaliana</i>	28%	52-99 F-box domain
CG9461		<i>D. melanogaster</i>	44%	51-92 F-box domain
T03F1.6b ¹		<i>C. elegans</i>	25%	51-193

Supplemental Table 1 (continued)

F-box protein (FBP)	Synonyms	Organism	Identity	Region of identity (aa)
Ydr131c		<i>S. cerevisiae</i>	100%	
(-)		<i>S. pombe</i>		
(-)		<i>H. sapiens</i>		
At3g08750	FBP	<i>A. thaliana</i>	32%	1-44 F-box domain
At3g21410	FBW1		36%	5-46 F-box domain
(-)		<i>D. melanogaster</i>		
(-)		<i>C. elegans</i>		
Ylr368w	MDM30p	<i>S. cerevisiae</i>	100%	
(-)		<i>S. pombe</i>		
FBXL3 iso1		<i>H. sapiens</i>	33%	15-68 F-box domain
At5g39490	FBP	<i>A. thaliana</i>	33%	19-60 F-box domain
(-)		<i>D. melanogaster</i>		
(-)		<i>C. elegans</i>		
Yml088w	Ufo1	<i>S. cerevisiae</i>	100%	
POF10	SPBC1703.06	<i>S. pombe</i>	22%	10-267
FBX31		<i>H. sapiens</i>	39%	4-49 F-box domain
At5g52880	FBP	<i>A. thaliana</i>	30%	2-60 F-box domain
At1g66290	FBP		21%	8-67 F-box domain
CG9461-PA		<i>D. melanogaster</i>	35%	10-87 F-box domain
(-)		<i>C. elegans</i>		
Yfl009w	CDC4	<i>S. cerevisiae</i>	100%	
SPAC4D7.03	POP2P	<i>S. pombe</i>	35%	236-744
Fbw7		<i>H. sapiens</i>	29%	247-743
(-)		<i>A. thaliana</i>		
CG15010		<i>D. melanogaster</i>	29%	247-743
Sel-10		<i>C. elegans</i>	28%	233-730
Ybr280c		<i>S. cerevisiae</i>	100%	
Pof9	FBP	<i>S. pombe</i>	35%	523-636
HERC2 ¹		<i>H. sapiens</i>	22%	364-566
(-)		<i>A. thaliana</i>		
CG11734		<i>D. melanogaster</i>	20%	364-605
Glo-4		<i>C. elegans</i>	26%	431-576

Supplemental Table 1 (continued)

F-box protein (FBP)	Synonyms	Organism	Identity	Region of identity (aa)
Yjl204c	Rcy1	<i>S. cerevisiae</i>	100%	
POF6	SPCC18.04	<i>S.pombe</i>	25%	96-840
(-)		<i>H. sapiens</i>		
(-)		<i>A. thaliana</i>		
CG17177		<i>D. melanogaster</i>	23%	359-47
C33H5.9		<i>C. elegans</i>	18%	555-822
Ynl230c	Ela1	<i>S. cerevisiae</i>	100%	
POF4	SPBC29A3.08	<i>S. pombe</i>	27%	1-77
Elongin A		<i>H. sapiens</i>	31%	1-82
(-)		<i>A. thaliana</i>		
CG6755		<i>D. melanogaster</i>	26%	3-85
R03D7.4	Elongin A	<i>C. elegans</i>	27%	1-124
Ynl311c		<i>S. cerevisiae</i>	100%	
(-)		<i>S. pombe</i>		
(-)		<i>H.sapiens</i>		
At1g32430	FBP	<i>A. thaliana</i>	26%	261-338
(-)		<i>D. melanogaster</i>		
(-)		<i>C. elegans</i>		
Ybr203c		<i>S. cerevisiae</i>	100%	
no orthologues				
Ymr094w	Ctf13	<i>S. cerevisiae</i>	100%	
no orthologues				
Ymr258c		<i>S. cerevisiae</i>	100%	
no orthologues				
Ylr224w		<i>S. cerevisiae</i>	100%	
no orthologues				

¹ In a few cases, orthology relationships as determined in our study differed from orthology relationships between animal F-box proteins established elsewhere (3).

² Generally, sequence homology outside of the F-box domain was a qualifying criteria for orthology. However, striking homology in the F-box domain itself was considered as an important criteria in a few exceptional cases.

³ This Arabidopsis F-box protein shares also significant homology with another yeast F-box protein.

Supplemental Table 2: Result of the *fbp7-3* microarray analysis

A. Genes that are induced in *fbp7-3*

Fold Change	Accession	Putative Gene Function	<i>fbp7-3</i> raw data	t-test p-value	wild type raw data	t-test p-value
25.34	At3g47320	hypothetical protein	19.24 (7.14 to 26.38)	0.021	0.67 (0.47 to 0.86)	0.328
7.959	At4g12470	lipid transfer family protein	2.38 (2.15 to 2.51)	0.578	318.3 (204.4 to 476.1)	0.415
7.93	At2g40330	Bet v I allergen family protein	40.69 (26.47 to 49.68)	0.702	7.13 (1.80 to 15.19)	0.516
6.343	At4g12490	lipid transfer family protein	325.1 (233.3 to 386.7)	0.377	51.23 (40.03 to 66.42)	0.687
6.236	At4g12480	lipid transfer family protein	1,155 (1,03 to 1,25)	0.552	186,3 (155 to 213,9)	0.42
6.183	At2g41230	expressed protein	49.72 (41.58 to 55.41)	0.517	10.23 (2.653 to 16.22)	0.858
5.701	At4g12500	lipid transfer family protein	178.6 (123.4 to 215.3)	0.38	31.81 (20.8 to 43.04)	0.728
5.14	At1g29090	peptidase C1A papain family	51.68 (28.56 to 76.89)	0.389	10.74 (4.076 to 15.24)	0.876
3.323	At5g45820	CBL-interacting protein kinase 20	126 (98.97 to 176.1)	0.504	37.5 (27.16 to 47.19)	0.369
3.117	At1g71200	bHLH family protein	35.93 (24.69 to 54.7)	0.436	11.62 (6.991 to 17.5)	0.868
2.952	At2g43620	chitinase, putative	986.5 (831.7 to 1,067)	0.396	336.7 (262 to 388.2)	0.273
2.935	At5g64120	peroxidase, putative	924.4 (726.3 to 1,074)	0.373	314 (275.8 to 378.9)	0.276
2.923	At4g22470	lipid transfer family protein	150.2 (132.1 to 164.4)	0.516	52.32 (37.64 to 60.72)	0.283
2.904	At3g16670	expressed protein	471.9 (448.2 to 492)	0.765	162.7 (151.1 to 176.5)	0.297
2.88	At1g22570	oligopeptide transporter	87.09 (69.2 to 107.3)	0.41	29.81 (27.77 to 32.21)	0.373
2.781	At5g48430	expressed protein	70.2 (49.51 to 88.09)	0.381	25.77 (19.38 to 37.65)	0.508
2.602	At1g76930	proline-rich family protein	1,121 (962.6 to 1,211)	0.443	431.1 (367.1 to 464.5)	0.262
2.586	At5g46050	oligopeptide transporter	135.5 (116.7 to 149.8)	0.464	53.07 (43.98 to 67.67)	0.238
2.576	At4g36670	mannitol transporter, putative	758.4 (666.4 to 881.2)	0.484	293.4 (264 to 326)	0.261
2.572	At1g19610	plant defensin-fusion protein	159.5 (141 to 173.2)	0.534	63.22 (47.07 to 80.06)	0.227
2.568	At2g26440	pectinesterase family protein	135.9 (113.5 to 161.5)	0.425	52.66 (45.39 to 58.42)	0.264
2.458	At2g25450	2-oxoglutarate-dependent dioxygenase	512 (457.1 to 606.4)	0.534	208.2 (179.8 to 242.4)	0.249
2.398	At1g52200	expressed protein	503.8 (449.8 to 572.6)	0.535	213.1 (178.4 to 273.8)	0.233
2.295	At5g46330	leucine-rich repeat protein kinase	70.33 (48.97 to 81.23)	0.366	30.36 (23.05 to 35.91)	0.301
2.294	At1g51790	leucine-rich repeat protein kinase	65.48 (57.32 to 80.62)	0.546	28.36 (24.29 to 31.86)	0.279
2.178	At2g05540	glycine-rich protein	691.2 (644.6 to 740.5)	0.687	319.7 (264.7 to 366.5)	0.234
2.169	At5g39580	peroxidase, putative	87.63 (61.42 to 102.7)	0.369	39.7 (35.42 to 47.05)	0.247
2.13	At2g39200	MLO12 family protein	122.5 (110.4 to 135.4)	0.594	58.25 (44.41 to 67.15)	0.215

Supplemental Table 2 (continued)

2.111	At5g06980	expressed protein	194.8 (160.5 to 260.4)	0.525	93.46 (60.42 to 118.2)	0.203
2.109	At2g05380	glycine-rich protein (GRP3S)	5.465 (4.735 to 6.144)	0.461	2.588 (2.297 to 2.886)	0.24
2.074	At5g44130	fasciclin-like arabinogalactan-protein	379.9 (298.4 to 434.9)	0.367	181.2 (172.3 to 198.8)	0.241
2.041	At1g24260	MADS-box protein (AGL9)	52.42 (43.9 to 57.07)	0.511	26.25 (21.59 to 35.52)	0.314

B. Genes that are repressed in *fbp7-3*

<u>Fold Change</u>	<u>Accession</u>	<u>Putative Gene Function</u>	<u><i>fbp7-3</i> raw data</u>	<u>t-test p-value</u>	<u>wild type raw data</u>	<u>t-test p-value</u>
0.0713	At1g21760	F-box family protein (AtFBP7)	27.76 (19.27 to 33.86)	0.0264	378.8 (373.3 to 387.6)	0.143
0.103	At3g15310	expressed protein	5.147 (0.966 to 13.25)	0.122	24.29 (20.86 to 27.03)	0.0977
0.124	At1g36920	hypothetical protein	7.239 (1.064 to 12.3)	0.118	39.26 (32.52 to 49.75)	0.0744
0.223	At2g41260	glycine-rich protein	42.04 (31.3 to 49.79)	0.0222	244.9 (80.48 to 494.5)	0.145
0.238	At1g73190	tonoplast intrinsic protein	48.55 (29.54 to 79.82)	0.0199	211.5 (104.8 to 364)	0.149
0.283	At2g02850	plantacyanin, putative	76.26 (66.36 to 90.95)	0.0184	270.7 (211.3 to 313.2)	0.146
0.307	At2g02120	plant defensin-fusion protein	46.03 (34.75 to 60.81)	0.0266	153.9 (105.8 to 226.2)	0.139
0.315	At3g04990	hypothetical protein	0.413 (0.243 to 0.7)	0.844	2.461 (0.275 to 6.163)	0.656
0.367	At1g08830	superoxide dismutase (Cu-Zn)	490.2 (424.6 to 589.9)	0.0175	1,331 (1,119 to 1,499)	0.164
0.381	At1g24070	glycosyl transferase family 2 protein	120.5 (92.02 to 150.2)	0.0206	312.3 (265.1 to 339.2)	0.155
0.408	At2g38905	low temperature responsive protein	17.38 (14.4 to 19.79)	0.0671	42.85 (35.26 to 53.39)	0.0675
0.409	At4g15440	hydroperoxide lyase (HPL1)	328 (236.9 to 398.7)	0.0198	785.8 (710.4 to 876.1)	0.164
0.414	At1g17180	glutathione S-transferase	83.95 (75.26 to 95.12)	0.0267	204.1 (167.9 to 243.8)	0.147
0.421	At1g66100	thionin, putative	83.41 (55.49 to 97.69)	0.0161	194.4 (157 to 235)	0.137
0.426	At4g33730	pathogenesis-related protein	22.72 (13.34 to 37.55)	0.0732	48.24 (45.09 to 51.43)	0.0975
0.432	At3g13784	beta-fructosidase, putative	20.96 (8.07 to 30.37)	0.16	44.62 (27.95 to 64.73)	0.0962
0.449	At4g19690	iron-responsive transporter (IRT1)	59.57 (43.15 to 87.01)	0.0159	133.2 (89.93 to 195.2)	0.107
0.456	At1g21770	expressed protein	445.7 (368.4 to 500.9)	0.0328	972.3 (884.1 to 1,018)	0.169
0.462	At1g72260	thionin (THI2.1)	267.9 (184.3 to 418.7)	0.0343	547.7 (446.5 to 668.6)	0.167
0.468	At5g42800	dihydroflavonol 4-reductase	30.4 (24.58 to 34)	0.0401	66.88 (43.31 to 85.24)	0.0826
0.478	At2g28190	superoxide dismutase (Cu-Zn)	338.6 (311.3 to 363.8)	0.0238	710.5 (640.1 to 812.9)	0.162
0.481	At5g04150	bHLH family protein	107.8 (87.37 to 127.6)	0.0195	231 (160.2 to 322.4)	0.136
0.489	At3g28270	expressed protein	519.2 (352.3 to 634.3)	0.0154	1,049 (886.3 to 1,344)	0.164
0.492	At1g49860	glutathione S-transferase	127 (101.2 to 157.2)	0.0289	254.7 (231.8 to 277.9)	0.155

III.III. Schwager et al., (manuscript of a research article)

Katja M. Schwager, Luz Irina A. Calderón Villalobos, Esther M.N.

Dohmann, Stephan Knierer, Carola Kuhnle, and Claus

Schwechheimer

**Characterization of the *VIER F-BOX PROTEINE (VFB)* genes
from *Arabidopsis* reveals their importance for plant growth
and development**

(Submitted to *Plant Cell*)

Characterization of the *VIER F-BOX PROTEINE (VFB)* genes from *Arabidopsis* reveals their importance for plant growth and development.

Katja M. Schwager, Luz Irina A. Calderon-Villalobos, Esther M. N. Dohmann, Stephan Knierer, Carola Kuhnle, and Claus Schwechheimer¹

Department of Development Genetics, Centre for Plant Molecular Biology, Tübingen University, Auf der Morgenstelle 5, 72076 Tübingen, Germany.

¹ To whom correspondence should be addressed: Phone: ++49 7071 2976669; Fax: ++49 7071 295135; Email: claus.schwechheimer@zmbp.uni-tuebingen.de

Word count (excluding references): 7231 words

Running title: Arabidopsis VFB F-box proteins

The author responsible for distribution of materials integral to the findings presented in this article in accordance with the policy described in the Instructions for Authors (www.plantcell.org) is: Claus Schwechheimer (claus.schwechheimer@zmbp.uni-tuebingen.de).

VIER F-BOX PROTEINE (VFB) is registered as a gene class symbol at www.arabidopsis.org.

Abstract

Eukaryotes use the ubiquitin-proteasome system for regulated protein degradation. E3 ubiquitin ligases (E3s) function as the degradation substrate receptors of the ubiquitin-proteasome system. In the SKP1/CDC53/F-box protein (SCF) E3 ligase complexes, the interchangeable F-box protein subunit recognizes the degradation substrate receptor and thereby confers specificity to the complex. The vast majority of the 694 F-box proteins encoded by the *Arabidopsis thaliana* genome remains to be characterized. Here, we characterize the *VIER F-BOX PROTEINE* (*VFB*; German for *FOUR F-BOX PROTEINS*) genes from *Arabidopsis* whose gene products are part of subfamily C3 of the *Arabidopsis* F-box protein superfamily. This subfamily also includes the F-box proteins TRANSPORT INHIBITOR RESISTANT1 (TIR1)/AUXIN SIGNALING F-BOX PROTEINS (AFBs) as well as the EIN3 BINDING FACTOR F-BOX (EBF) proteins, which have been shown to regulate auxin and ethylene responses, respectively. We show that loss of *VFB* function causes delayed plant growth and reduced lateral root formation. The expression of a number of auxin responsive genes is reduced in the *vfb* mutants indicating that VFB proteins may be required for proper auxin response. This hypothesis finds support in our observation that the activity of the auxin response reporter DR5:GUS is reduced in *vfb* mutants. Since we were unable to functionally complement the *tir1-1* mutant with *VFB2*, we propose that VFBs and TIR1/AFB F-box proteins regulate auxin responses via distinct mechanisms. (221 words)

Introduction

Eukaryotes use the ubiquitin-proteasome system for the targeted proteolysis of regulatory proteins such as cell cycle regulators and transcription factors (Hershko and Ciechanover, 1998; Schwechheimer and Schwager, 2004). Protein degradation by the 26S proteasome is generally preceded by the polyubiquitylation of the proteins targeted for degradation. Polyubiquitylation is the result of the consecutive activities of an E1 ubiquitin activating enzyme (E1), an E2 ubiquitin conjugating enzyme (E2) and an E3 ubiquitin ligase (E3)(Hershko and Ciechanover, 1998). E3s confer specificity to the system in that they specifically recognize the degradation targets and bring them into the vicinity of E2 enzymes for polyubiquitylation (Deshaies, 1999; Cardozo and Pagano, 2004; Schwechheimer and Villalobos, 2004).

Different types of E3 ligases have been described in eukaryotes. The so-called Cullin-RING E3s include the SCF (SKP1, CDC53, F-Box protein), VCB (Von-Hippel-Lindau, Elongin C, Elongin B), BTB/POZ (Bric-a-Brac, Tramtrack and Broad Complex/Pox Virus and Zinc-Finger) and DCX (Damaged DNA Binding Protein1, Cullin 4A, X-Box) complexes (Deshaies, 1999; Kamura et al., 1999; Higa et al., 2003; Xu et al., 2003; Cardozo and Pagano, 2004; Wertz et al., 2004). Common to these Cullin-RING E3s are the RING BOX1 (RBX1) and Cullin subunits (Cullin1 in SCF; Cullin2 or Cullin 5 in VCB; Cullin 3 in BTB/POZ; Cullin 4 in DCX). For each Cullin-RING E3, substrate specificity is brought about by the association of the Cullin-RBX1 core complex with specific substrate receptor proteins such as the F-box proteins in the case of SCF complexes.

Cullins are modified by the ubiquitin-related protein NEDD8 (neddylation) (Hori et al., 1999). Neddylation is essential for survival in higher eukaryotes (Osaka et al., 2000; Podust, 2000; Dharmasiri et al., 2003; Chiba and Tanaka, 2004). Although some experiments indicate that neddylation may control the assembly of E3 complexes or the association of E3 ligases with E2 ubiquitin conjugating enzymes, it appears that the precise role of neddylation for E3 function is at present not understood (Kawakami et al., 2001; Liu et al., 2002; Zheng et al., 2002a; Oshikawa et al., 2003; Cheng et al., 2004; Chuang et al., 2004; Feng et al., 2004; Min et al., 2005). NEDD8 is deconjugated from the Cullins (deneddylation) through the activity of COP9 signalosome (CSN) subunit 5 (CSN5) (Lyapina et al., 2001; Schwechheimer et al., 2001; Cope et al., 2002; Schwechheimer et al., 2002; Chiba and Tanaka,

2004; Gusmaroli et al., 2004; Dohmann et al., 2005a). Multiple studies from a range of organisms have shown that CSN interacts with Cullin-RING E3s and that proper E3 function is dependent on CSN and more specifically on CSN5-mediated deneddylation (Lyapina et al., 2001; Schwechheimer et al., 2001; Schwechheimer, 2004). Some recent studies suggest that deneddylation is required for E3 subunit stability or E3 complex assembly (Hetfeld et al., 2005; Wee et al., 2005; Wu et al., 2005). However, it has also been proposed that CSN is part of a proteasome-related complex (Peng et al., 2001; Peng et al., 2003). Regardless of its precise molecular mode of action, it can be said that CSN acts as a global regulator of Cullin-RING E3 activities. Loss of CSN in higher eukaryotes causes severe growth defects (Freilich et al., 1999; Lykke-Andersen et al., 2003; Schwechheimer, 2004; Tomoda et al., 2004; Dohmann et al., 2005a). Since it is expected that hundreds of Cullin-RING E3 functions are impaired in the respective *csn* mutants, these severe phenotype may be the result of the combined defects caused by the loss of individual E3 activities.

F-box proteins are the interchangeable substrate receptor subunits of SCF-type E3s (Deshai, 1999; Skowyra et al., 1999; Cardozo and Pagano, 2004). The F-box domain, which is typically located at the protein's N-terminus, serves for interactions with the adaptor protein of the Suppressor of Kinetochore1 (SKP1) protein family (Bai et al., 1996; Cardozo and Pagano, 2004). In addition, most F-box proteins contain recognizable protein-protein interaction domains such as leucine-rich repeats, WD40 repeats, or KELCH repeats that are thought to mediate interactions with the degradation substrates (Gagne et al., 2002; Jin et al., 2004). The Arabidopsis genome is predicted to encode 694 F-box proteins suggesting that protein degradation via SCF complexes is an important control mechanism in plants (Gagne et al., 2002). To date, the biological function of only approximately 20 F-box proteins has been elucidated based on available Arabidopsis mutants (Schwechheimer and Villalobos, 2004). These F-box proteins have been implicated in a wide range of physiological processes such as cell cycle control, circadian rhythms, floral development as well as many phytohormone responses.

The C3 subfamily of Arabidopsis F-box proteins is the best characterized F-box protein family from Arabidopsis. Most members of this family contain leucine-rich repeats as protein-protein interaction domains (Gagne et al., 2002). This subfamily includes AtSKP2;1 and AtSKP2;2, the putative Arabidopsis orthologues of the

mammalian SKP2 protein, which mediates the degradation of E2F transcription factor during the cell cycle (Marti et al., 1999b; del Pozo et al., 2002a). However, an unexpectedly large fraction of SKP2 relatives from this protein family has been shown to regulate plant hormone responses: TRANSPORT INHIBITOR RESISTANT1 (TIR1) and its three orthologues designated AUXIN SIGNALING F-BOX PROTEIN1 - 3 (AFB1 – AFB3) mediate the degradation of AUX/IAA repressors in response to auxin (Ruegger et al., 1998; Dharmasiri et al., 2005a; Dharmasiri et al., 2005b; Kepinski and Leyser, 2005). CORONATINE INSENSITIVE1 (COI1) controls the degradation of an as yet unknown protein in response to jasmonates (Xie et al., 1998). EIN3-BINDING F-BOX1 (EBF1) and EBF2 regulate ethylene signaling via degradation of the transcription factor ETHYLENE INSENSITIVE3 (EIN3) (Guo and Ecker, 2003; Potuschak et al., 2003; Gagne et al., 2004a). Some members of the C3 subfamily remain to be characterized. We were interested in an F-box protein family of the C3 subfamily, which we designated VIER F-BOX PROTEINE (VFB; *German for FOUR F-BOX PROTEINS*) (Gagne et al., 2002). We found that plants defective in all four *VFB* genes are delayed in general growth and are defective in lateral root formation. Transcript profiling indicated that a significant number of auxin responsive proteins is repressed in these mutants suggesting that the VFB proteins act upstream of auxin responses.

Results

Characterization of the VFB F-box protein family: The four F-box proteins At1g47056, At3g50080, At4g07400 and At5g67250 share significant sequence similarities (56% – 69% identity, 63% – 80% similarity) and together they form a distinct F-box protein family within the C3 subfamily of the Arabidopsis F-box protein superfamily (Figures 1A and 1C) (Gagne et al., 2002). We named this previously uncharacterized protein family VIER F-BOX PROTEINE (VFB), which is German for FOUR F-BOX PROTEINS, and we designated its individual members VFB1 (At1g47056), VFB2 (At3g50080), VFB3 (At4g07400), and VFB4 (At5g67250). The F-box proteins of the C3 subfamily also includes the cell cycle regulatory AtSKP2 proteins, the TIR1/AFB auxin receptor F-box proteins as well as the ethylene

response F-box proteins EBF1 and EBF2 (Figure 1C) (Xie et al., 1998; del Pozo et al., 2002a; Guo and Ecker, 2003; Potuschak et al., 2003; Gagne et al., 2004a; Dharmasiri et al., 2005a; Kepinski and Leyser, 2005). A unifying feature of these F-box proteins is the presence of an N-terminal F-box domain followed by a series of leucine-rich repeats (LRRs), which are predicted to interact with the respective degradation substrates (Figure 1B). We failed to identify non-plant proteins with a clear homology to the Arabidopsis VFB proteins. However, we found one putative tobacco homologue designated AVR9/CF-9 RAPIDLY ELICITED PROTEIN 189 (ACRE189) as well as two putative rice homologues ACRE189 and JNBb0002J11.1 (Figure 1C) (Navarro et al., 2004). Since we have been unable to assign these proteins unequivocally to a specific Arabidopsis VFB protein, we assume that the Arabidopsis VFBS and their putative orthologues from tobacco and rice originate from a common ancestor.

VFB2 interacts with the SCF-complex adaptor protein ASK2 and localizes to the cytoplasm: F-box proteins are the substrate receptors of SCF-type E3 complexes. F-box proteins interact via their F-box domain with the evolutionarily conserved SKP1 adaptor protein, which in turn binds to the Cullin1 subunit of SCF complexes (Bai et al., 1996; Deshaies, 1999; Zheng et al., 2002b; Risseuw et al., 2003). SCF complexes obtain distinct substrate specificities by association of the SKP1 adaptor with specific F-box proteins (Deshaies, 1999; Skowyra et al., 1999). In order to show that the VFB proteins have retained the ability to bind SKP1 proteins, we selected VFB2 as a representative family member and examined its interaction with ARABIDOPSIS SKP1-2 (ASK2), a predominant member of the Arabidopsis SKP1 protein family, using the yeast two-hybrid system (Risseuw et al., 2003; Zhao et al., 2003). Our analysis revealed a strong interaction between VFB2 and ASK2 but not between VFB2 and the two other SCF complex components AtRBX1 and AtCUL1 (Figure 2A) (del Pozo and Estelle, 1999; Schwechheimer et al., 2002; Risseuw et al., 2003). As expected, a VFB2 deletion variant lacking the F-box domain (VFB2 Δ F-box) failed to interact with ASK2 in the yeast assay (Figure 2A). Due to the high sequence conservation between the individual VFB family members, we are certain that these findings also hold true for VFB1, VFB3, and VFB4 proteins and suggest that these proteins act as F-box protein subunits of SCF^{VFB} complexes.

In order to examine the subcellular localisation of the VFB proteins, we generated constructs for the expression of VFB2:GREEN FLUORESCENT PROTEIN (GFP) and YELLOW FLUORESCENT PROTEIN (YFP):VFB2 fusion proteins under the control of the constitutive 35S CAULIFLOWER MOSAIC VIRUS (35S CaMV) promoter. We had to refrain to transient transformation of Arabidopsis protoplasts for the analysis of these constructs since repeated attempts to generate stable Arabidopsis transformants failed. Localization experiments with both constructs showed that the fusion proteins accumulate in the cytoplasm and are excluded from the nucleus (Figure 2B and data not shown). This finding invites the hypothesis that VFB2 acts in the cytoplasm. However, since we could not confirm the functionality of the fusion constructs e.g. by mutant complementation, these results have to be treated with the appropriate caution.

VFB gene expression: To examine the expression pattern of the four *VFB* genes, we fused 1 kb promoter fragments of each *VFB* gene to the β -glucuronidase (GUS) reporter. At least 10 transgenic lines were generated and analysed for each construct. While the promoter:GUS constructs for *VFB1*, *VFB2*, and *VFB4* showed strong GUS staining in the vascular system of hypocotyls, leaves, flowers and roots, the *VFB3*:GUS construct stained very weakly in any tissue type examined (Figures 3B – 3G). Interestingly, *VFB2* and *VFB4* also seem to be expressed in the cotyledons of bent cotyledon stage embryos but not at earlier stages of embryo development (Figure 3A).

Throughout this analysis, the impression arose that *VFB2* and *VFB4* have very similar staining patterns. We supported this observation by an analysis of publically available microarray data, which revealed an obvious correlation of the expression of *VFB2* and *VFB4* (Figure 4A) (Zimmermann et al., 2004). In a set of 1021 experiments with the Affymetrix ATH1 GeneChip, both genes were found to be expressed at high levels in the vast majority of tissue-types and experimental conditions examined. In contrast and as predicted by the *VFB3*:GUS analysis, *VFB3* is only weakly expressed in most tissue-types and experimental conditions (Figures 4B and 4C). Since *VFB1* is not represented on the Affymetrix ATH1 GeneChip, *VFB1* could not be included in this analysis. Taken together the expression analysis showed that *VFB1*, *VFB2*, and *VFB4* are actively transcribed members of this gene family, that *VFB2* and *VFB4*

expression is correlated, and that *VFB3* is the least strongly expressed gene of this family.

One previous report had identified *VFB4* as *AVR9/CF-9 RAPIDLY ELICITED PROTEIN189 (ACRE189)*, a gene that is induced after treatment of Arabidopsis cell cultures and seedlings with the bacterial elicitor peptide flagellin-22 (flg22)(Navarro et al., 2004). To substantiate these findings, we examined the expression of *VFB4* by semi-quantitative reverse transcription followed by polymerase chain reaction (RT-PCR). Consistent with the previous report, we observed a transient induction of *VFB4* expression two hours after flg22 induction (Figure 3H). *VFB4* may therefore be part of a plant defense response to bacterial attack.

***vfb1 vfb2 vfb3* triple mutants show no apparent growth defects:** To study the role of the *VFB* genes in plant growth and development, we identified and characterized T-DNA insertion mutant lines available for the four *VFB* genes (Figure 5A). We identified homozygous T-DNA insertion mutants for *VFB1* (SALK_128933, *vfb1-1*), *VFB2* (SALK_047600, *vfb2-1*), *VFB3* (SALK_054809, *vfb3-1*), and *VFB4* (GABI_414F09; *vfb4-1*). Using gene specific RT-PCRs, we then confirmed the absence of the respective full length transcript in *vfb1-1*, *vfb2-1*, and *vfb3-1*, which carry insertions in the only exon of the respective gene (Figure 5B). In contrast, *VFB4* expression appeared to be unaltered in the *vfb4-1* allele, which carries a T-DNA insertion 26 base pairs upstream of the ATG start codon and concluded that *vfb4-1* is not a *VFB4* knock-down or knock-out allele (Figure 5B). In any of the respective single mutants, we failed to detect apparent mutant phenotypes even when the mutants were subjected to a wide range of growth assays and physiological tests including all major phytohormone and stress treatments (Figure 5D). We therefore reasoned that the *VFB* genes may have redundant function and generated double mutant combinations and finally also a *vfb1-1 vfb2-1 vfb3-1* triple mutant (Figure 5C). However, neither of these mutants revealed any apparent defects in any experimental condition tested (Figure 5D).

Suppression of *VFB4* by RNAi causes growth defects: Since the mutant combinations generated so far did not include a mutant of the *VFB4* gene and since we knew that *VFB4* is a strongly expressed family member, we used RNA

interference (RNAi) to suppress *VFB4* function. For this purpose, a 114 base pair fragment of the *VFB4* 3'-terminus, the region with the highest sequence divergence between all four *VFB* genes, was selected to generate *vfb4* RNAi (Figure 6A). The *vfb4* (RNAi) transgene was introduced into the wild type and the *vfb1-1 vfb2-1 vfb3-1* triple mutant, and 20 transgenic lines were generated in each background. By semi-quantitative RT-PCR, we then showed a reduction of *VFB4* gene expression in these plants (Figure 6B). The analysis of the progeny of the *vfb4* (RNAi) and *vfb1-1 vfb2-1 vfb3-1 vfb4* (RNAi) transgenic plants revealed defects in lateral root formation in the seedlings and, in the case of the *vfb1-1 vfb2-1 vfb3-1 vfb4* (RNAi) plants, also a delay in root elongation as well as a general delay in plant growth as illustrated e.g. by their reduced rosette size at early stages of vegetative growth (Figures 6C – 6L). Cross sections of leaves indicated that the growth defects observed in the *vfb1-1 vfb2-1 vfb3-1 vfb4* (RNAi) mutants are due to a reduction in cell size and not due to a reduction of cell cycle activity (Figure 6M). Taken together, we showed that the *VFB4* gene in combination with the other three family members is required for normal plant growth.

Gene expression profiling of the *vfb* mutants: In order to gain an insight into the molecular mechanisms that underlie the phenotype observed in the *vfb1-1 vfb2-1 vfb3-1 vfb4-1*(RNAi) mutants (*vfb* mutants), we carried out gene expression profiling using Affymetrix ATH1 GeneChips of 10 day-old *vfb* mutant and wild type seedlings. This study identified 193 genes that are at least two-fold repressed and 179 genes that are at least two-fold induced in the mutant when compared to the wild type (Supplemental Tables 1 and 2). While the gene products of the misregulated genes have a wide variety of biochemical functions ranging from ABC transporters to CONSTANS-like zinc finger transcription factors, we noted that two gene families are overrepresented within the group of repressed genes, namely auxin response and signalling genes (12 genes; Table 1) and genes encoding cell wall metabolic enzymes (17 genes; Table 2).

The group of repressed auxin signalling genes includes the AUX/IAA repressors *IAA29*, *IAA19* (*MASSUGU2*, *MSG2*), *IAA6* (*SHORT HYPOCOTYL1*, *SHY1*), *IAA3* (*SHY2*), *IAA2*, and *IAA4* as well as six *SMALL AUXIN UP RNAs* (*SAURs*) (Gil et al., 1994; Leyser et al., 1996; Tian and Reed, 1999; Tatematsu et al.,

2004). The *AUX/IAA* genes encode unstable repressors that control the expression of auxin-induced genes in the absence of auxin (Reed, 2001; Tiwari et al., 2004). The expression of most *AUX/IAA* and at least some *SAUR* genes is induced by auxin, and *AUX/IAA* proteins repress their own transcription as part of a negative feedback mechanism (Reed, 2001; Tiwari et al., 2004). While the expression of cell wall metabolic enzyme genes is not under auxin control, all *AUX/IAA* and *SAUR* genes identified in our study are auxin induced as confirmed by analysis of publicly available expression data (Zimmermann et al., 2004). Since this finding suggested that the *VFB* genes act upstream of auxin response, we introduced the DR5:GUS reporter into the *vfb* mutant background (Ulmasov et al., 1997b). The DR5:GUS construct contains multiple binding sites for AUXIN RESPONSE FACTOR transcriptional activators whose activities are repressed by the *AUX/IAA* repressors (Ulmasov et al., 1997a). In agreement with previous reports, we detected strong DR5:GUS staining in the leaf margins, at sites of lateral root emergence and in root tips of wild type seedlings. However, the staining at these sites was strongly reduced in the *vfb* mutant background suggesting that the *VFB* protein function is required for the proper induction of auxin response genes (Figure 7A – 7F).

Auxin response via proteasomal degradation of *AUX/IAA* proteins is controlled by the auxin receptor F-box protein TIR1 and its three AFB orthologues (Dharmasiri et al., 2005a; Kepinski and Leyser, 2005). Similar to the *vfb* mutants, *tir1* mutants have fewer lateral roots than the wild type and fail to induce auxin-induced genes efficiently (Ruegger et al., 1998). In addition, *tir1-1* mutants are auxin insensitive when grown on auxin containing medium. To see whether the *vfb* mutants also share this feature of the *tir1-1* mutant phenotype, we tested auxin-sensitivity in *vfb* mutants. However, this analysis showed that the *vfb* mutants have normal auxin sensitivity and we therefore concluded that *VFB* proteins may not function together with TIR1/AFB in mediating auxin responses (Figure 7G). This conclusion was substantiated by the fact that we were unable to rescue the *tir1-1* mutant phenotype by overexpression of the *VFB2* gene in the mutant background (data not shown). In summary, these experiments suggest that the *VFB* genes are required for proper auxin response and that they function through a mechanism, which is distinct from that of the auxin receptor TIR1/AFB proteins.

A partial overlap between the gene expression defects of *vfb* mutants and mutants of the COP9 signalosome: The COP9 signalosome (CSN) interacts with SCF-type E3 ubiquitin ligases and is required for proper E3 activity (Schwechheimer et al., 2001). Arabidopsis mutants which lack CSN function have severe phenotypes that ultimately lead to growth arrest at the early seedling stage (Kwok et al., 1996; Schwechheimer, 2004; Dohmann et al., 2005a). Since Arabidopsis may contain close to one thousand different Cullin-RING E3s, the phenotype of the CSN mutants may be the combination of the growth defects conferred by malfunction of the individual E3-dependent pathways. Since CSN can be viewed as a global regulator of E3 activities, genes that are misexpressed in *vfb* mutants as identified above are expected to represent, at least in part, a fraction of the genes that are misexpressed in mutants of CSN (Schwechheimer et al., 2001; Schwechheimer et al., 2002; Dohmann et al., 2005b). We tested this hypothesis by comparing the gene expression changes between *vfb* mutants and *csn4* mutants that are deficient in CSN function since they carry a CSN destabilizing mutation in CSN subunit 4 (CSN4). In this comparative analysis, we identified a total of 87 genes that are repressed and 66 genes that are induced in both mutants (Supplemental data Tables 3 and 4). The list of genes whose expression is misregulated in both mutants includes many as yet uncharacterized signalling components and transcriptional regulators (Table 2). Most importantly, however, this list also includes four *AUX/IAA* genes, five *SAUR* genes as well as 11 genes that encode cell wall metabolic enzymes. Therefore, these gene families seem to represent common downstream targets of VFB F-box proteins and CSN.

Discussion

The four VFB proteins belong to the C3 subfamily of the Arabidopsis F-box protein superfamily: In the present study, we have characterized the four VFB F-box proteins from Arabidopsis. The VFB proteins form a distinct protein family within the C3 subfamily of Arabidopsis F-box proteins. The VFB proteins and the other *bona fide* members of this subfamily contain leucine-rich repeat domains for degradation substrate interaction (Gagne et al., 2002). Interestingly, this family also includes the predicted Arabidopsis orthologues of the human cell cycle regulatory F-box protein

SKP2. SKP2 in humans is required for the degradation of the cell cycle transcriptional regulator E2F as well as the cell cycle inhibitors p27^{Kip1} and p21^{Cip1} (Marti et al., 1999a; Sutterluty et al., 1999; Ungermannova et al., 2005; Wang et al., 2005). While the Arabidopsis genome does not contain clear orthologues of p27^{Kip1} and p21^{Cip1}, the E2F regulators are conserved in plants (del Pozo et al., 2002a). In addition, the degradation of the E2F transcription factors by the Arabidopsis SKP2 orthologues AtSKP2,1 and AtSKP2,2 appears to be also conserved between humans and plants and therefore these proteins may represent one evolutionary link to the human F-box protein family (del Pozo et al., 2002a).

While humans contain only 21 F-box proteins with leucine-rich repeat domains, plants seem to have undergone a dramatic expansion of this F-box protein family (Jin et al., 2004). The most exhaustive survey of this protein family predicts a total 202 leucine-rich repeat containing F-box proteins (Gagne et al., 2002). Plants seemingly have recruited F-box proteins of the C3 subfamily as regulators of plant specific pathways such as phytohormone responses, axillary branching and senescence (Xie et al., 1998; Woo et al., 2001; Stirnberg et al., 2002; Guo and Ecker, 2003; Potuschak et al., 2003; Gagne et al., 2004b; Dharmasiri et al., 2005a; Dharmasiri et al., 2005b; Kepinski and Leyser, 2005). Furthermore, our study suggests that the previously uncharacterized VFB proteins are plant growth regulators with an important role in controlling lateral root formation and plant growth in general. The close evolutionary relationship between the cell cycle regulatory AtSKP2 proteins and the other family members of the C3 subfamily invites the hypothesis that also these plant-specific F-box proteins may control plant growth by affecting cell cycle activity. However, while this hypothesis may potentially hold true for some members of this F-box protein family including the TIR1/AFBs and the VFBs it is very unlikely for others.

The proteins that are targeted for degradation by the VFBs remain to be identified. Molecular and genetic approaches may be used to identify such degradation targets. We have screened a yeast two-hybrid system library to search for interactors. However, this screen only resulted in the isolation of several ASK1 and ASK2 clones. That, in principle, such an approach is functional for this class of F-box proteins was demonstrated by the successful identification of EIN3 in a screen with the F-box proteins EBF1 and EBF2 (Potuschak et al., 2003). If however the

interacting substrate or the F-box protein requires a plant-specific post-translational modification for interaction, such a screen may not be fruitful in the heterologous yeast system. A second approach for the identification of degradation substrates would be a screen for suppressors of the *vfb* mutant phenotype. However, such a suppressor screen is only useful in a genetically stable background. In order to obtain such a stable mutation, we are currently trying to knock-out *VFB4* function through mobilization of an activatable DISSOCIATOR (DS) insertion element that is located 10 kilobases from the *VFB4* gene.

Auxin-induced genes are repressed in *vfb* mutants: Mutants deficient in *VFB* function lack lateral roots. Lateral root formation requires a functional auxin pathway and numerous auxin-signaling mutants with reduced lateral root formation have been identified. These include mutants that express stabilized versions of the AUX/IAA regulators IAA3/SHY2 and IAA19/MSG2 and loss-of-function mutants of the proteins required for AUX/IAA degradation including the TIR1/AFB F-box proteins, the proteins required for the neddylation of the SCF Cullin subunit and the proteins required for Cullin deneddylation, notably the COP9 signalosome (CSN) (Leyser et al., 1993; Tian and Reed, 1999; Gray et al., 2001; Schwechheimer et al., 2001; del Pozo et al., 2002b; Tian et al., 2003; Zenser et al., 2003; Tatematsu et al., 2004; Dharmasiri et al., 2005a; Dharmasiri et al., 2005b; Fukaki et al., 2005; Kepinski and Leyser, 2005). In the absence of auxin, AUX/IAA proteins repress their own expression as well as the expression of other auxin-induced genes. In the presence of auxin, AUX/IAA repressors are degraded allowing the expression of auxin-induced genes. Due to the stabilization of the AUX/IAA proteins in the various mutants mentioned above, auxin induced gene expression is not efficient in these mutants (Tian et al., 2002; Overvoorde et al., 2005). We observed a similar repression of *AUX/IAA* and auxin-induced genes in the *vfb* mutants. We therefore tested the hypothesis that *VFB* F-box proteins are also required for AUX/IAA degradation. However, our attempts to rescue *tir1-1* mutants by *VFB2* overexpression failed and we concluded that the *VFB* proteins cannot functionally replace TIR1. Furthermore, our fluorescent protein fusions with *VFB2* indicate that these proteins act in the cytoplasm. Identical protein fusions for TIR1 had shown that these proteins are active in the nucleus (Dharmasiri et al., 2005a; Dharmasiri et al., 2005b). Although their

different subcellular localization does not exclude the possibility that both proteins target the same substrates for degradation, it renders it very unlikely that both proteins can exert the same functions within the cell. We therefore suggest that the VFB proteins are required for proper auxin signaling but function through a mechanism that is distinct from that of the TIR1/AFB proteins.

Our microarray analysis also revealed that a number of cell wall metabolic genes are misregulated in the *vfb* mutants. Interestingly, a recent gene expression analysis of the *axr3-1/iaa17-1* gain-of-function mutants also showed the repression of a broad set of cell wall metabolic enzyme genes in this mutant (Overvoorde et al., 2005). Since the analysis of microarray data indicated that the expression of these cell wall metabolic enzyme genes is not induced by auxin, it may be that this gene expression pattern is a molecular consequence of an interrupted developmental program that is common to both types of mutants, such as the failure to efficiently induce lateral root formation.

A specific subset of genes is misregulated in *vfb* and *csn* mutants: CSN is an evolutionarily conserved regulator of Cullin-RING E3 activity. Arabidopsis *csn* mutants are characterized by their constitutive photomorphogenic phenotype, which includes loss of skotomorphogenic growth, chloroplast differentiation, and the expression of light-induced genes in the dark-grown seedlings (Chamovitz et al., 1996; Kwok et al., 1996). The seedling lethal *csn* mutants also fail to develop a proper root as well as lateral roots. This severe pleiotropic phenotype can be considered as the result of the malfunction of the hundreds of Cullin-RING E3s that can be formed in Arabidopsis (Schwechheimer and Villalobos, 2004). In plants, SCF^{TIR1}, SCF^{COI1}, and SCF^{UFO} have already been shown to interact physically with CSN (Schwechheimer et al., 2001; Feng et al., 2003; Wang et al., 2003). This taken together with numerous reports from other eukaryotes strongly suggests that all Cullin-RING E3 function in a CSN-dependent manner (Schwechheimer, 2004). We have examined whether there is a significant overlap between the misexpressed genes in the *vfb* mutants and the misexpressed genes in the *csn* mutants. We found that 153 genes, thus approximately one third of the misexpressed genes from *vfb* mutants, are also misexpressed in the *csn* mutants. Strikingly, the group of repressed genes includes a number of genes whose expression is normally controlled by auxin.

Therefore, this analysis identified reduced auxin response as a common denominator of both types of mutants. Reduced auxin responses in the *csn* mutants have so far been explained by defects in SCF^{TIR1} activity (Schwechheimer et al., 2001). However, the result of the present study indicates that SCF^{VFB} complexes may also participate in auxin responses and that SCF^{VFB} misfunction may account at least in part for the repression of auxin-induced gene expression observed in the *csn* mutants. In the same context, it should also be noted that the repression of auxin-induced gene expression is generally much stronger in the *csn* mutants than it is in the *vfb* mutants.

A limitation of the microarray approach is that it generally does not allow to distinguish between immediate early gene expression changes and late changes that are the result of non-functional downstream events. Nevertheless, these studies are very insightful and through gene expression profiling of more and more E3 mutants we will slowly but steadily obtain a very precise understanding of the genes that are controlled by the individual proteolysis-dependent components.

Materials and Methods

Biological material and T-DNA insertion mutants: All experiments were performed using *Arabidopsis thaliana* ecotype Columbia. The T-DNA insertion mutants SALK_128933 (*vfb1-1*), SALK_047599 (see below), SALK_047600 (*vfb2-1*), and SALK_054809 (*vfb3-1*) were identified in the SIGNAL database and obtained from the Nottingham Arabidopsis Stock Centre (NASC). The T-DNA insertion line GABI_414F09 (*vfb4-1*) was identified and obtained from the GABI-KAT collection. T-DNA insertions in the SALK lines were verified using the primer LbB1 5'-GCGTGGACCGCTTGCTGCAACT-3' in combination with the primers 5'-ATCGATAGGTAAGCATCACGCTAACGAAT-3' (SALK_128933; *vfb1-1*), 5'-ATGGGCCAAGCTCCGTCGTCTCCGGCGGAACCAAACGTA-3' (SALK_047600; *vfb2-1*), and 5'-GCCGGCTACTGGCTTCGACTTGATTCTGA-3' (SALK_054809; *vfb3-1*). We were unable to confirm the predicted T-DNA insertion of SALK_047599 in *VFB2*. The T-DNA insertion of GABI_414F09 (*vfb4-1*) was confirmed and analysed using the primers GABI T-DNA 5'-CCCATTTGGACGTGAATGTAGACAC-3' and the two gene specific primers 5'-ATATTGACCATCATACTCATTGC-3' and 5'-AGTAGAACTACTA GCATTATCATTGTGAGACCA -3. Double and triple mutant

combinations were obtained by crosses of the respective single mutants and T-DNA insertions in the respective loci were followed using PCR genotyping. A reporter line expressing the DR5:GUS (a gift from Jiri Friml, Tübingen, Germany) was crossed into a (*vfb1-1 vfb2-1 vfb3-1* RNAi (*VFB4*)) mutant line. Plants homozygous for the *vfb* mutations were identified and analysed in the F2 generation.

Sequence alignments: Protein sequence alignments were performed using the Lasergene DNASTar suite. The unrooted phylogenetic tree was generated using the CLUSTALW algorithm and the unrooted tree was generated with TreeViewPPC1. Leucine-rich repeats were predicted based on similar alignments presented in (Gagne et al., 2004a).

Yeast two-hybrid analysis: Full length *VFB2* and a deletion variant lacking the F-box domain (*VFB2*ΔF-box) were amplified using the primers 5'-CTCGAGTCTGAGATTCTCCCTTTCTTACCATGTATC-3' and 5'-CTCGAGATGGGCAAGCTCCGTCGTCTCCGGCGGAA-3' in combination with 5'-CTCGAGCTAAAGATCCTCCTCAGAAATAAGCTTTTGCTCAATGGAAGTAGCTTCACT-3'. The fragments were introduced into pER8 (a gift from Nam Hai Chua, New York, USA), sequence verified and then introduced as *Xho1* fragments into pLexA. The ASK2, AtRBX1 and AtCUL1 'prey' constructs were described previously (Schwechheimer et al., 2001; Risseeuw et al., 2003). Two-hybrid interactions were performed as described in (Schwechheimer and Deng, 2002).

***VFB2:GFP* fusion constructs and protein localization:** To generate a *VFB2:GFP* fusion construct, the *VFB2* open reading frame was amplified by PCR with the primers 5'-attB1-TCATGGGCCAAGCTCCGTCGTCTCGGGCG-3' and 5'-attB2-CAATGGAAGTAGTAGCTTCACTTTG-3'. The fragment was introduced into pDONR201 using Gateway™ technology, sequence verified and then transferred into the Gateway-compatible vector 35-S-(GW)-GFP (a gift from Jane Parker, Cologne, Germany). To generate a YFP:*VFB2* fusion construct, the *VFB2* gene was amplified with the oligonucleotides 5'-attB1-TCATGCGCCAAGCTCCGTCGTCTCCG-3' and 5'-attB2-CTCAAATGGAAGTAGTAGCTTCACTTTG-3'. As above, the fragment was introduced into pDONR201, sequence verified and then transferred into the

Gateway™-compatible vector pExtag-YFP-GW (a gift from Laurent Noel and Jane Parker, Cologne, Germany). All Gateway™-vector manipulations were performed using Gateway™ reagents and following the manufacturers instructions (Invitrogen, Carlsbad, CA). The subcellular localization of the resulting VFB2:GFP and YFP:VFB2 fusion proteins was examined in transiently transformed *Arabidopsis thaliana* protoplasts using a Leica TCS confocal microscope.

VFB gene expression analyses: To generate *VFB* promoter:GUS constructs, DNA fragments corresponding to an approximately 1000 base pair fragment upstream of the genes' ATG start codon were amplified using the primer combinations 5'-GAATTCTCCTATCGATCCAATTAAGTGGTT-3' and 5'-CCATGGACGAAAGTCTCCGGTGGTCGTTTCGT-3' (*VFB1*), 5'-GAATTCCTTCCGATAGAGTGTAAGTGGTC-3' and 5'-CCATGGTTGTGTGGTGAGTATTGGGTAAGG-3' (*VFB2*), 5'-GAATTCAGAGCTAGTCGATGCTCTACAGAGCCGGA-3' and 5'-CCATGGTTTTCTTTACAA GTTTTAATATAC-3' (*VFB3*), and 5'-GAATTCGTGGCACTTTCTTTTCTAAGTGTT-3' and 5'-CCATGGCCAACCGAATGGTTTCGATTTCCCT-3' (*VFB4*). The fragments were introduced into pCR2.1 (Invitrogen, Carlsbad, CA), sequence verified and then cloned into the *EcoR1* and *Nco1* cleavage sites of pCAMBIA 1391Z to generate the constructs VFB1:GUS through VFB4:GUS. The constructs were transformed into *Arabidopsis* wild type plants and for each construct at least ten transgenic lines were generated and analysed for GUS expression (Weigel and Glazebrook, 2002).

***vfb4* (RNAi):** To suppress *VFB4* gene expression by RNAi, a 114 base pair gene-specific fragment was amplified using the primers 5'-attB1-TCAGGTTGAAACCGTTGTGGAGG-3' and 5'-attB2-CACCTAATCATCGCTAATCTAC-3'. The fragment was inserted into pDONR201 using the Gateway™ technology (Invitrogen, Carlsbad, CA), sequence verified, and then transferred to the destination vector pJawohl17 (a gift from Imre Somssich, Cologne, Germany) to generate *vfb4* (RNAi). Using *Agrobacterium*-mediated transformation, the construct was introduced into wild type and *vfb1-1 vfb2-1 vfb3-1* triple mutant plants. At least 20 transgenic plants were generated for each construct.

Semi-quantitative RT-PCR: *VFB* gene expression was analysed by semi-quantitative RT-PCR based on a previously published protocol. Total RNA was extracted from 100 mg seedling or plant material using the Qiagen RNeasy kit (Qiagen, Hilden, Germany). 5 μ g RNA was used for reverse transcription with SuperScript II reverse transcriptase (Invitrogen, Carlsbad, CA) primed with the oligo-dT primer 5'-GACTCGAGTCGACATCGATTTTTTTTTTTTTTTTTTTT-3'. One μ L of the reverse transcription reaction was used to analyse gene expression of the individual *VFB* genes using gene-specific primer combinations: 5'-GACGACCACCGGAGACTTTCGTGGATGGGCCA-3' and 5'-ATCGATAGTAAGCATCACGCTAACGAAT-3' (*VFB1*), 5'-ATGGGCCAAGCTCCGTCGTCTCCGGCGGAA CCAAACGTA-3' and 5'-AATGGAACTAGTAGCTTCACTTTGA-3' (*VFB2*), 5'-GGGTGGCATTCTTGCCATTTCTCCACAT-3' and 5'-GCCGGCTACTGGCTTCGACTTGATTCTGA-3' (*VFB3*), and 5'-ATGGGCCAAGCGCCGTCGTCTACGGCG-3' and 5'-AGTAGAACTACTAGCATTATCATTGTGAGACCA-3' (*VFB4*). The expression of an unrelated gene was used as an input control for all experiments.

Microarray Analysis: Three replicate samples were harvested and prepared from 10 day-old light-grown wild type and *vfb1-1 vfb2-1 vfb3-1 vfb4-1* (RNAi) mutant seedlings. RNA for microarray analysis was extracted using the RNeasy™ kit (Quiagen, Hilden, Germany). Complementary RNA was prepared from 6 μ g of total RNA as described in the Affimetrix Expression Analysis Technical Manual using the One-Cycle Target Labeling and Control Reagents (Affimetrix, Santa Clara, CA). In brief, double-stranded cDNA was synthesized. Biotin-labeled target cRNA was prepared by cDNA *in vitro* transcription in the presence of biotinylated UTP and CTP. After purification, cRNA was fragmented and used to hybridize the Arabidopsis ATH1 GeneChip array (Affimetrix, Santa Clara, CA). Hybridization, washing, staining, scanning and data collection were performed in an Affymetrix GeneChip® Fluidics Station 450 and GeneArray® Scanner. The microarray computational analysis was performed on *.CEL and *.CHP data files. The microarray computational analysis was performed on CEL and CHIP data files and analyzed using the robust multi-array average (RMA) GC method of the GeneSpring XT software (SiliconGenetics). Data were subsequently filtered based on two-fold induction or repression, student's t-test ($p < 0.05$) and signal intensities (absent calls). An identical experiment was

conducted with 7 day old light-grown *csn4* (SALK_043720) mutant seedlings. The microarray data were submitted to the Gene Expression Omnibus and are available under the accession numbers GSM3863 (*vfb* mutant experiment) and GSM3865 (*csn4* mutant experiment).

Auxin sensitivity assay: To assay auxin sensitivity of Arabidopsis seedling roots, 5 day-old seedlings were transferred to 2,4-dichlorophenoxy acetic acid (2,4D) containing medium. Root elongation after transfer to auxin-containing medium was assayed after another 5 days of growth and calculated relative to the untreated control samples. The average and standard deviation of at least ten seedlings per experimental conditions were determined and plotted.

Accession numbers (AGI locus identifier): *VFB1* (At1g47056), *VFB2* (At3g50080), *VFB3* (At4g07400), *VFB4* (At5g67250), *Oryza sativa* ACRE189 (XP_450015.1), *Oryza sativa* JNBb0002J11.1 (XP_473092.1), *Nicotiana tabacum* ACRE189 (AAP03878.1); EBF1 (At2g25490), EBF2 (At5g25350), TIR1 (At3g62980), AFB1 (At4g03190), AFB2 (At3g26810), AFB3 (At1g12820), COI1 (At2g39940), MAX2/ORE9 (At2g42620), CSN4 (At5g42970). Microarray data: GSM3863 (*vfb* mutant experiment), GSM3865 (*csn4* mutant experiment).

Acknowledgements: We would like to thank our colleagues for helpful comments on the manuscript. We would like to acknowledge Markus Schmid and Detlef Weigel (Max-Planck Institute for Developmental Biology, Tübingen, Germany) for providing access to their microarray analysis facility, their supervision during hybridization and during the initial stages of data analysis. We acknowledge Klaus Harter, Joachim Kilian and Dierk Warnke (Tübingen University, Germany) for their instructive comments and support during microarray data analysis. We thank Andrea Gust (Tübingen University, Germany) for providing RNA samples of flg22 treated plant material and many colleagues for sharing unpublished vectors. We would like to thank the Nottingham Arabidopsis Stock Centre and GABI-Kat for providing seeds of T-DNA insertion lines. This research was supported by grants from the Arabidopsis Functional Genomics Network (SCHW 741/4-1 and SCHW741/4-2) and from the

Sonderforschungsbereich 446 (SFB446) of the Deutsche Forschungsgemeinschaft (DFG).

References:

- Bai, C., Sen, P., Hofmann, K., Ma, L., Goebel, M., Harper, J.W., and Elledge, S.J.** (1996). SKP1 connects cell cycle regulators to the ubiquitin proteolysis machinery through a novel motif, the F-box. *Cell* **86**, 263-274.
- Cardozo, T., and Pagano, M.** (2004). The SCF ubiquitin ligase: insights into a molecular machine. *Nat. Rev. Mol. Cell Biol.* **5**, 739 - 751.
- Chamovitz, D.A., Wei, N., Osterlund, M.T., von Arnim, A.G., Staub, J.M., Matsui, M., and Deng, X.-W.** (1996). The COP9 complex, a novel multisubunit nuclear regulator involved in light control of a plant developmental switch. *Cell* **86**, 115-121.
- Cheng, Y., Dai, X., and Zhao, Y.** (2004). AtCAND1, a HEAT-repeat protein that participates in auxin signaling in Arabidopsis. *Plant Phys.* **135**, 1020-1026.
- Chiba, T., and Tanaka, K.** (2004). Cullin-based ubiquitin ligase and its control by NEDD8-conjugating system. *Curr. Protein Pept. Sci.* **5**, 177-184.
- Chuang, H.W., Zhang, W., and Gray, W.M.** (2004). Arabidopsis ETA2, an apparent ortholog of the human cullin-interacting protein CAND1, is required for auxin responses mediated by the SCF(TIR1) ubiquitin ligase. *Plant Cell* **16**, 1883-1897.
- Cope, G.A., Suh, G.S.B., Aravind, L., Schwarz, S.E., Zipursky, S.L., Koonin, E.V., and Deshaies, R.J.** (2002). Role for predicted metalloprotease motif of JAB1/Csn5 in cleavage of NEDD8 from CUL1. *Science* **298**, 608 - 611.
- del Pozo, J.C., Boniotti, M.B., and Gutierrez, C.** (2002a). Arabidopsis E2Fc functions in cell division and is degraded by the ubiquitin-SCF(AtSKP2) pathway in response to light. *Plant Cell* **14**, 3057 - 3071.
- del Pozo, J.C., Dharmasiri, S., Hellmann, H., Walker, L., Gray, W.M., and Estelle, M.** (2002b). AXR1-ECC1-dependent conjugation of RUB1 to the Arabidopsis cullin AtCUL1 is required for auxin response. *Plant Cell* **14**, 421 - 433.
- del Pozo, J.L., and Estelle, M.** (1999). The Arabidopsis cullin AtCUL1 is modified by the ubiquitin-related protein RUB1. *Proc. Natl. Acad. Sci. USA* **96**, 15342-15347.
- Deshaies, R.J.** (1999). SCF and Cullin/RING H2-based ubiquitin ligases. *Annu. Rev. Cell Dev. Biol.* **15**, 435 - 467.
- Dharmasiri, N., Dharmasiri, S., and Estelle, M.** (2005a). The F-box protein TIR1 is an auxin receptor. *Nature* **435**, 441-445.
- Dharmasiri, N., Dharmasiri, S., Weijers, D., Lechner, E., Yamada, M., Hobbie, L., Ehrismann, J.S., Jurgens, G., and Estelle, M.** (2005b). Plant development is regulated by a family of auxin receptor F box proteins. *Dev. Cell* **9**, 109-119.
- Dharmasiri, S., Dharmasiri, N., Hellmann, H., and Estelle, M.** (2003). The RUB/Nedd8 conjugation pathway is required for early development in Arabidopsis. *EMBO J.* **22**, 1762 - 1770.
- Dohmann, E.M., Kuhnle, C., and Schwechheimer, C.** (2005a). Loss of the CONSTITUTIVE PHOTOMORPHOGENIC9 signalosome subunit 5 is sufficient to cause the *cop/det/fus* mutant phenotype in Arabidopsis. *Plant Cell* **17**, 1967-1978.
- Feng, S., Ma, L., Wang, X., Xie, D., Dinesh-Kumar, S.P., Wei, N., and Deng, X.-W.** (2003). The COP9 signalosome interacts physically with SCF^{COI1} and modulates jasmonate responses. *Plant Cell* **15**, 1083 - 1094.

- Feng, S., Shen, Y., Sullivan, J.A., Rubio, V., Xiong, Y., Sun, T.P., and Deng, X.W.** (2004). Arabidopsis CAND1, an unmodified CUL1-interacting protein, is involved in multiple developmental pathways controlled by ubiquitin/proteasome-mediated protein degradation. *Plant Cell* **16**, 1870-1882.
- Freilich, S., Oron, E., Kapp, Y., Nevo-Caspi, Y., Orgad, S., Segal, D., and Chamovitz, D.A.** (1999). The COP9 signalosome is essential for development of *Drosophila melanogaster*. *Curr Biol* **9**, 1187-1190.
- Fukaki, H., Nakao, Y., Okushima, Y., Theologis, A., and Tasaka, M.** (2005). Tissue-specific expression of stabilized SOLITARY-ROOT/IAA14 alters lateral root development in Arabidopsis. *Plant J* **44**, 382-395.
- Gagne, J.M., Downes, B.P., Shiu, S.H., Durski, A.M., and Vierstra, R.D.** (2002). The F-box subunit of the SCF E3 complex is encoded by a diverse superfamily of genes in Arabidopsis. *Proc. Natl. Acad. Sci. USA* **99**, 11519 - 11524.
- Gagne, J.M., Smalle, J., Gingerich, D.J., Walker, J.M., Yoo, S.-D., Yanagisawa, S., and Vierstra, R.** (2004a). Arabidopsis EIN3-binding F-box 1 and 2 form ubiquitin-protein ligases that repress ethylene action and promote growth by directing EIN3 degradation. *Proc. Natl. Acad. Sci. USA* **101**, 6803 - 6808.
- Gagne, J.M., Smalle, J., Gingerich, D.J., Walker, J.M., Yoo, S.-D., Yanagisawa, S., and Vierstra, R.D.** (2004b). Arabidopsis EIN3-binding F-box 1 and 2 form ubiquitin-protein ligases that repress ethylene action and promote growth by directing EIN3 degradation. *Proc. Natl. Acad. Sci. USA* **101**, 6803-6808.
- Gil, P., Liu, Y.-C., Orbovic, V., Verkamp, E., Poff, K.L., and Green, P.J.** (1994). Characterization of the auxin-inducible SAUR-AC1 gene for use as a molecular genetic tool in Arabidopsis. *Plant Phys.* **104**, 777-784.
- Gray, W.M., Kepinski, S., Rouse, D., Leyser, O., and Estelle, M.** (2001). Auxin regulates SCF^{TR1}-dependent degradation of AUX/IAA proteins. *Nature* **414**, 271 - 276.
- Guo, H., and Ecker, J.R.** (2003). Plant responses to ethylene gas are mediated by SCF(EBF1/EBF2)-dependent proteolysis of EIN3 transcription factor. *Cell* **115**, 667 - 677.
- Gusmaroli, G., Feng, S., and Deng, X.** (2004). The Arabidopsis CSN5A and CSN5B subunits are present in distinct COP9 signalosome complexes, and mutations in their JAMM domains exhibit differential dominant negative effects on development. *Plant Cell* **16**, 2984 - 3001.
- Hershko, A., and Ciechanover, A.** (1998). The ubiquitin system. *Annu. Rev. Biochem.* **67**, 425-479.
- Hetfeld, B.K., Helfrich, A., Kapelari, B., Scheel, H., Hofmann, K., Guterman, A., Glickman, M., Schade, R., Kloetzel, P.M., and Dubiel, W.** (2005). The zinc finger of the CSN-associated deubiquitinating enzyme USP15 is essential to rescue the E3 ligase Rbx1. *Curr. Biol.* **15**, 1217-1221.
- Higa, L.A.A., Mihaylov, I.S., Banks, D.P., Zhneg, J., and Zhang, H.** (2003). Radiation-mediated proteolysis of CDT1 by CUL4-ROC1 and CSN complexes constitutes a new checkpoint. *Nat. Cell Biol.* **5**, 1008 - 1015.
- Hori, T., Osaka, F., Chiba, T., Miyamoto, C., Okabayashi, K., Shimbara, N., Kato, S., and Tanaka, K.** (1999). Covalent modification of all members of human cullin family proteins by NEDD8. *Oncogene* **18**, 6829-6834.
- Jin, J., Cardozo, T., Lovering, R.C., Elledge, S.J., Pagano, M., and Harper, J.W.** (2004). Systematic analysis and nomenclature of mammalian F-box proteins. *Genes Dev.* **18**, 2573 - 2580.

- Kamura, T., Koepp, D.M., Conrad, M.N., Skowyra, D., Moreland, R.J., Iliopoulos, O., Lane, W.S., Kaelin, W.G.J., Elledge, S.J., Conaway, R.C., Harper, J.W., and Conaway, J.W.** (1999). RBX1, a component of the VHL tumor suppressor complex and SCF ubiquitin ligase. *Science* **284**, 657-661.
- Kawakami, T., Chiba, T., Suzuki, T., Iwai, K., Yamanaka, H., Minato, N., Suzuki, H., Shimbara, N., Hidaka, Y., Osaka, F., Omata, M., and Tanaka, K.** (2001). NEDD8 recruits E2-ubiquitin to SCF E3 ligase. *EMBO J.* **20**, 1 - 10.
- Kepinski, S., and Leyser, O.** (2005). The Arabidopsis F-box protein TIR1 is an auxin receptor. *Nature* **435**, 446-451.
- Kwok, S.F., Piekos, B., Miséra, S., and Deng, X.-W.** (1996). A complement of ten essential and pleiotropic Arabidopsis *COP/DET/FUS* genes is necessary for repression of photomorphogenesis in darkness. *Plant Phys.* **110**, 731-742.
- Leyser, H.M., Lincoln, C.A., Timpte, C., Lammer, D., Turner, J., and Estelle, M.** (1993). Arabidopsis auxin-resistance gene AXR1 encodes a protein related to ubiquitin-activating enzyme E1. *Nature* **364**, 161-164.
- Leyser, H.M.O., Pickett, F.B., Dharmasiri, S., and Estelle, M.** (1996). Mutations in the AXR3 gene of Arabidopsis result in altered auxin response including ectopic expression from the SAUR-AC1 promoter. *Plant J.* **10**, 403-413.
- Liu, J., Furukawa, M., Matsumoto, T., and Xiong, Y.** (2002). NEDD8 modification of CUL1 dissociates p120(CAND1), an inhibitor of CUL1-SKP1 binding and SCF ligases. *Mol. Cell* **10**, 1511-1518.
- Lyapina, S., Cope, G., Shevchenko, A., Serino, G., Zhou, C., Wolf, D.A., Wei, N., Shevchenko, A., and Deshaies, R.J.** (2001). COP9 Signalosome promotes cleavage of NEDD8-CUL1 conjugates. *Science* **292**, 1382 - 1385.
- Lykke-Andersen, K., Schaefer, L., Menon, S., Deng, X.-W., Miller, J.B., and Wei, N.** (2003). Disruption of the COP9 signalosome CSN2 subunit in mice causes deficient cell proliferation, accumulation of p53 and cyclin E, and early embryonic death. *Mol. Cell. Biol.* **23**, 6790 - 6797.
- Marti, A., Wirbelauer, C., Scheffner, M., and Krek, W.** (1999a). Interaction between ubiquitin-protein ligase SCFSKP2 and E2F-1 underlies the regulation of E2F-1 degradation. *Nat. Cell Biol.* **1**, 14-19.
- Marti, A., Wirbelauer, C., Scheffner, M., and Krek, W.** (1999b). Interaction between ubiquitin-protein ligase SCFSKP2 and E2F-1 underlies the regulation of E2F-1 degradation. *Nat. Cell Biol.* **1**, 14 - 19.
- Min, K.W., Kwon, M.J., Park, H.S., Park, Y., Yoon, S.K., and Yoon, J.B.** (2005). CAND1 enhances deneddylation of CUL1 by COP9 signalosome. *Biochem. Biophys. Res. Commun.* **334**, 867-874.
- Navarro, L., Zipfel, C., Rowland, O., Keller, I., Robatzek, S., Boller, T., and Jones, J.D.** (2004). The transcriptional innate immune response to flg22. Interplay and overlap with Avr gene-dependent defense responses and bacterial pathogenesis. *Plant Phys.* **135**, 1113-1128.
- Osaka, F., Saeki, M., Katayama, S., Aida, N., Toh-e, A., Kominami, K., Toda, T., Suzuki, T., Chiba, T., Tanaka, K., and Kato, S.** (2000). Covalent modifier NEDD8 is essential for SCF ubiquitin-ligase in fission yeast. *EMBO J.* **19**, 3475 - 3484.
- Oshikawa, K., Matsumoto, M., Yada, M., Kamura, T., Hatakeyama, S., and Nakayama, K.I.** (2003). Preferential interaction of TIP120A with Cul1 that is not modified by NEDD8 and not associated with Skp1. *Biochem. Biophys. Res. Commun.* **303**, 1209-1216.

- Overvoorde, P.J., Okushima, Y., Alonso, J.M., Chan, A., Chang, C., Ecker, J.R., Hughes, B., Liu, A., Onodera, C., Quach, H., Smith, A., Yu, G., and Theologis, A.** (2005). Functional Genomic Analysis of the AUXIN/INDOLE-3-ACETIC ACID Gene Family Members in *Arabidopsis thaliana*. *Plant Cell* **17**, 3282-3300.
- Peng, Z., Shen, Y., Feng, S., Wang, X., Chittetei, B.N., Vierstra, R.D., and Deng, X.W.** (2003). Evidence for a physical association of the COP9 signalosome, the proteasome, and specific SCF E3 ligases *in vivo*. *Curr. Biol.* **13**, R504 - R505.
- Peng, Z., Staub, J.M., Serino, G., Kwok, S.F., Kurepa, J., Bruce, B., Vierstra, R.D., Wei, N., and Deng, X.-W.** (2001). The cellular level of PR500, a protein complex related to the 19S regulatory particle of the proteasome, is regulated in response to stresses in plants. *Mol. Biol. Cell* **12**, 383 - 392.
- Podust, V.N., Brownell, J.E., Gladysheva, T.B., Luo, R.-S., Wang, C., Coggins, M.B., Pierce, J.W., Lightcap, E.S., Chau, V.** (2000). A Nedd8 conjugation pathway is essential for proteolytic targeting of p27^{Kip1} by ubiquitination. *Proc Natl. Acad. Sci. USA* **97**, 4579 - 4584.
- Potuschak, T., Lechner, E., Parmentier, Y., Yanagisawa, S., Grava, S., Koncz, C., and Genschik, P.** (2003). EIN3-dependent regulation of plant ethylene hormone signaling by two *Arabidopsis* F box proteins: EBF1 and EBF2. *Cell* **115**, 679 - 689.
- Reed, J.** (2001). Roles and activities of Aux/IAA proteins in *Arabidopsis*. *Trends Plant Sci.* **6**, 420 - 425.
- Risseuw, E.P., Daskalchuk, T.E., Banks, T.W., Liu, E., Cotelesage, J., Hellmann, H., Estelle, M., Somers, D.E., and Crosby, W.L.** (2003). Protein interaction analysis of SCF ubiquitin E3 ligase subunits from *Arabidopsis*. *Plant J.* **34**, 753 - 767.
- Ruegger, M., Dewey, E., Gray, W.M., Hobbie, L., Turner, J., and Estelle, M.** (1998). The TIR protein of *Arabidopsis* functions in auxin response and is related to human SKP2 and yeast Grr1p. *Genes Dev.* **12**, 198-207.
- Schwechheimer, C.** (2004). The COP9 signalosome (CSN): an evolutionary conserved proteolysis regulator in eukaryotic development. *Biochim. Biophys. Acta* **1695**, 45-54.
- Schwechheimer, C., and Deng, X.W.** (2002). Studying protein-protein interactions with the yeast two-hybrid system. In *Molecular Plant Biology*, P.M. Gilmartin and C. Bowler, eds (Oxford: Oxford University Press), pp. 173 - 198.
- Schwechheimer, C., and Villalobos, L.I.** (2004). Cullin-containing E3 ubiquitin ligases in plant development. *Curr. Opin. Plant Biol.* **7**, 677-686.
- Schwechheimer, C., and Schwager, K.** (2004). Regulated proteolysis and plant development. *Plant Cell Rep.* **23**, 353-364.
- Schwechheimer, C., Serino, G., and Deng, X.-W.** (2002). Multiple ubiquitin-ligase-mediated processes require COP9 signalosome and AXR1 function. *Plant Cell* **14**, 2553 - 2563.
- Schwechheimer, C., Serino, G., Callis, J., Crosby, W.L., Lyapina, S., Deshaies, R.J., Gray, W.M., Estelle, M., and Deng, X.-W.** (2001). Interactions of the COP9 signalosome with the E3 ubiquitin ligase SCF^{TIR1} in mediating auxin response. *Science* **292**, 1379 - 1382.
- Skowyra, D., Koepp, D.M., Kamura, T., Conrad, M.N., Conaway, R.C., Conaway, J.W., Elledge, S.J., and Harper, J.W.** (1999). Reconstitution of G1 cyclin

- ubiquitination with complexes containing SCF^{Grr1} and Rbx1. *Science* **284**, 662-665.
- Stirnberg, P., van de Sande, K., and Leyser, H.M.O.** (2002). MAX1 and MAX2 control shoot lateral branching in Arabidopsis. *Development* **129**, 1131 - 1141.
- Sutterluty, H., Chatelain, E., Marti, A., Wirbelauer, C., Senften, M., Muller, U., and Krek, W.** (1999). p45SKP2 promotes p27Kip1 degradation and induces S phase in quiescent cells. *Nat. Cell Biol.* **1**, 207-214.
- Tatematsu, K., Kumagai, S., Muto, H., Sato, A., Watahiki, M.K., Harper, R.M., Liscum, E., and Yamamoto, K.T.** (2004). MASSUGU2 encodes Aux/IAA19, an auxin-regulated protein that functions together with the transcriptional activator NPH4/ARF7 to regulate differential growth responses of hypocotyl and formation of lateral roots in Arabidopsis thaliana. *Plant Cell* **16**, 379 - 393.
- Tian, Q., and Reed, J.W.** (1999). Control of auxin-regulated root development by the Arabidopsis thaliana SHY2/IAA3 gene. *Development* **126**, 711-721.
- Tian, Q., Uhlir, N.J., and Reed, J.W.** (2002). Arabidopsis SHY2/IAA3 inhibits auxin-regulated gene expression. *Plant Cell* **14**, 301-319.
- Tian, Q., Nagpal, P., and Reed, J.W.** (2003). Regulation of Arabidopsis SHY2/IAA3 protein turnover. *Plant J.* **36**, 643 - 651.
- Tiwari, S.B., Hagen, G., and Guilfoyle, T.J.** (2004). Aux/IAA proteins contain a potent transcriptional repression domain. *Plant Cell* **16**, 533 - 543.
- Tomoda, K., Yoneda-Kato, N., Fukumoto, A., Yamanaka, S., and Kato, J.-y.** (2004). Multiple functions of Jab1 are required for early embryonic development and growth potential in mice. *J. Biol. Chem.* **279**, 43013 - 43018.
- Ulmasov, T., Hagen, G., and Guilfoyle, T.J.** (1997a). ARF1, a transcription factor that binds to auxin response elements. *Science* **276**, 1865-1868.
- Ulmasov, T., Murfett, J., Hagen, G., and Guilfoyle, T.J.** (1997b). Aux/IAA proteins repress expression of reporter genes containing natural and highly active synthetic auxin response elements. *Plant Cell* **9**, 1963-1971.
- Ungermannova, D., Gao, Y., and Liu, X.** (2005). Ubiquitination of p27Kip1 requires physical interaction with cyclin E and probable phosphate recognition by SKP2. *J. Biol. Chem.* **280**, 30301-30309.
- Wang, W., Nacusi, L., Sheaff, R.J., and Liu, X.** (2005). Ubiquitination of p21(Cip1/WAF1) by SCF(Skp2): Substrate Requirement and Ubiquitination Site Selection. *Biochem.* **44**, 14553-14564.
- Wang, X., Feng, S., Nakayama, N., Crosby, W.L., Irish, V.F., Deng, X.W., and Wei, N.** (2003). The COP9 Signalosome interacts with SCFUFO and participates in Arabidopsis flower development. *Plant Cell* **15**, 1071 - 1082.
- Wee, S., Geyer, R.K., Toda, T., and Wolf, D.A.** (2005). CSN facilitates Cullin-RING ubiquitin ligase function by counteracting autocatalytic adapter instability. *Nat. Cell. Biol.* **7**, 387-391.
- Weigel, D., and Glazebrook, J.** (2002). Arabidopsis: A laboratory manual. (Cold Spring Harbor, New York: CSHL Press).
- Wertz, I.E., O'Rourke, K.M., Zhang, Z., Dornan, D., Arnott, D., Deshaies, R.J., and Dixit, V.M.** (2004). Human De-Etiolated-1 Regulates c-Jun by assembling a CUL4A Ubiquitin Ligase. *Science* **303**, 1371 -1374.
- Woo, H.R., Chung, K.M., Park, J.-H., Oh, S.A., Ahn, T., Hong, S.H., Jang, S.K., and Nam, H.G.** (2001). ORE9, an F-box protein that regulates leaf senescence in Arabidopsis. *Plant Cell* **13**, 1779 - 1790.

- Wu, J.T., Lin, H.C., Hu, Y.C., and Chien, C.T.** (2005). Neddylation and deneddylation regulate Cul1 and Cul3 protein accumulation. *Nat. Cell Biol.* **7**, 1014-1020.
- Xie, D.-X., Feys, B.F., James, S., Nieto-Rostro, M., and Turner, J.G.** (1998). COI1: An Arabidopsis gene required for jasmonate-regulated defense and fertility. *Science* **280**, 1091 - 1094.
- Xu, L., Wei, Y., Reboul, J., Vaglio, P., Shin, T.-H., Vidal, M., Elledge, S.J., and Harper, J.W.** (2003). BTB proteins are substrate-specific adaptors in an SCF-like modular ubiquitin ligase containing Cul-3. *Nature* **425**, 316-321.
- Zenser, N., Dreher, K.A., Edwards, S.R., and Callis, J.** (2003). Acceleration of Aux/IAA proteolysis is specific for auxin and independent of AXR1. *Plant J.* **35**, 285 - 294.
- Zhao, D., Ni, W., Feng, B., Han, T., Petrasek, M.G., and Ma, H.** (2003). Members of the *Arabidopsis-SKP1-like* gene family exhibit a variety of expression patterns and may play diverse roles in Arabidopsis. *Plant Phys.* **133**, 203 -217.
- Zheng, J., Yang, X., Harrell, J.M., Ryzhikov, S., Shim, E.H., Lykke-Andersen, K., Wei, N., Sun, H., Kobayashi, R., and Zhang, H.** (2002a). CAND1 binds to unneddylated CUL1 and regulates the formation of SCF ubiquitin E3 ligase complex. *Mol. Cell* **10**, 1519-1526.
- Zheng, N., Schulman, B.A., Song, L., Miller, J.J., Jeffrey, P.D., Wang, P., Chu, C., Koepp, D.M., Elledge, S.J., Pagano, M., Conaway, R.C., Conaway, J.W., Harper, J.W., and Pavletich, N.P.** (2002b). Structure of the Cul1-Rbx1-Skp1-F boxSkp2 SCF ubiquitin ligase complex. *Nature* **416**, 703 - 709.
- Zimmermann, P., Hirsch-Hoffmann, M., Hennig, L., and Gruissem, W.** (2004). GENEVESTIGATOR. Arabidopsis microarray database and analysis toolbox. *Plant Phys.* **136**, 2621-2632.

Figures and Legends

A

```

MNIYIFSKKKKKVYCDNLKTRGRRREHCEPHRRRMGQSTLFRFRSKTTFTSP 55
HG-----QSTAAAGNLLNRRSKSFILMFP-----WSR 24
HG-----DAPSSAESMGRLELRL-----WSR 24
HG-----

VLPNLRQNSGADPEVQVSNLPDECLLTFQSLTCAQLKRCCLVDRRMLTIEGQ 110
--I--FSTFSESSQDNTSLDDECLAVFQFNGLRKRRCALVGRMLVIEGQ 76
FLDCESSDFEFGDQDFLMDDDCLAFIFQFSLAGDRKRCCLVGRMLVIEGQ 77
IVAGGESHMAVGMVVDQDFDGLDDECLAVHVFQFLGAGDRKRCCLVGRMLVIEGQ 79

GRRLSLMAKSDLTQVHPSLFRFDSVTRLVLRGDRRSLGICDHALVMSSVGRN 165
NRRLSLMAKSDLTQVHPSLFRFDSVTRLVLRGDRRSLGICDHALVMSSVGRN 121
NRRLSLMAKSDLTQVHPSLFRFDSVTRLVLRGDRRSLGICDHALVMSSVGRN 122
NRRLSLMAKSDLTQVHPSLFRFDSVTRLVLRGDRRSLGICDHALVMSSVGRN 123
NRRLSLMAKSDLTQVHPSLFRFDSVTRLVLRGDRRSLGICDHALVMSSVGRN 124
NRRLSLMAKSDLTQVHPSLFRFDSVTRLVLRGDRRSLGICDHALVMSSVGRN 125
NRRLSLMAKSDLTQVHPSLFRFDSVTRLVLRGDRRSLGICDHALVMSSVGRN 126
NRRLSLMAKSDLTQVHPSLFRFDSVTRLVLRGDRRSLGICDHALVMSSVGRN 127
NRRLSLMAKSDLTQVHPSLFRFDSVTRLVLRGDRRSLGICDHALVMSSVGRN 128
NRRLSLMAKSDLTQVHPSLFRFDSVTRLVLRGDRRSLGICDHALVMSSVGRN 129
NRRLSLMAKSDLTQVHPSLFRFDSVTRLVLRGDRRSLGICDHALVMSSVGRN 130
NRRLSLMAKSDLTQVHPSLFRFDSVTRLVLRGDRRSLGICDHALVMSSVGRN 131
NRRLSLMAKSDLTQVHPSLFRFDSVTRLVLRGDRRSLGICDHALVMSSVGRN 132
NRRLSLMAKSDLTQVHPSLFRFDSVTRLVLRGDRRSLGICDHALVMSSVGRN 133
NRRLSLMAKSDLTQVHPSLFRFDSVTRLVLRGDRRSLGICDHALVMSSVGRN 134

LTRLKLRGDELDSDGLITGFLEHQRSLKRVYDSCDFGQGHMLLHNLQLEEL 220
LTRLKLRGDELDSDGLITGFLEHQRSLKRVYDSCDFGQGHMLLHNLQLEEL 186
LTRLKLRGDELDSDGLITGFLEHQRSLKRVYDSCDFGQGHMLLHNLQLEEL 187
LTRLKLRGDELDSDGLITGFLEHQRSLKRVYDSCDFGQGHMLLHNLQLEEL 189

SVKRLRGGA-GAEI-LGPPGAAAGSLKVTCLKEHNGQCFAPLLSAAQGLRLK 273
SKRLRGFTDIDPEM-IGDQVAAASSLKSCLKEHNGQCFAPLLSAAQGLRLK 240
SKRLRGFTDIDPEM-IGDQVAAASSLKSCLKEHNGQCFAPLLSAAQGLRLK 238
SVKRLRGGA-GAEI-LGPPGAAAGSLKVTCLKEHNGQCFAPLLSAAQGLRLK 244

FRSGDQDQVAVRDKVYNATVETHLERMMDQGLLALCKKCVVLLVKTDP 229
FRSGDQDQVAVRDKVYNATVETHLERMMDQGLLALCKKCVVLLVKTDP 295
FRSGDQDQVAVRDKVYNATVETHLERMMDQGLLALCKKCVVLLVKTDP 293
FRSGDQDQVAVRDKVYNATVETHLERMMDQGLLALCKKCVVLLVKTDP 299

CTVGLALVAEACKLRLKLIIDGKTRNTRDDEGLIVAKVCHLQELVIGVNT 383
CTVGLALVAEACKLRLKLIIDGKTRNTRDDEGLIVAKVCHLQELVIGVNT 350
CTVGLALVAEACKLRLKLIIDGKTRNTRDDEGLIVAKVCHLQELVIGVNT 348
CTVGLALVAEACKLRLKLIIDGKTRNTRDDEGLIVAKVCHLQELVIGVNT 354

KLSLEAVENCNLERLALCGSDTVSDTELCIAEKLLALRKLKZRHCPIDDEGT 438
TSLGMLAKKCNLERLALCGSDTVSDTELCIAEKLLALRKLKZRHCPIDDEGT 405
YMSLVAASNCNLERLALCGSDTVSDTELCIAEKLLALRKLKZRHCPIDDEGT 403
HMSLVAASNCNLERLALCGSDTVSDTELCIAEKLLALRKLKZRHCPIDDEGT 409

VALRGCPILLVVKKCKVVTGEGADLLRERALLVHLDAPETP---IDGSA 490
ENVAAGCPILLVVKKCKVVTGEGADLLRERALLVHLDAPETP---IDGSA 457
QALAGCPILLVVKKCKVVTGEGADLLRERALLVHLDAPETP---IDGSA 458
EALVAGCPILLVVKKCKVVTGEGADLLRERALLVHLDAPETP---IDGSA 464

GE--GTEHAFVFPSSRLDPTIILASDITQSSSEFLKGLLSGHLVQALR 543
NDVVGQVQENGFEFPLNSDMMASALSSNRSGYKSGTGFSGMLVPPCT 511
QRVLETVVEE--DPIVDGDLGAVAGGRGLAIEKTLGLLAGRNLYACTR 511
ETVVEEPVVAQ--GGIYAEVGSINGGGSRLLAM--IRKLGFLAGRNLYCTFR 515

ALGRSRSRNE 554 VFB3 (At1g07400)
--SRRAASR 518 VFB1 (At1g47056)
RWQNSLAFV 522 VFB2 (At3g00800)
RWQNSLAFV 527 VFB4 (At5g67250)
    
```

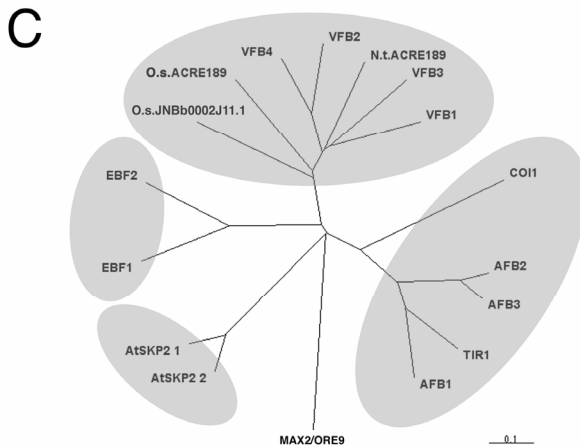
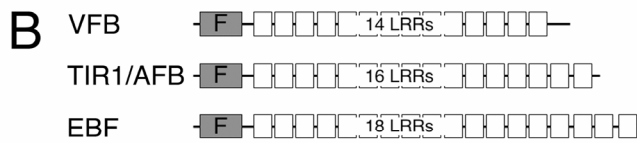


Figure 1

Figure 1: The VFB proteins are leucine-rich repeat containing F-box proteins of the C3 subfamily of the Arabidopsis F-box protein superfamily. **A.** Pretty box of a clustal alignment of the VFB proteins VFB1 (At1g47056), VFB2 (At3g50080), VFB3 (At4g07400) and VFB4 (At5g67250). The F-box domain is boxed, the individual leucine-rich repeats are flanked by brackets and were identified as described in (Gagne et al., 2004a). **B.** Schematic view of the VFB F-box proteins in comparison with the auxin-receptor TIR1/AFB F-box proteins and the ethylene-response EBF F-box proteins. F, F-box domain; LRR, leucine-rich repeat. **C.** Unrooted phylogenetic tree of the Arabidopsis VFB proteins, two apparent orthologues from rice (*Oryza sativa*, O.s.) annotated as ACRE189 and JNBb0002J11.1, one apparent orthologue from tobacco (*Nicotiana tabacum*, N.t.) annotated as ACRE189 and several previously characterized F-box proteins from *Arabidopsis thaliana*. A.t., *Arabidopsis thaliana*, O.s., *Oryza sativa*; N.t., *Nicotiana tabacum*. Please refer to the text for other abbreviations. Accession numbers are listed in Materials and Methods.

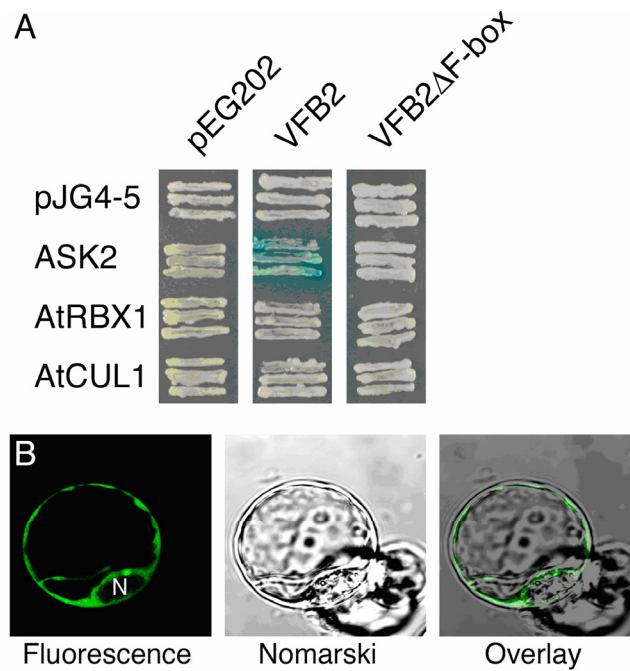


Figure 2

Figure 2: A. A yeast two-hybrid interaction study between VFB2 and the SCF-complex components ASK2, AtRBX1 and AtCUL1 reveals a specific and F-box domain dependent interaction between VFB2 and ASK2. ASK2, AtRBX1 and AtCUL1 full-length proteins were expressed from the ,bait' vector pJG4-5. VFB2 and VFB2 Δ F-box, a VFB2 variant lacking the protein's N-terminus including the F-box domain, were expressed from the ,prey' vector pEG202. Blue staining identifies LacZ reporter activity and protein-protein interaction. **B.** Confocal microscopy image of *Arabidopsis thaliana* protoplasts transiently transformed with a construct for the overexpression of a VFB2:GFP fusion protein. Left panel, confocal image; middle panel, Nomarski image; right panel, overlay. This analysis and a similar analysis with a YFP:VFB2 protein (data not shown) suggests a cytoplasmic localization of VFB2. N, nucleus.

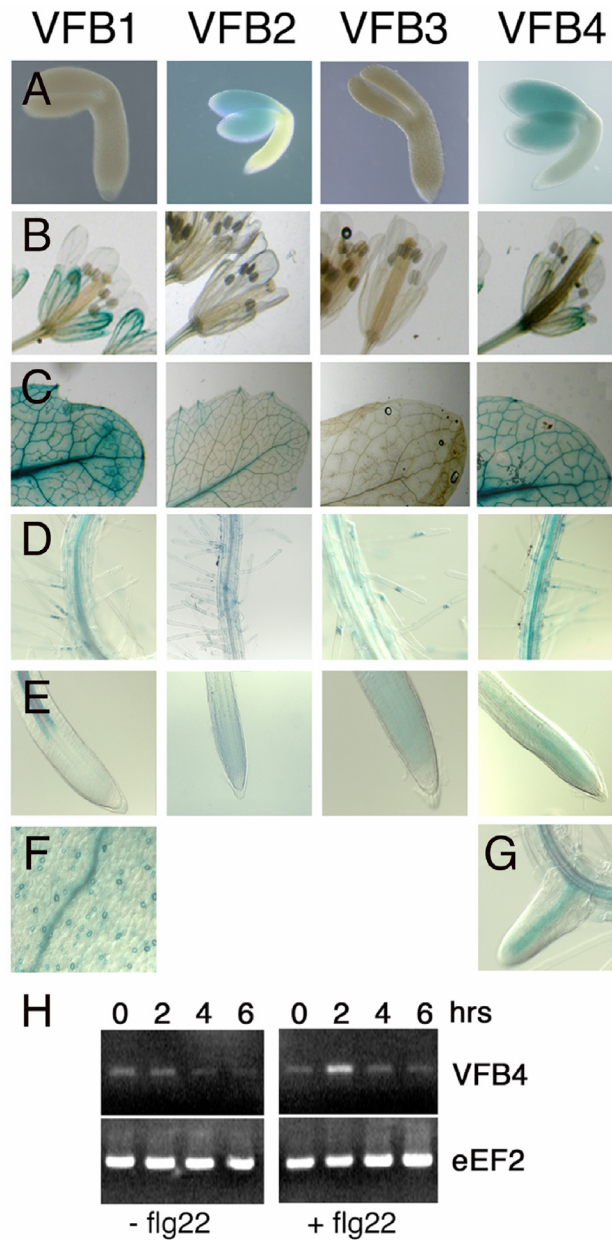


Figure 3

Figure 3: GUS staining of promoter:GUS expressing lines predict distinct but also overlapping expression patterns for the *VFB* genes. Transgenic plants expressing promoter:GUS fusions for each of the four *VFB* genes were examined in bent cotyledon stage embryos (**A**), flowers (**B**), leaves (**C**), roots (**D**), and root tips (**E**). Noteworthy is also the strong expression of *VFB1* in stomata (**F**) and of *VFB4* in lateral roots (**G**). Representative staining patterns are shown. **H.** RT-PCR analysis (25 PCR cycles) of *VFB4* expression following flg22 treatment reveals the transient induction of the *VFB4* gene. *ACTIN* served as a normalization control of the experiment.

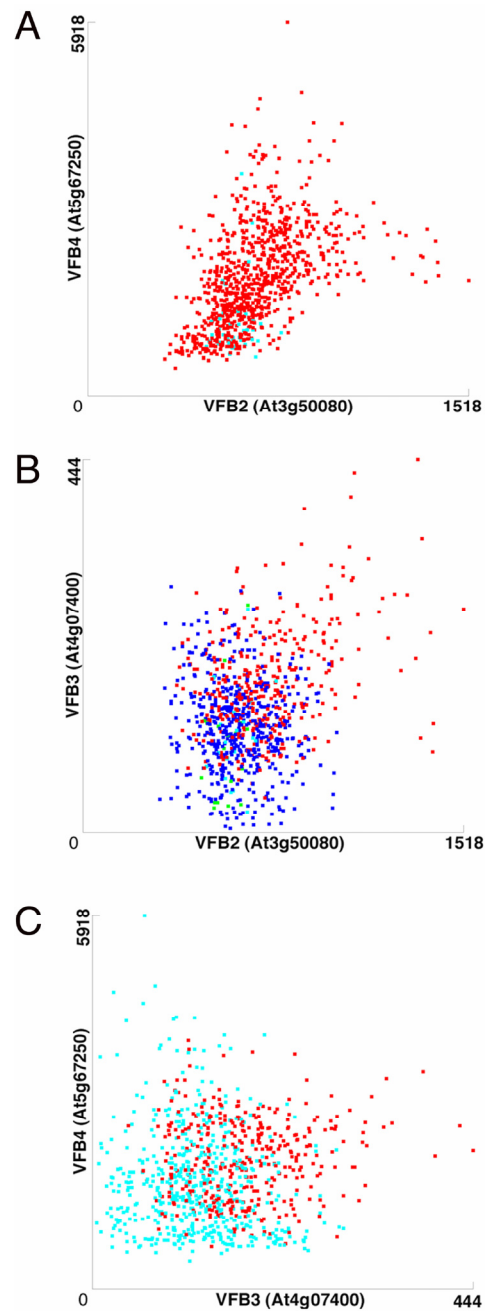


Figure 4

Figure 4: Analysis of published *VFB* gene expression data (1021 microarray data sets). **A.** *VFB2* and *VFB4* are expressed under any condition examined and both genes show strongly correlated gene expression changes. In turn, *VFB3* expression is not well correlated with expression of *VFB2* (**B**) and *VFB4* (**C**). *VFB1* could not be included in this analysis since it is not represented on the Affymetrix ATH1 GeneChip. The graphs are in linear scale. Red squares, both genes are expressed above threshold; dark blue squares, the Y-axis gene is expressed below threshold, light blue squares, the X-axis gene is expressed below threshold.

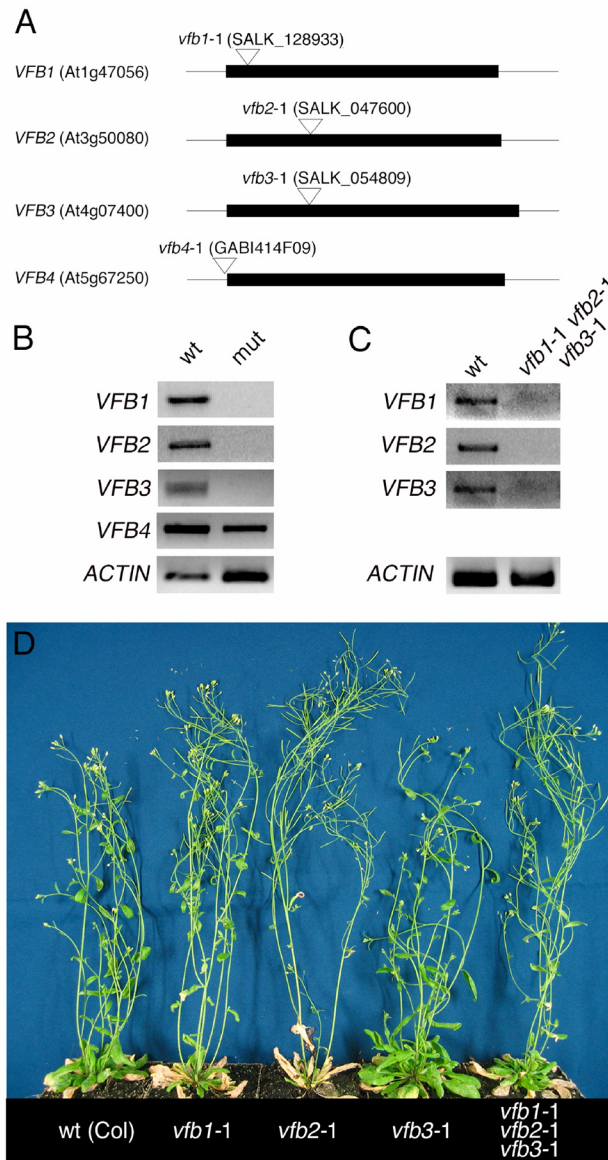


Figure 5

Figure 5: *vfb1*, *vfb2*, and *vfb3* mutant combinations do not have an apparent phenotype. **A.** The *VFB* genes are composed of a single exon (black bar). The T-DNA insertion lines that have been characterized in this study are indicated. **B.** Semi-quantitative RT-PCR (30 cycles) of *VFB* gene expression in the *vfb1-1*, *vfb2-1*, and *vfb3-1* mutants reveals that the full-length transcripts are missing from the respective mutants. The T-DNA insertion upstream of the *VFB4* open reading frame in GABI_414F09 does not affect *VFB4* expression. **C.** Semi-quantitative RT-PCR (30 cycles) for *VFB* gene expression in the *vfb1-1 vfb2-1 vfb3-1* triple mutants. **D.** 5 week-old single and triple *vfb* mutants (5 week-old plants shown here) do not show apparent phenotypes when grown under standard growth conditions and in a wide range of physiological assays. Double mutants are not shown.

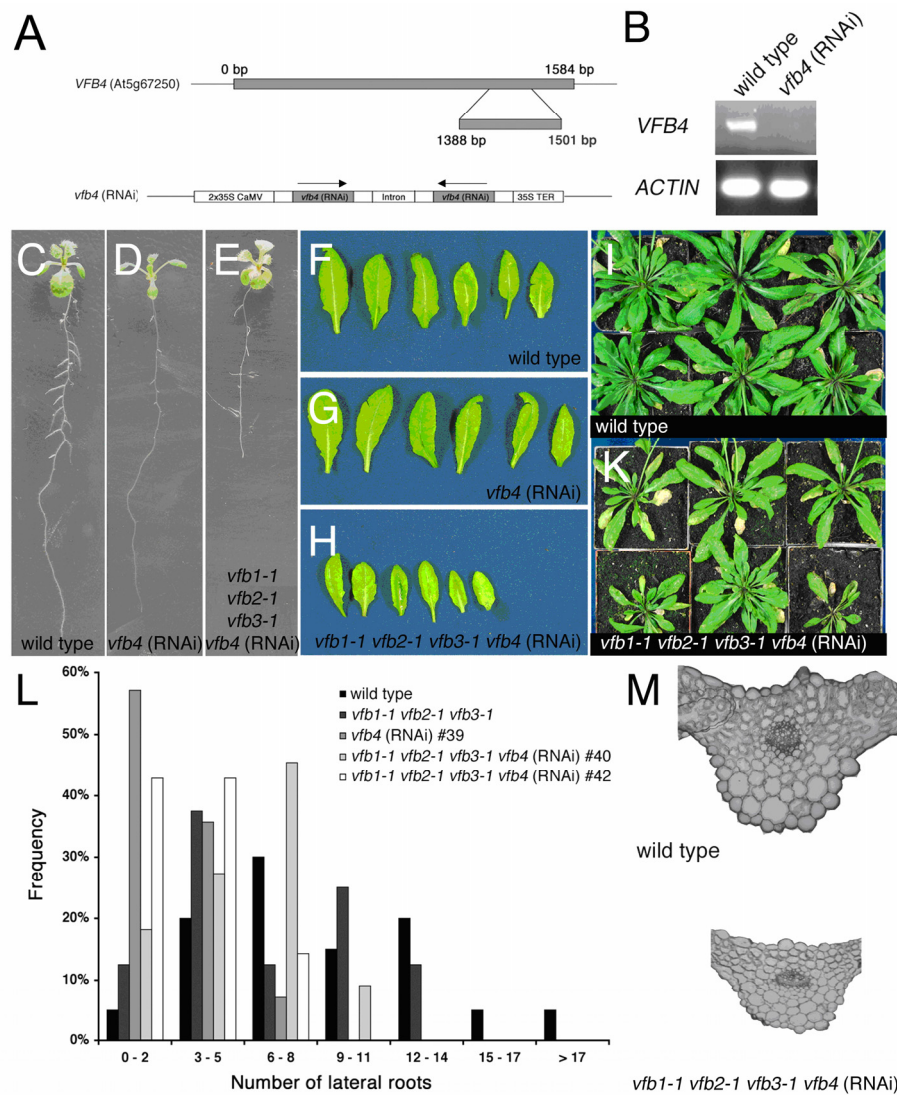


Figure 6

Figure 6: RNAi suppression of *VFB4* reveals a role for the *VFB* gene family in development. **A:** Schematic representation of the *VFB4* gene (upper panel) and the *vfb4* (RNAi) construct (lower panel) that was selected for suppression of *VFB4* expression. Magnified is the 114 base pair (bp) region between bp 1388 and bp 1501 of the *VFB4* open reading frame, which shows the highest sequence divergence between all four *VFB* family members and was selected for RNAi suppression of *VFB4*. **B.** Semiquantitative RT-PCR (33 cycles) indicates that *VFB4* gene expression is strongly reduced in selected *vfb4* (RNAi) lines. **C. – E.** A comparative analysis of ten day-old light grown seedlings reveals differences in root growth and lateral root formation between the wild type (**C**), the wild type transformed with the *vfb4* (RNAi) construct (**D**) and *vfb1-1 vfb2-1 vfb3-1* mutants containing *vfb4* (RNAi) (**E**). **F. – K.**

vfb4 RNAi suppression in the *vfb1-1 vfb2-1 vfb3-1* triple mutant (**H** and **K**) but not in the wild type (**G** and **I**) causes growth delay as indicated by the plants' reduced rosette size. Shown are representative leaves (**F** – **H**) and rosettes (**I** and **K**) of three week old plants. **L**. Quantitative analysis of lateral root formation in 10 day-old Arabidopsis seedlings. The histogram shows the distribution of plants with a given number of lateral roots for the genotypes indicated. $n \geq 20$. **M**. A cross-section from rosette leaves indicates that growth differences in the *vfb1-1 vfb2-1 vfb3-1 vfb4* (RNAi) mutants are due to reduced cell size and not due to reduced cell number. Photographs of both sections were taken at the same magnification.

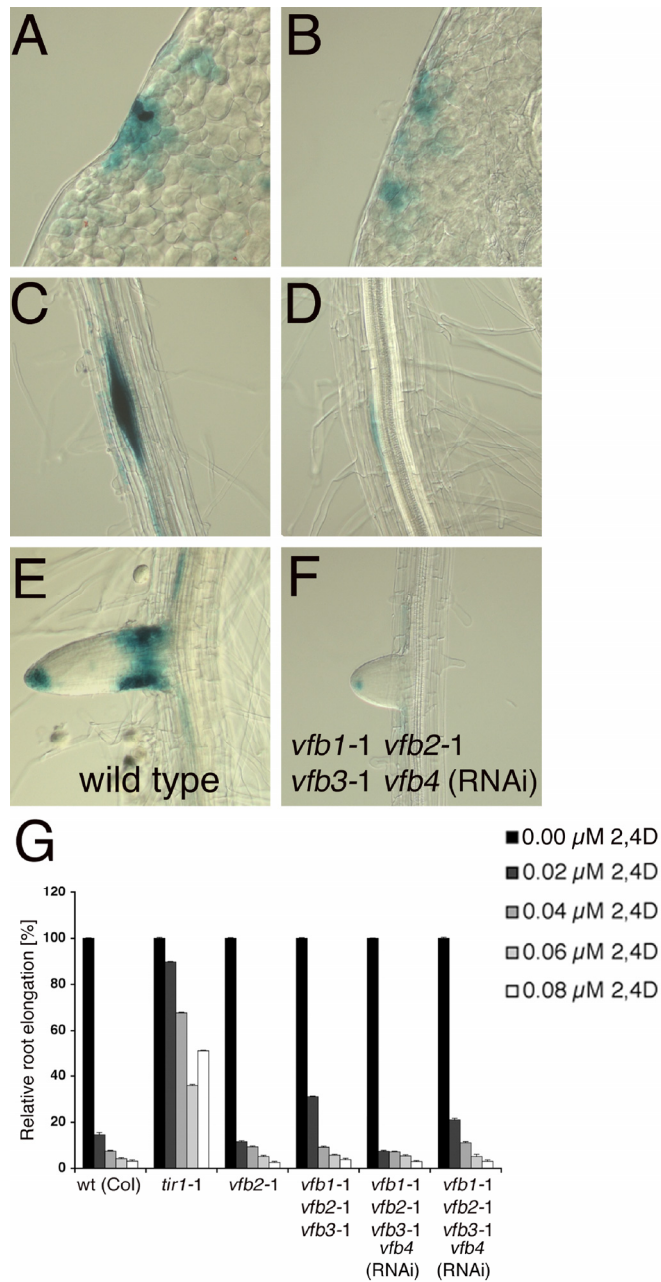


Figure 7

Figure 7: Auxin responses are impaired in the *vfb1-1 vfb2-1 vfb3-1 vfb4* (RNAi) mutants. **A** – **F**. The activity of the DR5:GUS was compared between the wild type and *vfb1-1 vfb2-1 vfb3-1 vfb4* (RNAi) mutants. A general reduction of GUS reporter activity was obtained in leaf margins, lateral root initials, and root tips in the *vfb1-1 vfb2-1 vfb3-1 vfb4* (RNAi) mutants (**B**, **D**, and **F**) when compared to the wildtype (**A**, **C**, and **E**). **G**. Auxin sensitivity assay of *vfb* mutants compared to the wild type and the auxin insensitive *tir1-1* mutant.

Table 1. List of genes that are repressed in *vfb1-1 vfb2-1 vfb3-1 vfb4* (RNAi) mutants (*vfb* mutants) versus the wild type.

Fold repression	Gene Identity	Wt (Col) Raw data	t-test p-value	<i>vfb</i> mutant Raw data	t-test p-value
Auxin response and auxin induced					
6.17	At4g32280 IAA29	174.4 (119.6 to 235.7)	0.057	28.27 (23.33 to 34.51)	0.012
5.54	At3g15540 IAA19 (MASSUGU2)	357.7 (280.6 to 439.3)	0.033	64.53 (57.24 to 73.1)	0.004
2.79	At1g52830 IAA6 (SHY1)	48.94 (46.96 to 50.64)	0.004	17.55 (11.91 to 23.54)	0.064
2.66	At1g04240 IAA3 (SHY2)	299.5 (275.5 to 321.4)	0.011	112.7 (96.26 to 121.2)	0.017
2.64	At3g23030 IAA2	1,144 (989.1 to 1,241)	0.024	433.9 (379.9 to 472.6)	0.015
2.26	At5g43700 IAA4	521.3 (452.5 to 579.6)	0.029	230.2 (227.3 to 234.1)	0.0004
Auxin induced					
4.30	At5g18060 auxin-responsive protein (SAUR)	266.3 (176.9 to 355.9)	0.067	61.97 (58.06 to 66.91)	0.003
3.66	At1g29430 auxin-responsive family protein (SAUR)	346.7 (256.6 to 472.7)	0.078	94.76 (69.35 to 109.3)	0.043
3.05	At3g03830 auxin-responsive family protein (SAUR)	39.22 (34.98 to 45.5)	0.031	12.84 (10.06 to 15.37)	0.030
2.82	At2g21200 auxin-responsive protein (SAUR)	47.64 (45.3 to 49.86)	0.005	16.89 (12.71 to 20.89)	0.047
2.40	At1g29510 auxin-responsive protein (SAUR)	282.4 (225.6 to 349.4)	0.078	117.7 (92.58 to 137.4)	0.062
2.35	At1g29500 auxin-responsive protein (SAUR)	257.6 (216.6 to 337.9)	0.119	109.5 (95.04 to 125.6)	0.030
Cell wall metabolism					
2.65	At1g02640 glycosyl hydrolase family 3 protein	448.6 (399.7 to 513.7)	0.032	169.6 (121.5 to 196.8)	0.063
2.57	At5g48900 pectate lyase family protein	509.4 (407.5 to 567.5)	0.044	198 (175.3 to 209.7)	0.017
2.57	At1g05310 pectinesterase family protein	44.16 (36.02 to 54.87)	0.079	17.2 (13.73 to 21.6)	0.056
2.50	At5g04960 pectinesterase family protein	62.97 (52.05 to 70.71)	0.039	25.21 (24.26 to 27.04)	0.006
2.44	At1g03870 fasciclin-like arabinogalactan-protein (FLA9)	1,985 (1,870 to 2,161)	0.01	812.5 (657.2 to 948.5)	0.034
2.44	At1g65310 xyloglucan:xyloglucosyl transferase	86.83 (84.98 to 87.91)	0.001	35.65 (27.98 to 42.67)	0.039
2.43	At5g65390 arabinogalactan-protein (AGP7)	439.9 (432.8 to 447)	0.0009	180.8 (150.9 to 218.2)	0.030
2.41	At3g26610 polygalacturonase/pectinase	36.79 (33.07 to 39.11)	0.019	15.29 (11.26 to 17.52)	0.067
2.37	At5g01930 (1-4)-beta-mannan endohydrolase	74.88 (63.45 to 89.34)	0.055	31.6 (24.25 to 35.35)	0.066
2.20	At2g32860 glycosyl hydrolase family 1 protein	449.8 (434.2 to 471.3)	0.006	204.9 (184.9 to 224.2)	0.013
2.15	At2g06850 xyloglucan:xyloglucosyl transferase	4,292 (4,012 to 4,602)	0.015	1,994 (1,830 to 2,250)	0.018
2.14	At1g05630 endonuclease/exonuclease/phosphatase family protein	93.87 (87.1 to 102.8)	0.022	43.89 (38.2 to 49.18)	0.026
2.12	At2g48030 endonuclease/exonuclease/phosphatase family protein	169.3 (154.5 to 185.9)	0.024	9.84 (68.04 to 86.09)	0.032
2.08	At4g03210 xyloglucan:xyloglucosyl transferase	3,750 (3,619 to 3,873)	0.006	1,804 (1,536 to 2,229)	0.049
2.05	At1g24170 glycosyl transferase family 8 protein	558.9 (492.9 to 669.7)	0.076	272.8 (228.5 to 306)	0.047
2.03	At3g07010 pectate lyase family protein	302.2 (294 to 313)	0.005	148.6 (127.3 to 174.2)	0.036
2.01	At3g54920 pectate lyase/powdery mildew susceptibility protein	615.1 (585.8 to 660.6)	0.020	306 (266.7 to 364.7)	0.041

Table 2. Genes that misexpressed in *vfb1-1 vfb2-1 vfb3-1 vfb4* (RNAi) mutants (*vfb* mutants) and COP9 signalosome mutants (*csn4*) when compared to the wild type.

A. Repressed genes											
Gene Identity	Wt (Col) Raw data	t-test p-value	<i>vfb</i> mutant	t-test p-value	Fold repression	Wt (Col) Raw data	t-test p-value	<i>csn4</i> (SALK 043720)	t-test p-value	Fold repression	
Auxin response and auxin induced											
A14g32280	IAA29	174.4 (119.6 to 235.7)	0.057	28.27 (23.33 to 34.51)	0.012	6.2	380.3 (369.6 to 385.8)	8.07e-5	53.61 (31.12 to 73.34)	0.226	7.1
A13g15540	IAA19	357.7 (280.6 to 439.3)	0.033	64.53 (57.24 to 73.1)	0.004	5.5	847.1 (728.5 to 1,009)	0.001	49.64 (35.75 to 68.37)	0.707	17.1
A13g23030	IAA2	1,144 (989.1 to 1,241)	0.024	433.9 (379.9 to 472.6)	0.015	2.6	2,495 (2,304 to 2,700)	0.0003	278.3 (177.7 to 346.1)	0.34	9.0
A15g43700	IAA4	521.3 (452.5 to 579.6)	0.029	230.2 (227.3 to 234.1)	0.0004	2.3	504.3 (478.3 to 631.1)	0.001	56.5 (27.45 to 79.35)	0.893	9.6
Auxin induced											
A15g18060	auxin-responsive protein (SAUR)	266.3 (176.9 to 355.9)	0.067	61.97 (58.06 to 66.91)	0.003	4.3	414.4 (374.3 to 455.1)	0.0006	46.18 (28.88 to 73.89)	0.755	9.0
A11g29430	auxin-responsive family protein (SAUR)	346.7 (256.6 to 472.7)	0.078	94.76 (69.35 to 109.3)	0.043	3.7	346.8 (302 to 429.5)	0.001	15.27 (6.704 to 23.25)	0.901	22.7
A13g03830	auxin-responsive protein (SAUR)	39.22 (34.98 to 45.5)	0.031	12.84 (10.06 to 15.37)	0.030	3.1	43.92 (40.24 to 47.05)	0.001	1.709 (1.226 to 2.041)	0.006	25.7
A11g29610	auxin-responsive protein (SAUR)	282.4 (225.6 to 349.4)	0.078	117.7 (92.58 to 137.4)	0.062	2.4	244 (234.3 to 250.9)	6.31e-5	14.89 (10.71 to 31.74)	0.466	16.4
A11g29500	auxin-responsive protein (SAUR)	257.6 (216.6 to 337.9)	0.119	109.5 (95.04 to 125.6)	0.030	2.4	302.7 (270.1 to 321.6)	0.0002	10.67 (0.692 to 26.56)	0.461	28.4
Cell wall metabolism											
A14g02290	glycosyl hydrolase family 9 protein	493.6 (353 to 570.6)	0.053	140.9 (119.3 to 153.1)	0.018	3.5	216.5 (166.2 to 246.6)	0.02	70.76 (49.78 to 97.28)	0.301	3.1
A11g02640	glycosyl hydrolase family 3 protein	448.6 (399.5 to 513.7)	0.032	169.6 (121.5 to 196.8)	0.063	2.6	973.2 (896.7 to 1,091)	0.0007	68.19 (57.46 to 86.84)	0.054	14.3
A15g48900	pectate lyase family protein	509.4 (407.5 to 567.5)	0.044	198 (175.3 to 209.7)	0.017	2.6	506.3 (448.8 to 590.4)	0.005	166.2 (115 to 208.5)	0.748	3.0
A11g03870	fasciclin-like arabinogalactan-protein (FLA9)	1,985 (1,870 to 2,161)	0.016	812.5 (657.2 to 948.5)	0.034	2.4	3,214 (2,992 to 3,570)	0.001	577.2 (412.1 to 686.7)	0.565	5.6
A11g65310	xyloglucan:xyloglucosyl transferase	86.83 (84.98 to 87.91)	0.001	35.65 (27.98 to 42.67)	0.039	2.4	133.9 (121.1 to 145.7)	0.003	60.26 (46.09 to 69.37)	0.728	2.2
A15g65390	arabinogalactan-protein (AGP7)	439.9 (432.8 to 447)	0.0009	180.8 (150.9 to 218.2)	0.030	2.4	1,250 (1,157 to 1,378)	0.0009	218.6 (117.9 to 377)	0.615	5.7
A12g32860	glycosyl hydrolase family 1 protein	449.8 (434.2 to 471.3)	0.006	204.9 (184.9 to 224.2)	0.013	2.2	271.5 (245.6 to 293.5)	0.0006	36.23 (26.88 to 47.29)	0.934	7.5
A12g08850	xyloglucan:xyloglucosyl transferase	4,292 (4,012 to 4,602)	0.015	1,594 (1,830 to 2,250)	0.018	2.2	6,247 (5,987 to 6,671)	0.0006	1,814 (1,484 to 2,263)	0.803	3.4
A14g03210	xyloglucan:xyloglucosyl transferase	3,750 (3,619 to 3,873)	0.006	1,804 (1,536 to 2,229)	0.049	2.1	2,373 (2,142 to 2,622)	0.002	1,184 (953.6 to 1,581)	0.232	2.0
A13g07010	pectate lyase family protein	302.2 (294 to 313)	0.005	148.6 (127.3 to 174.2)	0.036	2.0	313.1 (293.2 to 343)	0.001	83.9 (67.97 to 106.4)	0.76	3.7
A13g54920	pectate lyase	615.1 (585.8 to 660.6)	0.020	306 (266.7 to 364.7)	0.041	2.0	826.1 (798.9 to 869)	0.001	375.4 (277 to 459.6)	0.716	2.2
Signalling components											
A15g02760	protein phosphatase 2C family protein / PP2C family protein745	502.5 (502.5 to 922.4)	0.070	186.9 (150.9 to 244)	0.039	4.0	2,407 (2,115 to 2,695)	0.0004	52.19 (43.03 to 60.89)	0.023	46.1
A13g59350	serine/threonine protein kinase	768.1 (586.4 to 992)	0.061	217.3 (179.7 to 249.6)	0.020	3.5	716.8 (617.6 to 847.4)	0.003	127.1 (78.51 to 169.3)	0.637	5.6
A11g66940	protein kinase-related	1,051 (970.3 to 1,131)	0.013	434.1 (397.7 to 464.5)	0.008	2.4	762.6 (737.9 to 796.1)	0.0002	162.4 (115.5 to 286.5)	0.855	4.2
Transcriptional regulators											
A14g16780	homeobox-leucine zipper protein 4 (HAT4)	180.7 (122.4 to 243.9)	0.068	38.18 (33.78 to 46.2)	0.015	4.7	384.5 (290.3 to 463.1)	0.013	107 (82.07 to 133.5)	0.537	3.6
A13g58120	bZIP transcription factor family protein	449.9 (396.4 to 482.8)	0.018	150.4 (109.6 to 178.2)	0.046	3.0	547.1 (516.5 to 600.5)	0.0001	12.8 (4.729 to 24.72)	0.379	42.7
A15g47370	homeobox-leucine zipper protein 2 (HAT2)	442 (385.5 to 466.9)	0.014	166.2 (161.8 to 170.9)	0.0008	2.7	730.3 (660.4 to 817.3)	0.0006	68 (45.18 to 100.1)	0.839	10.6
A13g50650	scarecrow-like transcription factor 7 (SCL7)	116.2 (110.7 to 125.5)	0.011	44.72 (41.11 to 50.24)	0.010	2.6	97.87 (87.74 to 108.2)	0.009	38.88 (37.35 to 39.7)	0.004	2.5
A11g73830	basic helix-loop-helix (bHLH) family protein	219.5 (159.4 to 250)	0.079	88.79 (77.04 to 101.8)	0.039	2.5	699.1 (631.7 to 738.1)	0.0008	128.2 (122.5 to 137.7)	0.421	5.5
A13g7795	bHLH transcription factor	287.9 (257.4 to 312.9)	0.022	127.1 (121.4 to 137.4)	0.008	2.3	315.9 (302.8 to 329.8)	0.0005	91.2 (81.84 to 103.9)	0.135	3.5
A11g14920	gibberellin response modulator (GA)	667.6 (556.8 to 771.4)	0.061	312.8 (255.6 to 363.7)	0.061	2.1	902 (848.6 to 976.8)	0.0006	122.2 (113.8 to 128.5)	0.011	7.4
A11g18400	basic helix-loop-helix (bHLH) family protein	100.3 (94.19 to 106.9)	0.014	47.61 (38.79 to 53.52)	0.045	2.1	259.6 (231.9 to 302.7)	0.002	39.03 (25.16 to 59.68)	0.274	6.7
A15g50570	squamosa promoter-binding protein, putative	416.1 (388 to 457.5)	0.028	198 (152.8 to 234.7)	0.066	2.1	283.1 (240.9 to 322.7)	0.013	134.9 (90.1 to 166.5)	0.869	2.1
B. Induced genes											
Gene Identity	Wt (Col) Raw data	t-test p-value	<i>vfb</i> mutant	t-test p-value	Fold induction	Wt (Col) Raw data	t-test p-value	<i>csn4</i> (SALK 043720)	t-test p-value	Fold induction	
Signalling components											
A12g24540	kelch repeat-containing F-box family protein	61.36 (56.86 to 66.94)	0.004	199.3 (186.4 to 217.9)	0.010	3.2	66.38 (62.28 to 68.85)	0.0003	347.7 (199.7 to 444.1)	0.926	5.2
A15g11410	protein kinase family protein	16.49 (12.68 to 21.41)	0.036	53.27 (49.03 to 58.5)	0.015	3.2	10.68 (8.582 to 13.48)	0.002	238.4 (215.6 to 258.9)	0.030	22.3
A14g23300	protein kinase family protein	100.5 (78.67 to 123)	0.042	263.7 (241 to 332.9)	0.043	2.8	79.84 (65.34 to 90.51)	0.007	371.5 (331.3 to 410.3)	0.018	4.7
A14g23290	protein kinase family protein	163.3 (136.8 to 220.8)	0.068	415.4 (346.3 to 465.6)	0.052	2.5	168.1 (140.6 to 187.5)	0.005	710.1 (536.8 to 928.8)	0.239	4.2
A11g07580	leucine-rich repeat family protein	57.64 (48.67 to 63.37)	0.022	136.5 (134.6 to 143.7)	0.003	2.4	54.84 (51.43 to 61.11)	0.001	252.4 (209.3 to 305.2)	0.946	4.6
A11g53090	WD40 repeat family protein / phytochrome A-related	70.86 (64.43 to 77.32)	0.017	154.4 (132.2 to 173.5)	0.040	2.2	83.15 (61.35 to 94.26)	0.012	306.1 (250.6 to 407.1)	0.789	3.7
A14g03260	leucine-rich repeat family protein	255.8 (232.3 to 274.8)	0.013	551.9 (507.3 to 592.7)	0.016	2.2	278.2 (246.2 to 302)	0.003	764.9 (640.6 to 849.7)	0.345	2.7
Transcriptional regulators											
A12g21320	zinc finger (B-box type) family protein	27.89 (15.5 to 41.57)	0.047	178.4 (140.6 to 198.5)	0.028	6.4	33.51 (26.18 to 45.14)	0.023	150.4 (94.72 to 225.9)	0.264	4.5
A13g17610	bZIP transcription factor	49.69 (37.62 to 63.57)	0.029	198.5 (166.3 to 237.8)	0.035	4.0	71.9 (68.15 to 77.94)	0.0008	377.2 (316.6 to 444.2)	0.127	5.2
A15g24120	RNA polymerase sigma subunit SigE (sigE)	93.13 (85.42 to 100.3)	0.004	356.2 (281.1 to 465.7)	0.057	3.8	85.68 (67.86 to 97.43)	0.009	271.8 (158.3 to 373.8)	0.940	3.2
A13g61890	homeobox-leucine zipper protein 12 (HB-12)	67.72 (58.36 to 76.74)	0.032	138.2 (130.7 to 142.6)	0.009	2.0	93.94 (91.46 to 96.06)	0.0004	221.3 (206.1 to 249.7)	0.115	2.4

Supplemental Data

Table 1. Genes that are repressed in *vfb1-1 vfb2-1 vfb3-1 vfb4* (RNAi) mutants (*vfb* mutants) compared to the wild type.

Fold repression	Gene Identity	Wt (Col) Raw data	t-test p-value	<i>vfb</i> mutant Raw data	t-test p-value
73.54	At5g24240 phosphatidylinositol 3- and 4-kinase family protein	187.3 (177.7 to 193.1)	0.001	2.547 (1.227 to 3.867)	0.008
20.68	At1g52820 2-oxoglutarate-dependent dioxygenase	47.72 (35.68 to 69.63)	0.061	2.308 (0.57 to 4.254)	0.053
8.09	At5g62280 expressed protein	307.6 (271.5 to 365.2)	0.018	38.02 (32.14 to 43.56)	0.003
7.56	At5g12050 expressed protein	791.8 (704.2 to 885.9)	0.010	104.8 (86.3 to 127.6)	0.006
6.17	At4g32280 IAA29	174.4 (119.6 to 235.7)	0.057	28.27 (23.33 to 34.51)	0.012
5.60	At5g57760 expressed protein	147 (139 to 152.1)	0.002	26.27 (20.72 to 33.04)	0.012
5.54	At3g15540 IAA19	357.7 (280.6 to 439.3)	0.033	64.53 (57.24 to 73.1)	0.004
5.49	At2g37820 DC1 domain-containing protein	9.496 (6.958 to 14.19)	0.686	1.73 (1.497 to 2.169)	0.004
4.77	At1g22740 Ras-related protein (RAB7)/AtRab75	402.2 (332.5 to 457.4)	0.025	84.35 (60.61 to 111.1)	0.029
4.73	At4g16780 homeobox-leucine zipper protein 4 (HAT4)	180.7 (122.4 to 243.9)	0.068	38.18 (33.78 to 46.2)	0.015
4.72	At2g47880 glutaredoxin family protein	130.2 (110.7 to 145.1)	0.022	27.56 (19.07 to 42.36)	0.049
4.32	At3g23550 MATE efflux family protein	265.2 (204.7 to 351.8)	0.071	61.34 (44.35 to 88.09)	0.048
4.30	At5g18060 auxin-responsive protein	266.3 (176.9 to 355.9)	0.067	61.97 (58.06 to 66.91)	0.003
4.21	At5g59670 leucine-rich repeat protein kinase	47.72 (38.11 to 53.37)	0.030	11.33 (6.799 to 13.71)	0.063
4.14	At3g45860 receptor-like protein kinase	292 (238.1 to 393.6)	0.070	70.47 (55.47 to 78.84)	0.018
4.13	At2g25940 vacuolar processing enzyme alpha	29.8 (28.05 to 30.69)	0.005	7.217 (4.895 to 11.66)	0.060
4.12	At1g49860 glutathione S-transferase	308.2 (290.7 to 330.9)	0.007	74.74 (58.84 to 102.7)	0.029
4.09	At3g04210 putative disease resistance protein (TIR-NBS class)	380.2 (336.4 to 457.9)	0.032	92.85 (70.35 to 106.9)	0.021
3.99	At5g02760 protein phosphatase 2C family protein	745 (502.5 to 922.4)	0.070	186.9 (150.9 to 244)	0.039
3.91	At5g49350 pseudogene, glycine-rich protein	35.34 (23.43 to 47.42)	0.077	9.028 (7.327 to 10.53)	0.026
3.91	At1g13420 sulfotransferase family protein	57.18 (44.78 to 64.09)	0.040	14.62 (10.65 to 19.76)	0.044
3.90	At2g14560 expressed protein	584.5 (479.9 to 701.9)	0.037	150 (119.3 to 187.1)	0.024
3.83	At2g42870 expressed protein	274.5 (232 to 324.6)	0.030	71.61 (58.94 to 82.64)	0.015
3.75	At1g19530 expressed protein	76.91 (53.54 to 110)	0.097	20.49 (17.89 to 24.54)	0.021
3.75	At1g78970 lupeol synthase (LUP1)	274.3 (250.6 to 306.9)	0.013	73.22 (69.13 to 76.2)	0.001
3.74	At3g06370 sodium proton exchanger (NHX3)	66.82 (64.16 to 69.75)	0.002	17.88 (14.94 to 21.3)	0.013
3.70	At4g31940 cytochrome P450	75.82 (71.16 to 78.28)	0.004	20.5 (15.24 to 25.31)	0.027
3.68	At4g14060 major latex protein-related	116.4 (99.81 to 134.6)	0.025	31.65 (29.26 to 36.17)	0.008
3.66	At1g29430 auxin-responsive family protein (SAUR)	346.7 (256.6 to 472.7)	0.078	94.76 (69.35 to 109.3)	0.043
3.64	At2g16060 non-symbiotic hemoglobin 1 (HB1)	229.6 (198 to 246.3)	0.020	63.12 (52.53 to 79.61)	0.024
3.53	At3g59350 serine/threonine protein kinase	768.1 (586.4 to 992)	0.061	217.3 (179.7 to 249.6)	0.020
3.50	At4g02290 glycosyl hydrolase family 9 protein	493.6 (353 to 570.6)	0.053	140.9 (119.3 to 153.1)	0.018
3.39	At1g69230 expressed protein	147.1 (135.5 to 170)	0.027	43.41 (38.67 to 51.38)	0.013
3.28	At3g22231 expressed protein	3,863 (3,309 to 4,308)	0.022	1,178 (1,110 to 1,272)	0.003
3.22	At5g43890 flavin-containing monooxygenase family protein	54.2 (36.55 to 65.26)	0.078	16.84 (13.6 to 20.35)	0.043
3.16	At1g49230 zinc finger (C3HC4-type RING finger) family protein	143.5 (127.1 to 163.1)	0.020	45.35 (44.38 to 46)	0.0002
3.11	At1g28330 dormancy-associated protein (DRM1)	1,443 (1,357 to 1,566)	0.013	463.4 (289.6 to 635.6)	0.070
3.06	At2g31010 serine/threonine kinase	69.37 (58.25 to 84.65)	0.059	22.66 (17.53 to 30.65)	0.053
3.05	At3g03830 auxin-responsive family protein (SAUR)	39.22 (34.98 to 45.5)	0.031	12.84 (10.06 to 15.37)	0.030
3.04	At1g08430 expressed protein	125.6 (112.7 to 135.8)	0.015	41.3 (35.4 to 49.43)	0.020
2.99	At3g58120 bZIP transcription factor	449.9 (396.4 to 482.8)	0.018	150.4 (109.6 to 178.2)	0.047
2.99	At2g34510 expressed protein	1,220 (965.8 to 1,380)	0.043	408.4 (299.7 to 466.8)	0.056

Supplemental Data

Table 1 (continued)

Fold repression	Gene Identity	Wt (Col) Raw data	t-test p-value	vfb mutant Raw data	t-test p-value
2.97	At1g43790 expressed protein	288.8 (265 to 318.3)	0.014	97.23 (78.92 to 108)	0.022
2.92	At1g21250 wall-associated kinase 1 (WAK1)	617.3 (548.6 to 719.7)	0.034	211.3 (151.3 to 248.4)	0.052
2.91	At2g31010 protein kinase family protein	134.7 (99.13 to 165.5)	0.063	46.35 (43.78 to 50.29)	0.007
2.91	At2g18480 mannitol transporter	39.63 (34.27 to 46.1)	0.040	13.64 (10.36 to 17.73)	0.050
2.90	At3g21550 expressed protein	185.4 (156.2 to 203)	0.036	63.86 (47.03 to 84.97)	0.060
2.88	At1g06830 glutaredoxin family protein	182.3 (150.1 to 223.6)	0.059	63.31 (54.14 to 77.41)	0.031
2.88	At5g37990 S-adenosyl-L-methionine:carboxyl methyltransferase	465.9 (387.6 to 519.2)	0.038	161.9 (135.7 to 205.2)	0.04
2.87	At1g33700 expressed protein	80.12 (61.98 to 89.31)	0.060	27.87 (22.5 to 36.73)	0.059
2.87	At1g52290 protein kinase family protein	228.6 (192.1 to 284.8)	0.066	79.73 (68.22 to 97.44)	0.030
2.86	At2g44500 expressed protein	382.7 (344.6 to 438.4)	0.028	133.8 (105.2 to 156.1)	0.032
2.85	At5g61660 glycine-rich protein	716 (661.2 to 763.1)	0.012	251.3 (199.6 to 323)	0.039
2.82	At5g23210 serine carboxypeptidase S10 family protein	723.9 (599.1 to 889.6)	0.053	256.6 (242.1 to 284)	0.008
2.82	At2g21200 auxin-responsive protein (SAUR)	47.64 (45.3 to 49.86)	0.005	16.89 (12.71 to 20.89)	0.047
2.79	At1g52830 IAA6	48.94 (46.96 to 50.64)	0.004	17.55 (11.91 to 23.54)	0.064
2.78	At1g22330 RNA recognition motif (RRM)-containing protein	111.1 (105.8 to 118.8)	0.009	39.93 (32.6 to 48.49)	0.028
2.78	At3g46490 oxidoreductase, 2OG-Fe(II) oxygenase family protein	133.3 (125.8 to 146.5)	0.016	48.03 (41.8 to 57.16)	0.020
2.77	At1g17430 hydrolase, alpha/beta fold family protein	129 (105.5 to 163)	0.073	46.58 (37.84 to 55.76)	0.037
2.76	At2g28780 expressed protein	73.03 (68.74 to 75.65)	0.005	26.45 (20.14 to 30.24)	0.038
2.74	At2g34770 fatty acid hydroxylase (FAH1)	1,107 (989.4 to 1,282)	0.041	403.6 (303.8 to 531.4)	0.055
2.71	At2g26560 patatin	375.6 (337.8 to 438.5)	0.042	138.6 (119.1 to 172.2)	0.033
2.69	At4g16515 expressed protein	216.2 (186.6 to 267.4)	0.061	80.27 (69.62 to 88.63)	0.016
2.68	At2g17230 phosphate-responsive 1 family protein	1,047 (914.7 to 1,147)	0.028	391 (335.7 to 494.2)	0.040
2.67	At1g61170 expressed protein	87.81 (78.08 to 98.13)	0.026	32.88 (27.76 to 39.65)	0.029
2.67	At2g33570 expressed protein	310.8 (286.9 to 326.6)	0.010	116.5 (84.47 to 138.6)	0.054
2.66	At5g47370 homeobox-leucine zipper protein 2 (HAT2)	442 (395.5 to 466.9)	0.014	166.2 (161.8 to 170.9)	0.0008
2.66	At4g14400 ankyrin repeat family protein	584.6 (485.2 to 681.9)	0.042	219.9 (179.3 to 245.4)	0.034
2.66	At1g04240 IAA3	299.5 (275.5 to 321.4)	0.011	112.7 (96.26 to 121.2)	0.017
2.65	At1g02640 glycosyl hydrolase family 3 protein	448.6 (399.7 to 513.7)	0.032	169.6 (121.5 to 196.8)	0.063
2.64	At3g23030 IAA2	1,144 (989.1 to 1,241)	0.024	433.9 (379.9 to 472.6)	0.015
2.60	At3g50650 scarecrow-like transcription factor 7	116.2 (110.7 to 125.5)	0.011	44.72 (41.11 to 50.24)	0.010
2.59	At5g44400 FAD-binding domain-containing protein	493.8 (434.2 to 590.3)	0.049	190.9 (167.8 to 213.3)	0.016
2.58	At3g47340 glutamine-dependent asparagine synthetase 1 (ASN1)	1,376 (1,256 to 1,538)	0.023	533.1 (386.9 to 611.8)	0.060
2.57	At5g48900 pectate lyase family protein	509.4 (407.5 to 567.5)	0.044	198 (175.3 to 209.7)	0.017
2.57	At1g05310 pectinesterase family protein	44.16 (36.02 to 54.87)	0.079	17.2 (13.73 to 21.6)	0.056
2.56	At5g46330 leucine-rich repeat transmembrane protein kinase	135.8 (134 to 137.3)	0.001	53.04 (43.08 to 58.99)	0.025
2.53	At2g30930 expressed protein	1,025 (888.8 to 1,251)	0.071	405.4 (324.5 to 501.5)	0.047
2.53	At3g01670 expressed protein	271.7 (254.5 to 285.5)	0.008	107.5 (88.75 to 122.1)	0.026
2.51	At1g19330 expressed protein	285.6 (234.4 to 361.3)	0.076	113.8 (92.24 to 126.6)	0.042
2.51	At1g31950 terpene synthase/cyclase family protein	62.98 (56.98 to 73.42)	0.039	25.1 (20.33 to 27.74)	0.033
2.50	At5g04960 pectinesterase family protein	62.97 (52.05 to 70.71)	0.039	25.21 (24.26 to 27.04)	0.006
2.48	At1g07000 exocyst subunit EXO70 family protein	181.7 (156.8 to 204.4)	0.032	73.13 (66.28 to 81.83)	0.015
2.47	At4g19530 disease resistance protein (TIR-NBS-LRR class)	1,075 (1,020 to 1,109)	0.004	434.4 (371.7 to 468.2)	0.018

**Supplemental Data
Table 1 (continued)**

Fold repression	Gene Identity	Wt (Col) Raw data	t-test p-value	vfb mutant Raw data	t-test p-value
2.47	At1g73830 bHLH transcription factor	219.5 (159.4 to 250)	0.079	88.79 (77.04 to 101.8)	0.039
2.47	At3g26460 major latex protein-related	75.04 (64.13 to 83.69)	0.035	30.41 (22.03 to 35.15)	0.077
2.46	At1g61100 disease resistance protein (TIR class)	494.2 (430.5 to 589.2)	0.063	200.8 (165 to 252.9)	0.050
2.45	At2g42580 tetra-tricopeptide repeat (TPR)-containing protein	601.5 (585.8 to 612.9)	0.001	245.2 (235 to 261.4)	0.003
2.45	At1g08500 plastocyanin-like domain-containing protein	97.13 (88 to 105.4)	0.018	39.65 (29.83 to 44.99)	0.057
2.44	At1g03870 fasciclin-like arabinogalactan-protein (FLA9)	1,985 (1,870 to 2,161)	0.01	812.5 (657.2 to 948.5)	0.034
2.44	At1g65310 xyloglucan:xyloglucosyl transferase	86.83 (84.98 to 87.91)	0.001	35.65 (27.98 to 42.67)	0.039
2.43	At5g65390 arabinogalactan-protein (AGP7)	439.9 (432.8 to 447)	0.0009	180.8 (150.9 to 218.2)	0.030
2.43	At1g22335 expressed protein	182.8 (169.7 to 199.9)	0.016	75.16 (61.03 to 82.82)	0.033
2.42	At1g66940 protein kinase-related	1,051 (970.3 to 1,131)	0.013	434.1 (397.7 to 464.5)	0.008
2.42	At4g25940 epsin N-terminal homology domain-containing protein	84.63 (78.95 to 89.5)	0.014	35.02 (25.73 to 45.87)	0.068
2.41	At3g26610 polygalacturonase/pectinase	36.79 (33.07 to 39.11)	0.019	15.29 (11.26 to 17.52)	0.067
2.40	At4g31000 calmodulin-binding protein	107.2 (80.93 to 124.9)	0.071	44.58 (37.89 to 50.54)	0.042
2.40	At2g41090 calmodulin-like calcium-binding protein, 22 kDa	3,146 (2,742 to 3,387)	0.033	1,309 (1,110 to 1,633)	0.047
2.40	At1g29510 auxin-responsive protein (SAUR)	282.4 (225.6 to 349.4)	0.078	117.7 (92.58 to 137.4)	0.062
2.40	At5g58670 phosphoinositide-specific phospholipase C (PLC1)	155.1 (126.8 to 183)	0.052	64.68 (59.25 to 69.84)	0.012
2.39	At1g80240 expressed protein	72.32 (69.12 to 75.24)	0.005	30.28 (26.97 to 34.32)	0.016
2.39	At1g11080 serine carboxypeptidase S10 family protein	233.6 (218.6 to 250.5)	0.014	97.92 (80.98 to 117.9)	0.036
2.39	At1g14790 RNA-dependent RNA polymerase	75.69 (67.1 to 83.73)	0.030	31.73 (22.8 to 38.04)	0.077
2.38	At5g56080 nicotianamine synthase	184.5 (146.5 to 207.9)	0.052	77.57 (72.18 to 83.41)	0.011
2.37	At4g35350 cysteine endopeptidase, papain-type (XCP1)	219 (190.7 to 234.7)	0.027	92.3 (76.48 to 103.2)	0.035
2.37	At4g22160 expressed protein	94.06 (84.96 to 103.5)	0.026	39.68 (30.74 to 48.13)	0.054
2.37	At5g01930 (1-4)-beta-mannan endohydrolase	74.88 (63.45 to 89.34)	0.055	31.6 (24.25 to 35.35)	0.066
2.35	At1g59710 expressed protein	195.3 (187.3 to 204.6)	0.007	82.99 (71.6 to 100)	0.031
2.35	At1g29500 auxin-responsive protein (SAUR)	257.6 (216.6 to 337.9)	0.119	109.5 (95.04 to 125.6)	0.030
2.35	At4g11190 disease resistance-responsive family protein	176.8 (161.6 to 194.4)	0.028	75.18 (58.92 to 96.57)	0.060
2.34	At5g47990 cytochrome P450 family protein	186.5 (158.8 to 212.5)	0.040	79.74 (65.88 to 87.69)	0.040
2.32	At4g30410 expressed protein	134.9 (134.2 to 135.3)	6.44e-5	58.07 (50.94 to 62.91)	0.014
2.32	At3g62040 haloacid dehalogenase-like hydrolase family protein	385.2 (329.7 to 427.7)	0.036	166 (151.1 to 187.3)	0.020
2.31	At1g02340 long hypocotyl in far-red 1 (HFR1)	67.47 (60.66 to 79.69)	0.065	29.22 (24.22 to 36.08)	0.048
2.31	At1g67870 glycine-rich protein	928.5 (846 to 985.4)	0.016	402.4 (311.1 to 449.9)	0.056
2.31	At5g06610 expressed protein	80.58 (75.63 to 85.41)	0.010	34.95 (31.49 to 39.18)	0.015
2.30	At3g12920 expressed protein	482.6 (456.3 to 515.9)	0.009	210 (203.6 to 217.1)	0.001
2.29	At4g26070 mitogen-activated protein kinase kinase (MAPKK)	313.7 (295.5 to 343.8)	0.019	136.7 (119.9 to 153.1)	0.019
2.29	At4g33810 glycosyl hydrolase family 10 protein	67.2 (53.67 to 79.1)	0.061	29.4 (25.35 to 32.19)	0.034
2.28	At3g54260 expressed protein	806.4 (668.7 to 947)	0.051	353.9 (341 to 373.6)	0.005
2.28	At1g25230 purple acid phosphatase family protein	1,025 (967 to 1,100)	0.012	450.4 (391.8 to 503.2)	0.020
2.27	At3g57795 bHLH transcription factor	287.9 (257.4 to 312.9)	0.022	127.1 (121.4 to 137.4)	0.008
2.26	At5g43700 IAA4	521.3 (452.5 to 579.6)	0.029	230.2 (227.3 to 234.1)	0.0004
2.26	At1g64360 expressed protein	150.7 (147.3 to 155.1)	0.002	66.81 (54.09 to 78.29)	0.038
2.25	At2g35880 expressed protein	402.2 (370.7 to 440.6)	0.018	178.8 (172 to 187.5)	0.003
2.24	At3g06210 expressed protein	88.15 (85.34 to 90.78)	0.003	39.34 (33.75 to 44.08)	0.023

Supplemental Data

Table 1 (continued)

Fold repression	Gene Identity	Wt (Col) Raw data	t-test p-value	vfb mutant Raw data	t-test p-value
2.23	At1g21270 wall-associated kinase 2 (WAK2)	289.2 (252.2 to 317.1)	0.032	129.5 (111.3 to 145.3)	0.030

2.23	At2g33790 pollen Ole e 1 allergen and extensin family protein	90.32 (84.09 to 100.2)	0.031	40.47 (34.14 to 49.24)	0.042
2.22	At1g52070 jacalin lectin family protein	56.64 (53.37 to 62.65)	0.024	25.46 (21.54 to 28.33)	0.028
2.22	At5g09520 hydroxyproline-rich glycoprotein family protein	90.49 (82.46 to 97.94)	0.024	40.72 (35.36 to 49.78)	0.043
2.22	At5g03120 expressed protein	208.2 (156.5 to 256.1)	0.081	93.76 (91.39 to 98.1)	0.005
2.21	At4g03190 F-box family protein (FBL18)	426.4 (383 to 497.9)	0.046	193.2 (183 to 203.9)	0.005
2.20	At5g65040 senescence-associated protein-related	123.3 (121.1 to 126.2)	0.001	55.92 (42.5 to 64.62)	0.056
2.20	At4g01120 G-box binding factor 2 (GBF2)	212 (201.9 to 228.5)	0.014	96.17 (81.22 to 107.5)	0.028
2.20	At1g76040 calcium-dependent protein kinase	63.15 (62.2 to 64.61)	0.001	28.71 (22.77 to 33.31)	0.044
2.20	At5g07000 sulfotransferase family protein	74.62 (69.33 to 82.33)	0.023	33.94 (29.35 to 37.42)	0.024
2.20	At4g11310 cysteine proteinase	667.7 (613.9 to 735.8)	0.023	304 (263.5 to 333.5)	0.024
2.20	At2g32860 glycosyl hydrolase family 1 protein	449.8 (434.2 to 471.3)	0.006	204.9 (184.9 to 224.2)	0.013
2.19	At3g24110 calcium-binding EF hand family protein	41.04 (34.57 to 51.9)	0.097	18.74 (16.97 to 20.82)	0.021
2.19	At1g71960 ABC transporter family protein	120.1 (108.5 to 134.2)	0.026	54.87 (54.45 to 55.45)	0.0001
2.19	At1g50630 expressed protein	111.4 (106 to 121.6)	0.020	50.97 (40.16 to 57.87)	0.050
2.18	At3g45160 expressed protein	953.6 (832.1 to 1,070)	0.036	436.5 (393.5 to 476.6)	0.018
2.17	At5g44680 methyladenine glycosylase family protein	1,641 (1,558 to 1,786)	0.025	756.9 (614.9 to 957.2)	0.057
2.16	At3g16180 proton-dependent oligopeptide transport family protein	328.1 (309.7 to 356.2)	0.019	151.7 (109.5 to 173.6)	0.085
2.16	At1g22530 SEC14 cytosolic factor family protein	797.9 (717.7 to 916.5)	0.044	369.1 (312.9 to 414.1)	0.034
2.16	At1g14290 acid phosphatase	452.6 (430.2 to 479.1)	0.008	209.4 (192.4 to 219.3)	0.008
2.16	At5g63560 transferase family protein	141.4 (131.4 to 161.3)	0.044	65.61 (54.26 to 74.66)	0.039
2.15	At2g06850 xyloglucan:xyloglucosyl transferase	4,292 (4,012 to 4,602)	0.015	1,994 (1,830 to 2,250)	0.018
2.15	At2g15960 expressed protein	1,967 (1,740 to 2,264)	0.047	914.5 (831.1 to 1,037)	0.024
2.15	At5g02540 short-chain dehydrogenase/reductase family protein	121 (101.4 to 135.7)	0.051	56.26 (51.82 to 64.54)	0.031
2.15	At4g29270 acid phosphatase class B family protein	277.2 (214.3 to 342.6)	0.084	128.9 (123.6 to 137.4)	0.010
2.14	At1g05630 endonuclease/exonuclease/phosphatase family protein	93.87 (87.1 to 102.8)	0.022	43.89 (38.2 to 49.18)	0.026
2.13	At1g14920 gibberellin response modulator (GAI)	667.6 (556.8 to 771.4)	0.061	312.8 (255.6 to 363.7)	0.061
2.13	At5g19530 spermine/spermidine synthase family protein	298.2 (280.1 to 314)	0.011	139.9 (107.2 to 156.9)	0.066
2.13	At5g59000 zinc finger (C3HC4-type RING finger) family protein	76.68 (62.79 to 84.88)	0.055	35.98 (33.42 to 40.06)	0.023
2.13	At4g26690 glycerophosphoryl diester phosphodiesterase protein	573.7 (540.9 to 609.9)	0.011	269.4 (257.1 to 289.2)	0.007
2.13	At2g16660 nodulin family protein	668.7 (549.8 to 737.9)	0.059	314.2 (247.4 to 366.8)	0.079
2.12	At2g48030 endonuclease/exonuclease/phosphatase family protein	169.3 (154.5 to 185.9)	0.024	9.84 (68.04 to 86.09)	0.032
2.11	At1g08900 sugar transporter-related	97.22 (86.34 to 108)	0.036	45.98 (38.41 to 52.87)	0.045
2.11	At1g64330 myosin heavy chain-related	152.4 (137.7 to 169.6)	0.036	72.2 (58.37 to 85.14)	0.055
2.11	At1g18400 bHLH transcription factor	100.3 (94.19 to 106.9)	0.014	47.61 (38.79 to 53.52)	0.045
2.11	At2g47200 expressed protein	76.41 (68.1 to 86.62)	0.049	36.27 (29.25 to 44.09)	0.062
2.11	At1g30510 ferredoxin--NADP(+) reductase	748.9 (695.2 to 846.7)	0.038	355.6 (322.2 to 391.7)	0.017
2.10	At5g50570 squamosa promoter-binding protein	416.1 (388 to 457.5)	0.028	198 (152.8 to 234.7)	0.066
2.09	At3g26970 ubiquitin-realted protein	270.8 (219.6 to 345.8)	0.101	129.5 (122.1 to 138.4)	0.012
2.09	At1g75780 tubulin beta-1 chain (TUB1)	251.9 (240.2 to 269)	0.013	120.6 (108.3 to 134.7)	0.019
2.09	At5g06690 thioredoxin family protein	645 (609.2 to 705.6)	0.021	308.9 (269.8 to 335.9)	0.023
2.08	At1g64640 plastocyanin-like domain-containing protein	186.9 (170.3 to 211.3)	0.039	89.67 (77.15 to 99.98)	0.032

Supplemental Data Table 1 (continued)

Fold repression	Gene Identity	Wt (Col) Raw data	t-test p-value	vfb mutant Raw data	t-test p-value
2.08	At3g21770 peroxidase 30 (PER30) (P30) (PRXR9)	402 (342 to 449.5)	0.044	192.9 (184.7 to 208.4)	0.011
2.08	At4g03210 xyloglucan:xyloglucosyl transferase	3,750 (3,619 to 3,873)	0.006	1,804 (1,536 to 2,229)	0.049
2.07	At3g61210 embryo-abundant protein-related	347.2 (323 to 383)	0.025	167.4 (153.1 to 181.6)	0.014
2.07	At1g69080 universal stress protein (USP) family protein	92.56 (90.05 to 96.55)	0.004	44.65 (42.63 to 46.04)	0.003

2.07	At5g22500 acyl CoA reductase/male-sterility protein	354.3 (295 to 387.2)	0.050	171 (158.8 to 187)	0.018
2.07	At3g10120 expressed protein	162.9 (146.3 to 194.9)	0.079	78.7 (67.81 to 89.75)	0.036
2.06	At5g10830 embryo-abundant protein-related	138.1 (128 to 150.7)	0.030	67 (56.53 to 82.85)	0.056
2.06	At5g46240 inward rectifying potassium channel (KAT1)	160.6 (141.1 to 178.4)	0.043	78 (62.46 to 91.83)	0.066
2.06	At5g63590 flavonol synthase	96.31 (88.9 to 100.5)	0.014	46.78 (42.54 to 49.91)	0.014
2.06	At1g69040 ACT domain containing protein (ACR4)	400.5 (378 to 435.4)	0.019	194.7 (176.2 to 211.2)	0.015
2.05	At3g20590 non-race specific disease resistance protein	125.1 (112.9 to 144.3)	0.047	60.89 (58.33 to 65.13)	0.008
2.05	At5g22580 expressed protein	728.7 (647.1 to 815.3)	0.036	354.7 (337 to 385.4)	0.012
2.05	At5g58860 cytochrome P450 86A1 (CYP86)	154 (132.1 to 183.4)	0.060	75.02 (73.34 to 77.5)	0.002
2.05	At1g24170 glycosyl transferase family 8 protein	558.9 (492.9 to 669.7)	0.076	272.8 (228.5 to 306)	0.047
2.04	At3g58620 tetratricopeptide repeat-containing protein	368.8 (342.1 to 406.5)	0.027	180.8 (158.8 to 201.1)	0.026
2.03	At3g07010 pectate lyase family protein	302.2 (294 to 313)	0.005	148.6 (127.3 to 174.2)	0.036
2.03	At3g11420 fringe-related protein	170.3 (162.4 to 177.5)	0.008	83.77 (73.05 to 97.44)	0.034
2.03	At5g14450 GDSL-motif lipase/hydrolase family protein	414.3 (360.1 to 486.4)	0.072	204.4 (170.2 to 242.1)	0.059
2.01	At2g47440 DNAJ heat shock N-terminal domain-containing protein	973.4 (899.1 to 1,030)	0.019	483.3 (426.6 to 558)	0.034
2.01	At2g34200 zinc finger (C3HC4-type RING finger) family protein	75.43 (72.8 to 78.79)	0.007	37.48 (30.32 to 41.9)	0.050
2.01	At3g54920 pectate lyase/powdery mildew susceptibility protein	615.1 (585.8 to 660.6)	0.020	306 (266.7 to 364.7)	0.041
2.01	At5g54380 protein kinase family protein	515.7 (459.5 to 566.8)	0.037	256.6 (207.2 to 295.5)	0.064
2.01	At4g36790 transporter-related	116 (106.9 to 126.7)	0.026	57.73 (46.1 to 65.03)	0.062
2.01	At2g40480 expressed protein	121.5 (118.8 to 123.3)	0.001	60.53 (56.56 to 62.69)	0.006
2.00	At3g25930 universal stress protein (USP) family protein	126 (121.6 to 131.5)	0.007	63.03 (57.48 to 71.52)	0.023

Supplemental Data

Table 2. Genes that are induced in *vfb1-1 vfb2-1 vfb3-1 vfb4* (RNAi) mutants (*vfb* mutants) compared to the wild type.

Fold induction	Gene Identity	Wt (Col) Raw data	t-test p-value	<i>vfb</i> mutant Raw data	t-test p-value
16.40	At3g28270 expressed protein	68.06 (58.7 to 77.6)	0.002	1,116 (683.6 to 1,502)	0.047
9.90	At5g24420 glucosamine/galactosamine-6-phosphate isomerase	113.6 (98.07 to 129.8)	0.005	1,125 (519.3 to 1,649)	0.081
8.72	At4g31870 glutathione peroxidase	23.28 (21.96 to 25.61)	0.001	203 (148 to 274.6)	0.045
8.55	At1g02820 late embryogenesis abundant 3 family protein	70.7 (49 to 87.04)	0.014	604.6 (493.5 to 774)	0.034
7.85	At3g28220 MATH domain-containing protein	396.7 (303.1 to 457)	0.012	3,115 (1,968 to 4,461)	0.064
7.47	At2g27420 cysteine proteinase	8.392 (5.076 to 14.77)	0.053	62.69 (47.74 to 82.9)	0.054
7.19	At2g04040 MATE efflux family protein	17.53 (9.59 to 25.04)	0.034	126 (116.3 to 136.9)	0.006
7.15	At2g15020 expressed protein	10.73 (8.869 to 13.14)	0.007	76.76 (67 to 82.61)	0.010
6.40	At2g21320 zinc finger (B-box type) family protein)	27.89 (15.5 to 41.57)	0.047	178.4 (140.6 to 198.5)	0.028
6.30	At1g52100 jacalin lectin family protein	75.52 (55.74 to 103.5)	0.019	475.5 (419.4 to 512)	0.010
6.25	At1g09500 cinnamyl-alcohol dehydrogenase family/CAD family	28.14 (26.76 to 29.43)	0.0006	175.9 (132.4 to 241.8)	0.054
5.86	At3g59930 expressed protein	26.58 (19.31 to 35.09)	0.023	155.8 (121 to 180.1)	0.030
5.70	At3g45130 cycloartenol synthase	9.791 (7.732 to 13.52)	0.029	55.78 (38.47 to 73.82)	0.060
5.61	At2g05540 glycine-rich protein	462.8 (389.6 to 509.3)	0.006	2,595 (2,037 to 3,107)	0.029
5.60	At4g08870 arginase	188.3 (166.9 to 209.6)	0.007	1,055 (592.5 to 1,699)	0.106
5.36	At2g31380 zinc finger (B-box type) family protein	67.9 (54.21 to 77.92)	0.010	363.7 (307.9 to 408.1)	0.017
5.07	At1g62510 protease inhibitor/seed storage/lipid transfer protein	266.3 (181 to 322.7)	0.026	1,349 (1,199 to 1,434)	0.010
5.03	At1g19610 plant defensin-fusion protein (PDF1.4)	52.37 (40.47 to 73.55)	0.031	263.4 (214.5 to 296.4)	0.026
4.82	At5g42760 O-methyltransferase N-terminus domain-protein	39.61 (38.35 to 40.57)	0.0003	190.8 (145.3 to 230.1)	0.035
4.61	At1g47400 expressed protein	331.5 (287.5 to 356.3)	0.005	1,527 (1,350 to 1,653)	0.011
4.52	At5g17300 myb family transcription factor	64.9 (52.41 to 72.94)	0.014	293.5 (229.7 to 383.6)	0.052
4.47	At2g32540 cellulose synthase family protein	147.8 (122 to 185.4)	0.014	660.4 (620.9 to 694.9)	0.004
4.45	At1g08630 L-allo-threonine aldolase-related	13.18 (8.674 to 18.35)	0.047	58.64 (47.34 to 70.51)	0.038
4.40	At5g46050 proton-dependent oligopeptide transport (POT) protein	63.06 (53.08 to 72.81)	0.010	277.6 (228.9 to 323.9)	0.027
4.36	At5g58770 dehydrodolichyl diphosphate synthase	62.45 (58.24 to 64.62)	0.001	272.4 (263.1 to 282.3)	0.001
4.34	At4g15680 glutaredoxin family protein	47.46 (43.49 to 51.99)	0.004	205.8 (152.4 to 259.2)	0.048
4.25	At2g46830 myb-related transcription factor (CCA1)	78.88 (72.85 to 83.18)	0.002	335.5 (283.7 to 380.4)	0.020
4.22	At2g41250 haloacid dehalogenase-like hydrolase family protein	142.6 (115.9 to 159.8)	0.012	602.3 (539.6 to 636.7)	0.009
4.18	At3g02380 zinc finger protein CONSTANS-LIKE 2 (COL2)	74.7 (68.49 to 83.63)	0.007	312.6 (216.1 to 367.4)	0.053
4.10	At5g36910 thionin (THI2.2)	88.85 (81.7 to 96.69)	0.004	364.2 (272 to 447.5)	0.045
4.07	At1g64500 glutaredoxin family protein	61.45 (55.09 to 73.11)	0.009	250.3 (240.5 to 261.2)	0.002
4.02	At3g21670 nitrate transporter (NTP3)	171.3 (157.5 to 195.1)	0.005	687.9 (646.2 to 711.3)	0.003
3.99	At3g17610 bZIP transcription factor	49.69 (37.62 to 63.57)	0.029	198.5 (166.3 to 237.8)	0.035
3.91	At5g09570 expressed protein	30.59 (23.39 to 35.37)	0.029	119.6 (90.06 to 143)	0.045
3.91	At5g62430 Dof-type zinc finger domain-containing protein	55.9 (32.24 to 72.55)	0.070	218.4 (185.1 to 246.8)	0.025
3.86	At1g55960 expressed protein	154.2 (144.1 to 168.3)	0.003	594.6 (522.5 to 715.2)	0.032
3.82	At5g24120 RNA polymerase sigma subunit SigE (sigE)	93.13 (85.42 to 100.3)	0.004	356.2 (281.1 to 465.7)	0.057
3.81	At5g48430 expressed protein	31.73 (23.11 to 40.44)	0.037	120.9 (98.56 to 133.9)	0.030
3.78	At5g24150 squalene monooxygenase 1,1	201 (173 to 229.8)	0.012	758.8 (600.2 to 911.5)	0.039
3.75	At3g44450 expressed protein	39.53 (33.27 to 45.84)	0.020	148.3 (101.8 to 204.1)	0.082
3.72	At5g20150 SPX (SYG1/Pho81/XPR1) domain-containing protein	122.9 (104.2 to 132.4)	0.014	457.2 (336.9 to 522.1)	0.045
3.52	At3g17790 acid phosphatase type 5 (ACP5)	131.3 (101.1 to 154.4)	0.045	461.9 (306 to 614.4)	0.083

Supplemental Data

Table 2. (continued)

Fold induction	Gene Identity	Wt (Col) Raw data	t-test p-value	vfb mutant Raw data	t-test p-value
3.44	At3g26290 cytochrome P450 71B26 (CYP71B26)	133.2 (117.2 to 144.6)	0.009	458.4 (360.2 to 540.6)	0.039
3.35	At2g36790 UDP-glucuronosyl/UDP-glucosyltransferase family protein	43.73 (35.39 to 51.94)	0.018	146.5 (141.3 to 156.4)	0.006
3.31	At3g12320 expressed protein	61.81 (57.83 to 68.53)	0.008	204.5 (148.5 to 239.6)	0.055
3.28	At3g28740 cytochrome P450 family protein	141.3 (116.1 to 175.1)	0.025	463.3 (414.5 to 495.1)	0.014
3.27	At5g20790 expressed protein	21.77 (15.05 to 30.06)	0.059	71.22 (61.41 to 87.79)	0.061
3.25	At2g24540 kelch repeat-containing F-box family protein	61.36 (56.86 to 66.94)	0.004	199.3 (186.4 to 217.9)	0.010
3.23	At5g11410 protein kinase family protein	16.49 (12.68 to 21.41)	0.036	53.27 (49.03 to 58.5)	0.015
3.20	At3g47420 glycerol-3-phosphate transporter	70.71 (60.18 to 77.12)	0.018	226.3 (169.3 to 293.9)	0.067
3.20	At1g64900 cytochrome P450	105.8 (86.65 to 123.6)	0.019	338.1 (308.7 to 374.6)	0.015
3.16	At1g05680 UDP-glucuronosyl/UDP-glucosyl transferase family protein	52.81 (43.17 to 57.72)	0.022	166.9 (139.9 to 202.5)	0.042
3.12	At4g26200 1-aminocyclopropane-1-carboxylate synthase	33.69 (25.51 to 45.83)	0.063	105.1 (80.54 to 118.4)	0.059
3.10	At2g37770 aldo/keto reductase family protein	51.87 (45.58 to 62.16)	0.026	160.9 (122.3 to 183.8)	0.052
3.09	At5g64170 dentin sialophosphoprotein-related	87.06 (79.83 to 91.48)	0.006	269.2 (206 to 314.8)	0.046
3.08	At1g18330 myb family transcription factor	65.2 (57.06 to 72.21)	0.009	201 (185.9 to 228.9)	0.022
3.04	At5g39520 expressed protein	25.55 (21.06 to 32.31)	0.028	77.69 (73.93 to 79.62)	0.004
3.03	At3g57020 strictosidine synthase family protein	345.1 (249.5 to 411.1)	0.055	1,044 (847.7 to 1,269)	0.051
3.02	At3g56980 bHLH transcription factor	174.2 (157.9 to 200.5)	0.016	525.4 (413.4 to 613)	0.046
2.97	At3g18250 expressed protein	88.63 (75.21 to 104.7)	0.018	262.9 (246.1 to 286.5)	0.012
2.97	At1g01060 myb family transcription factor	157.6 (116.4 to 180.4)	0.041	467.3 (426.8 to 539.3)	0.029
2.94	At5g02830 pentatricopeptide (PPR) repeat-containing protein	132.6 (106 to 165.4)	0.047	390.1 (296.2 to 479.7)	0.068
2.93	At4g20000 VQ motif-containing protein	19.51 (15.31 to 27.79)	0.066	57.19 (49.78 to 65.31)	0.039
2.91	At1g78510 solanesyl diphosphate synthase (SPS)	70.66 (68.3 to 72.25)	0.0007	205.9 (189.6 to 221.4)	0.009
2.91	At4g28290 expressed protein	86.28 (78.67 to 93.79)	0.01	251 (190.9 to 315.1)	0.063
2.90	At3g47500 Dof-type zinc finger domain-containing protein	143 (129.8 to 149.8)	0.008	414.5 (322.9 to 476.3)	0.044
2.87	At5g67370 expressed protein	448.7 (407.2 to 474.5)	0.005	1,290 (1,240 to 1,354)	0.004
2.82	At4g23300 protein kinase family protein	100.5 (78.67 to 123)	0.042	283.7 (241 to 332.9)	0.043
2.81	At5g49480 sodium-inducible calcium-binding protein (ACP1)	395.1 (285.1 to 503.2)	0.071	1,111 (877.8 to 1,263)	0.054
2.80	At3g14770 nodulin MtN3 family protein	89.38 (73.03 to 106.7)	0.034	250.1 (205.7 to 300.4)	0.052
2.78	At1g07180 pyridine nucleotide-disulphide oxidoreductase protein	111 (80.93 to 129.9)	0.059	308.7 (259.4 to 373.2)	0.052
2.77	At1g22500 zinc finger (C3HC4-type RING finger) family protein	95.08 (81.42 to 106.3)	0.022	263.3 (211.4 to 291)	0.041
2.77	At2g44370 DC1 domain-containing protein	66.14 (43.74 to 80.59)	0.065	182.9 (179.7 to 188)	0.001
2.76	At4g15490 UDP-glucuronosyl/UDP-glucosyl transferase protein	65.66 (57.29 to 71.02)	0.011	181 (175 to 186.3)	0.002
2.75	At4g20860 FAD-binding domain-containing protein	135.3 (131.2 to 143.3)	0.002	371.9 (330.4 to 407.1)	0.018
2.75	At1g18810 phytochrome kinase substrate-related	61.03 (58.57 to 63.87)	0.002	167.6 (138.9 to 195.8)	0.038
2.74	At3g28540 AAA-type ATPase family protein	28.52 (24.22 to 33.97)	0.030	78.28 (64.54 to 98.5)	0.072
2.72	At1g10370 glutathione S-transferase (ERD9)	67.05 (57.35 to 76.2)	0.018	182.6 (165.6 to 198)	0.015
2.72	At5g18670 beta-amylase (BMY3)	130.1 (110.9 to 144.5)	0.029	354.2 (259.9 to 427.8)	0.068
2.72	At1g31820 amino acid permease family protein	41.54 (34.8 to 49.44)	0.027	112.8 (101 to 128)	0.028
2.71	At3g56290 expressed protein	262.9 (212.2 to 288.7)	0.033	712.7 (608.2 to 864.4)	0.050
2.70	At3g54500 expressed protein	164.1 (154.2 to 169.2)	0.003	443.2 (381.4 to 507.5)	0.029
2.69	At4g14690 chlorophyll A-B binding family protein	67.44 (46.43 to 85.84)	0.069	181.1 (164 to 202.8)	0.027

**Supplemental Data
Table 2. (continued)**

Fold induction	Gene Identity	Wt (Col) Raw data	t-test p-value	vfb mutant Raw data	t-test p-value
2.68	At4g24700 expressed protein	66.03 (64.07 to 68.57)	0.001	176.7 (149.3 to 193)	0.027
2.66	At5g24160 squalene monooxygenase 1,2	271.7 (231.3 to 324.3)	0.031	721.7 (608 to 829.3)	0.041
2.66	At3g19550 expressed protein	19.42 (18.54 to 20.44)	0.002	51.57 (47.13 to 56.31)	0.014
2.65	At5g26340 hexose transporter	114.3 (84.53 to 143.6)	0.055	303.2 (273.1 to 332.6)	0.022
2.63	At1g69930 glutathione S-transferase	18.48 (13.02 to 22.43)	0.066	48.69 (43.87 to 53.32)	0.021
2.60	At1g60590 polygalacturonase/pectinase	157.6 (137.9 to 169.6)	0.014	409.2 (370.2 to 478.3)	0.037
2.56	At1g32900 starch synthase	188.1 (159.7 to 213.4)	0.028	481.6 (399.2 to 616.2)	0.083
2.56	At5g52570 beta-carotene hydroxylase	98.97 (87.77 to 117.5)	0.028	253.2 (216.3 to 278.4)	0.033
2.52	At4g15530 pyruvate phosphate dikinase family protein	283.1 (206.8 to 324.7)	0.06	714.7 (658.5 to 761)	0.012
2.50	At4g23290 protein kinase family protein	166.3 (136.8 to 220.8)	0.068	415.4 (346.3 to 465.6)	0.052
2.49	At4g37370 cytochrome P450	69.1 (60.43 to 83.38)	0.033	172.3 (149.5 to 192.4)	0.034
2.49	At2g25470 leucine-rich repeat family protein	23.86 (21.5 to 27.29)	0.030	59.41 (43.5 to 71.97)	0.080
2.48	At4g36670 mannitol transporter	384.6 (314.5 to 430.3)	0.031	955.2 (875.7 to 1,049)	0.018
2.48	At1g52200 expressed protein	428.2 (361.7 to 474)	0.025	1,063 (942.9 to 1,224)	0.035
2.47	At3g04110 glutamate receptor family protein (GLR1.1)	47.96 (40.79 to 58.48)	0.032	118.3 (111.9 to 127.4)	0.013
2.46	At4g19170 9-cis-epoxycarotenoid dioxygenase	289.1 (258.5 to 324.7)	0.019	710.8 (590.5 to 795.3)	0.041
2.45	At4g23680 major latex protein-related	554.8 (449.3 to 622.8)	0.035	1,361 (1,237 to 1,432)	0.014
2.42	At4g27820 glycosyl hydrolase family 1 protein	72.53 (62.7 to 84.19)	0.033	175.7 (143.2 to 222.8)	0.087
2.42	At1g71030 myb family transcription factor	340.4 (326.6 to 355.5)	0.002	824.3 (725.6 to 945.1)	0.032
2.42	At1g07390 leucine-rich repeat family protein	57.64 (48.57 to 63.37)	0.022	139.5 (134.6 to 143.7)	0.003
2.42	At3g02040 glycerophosphoryl diester phosphodiesterase family protein	68.4 (61.2 to 75.32)	0.021	165.2 (128.7 to 197.5)	0.065
2.41	At5g45820 CBL-interacting protein kinase 20 (CIPK20)	103.8 (81.89 to 117.2)	0.048	250.3 (218.7 to 282.7)	0.033
2.41	At5g58570 expressed protein	78.52 (65.35 to 92.16)	0.034	189.1 (169.6 to 210.7)	0.028
2.40	At3g01060 expressed protein	176.4 (154 to 209.7)	0.026	422.6 (400.6 to 441.8)	0.007
2.38	At4g02410 lectin protein kinase family protein	107.3 (94.35 to 127.5)	0.027	255.4 (237.8 to 283.7)	0.026
2.37	At5g48540 33 kDa secretory protein-related	108.7 (79.54 to 128.5)	0.064	257.1 (241.7 to 270.1)	0.009
2.36	At2g41730 expressed protein	85.88 (73.44 to 104.7)	0.034	203 (193.4 to 215)	0.009
2.36	At5g35970 DNA-binding protein	383.6 (349.9 to 433.1)	0.020	905 (758.1 to 1,066)	0.053
2.35	At1g03020 glutaredoxin family protein	23.96 (21.94 to 26.17)	0.009	56.27 (53.52 to 60.45)	0.011
2.34	At2g41290 strictosidine synthase family protein	78.09 (74.56 to 84.63)	0.007	183 (169.5 to 191.3)	0.010
2.33	At1g02850 glycosyl hydrolase family 1 protein	270.4 (216.3 to 313.2)	0.047	630.6 (557.2 to 669.7)	0.025
2.33	At5g16980 NADP-dependent oxidoreductase	33.22 (29.55 to 36.96)	0.029	77.43 (58.38 to 97.12)	0.087
2.32	At4g26850 expressed protein	615.8 (561.3 to 717.5)	0.025	1,430 (1,281 to 1,660)	0.046
2.31	At5g62130 Per1-like protein-related	70.15 (56.63 to 80.16)	0.042	162.2 (146.3 to 187.8)	0.044
2.31	At5g26270 expressed protein	65.53 (63.88 to 66.5)	0.001	151.2 (113.7 to 181.4)	0.069
2.29	At1g57770 amine oxidase family	118 (102.5 to 131.2)	0.023	270.4 (240 to 299.4)	0.028
2.29	At3g09440 heat shock cognate 70 kDa protein 3	380.7 (361.4 to 418.3)	0.013	870.1 (738.1 to 1,126)	0.108
2.28	At2g42360 zinc finger (C3HC4-type RING finger) family protein	21.34 (18.8 to 23.79)	0.021	48.73 (43.53 to 57.24)	0.050
2.27	At5g47610 zinc finger (C3HC4-type RING finger) family protein	53.14 (51.74 to 54.96)	0.001	120.7 (118.7 to 122.7)	0.0008
2.27	At3g26280 cytochrome P450 family protein	109.8 (103.6 to 121)	0.012	249.3 (218.9 to 265.1)	0.026
2.27	At3g61220 short-chain dehydrogenase/reductase (SDR) family protein	348.4 (286.7 to 411.9)	0.054	791 (647.3 to 902.2)	0.058
2.26	At2g28110 exostosin family protein	59.14 (49.39 to 67.26)	0.033	133.7 (122.8 to 150.2)	0.031

Supplemental Data Table 2. (continued)

Fold induction	Gene Identity	Wt (Col) Raw data	t-test p-value	vfb mutant Raw data	t-test p-value
2.26	At1g23205 invertase/pectin methylesterase inhibitor family protein	79.49 (62.89 to 98.27)	0.058	179.7 (161.5 to 210.4)	0.062

2.25	At4g12310 cytochrome P450	217.2 (201.4 to 234.4)	0.007	489.3 (475.6 to 510.1)	0.004
2.25	At3g03470 cytochrome P450	112.1 (99.99 to 126.1)	0.018	252.5 (235.4 to 283.4)	0.031
2.25	At5g15850 zinc finger protein CONSTANS-LIKE 1 (COL1)	251.5 (216.4 to 270.9)	0.030	566.4 (482.5 to 624.4)	0.036
2.24	At3g47640 bHLH transcription factor	71.44 (66.66 to 79.37)	0.023	159.9 (123.1 to 190.3)	0.075
2.24	At5g67330 NRAMP metal ion transporter 4	509.6 (491.5 to 521.9)	0.002	1,140 (985.3 to 1,239)	0.029
2.23	At5g43450 2-oxoglutarate-dependent dioxygenase	140 (117.4 to 174.4)	0.052	311.8 (281.4 to 339.7)	0.029
2.22	At4g37310 cytochrome P450	118.5 (89.15 to 140.6)	0.075	263.4 (231.4 to 289.2)	0.034
2.22	At2g25450 2-oxoglutarate-dependent dioxygenase	1,957 (1,675 to 2,391)	0.040	4,349 (4,146 to 4,524)	0.007
2.22	At3g51860 cation exchanger (CAX3)	103.4 (85.64 to 112.4)	0.036	229.7 (212.7 to 244.5)	0.013
2.22	At2g36080 DNA-binding protein	47.73 (39.33 to 57.44)	0.041	105.9 (101.6 to 109.2)	0.005
2.20	At4g01870 tolB protein-related	229.1 (176.7 to 268.9)	0.058	504.5 (473.5 to 531.7)	0.012
2.20	At2g46340 phytochrome A suppressor spa1	252.1 (234.2 to 283.1)	0.023	554.3 (458.9 to 648.8)	0.059
2.20	At2g44380 DC1 domain-containing protein	98.21 (90.12 to 113.7)	0.040	215.9 (168.7 to 243.8)	0.072
2.20	At4g01700 chitinase	160.5 (126.8 to 195.4)	0.068	352.8 (301.4 to 390.8)	0.047
2.19	At5g61820 expressed protein	774.2 (671.6 to 874.3)	0.031	1,695 (1,464 to 1,821)	0.035
2.19	At1g77760 nitrate reductase 1 (NR1)	1,471 (1,377 to 1,646)	0.020	3,217 (2,707 to 4,056)	0.096
2.18	At1g53090 WD-40 repeat family protein/phytochrome A-related	70.86 (64.43 to 77.32)	0.017	154.4 (132.2 to 173.5)	0.040
2.18	At4g27410 no apical meristem (NAM) family protein (RD26)	118.9 (95.21 to 143)	0.058	258.8 (230 to 289.3)	0.039
2.17	At5g51390 expressed protein	50.77 (44.78 to 58.13)	0.028	110.3 (99.03 to 117)	0.023
2.16	At1g35560 TCP family transcription factor	42.96 (40.16 to 45.47)	0.010	92.89 (76.93 to 117.7)	0.091
2.16	At4g03260 leucine-rich repeat family protein	255.8 (232.3 to 274.8)	0.013	551.9 (507.3 to 592.7)	0.016
2.16	At4g15430 early-responsive to dehydration protein-related	25.65 (23.85 to 27.95)	0.012	55.31 (48.92 to 59.56)	0.027
2.15	At1g52400 glycosyl hydrolase family 1 protein	3,678 (3,339 to 4,125)	0.034	7,911 (6,042 to 9,288)	0.081
2.15	At3g29810 COBRA cell expansion protein COBL2	63.09 (54.11 to 69.17)	0.035	135.6 (116.5 to 157.6)	0.051
2.14	At1g66540 cytochrome P450	22.92 (18.33 to 27.52)	0.068	49.11 (41.66 to 56.95)	0.063
2.14	At2g37760 aldo/keto reductase family protein	356.2 (306.9 to 448.4)	0.063	762.9 (667.6 to 872)	0.058
2.14	At5g65010 asparagine synthetase 2 (ASN2)	1,163 (995.5 to 1,345)	0.043	2,485 (2,106 to 2,859)	0.056
2.12	At4g22200 potassium channel protein 2 (AKT2) (AKT3)	77.11 (60.8 to 85.99)	0.066	163.8 (144.8 to 188.2)	0.046
2.12	At3g22370 alternative oxidase 1a, mitochondrial (AOX1A)	236.5 (228.3 to 247)	0.004	501.4 (429.8 to 592.4)	0.054
2.12	At3g15720 glycoside hydrolase family 28 protein/polygalacturonase (pectinase)	27.61 (27.04 to 28.57)	0.003	58.47 (44.18 to 68.72)	0.076
2.12	At4g11280 1-aminocyclopropane-1-carboxylate synthase 6	98.69 (84.42 to 106.1)	0.032	208.8 (188.5 to 223.4)	0.021
2.11	At1g07010 calcineurin-like phosphoesterase family protein	243.8 (220.7 to 269.9)	0.020	514.4 (454.2 to 553.6)	0.029
2.11	At2g42750 DNAJ heat shock N-terminal domain-containing protein	489.8 (474.6 to 519.3)	0.005	1,032 (915.5 to 1,211)	0.052
2.10	At1g26420 FAD-binding domain-containing protein	33.28 (31.46 to 36.09)	0.016	70 (55.87 to 87.18)	0.089
2.09	At1g54010 myrosinase-associated protein	428.8 (396.5 to 452.2)	0.010	897.4 (800.1 to 980.1)	0.026
2.09	At5g03555 allantoin family protein	126.6 (124.2 to 129.6)	0.001	264.2 (240.4 to 295.3)	0.028
2.08	At2g38870 protease inhibitor	1,671 (1,356 to 1,887)	0.050	3,477 (3,219 to 3,694)	0.016
2.08	At1g13080 cytochrome P450 family protein	181.8 (152.3 to 206.9)	0.057	378.2 (309.5 to 437.7)	0.067
2.07	At1g13990 expressed protein	220.8 (199.1 to 243.2)	0.017	458 (434 to 491)	0.014
2.07	petD petD	68.49 (64.44 to 71.43)	0.012	141.6 (108.7 to 168.1)	0.077
2.07	At1g04770 male sterility MS5 family protein	227.8 (210.5 to 255.7)	0.020	470.8 (432.9 to 495.5)	0.017

Supplemental Data

Table 2. (continued)

Fold induction	Gene Identity	Wt (Col) Raw data	t-test p-value	vfb mutant Raw data	t-test p-value
2.06	At1g51700 Dof-type zinc finger domain-containing protein (ADOF1)	111.9 (105 to 123.6)	0.020	230.1 (194.9 to 252.9)	0.046
2.05	At2g30510 RPT2	958.7 (939.7 to 996.6)	0.003	1,966 (1,638 to 2,308)	0.058
2.04	At4g38540 monooxygenase (MO2)	200.6 (170 to 222.3)	0.036	409.9 (383 to 437.7)	0.015
2.04	At3g61890 homeobox-leucine zipper protein 12 (HB-12)	67.72 (58.36 to 76.74)	0.032	138.2 (130.7 to 142.6)	0.009

2.04	At1g06570 4-hydroxyphenylpyruvate dioxygenase (HPD)	241.9 (231.5 to 250.8)	0.003	493.4 (473.4 to 532.1)	0.015
2.03	At4g36380 cytochrome P450 90C1 (CYP90C1)	59.75 (57.95 to 62.59)	0.005	121.4 (102.5 to 137.4)	0.047
2.03	At4g27030 expressed protein	209.6 (181 to 227.7)	0.046	425.2 (347.9 to 490.6)	0.063
2.02	At2g37970 SOUL heme-binding family protein	326.8 (299.9 to 371.7)	0.027	659.6 (597 to 704.3)	0.025
2.02	At3g52740 expressed protein	41.06 (33.97 to 51.53)	0.061	82.87 (79.28 to 86.3)	0.010
2.01	At1g73680 pathogen-responsive alpha-dioxygenase	142.3 (125.2 to 170.8)	0.046	286.1 (263.4 to 298.8)	0.021
2.01	At5g44190 myb family transcription factor (GLK2)	216.4 (202.5 to 229.4)	0.007	434.5 (432.1 to 438.4)	0.0002
2.00	At5g47560 sodium/dicarboxylate cotransporter	489.4 (435.2 to 538)	0.022	977.4 (919 to 1,025)	0.011

Table 3. (Continued)

<u>Fold Induction</u>	<u>Gene Identity</u>	<u>Wt (Col) Raw data</u>	<u>t-test p-value</u>	<u>v7h mutant</u>	<u>t-test p-value</u>	<u>Fold Induction</u>	<u>Wt (Col) Raw data</u>	<u>t-test p-value</u>	<u>csn4 (SALK_043720)</u>	<u>t-test p-value</u>	<u>Fold Induction</u>
At1g18400	basic helix-loop-helix (bHLH) family protein	100.3 (94.19 to 106.9)	0.014	47.61 (38.79 to 53.52)	0.045	2.1	259.6 (231.9 to 302.7)	0.002	39.03 (25.16 to 59.68)	0.274	6.7
At5g50570	squamosa promoter-binding protein, putative	416.1 (389 to 457.6)	0.028	198 (152.8 to 234.7)	0.066	2.1	283.1 (240.9 to 322.7)	0.013	134.9 (90.1 to 186.5)	0.869	2.1
At5g06690	thioredoxin family protein	645 (609.2 to 705.6)	0.021	308.9 (269.8 to 335.9)	0.023	2.1	440.4 (421.8 to 451.5)	0.0002	83.4 (37.49 to 116.7)	0.509	5.3
At1g64640	plastocyanin-like domain-containing protein	186.9 (170.3 to 211.3)	0.039	89.67 (77.15 to 99.98)	0.032	2.1	309.4 (275.9 to 347.4)	0.001	35.32 (28.73 to 44.98)	0.047	8.8
At4g03210	xyloglucan:xyloglucosyl transferase,	3,750 (3,619 to 3,873)	0.006	1,804 (1,536 to 2,229)	0.049	2.1	2,373 (2,142 to 2,522)	0.002	1,184 (953.6 to 1,581)	0.232	2.0
At3g61210	embryo-abundant protein-related	347.2 (323 to 363)	0.025	167.4 (153.1 to 181.6)	0.014	2.1	183.5 (155.4 to 227.2)	0.009	40.94 (29.68 to 56.89)	0.199	4.5
At5g22500	acyl CoA reductase, putative / male-sterility protein	354.3 (295 to 387.2)	0.050	171 (158.8 to 187)	0.018	2.1	534.8 (475.2 to 565.5)	0.004	176.2 (154.4 to 192.9)	0.066	3.0
At3g10120	expressed protein	162.9 (146.3 to 194.9)	0.079	78.7 (67.81 to 89.75)	0.036	2.1	137.9 (136.4 to 139.5)	3.48e-5	39.45 (31.48 to 45.37)	0.276	3.5
At3g58620	tetratricopeptide repeat (TPR)-containing protein	368.8 (342.1 to 406.5)	0.027	180.8 (158.8 to 201.1)	0.026	2.0	336.3 (327.2 to 341.3)	0.0001	127.1 (107.3 to 155.4)	0.893	2.6
At3g07010	pectate lyase family protein	302.2 (294 to 313)	0.005	148.6 (127.3 to 174.2)	0.036	2.0	313.1 (293.9 to 343)	0.001	63.9 (67.97 to 106.4)	0.76	3.7
At5g14450	GDSL-motif lipase/hydrolase family protein	414.3 (380.1 to 486.4)	0.072	204.4 (170.2 to 242.1)	0.059	2.0	289.3 (277.8 to 308.3)	0.001	101.9 (61.22 to 130.4)	0.436	2.8
At3g54920	pectate lyase, putative	615.1 (585.8 to 660.6)	0.020	306 (266.7 to 364.7)	0.041	2.0	826.1 (798.2 to 869)	0.001	375.4 (277 to 459.6)	0.716	2.2
At2g40480	expressed protein	121.5 (118.8 to 123.3)	0.001	60.53 (56.56 to 62.69)	0.006	2.0	101.1 (88.04 to 114.9)	0.001	30.75 (18.23 to 40.84)	0.173	3.3
At3g25930	universal stress protein (USP) family protein	126 (121.6 to 131.5)	0.007	63.03 (57.48 to 71.52)	0.023	2.0	131.9 (112.4 to 143.7)	0.005	40.21 (30.18 to 49.98)	0.475	3.3

III.IV. Calderón Villalobos et al. 2005 (research article)

Luz Irina A. Calderón Villalobos, Carola Kuhnle, Esther M.N.
Dohmann, Hanbing Li, Mike Bevan, and Claus Schwechheimer

**The evolutionarily conserved TOUGH protein is required for
proper development of *Arabidopsis thaliana***

Plant Cell, 17, 2473-2485

(2005)

The Evolutionarily Conserved TOUGH Protein Is Required for Proper Development of *Arabidopsis thaliana* ^W

Luz I.A. Calderon-Villalobos,^a Carola Kuhnle,^a Esther M.N. Dohmann,^a Hanbing Li,^a Mike Bevan,^b and Claus Schwechheimer^{a,1}

^aCentre for Plant Molecular Biology, Developmental Genetics, Tübingen University, 72076 Tübingen, Germany

^bJohn Innes Centre, Department of Molecular and Cellular Biology, Norwich, Norfolk, NR4 7UH, United Kingdom

In this study, we characterize the evolutionarily conserved TOUGH (TGH) protein as a novel regulator required for *Arabidopsis thaliana* development. We initially identified TGH as a yeast two-hybrid system interactor of the transcription initiation factor TATA-box binding protein 2. TGH has apparent orthologs in all eukaryotic model organisms with the exception of the budding yeast *Saccharomyces cerevisiae*. TGH contains domains with strong similarity to G-patch and SWAP domains, protein domains that are characteristic of RNA binding and processing proteins. Furthermore, TGH colocalizes with the splicing regulator SRp34 to subnuclear particles. We therefore propose that TGH plays a role in RNA binding or processing. *Arabidopsis tgh* mutants display developmental defects, including reduced plant height, polycotyly, and reduced vascularization. We found *TGH* expression to be increased in the *amp1-1* mutant, which is similar to *tgh* mutants with respect to polycotyly and defects in vascular development. Interestingly, we observed a strong genetic interaction between *TGH* and *AMP1* in that *tgh-1 amp1-1* double mutants are extremely dwarfed and severely affected in plant development in general and vascular development in particular when compared with the single mutants.

INTRODUCTION

Throughout their life cycle, plants produce new cells that subsequently differentiate to give rise to new cell types and organs. Cell differentiation and organ formation are closely linked to the activities of the phytohormones auxin and cytokinin. Applications of specific concentrations of auxin and cytokinin can stimulate the formation of undifferentiated callus from differentiated tissue and conversely the formation of differentiated shoot and root tissue from undifferentiated callus (Murashige and Skoog, 1962). Within the plant, the proper distribution of auxin and cytokinin as well as the activities of hormone-specific signal transduction pathways appear to be the main determinants of the effects of these hormones during differentiation (Murashige and Skoog, 1962; Reinhardt, 2003).

Cotyledons and leaves of dicotyledonous plants have an interconnected vascular network that transports essential nutrients throughout the plant. The differentiation of the vascular system requires proper auxin transport and response (Mattsson et al., 1999, 2003). Auxin is produced in the margins of cotyledons and leaves and from there transported inwards, resulting in auxin accumulation within specific cells. Most but not all phenomena associated with vascular differentiation can be ex-

plained by the canalization hypothesis, which suggests that these auxin-accumulating cells subsequently differentiate and connect to give rise to the vascular networks of cotyledons and leaves (Sachs, 1991; Reinhardt, 2003). The role of auxin transport and signaling in vascular development is supported by physiological experiments as well as by several *Arabidopsis thaliana* mutants defective in proteins that presumably participate in the transport of auxin (e.g., GNOM and PIN-FORMED1) or in the transcriptional regulation of auxin-induced gene expression (e.g., BODENLOS, MONOPTEROS, and AUXIN-RESISTANT6) (Gälweiler et al., 1998; Hardtke and Berleth, 1998; Mattsson et al., 1999, 2003; Steinmann et al., 1999; Christensen et al., 2000; Hobbie et al., 2000; Carland et al., 2002; Hamann et al., 2002; Hellmann et al., 2003; Willemsen et al., 2003). In addition, mutants of the cell cycle-regulated *HOBBIT* gene, which encodes a protein with homology to the CDC27 subunit of the anaphase promoting complex, display reduced auxin responses, suggesting that cell cycle regulation, auxin response, and cell differentiation may be tightly interconnected processes (Willemsen et al., 1998; Bliilou et al., 2002).

In addition to the proteins and mutants described above, several other mutants defective in vascular development have been described that can at present not be linked to auxin transport or auxin signaling. The gene *ALTERED MERISTEM PATTERNING1* (*AMP1*) was isolated in multiple mutant screens (Jürgens et al., 1991; Chaudhury et al., 1993; Hou et al., 1993; Conway and Poethig, 1997). The *amp1* mutant has elevated cytokinin levels, expresses higher levels of the cytokinin-induced cell cycle regulator cyclin D3 (*CYCD3*), and has an enlarged meristem (Chaudhury et al., 1993; Riou-Khamlich et al., 1999). Increased *CYCD3* expression, cell cycle activity, and enlarged meristem size may be the cause for the supernumerary cotyledons and the

¹To whom correspondence should be addressed. E-mail claus.schwechheimer@zmbp.uni-tuebingen.de; fax 49-7071-295135.

The author responsible for distribution of materials integral to the findings presented in this article in accordance with the policy described in the Instructions for Authors (www.plantcell.org) is: Claus Schwechheimer (claus.schwechheimer@zmbp.uni-tuebingen.de).

^WOnline version contains Web-only data.

Article, publication date, and citation information can be found at www.plantcell.org/cgi/doi/10.1105/tpc.105.031302.

faster vegetative growth observed in the *amp1* mutant. Interestingly, *amp1* mutants fail to form a proper vascular system in leaves, and it may be suggested that increased cell cycle activity in the *amp1* mutant prevents proper leaf vascularization (Conway and Poethig, 1997).

To specify the set of available proteins in specific cells or cell types, eukaryotes control gene expression at the transcriptional level or posttranscriptionally by pre-mRNA processing and alternative splicing (Smith and Valcarcel, 2000; Orphanides and Reinberg, 2002; Proudfoot et al., 2002). Pre-mRNA processing involves the removal of introns by the spliceosome, capping of the mRNA 5'-end, polyadenylation of the mRNA 3'-end, and transport of the mature mRNAs to the cytoplasm (Orphanides and Reinberg, 2002). Alternative splicing, the alternative removal of exons or introns by differential selection of 5' and 3' splice sites, permits the generation of different polypeptides from one pre-mRNA (Blencowe et al., 1999; Graveley, 2000). Thereby, alternative splicing not only enhances the number of different proteins encoded from a limited number of genes but it also represents an important regulatory mechanism during gene expression. RNA binding proteins such as the Ser Arg (SR) proteins have not only been implicated in RNA processing but also in transcriptional activation and elongation, suggesting that transcription and pre-mRNA processing are tightly linked (Fong and Zhou, 2001; Orphanides and Reinberg, 2002; Proudfoot et al., 2002).

In plants, pre-mRNA processing, alternative splicing, and other RNA-directed protein activities are required for various processes, including floral transition, floral patterning, vegetative phase change, and signal transduction (Chen and Cheng, 2004). However, little is known about the role of RNA binding and processing proteins when compared with the large set of proteins with a proposed role in these processes (Lorkovic and Barta, 2002). Here, we describe the previously uncharacterized and evolutionarily conserved TOUGH (TGH) protein, which we initially isolated as a yeast two-hybrid interactor of TATA binding protein 2 (TBP2). TGH contains two conserved protein domains found in proteins with a role in RNA binding and RNA processing, and TGH localizes with the *Arabidopsis* splicing regulator SRp34 to specific subnuclear particles. Both observations are indicative for a role of TGH in RNA binding or processing. *Arabidopsis tgh* mutants are defective in vascular patterning, and *TGH* expression is increased in the *amp1-1* mutant. Interestingly, *TGH* interacts genetically with *AMP1*, and our data suggest that both proteins control growth in general and vascular patterning in particular.

RESULTS

TGH Is an Evolutionarily Conserved Protein

TGH (At5g23080) is a previously uncharacterized protein from *Arabidopsis*. The *TGH* open reading frame is composed of 16 exons and encodes a 931-amino acid protein with a calculated molecular mass of 104.9 kD (Figure 1A). BLASTP searches using full-length TGH protein reveal that TGH is not related to any other *Arabidopsis* protein. However, proteins clearly related to TGH are present in rice (*Oryza sativa*) and in many eukaryotic model

organisms, including all model animal species and the fission yeast *Schizosaccharomyces pombe*, although not in the budding yeast *Saccharomyces cerevisiae* (Figures 1B and 1C). Since, with the exception of budding yeast, each organism subjected to analysis was found to contain exactly one protein with obvious similarity to TGH, we assume that these proteins arose from one common ancestor and that they are TGH orthologs. The TGH orthologs share highest sequence similarity within their N termini, and these similarities range from 69% sequence identity (83% similarity) between *Arabidopsis* and rice TGH to 52% identity (72% similarity) between *Arabidopsis* and *Caenorhabditis elegans* TGH, the most distantly related TGH identified in our analyses (Figure 1B). Since the N-terminal domain is specific to *Arabidopsis* TGH and its orthologs, we named it the TGH domain (Figures 1A and 1B).

In addition to the highly conserved and specific TGH domain, the TGH orthologs contain two recognizable conserved protein domains, a G-patch and a Suppressor-of-white-apricot (SWAP) domain (Figures 1A, 1C, and 1D) (Denhez and Lafyatis, 1994; Spikes et al., 1994; Aravind and Koonin, 1999). The G-patch is defined by a series of conserved Gly residues, and G-patches are exclusively found in proteins with a predicted or known role in RNA binding or RNA processing (Aravind and Koonin, 1999) (Figure 1C). The SWAP domain is a conserved domain with a presumed function in RNA binding that was first identified in the splicing regulator SWAP from *Drosophila melanogaster* (Denhez and Lafyatis, 1994; Spikes et al., 1994) (Figure 1D). The G-patch and the SWAP domains have unknown biochemical properties or functions. Nevertheless, these domains have only been found together in proteins with a role in RNA binding and RNA processing, inviting the hypothesis that SWAP and G-patch domain-containing proteins and therefore also TGH may play a role in these processes (Aravind and Koonin, 1999). With regard to the G-patch, we also noted that several conserved residues of the G-patch are not conserved in *Arabidopsis* and rice TGH but in their animal counterparts (Figure 1C). It can therefore not be ruled out that the G-patch has lost or changed functionality during plant evolution.

The G-patch domain is often accompanied by the repetitive RS (Arg, Ser) and RGG (Arg, Gly, Gly) sequences (Blencowe et al., 1999; Graveley, 2000). RS and RGG sequences are found in splicing regulators, such as SR proteins, and have been proposed to mediate protein-RNA or protein-protein interactions (Aravind and Koonin, 1999). While canonical RS and RGG sequences are absent from TGH, the domain comprising the C-terminal 170 amino acids of *Arabidopsis* TGH is significantly enriched in basic (53; 31%) and acidic (36; 21%) amino acids and in Ser residues (36; 21%). This domain was therefore designated KRDES (Lys, Arg, Asp, Glu, Ser) domain (Figure 1A; data not shown). The KRDES domain seems to be unique to *Arabidopsis* TGH.

TGH May Interact with TATA Binding Protein

Our interest in TGH was initially triggered by its identification as an interactor of the general transcription factor TBP2. We found that the TGH full-length protein and the TGH C-terminal 245 amino acids, including the KRDES domain, interact with

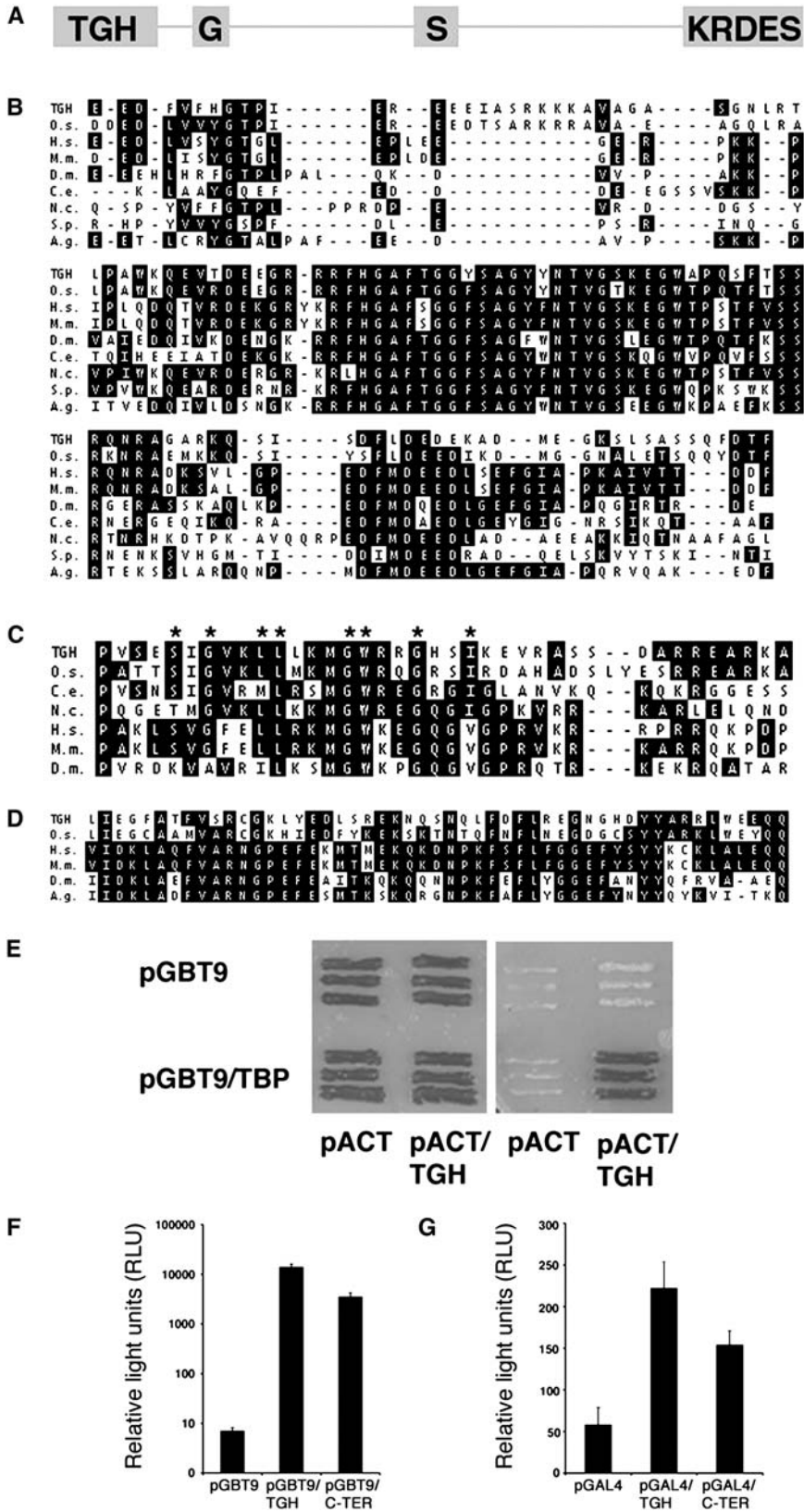


Figure 1. The TGH Protein Is Evolutionarily Conserved and May Interact with TBP2.

Arabidopsis TBP2 (At1g55520) in the yeast two-hybrid system (Figure 1E). TBPs recognize the TATA-box in eukaryotic gene promoters, where they initiate the assembly of other general transcription factors to form the preinitiation complex, a prerequisite for RNA polymerase II binding (Orphanides and Reinberg, 2002; Proudfoot et al., 2002). TBPs interact with transcriptional coactivators, such as the TBP-associated factors (TAFs), which in turn serve as interaction platforms for transcription activators (Tansey and Herr, 1997; Wu and Chiang, 2001). To make an allusion to the TBP-interacting TAF proteins, the hitherto uncharacterized TBP-interacting protein At5g23080 was designated TGH.

Numerous studies show that the interactions between TBP and transcriptional regulators, such as the TAFs, are essential for transcriptional activation (Dymlacht et al., 1991; Goodrich and Tjian, 1994; Lieberman and Berk, 1994; Tjian and Maniatis, 1994; Verrijzer and Tjian, 1996). We therefore examined whether TGH functions as a transcriptional regulator. To this end, we fused the full-length TGH protein as well as its C terminus including the KRDES domain to the DNA binding domain of the GAL4 transcription factor. We found that the TGH full-length protein as well as the TGH C terminus can activate gene expression from a GAL4-responsive reporter in yeast and in transiently transformed tobacco (*Nicotiana tabacum*) mesophyll protoplasts (Figures 1F and 1G). It could therefore be envisioned that TGH regulates gene expression as a transcriptional activator or as a regulator of another process that occurs cotranscriptionally and that possibly requires TBP2 interaction.

Subcellular Localization of TGH

The observed yeast two-hybrid interaction with TBP2 and the presence of several predicted nuclear targeting sequences within the KRDES domain (RKKR, RRRKR, KKRRR, and RRESREKRSSHKKHS) are suggestive of a nuclear localization (Dingwall and Laskey, 1991). To study the subcellular localization

of TGH, we generated transgenic *Arabidopsis* lines expressing TGH:green fluorescent protein (GFP) fusions. Transgenic plants transformed with construct TGH:TGH:GFP express the genomic *TGH* gene fragment fused to *GFP* under control of a 1-kb *TGH* promoter fragment. Transgenic plants transformed with 35S:TGH:GFP express the *TGH* cDNA fused to GFP under control of the constitutive 35S promoter of *Cauliflower mosaic virus*. Both constructs produce a functional TGH:GFP fusion protein that is able to rescue the mutant phenotype (Figures 2M to 2P; see Supplemental Table 1 online). In transgenic lines transformed with either construct, we found TGH:GFP to accumulate exclusively in the nucleus of all cells amenable to fluorescence microscopy (Figures 3A to 3C). When we analyzed TGH:GFP localization in transiently transformed *Arabidopsis* protoplasts, we noticed that the fusion protein is present in subnuclear particles that varied in size and shape in different cells examined, regardless of the TGH:GFP construct used (Figures 3D and 3G). To study the identity of these subnuclear particles, we conducted colocalization experiments between the TGH:GFP constructs and SRp34:DsRED as well as between the TGH:GFP constructs and RSZ33:DsRED. SRp34 is one of two proteins present in *Arabidopsis* closely related to human SPLICING FACTOR2/ALTERNATIVE SPLICING FACTOR, which is required for pre-mRNA processing (Lopato et al., 1999). RSZ33 is a plant-specific protein with a predicted role in RNA binding and processing (Lopato et al., 2002; Lorkovic et al., 2004b). Both SRp34 and RSZ33 are known to localize to distinct particles within the nucleus. As observed with the TGH:GFP constructs, SRp34:DSRED and RSZ33:DsRED proteins also accumulate in subnuclear particles that had different sizes and shapes in different cells examined. Regardless of these differences in size and shape, our studies revealed colocalization of the TGH:GFP constructs with SRp34:DsRED in all of the cells examined (Figures 3D to 3F) but not of the TGH:GFP constructs with RSZ33:DsRED (Figures 3G to 3I). We therefore propose that the TGH protein functions close to the *Arabidopsis* splicing regulator SRp34.

Figure 1. (continued).

(A) Schematic representation of the TGH protein. Gray boxes indicate the conserved TGH (TGH), the G-patch (G), and the SWAP (S) domains (drawn to scale). The KRDES domain of *Arabidopsis* TGH is enriched in basic and acidic amino acids as well as in Ser residues.

(B) Protein sequence alignment of the highly conserved N termini of TGH (amino acids 5 to 123) and its orthologs from rice (O.s.; amino acids 6 to 124), human (H.s.; amino acids 9 to 116), mouse (M.m.; amino acids 9 to 116), *Drosophila* (D.m.; amino acids 3 to 111), *C. elegans* (C.e.; amino acids 5 to 111), *Neurospora crassa* (N.c.; amino acids 18 to 131), *S. pombe* (S.p.; amino acids 18 to 119), and *Anopheles gambiae* (A.g.; amino acids 3 to 112). Identical conserved amino acids are shaded.

(C) Protein sequence alignment of the G-patch domains of TGH orthologs from *Arabidopsis* (TGH; amino acids 157 to 197), rice (O.s.; amino acids 158 to 197), *C. elegans* (C.e.; amino acids 143 to 191), *N. crassa* (N.c.; amino acids 146 to 197), human (H.s.; amino acids 150 to 199), mouse (M.m.; amino acids 150 to 199), and *Drosophila* (D.m.; amino acids 151 to 200). Accession numbers are listed in Methods. Identical conserved amino acids are shaded. Conserved Gly residues of the G-patch are indicated by asterisks.

(D) Protein sequence alignment of the SWAP domains of TGH from *Arabidopsis* (TGH; amino acids 405 to 455) and rice (O.s.; amino acids 408 to 458) and SWAP domain containing proteins from human (H.s.; amino acids 15 to 65), mouse (M.m.; amino acids 15 to 65), *Drosophila* (D.m.; amino acids 14 to 63), and *A. gambiae* (A.g.; amino acids 36 to 85). Accession numbers are listed in Methods. Identical amino acids are shaded. Conserved residues of the SWAP domain are indicated by asterisks. Sequence alignments in **(B)** to **(D)** were performed using the Jotun-Hein algorithm (gap penalty 11, gap length penalty 3, Ktuple 2).

(E) The yeast two-hybrid interaction between TBP and TGH visualized by differential growth on full media (cotransformation control, left panel) and on selective media (interaction experiment, right panel). The respective empty vector controls with pGBT9 and pACT fail to grow on selective media.

(F) and **(G)** Protein fusions of the GAL4 DNA binding domain to TGH or to the TGH KRDES domain activate transcription from a GAL4-responsive LACZ reporter in yeast **(F)** or a luciferase reporter construct in transiently transformed tobacco mesophyll protoplasts **(G)**.

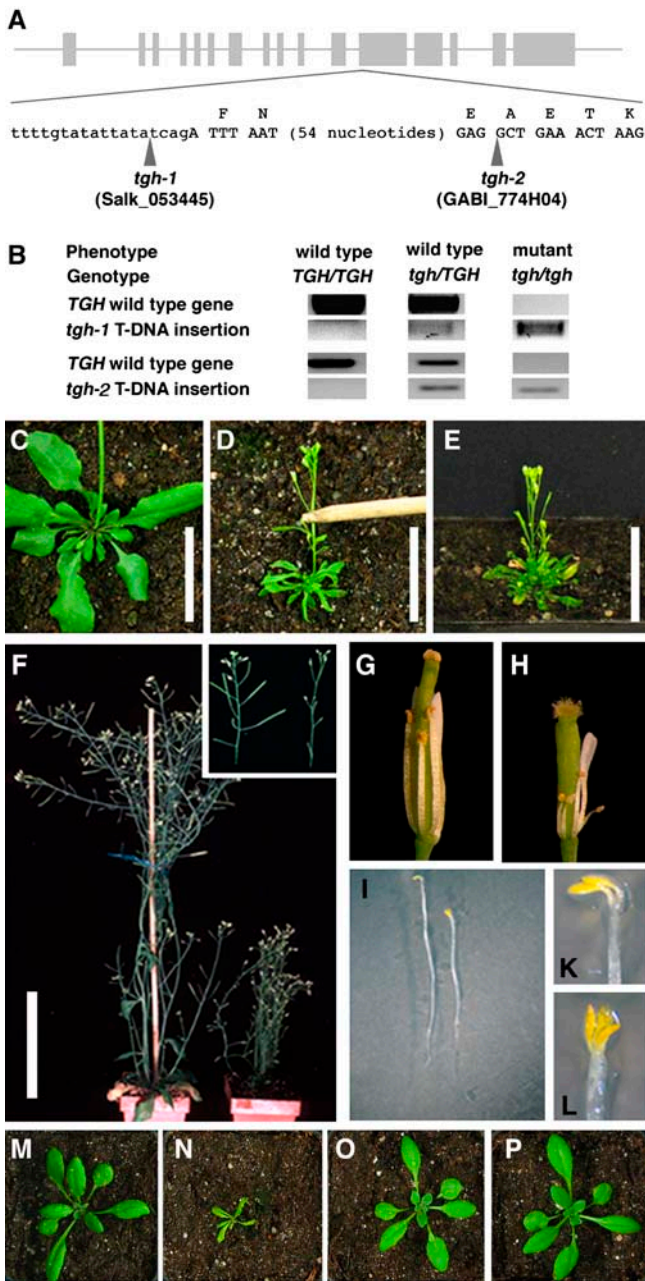


Figure 2. Mutations in the *TGH* Gene Cause Severe Growth Defects. **(A)** Genomic organization of the *TGH* gene. Gray boxes indicate exons, and lines indicate introns (drawn to scale). The T-DNA insertion positions of *tgh-1* and *tgh-2* are indicated by arrowheads. **(B)** Result of PCR genotyping of segregants from a *tgh-1/TGH* and a *tgh-2/TGH* population. The presence or absence of a band indicates the presence or absence of the gene indicated on the left side of the panel. Only plants homozygous for the T-DNA insertions show the mutant phenotype. **(C) to (E)** Three-week-old *tgh-1* **(D)** and *tgh-2* **(E)** mutants are dwarfed compared with the wild type **(C)**. Bars = 3 cm. **(F)** *tgh-1* mutant plants (right) have an increased number of lateral shoots and are sterile (inset). Bar = 5 cm. **(G)** and **(H)** Partially dissected wild-type **(G)** and *tgh-1* mutant **(H)** flower showing reduced stamen length and sterility in the *tgh* mutants. **(I)** Reduced hypocotyl elongation and apical hook formation in 5-d-old dark-grown wild-type (left) and *tgh-1* mutant (right) seedlings. **(K)** and **(L)** *tgh* mutants frequently develop three cotyledons. **(K)**, the wild type; **(L)**, *tgh-1* mutant. **(M) to (P)** The TGH:GFP fusion constructs complement the *tgh-1* mutant phenotype. Phenotype of an 18-d-old wild-type plant **(M)** and *tgh-1* mutants containing no TGH:GFP transgene **(N)**, containing the TGH:GFP transgene **(O)**, and the 35S:TGH:GFP transgene **(P)**.

TGH Is Required for Proper *Arabidopsis* Development

To gain insight into the biological function of *TGH*, we examined two *TGH* T-DNA insertion mutants, namely SALK_053445 (*tgh-1*) and GABI_774H04 (*tgh-2*) (Figure 2A). The T-DNA insertions are located at the end of intron 11 and at the beginning of exon 12, respectively (Figure 2A). Plants homozygous for the *TGH* T-DNA insertions were isolated by PCR-based genotyping from a large segregating population (Figures 2B to 2E). Plants homozygous for both *TGH* gene insertions displayed identical phenotypes that clearly distinguished them from wild-type and hemizygous segregants (Figures 2B to 2E). In general terms, adult *tgh* mutant plants have a reduced stature and significantly smaller lanceolate leaves (Figures 2C to 2F). Elongation defects could also be observed in the anthers of *tgh* mutant flowers, which fail to elongate and produce pollen (Figures 2G and 2H). At the seedling stage, *tgh* mutant seedlings are recognizable by developmental defects, including triple cotyledons, altered cotyledon shape, and reduced elongation growth in dark-grown seedlings (Figures 2I to 2L; data not shown). The triple cotyledon phenotype is, however, not fully penetrant (e.g., only 7 of 362 progeny seedlings of a *TGH/tgh-1* parent line displayed the triple cotyledon phenotype corresponding to a penetrance of 7.7%). Due to the almost complete infertility of *tgh* mutants, all subsequent analyses were performed with segregants of heterozygous *TGH/tgh-1* and *TGH/tgh-2* plants.

TGH Is Required for the Initiation of Vascular Development

Altered cotyledon number as observed in the *tgh* mutants is frequently associated with defects in cotyledon and leaf vascular initiation (Chaudhury et al., 1993; Hardtke and Berleth, 1998; Hamann et al., 1999; Hobbie et al., 2000; Mattsson et al., 2003). We therefore examined vascularization in cotyledons and leaves of *tgh-1* and *tgh-2* mutants and found that both *tgh* mutant alleles form an incomplete vascular system (Figure 4). While wild-type cotyledons typically have a simple interconnected vascular system, *tgh* mutant cotyledons have an imperfect vascular system with differentiated but frequently unconnected vascular strands (Figures 4A and 4D). The defects in vascularization are also detectable in leaves where second and third order vascular strands often remain unconnected in *tgh* mutants, while they are almost always interconnected in the wild type (Figures 4B and 4E). While the vascular network is altered in the *tgh* mutants, no obvious defects were observed with respect to vascular strand positions and vascular strand alignment.

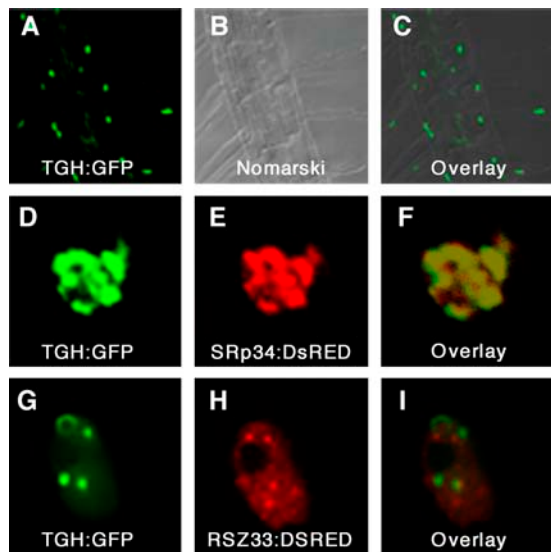


Figure 3. TGH:GFP and SRp34:DsRED Colocalize to Subnuclear Particles.

(A) to (C) 35S:TGH:GFP and TGH:TGH:GFP accumulate in the nuclei of root cells of transgenic *Arabidopsis* seedlings. Confocal fluorescence image (A), Nomarski image (B), and merged image (C) of a root expressing 35S:TGH:GFP.

(D) to (I) Confocal images of *Arabidopsis* protoplast nuclei expressing 35S:TGH:GFP (D) and (G) and SRp34:DsRED (E) or RSZ33:DsRED (H). 35S:TGH:GFP and SRp34:DsRED (D) to (F) but not 35S:TGH:GFP and RSZ33:DsRED (G) to (I) colocalize in subnuclear particles.

The morphological examination of cleared tissue only allows the visualization of differentiated vascular tissue but not the visualization of provascular cells. The expression of the *Arabidopsis* gene *HOMEBOX GENE 8* (*AtHB-8*) as monitored with the *AtHB-8*: β -glucuronidase (*GUS*) transgene is strong in provascular cells and reduced after vascularization is complete (Baima et al., 1995). To differentiate between defects at the level of vascular initiation and vascular differentiation, we examined the expression of *AtHB-8*:*GUS* in the *tgh-1* mutant. We found that *GUS* staining in *tgh-1* mutant embryonic and mature cotyledons delineates the interrupted vascularization pattern observed in the clearing sections (Figures 4C and 4F). Taken together, this shows that *tgh* mutants have defects in the initiation of vascular development as determined by the expression of the *AtHB-8*:*GUS* reporter construct.

To examine whether *TGH* gene expression can be correlated with its apparent role in vascular development, we generated transgenic lines that express the *GUS* reporter under control of a 1021-bp *TGH* promoter fragment. The same promoter fragment had been used in the TGH:TGH:GFP expression construct, which was able to rescue the *tgh* mutant phenotype. Analysis of *TGH* expression by virtue of *GUS* reporter activity allowed us to reproducibly detect strong *GUS* expression in the cotyledons of embryos, in the vasculature of cotyledons and leaves, in young meristematic tissue, in trichomes, and in the pistil (Figures 4G to 4L). Hence, in this analysis *TGH* expression in the vascular system can be correlated with its role in vascular development.

Auxin Response Is Not Altered in the *tgh* Mutant

Vascular differentiation requires auxin transport and auxin signal transduction (Mattsson et al., 2003; Fukuda, 2004). The importance of auxin transport for vascularization is supported by the observation that *Arabidopsis* mutants of auxin transport proteins (e.g., *pin-formed1* [*pin1*] and *pinoid*) or of proteins involved in the proper localization of auxin transport proteins (e.g., *gnom*) fail to form a proper vascular system (Gälweiler et al., 1998; Steinmann et al., 1999; Christensen et al., 2000). The importance of auxin signal transduction for vascular development is suggested by the discontinuous vascular system observed in the *Arabidopsis* mutants *monopteros* (*mp*), *bodenlos* (*bdl*), and *auxin-resistant 6* (*axr6*) (Hardtke and Berleth, 1998; Hobbie et al., 2000; Hamann et al., 2002). The current model of auxin signal transduction predicts that these mutants fail to express a subset of auxin-induced genes required for proper vascular development since they lack the transcription activator MP or are unable to degrade the repressor BDL. To examine a possible role for TGH in auxin response, we investigated the possibility that TGH participates in auxin-induced gene expression. To this end, we compared the expression of the three auxin-induced genes *GH3*, *IAA19*, and *SAUR10* by reverse transcription PCR in *tgh-1* mutant and in wild-type seedlings that had been subjected to a 2-h treatment with 5 and 50 μ M of the synthetic auxin 2,4-D (Figure 5A). In these

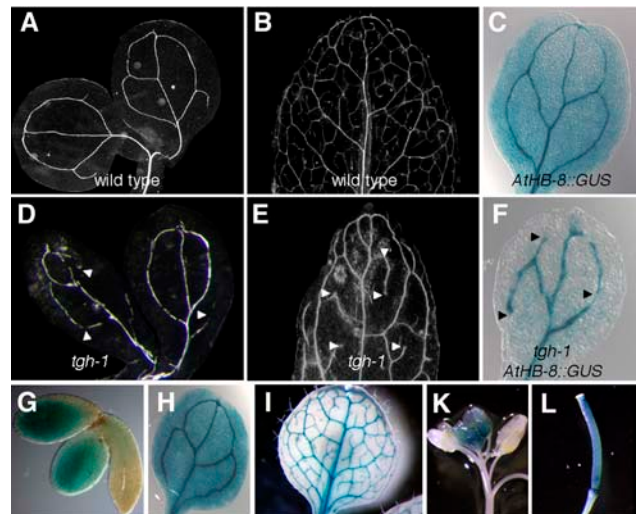


Figure 4. Vascularization Defects in the *tgh* Mutants.

(A) and (B) Cleared cotyledons and leaf of wild-type plants. (C) *GUS* staining of *AtHB-8*:*GUS* in cotyledons of 5-d-old *Arabidopsis* seedlings clearly delineates the vascular system. (D) and (E) Cleared cotyledons and leaf of the *tgh-1* mutant reveal defects in vascularization. Arrowheads mark unconnected vascular strands. (F) *GUS* staining of *AtHB-8*:*GUS* in the cotyledons of *tgh-1* seedlings delineates the interrupted vascular system observed in these mutants. Arrowheads mark unconnected vascular strands. (G) to (L) *GUS* expression in embryos (G), cotyledon (H), leaf (I), young inflorescence (K), and the pistil (L) of transgenic lines expressing the reporter *GUS* under control of a 1021-bp *TGH* promoter fragment.

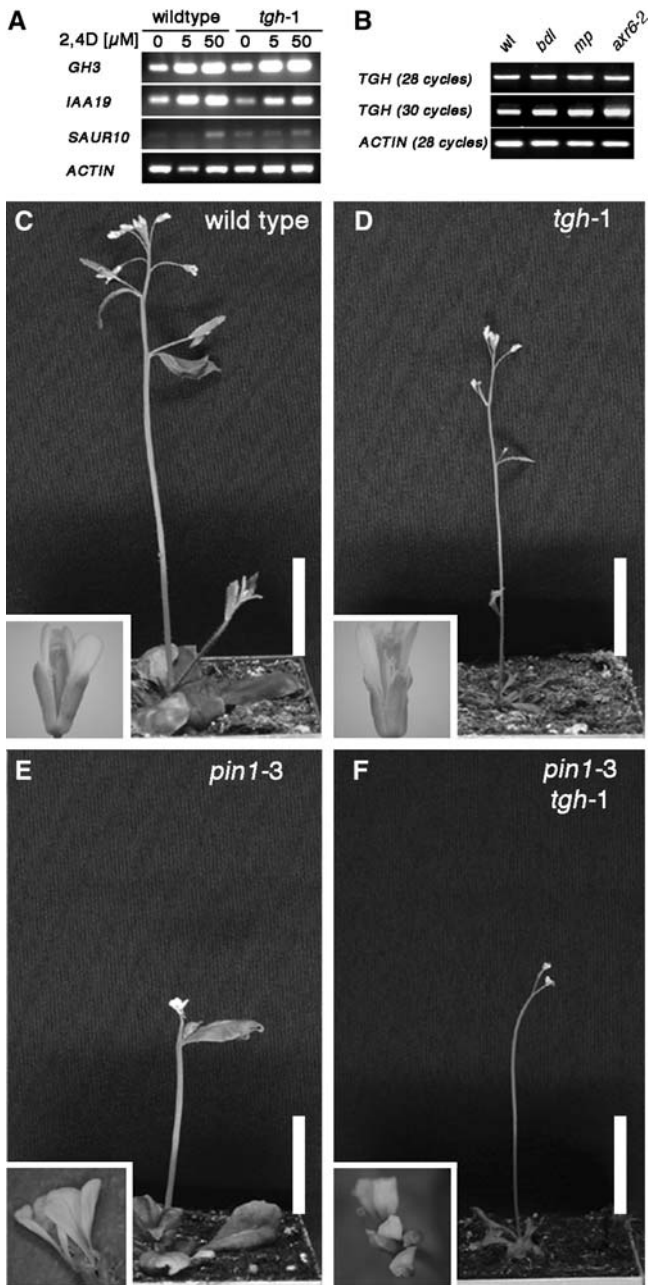


Figure 5. Auxin Response and Auxin Transport Are Not Affected in the *tgh-1* Mutant.

(A) Auxin-induced gene expression of the genes *GH3*, *IAA19*, and *SAUR10* is not impaired in *tgh-1* mutants compared with the wild type. Three-week-old plants were treated for 2 h with the synthetic auxin 2,4-D and subsequently analyzed by reverse transcription followed by 28 PCR amplification cycles.

(B) *TGH* gene expression is obviously unaltered in 7-d-old *bdl*, *mp*, and *axr6-2* mutant seedlings as determined by RT-PCR analysis. *ACTIN* served as an input control for all experiments. Number of PCR amplification cycles is indicated in parentheses.

(C) to (F) Mutants defective in *TGH* and *PIN1* show additive phenotypes. Shown are 4-week-old wild-type **(C)**, *tgh-1* **(D)**, *pin1-3* **(E)**, and *pin1-3 tgh-1* double mutant **(F)** plants as well as flowers (insets). Bars = 1.5 cm.

analyses, we detected different levels of auxin-induced gene expression for all three genes; however, we failed to detect any obvious differences between the wild type and the *tgh-1* mutant (Figure 5A). These data suggest that *TGH* is not required for auxin-induced gene expression.

Next, we examined whether *TGH* is a downstream target of the gene expression system that is composed of MP, BDL, and AXR6 (Hardtke and Berleth, 1998; Hamann et al., 2002; Hellmann et al., 2003). To this end, we tested whether *TGH* expression is altered in a loss-of-function allele of the transcriptional activator MP identified in the Salk T-DNA collection, as well as in the *bdl* and *axr6-2* mutants that fail to degrade BDL in response to auxin (Hardtke and Berleth, 1998; Hamann et al., 2002; Hellmann et al., 2003; D. Weijers and G. Jürgens, unpublished data). When we examined *TGH* gene expression by RT-PCR, we failed to detect any obvious differences in any of the mutants examined when compared with the wild type (Figure 5B). We therefore suggest that *TGH* acts independently of the BDL, MP, and AXR6 proteins and conclude furthermore that *TGH* is not a component of the auxin response pathway.

Additionally, we examined whether *TGH* is required for proper auxin transport. Mutants of the putative auxin efflux carrier *PIN1* fail to form a proper vascular system (Gälweiler et al., 1998). We therefore investigated the genetic interaction of *TGH* and *PIN1* in a *pin1-3 tgh-1* double mutant. Since this double mutant displayed the additive phenotype of the respective single mutants with respect to plant size, leaf shape, and flower morphology, we conclude that *TGH* and *PIN1* regulate vascular development by independent mechanisms (Figures 5C to 5F).

Genetic Interaction of *TGH* and *AMP1*

Arabidopsis AMP1 has been identified in several mutant screens (Jürgens et al., 1991; Chaudhury et al., 1993; Hou et al., 1993; Conway and Poethig, 1997). *amp1* mutants fail to form proper cotyledon and leaf vasculature and frequently produce multiple cotyledons (Chaudhury et al., 1993; Conway and Poethig, 1997). Furthermore, *amp1* mutants are constitutively photomorphogenic, grow fast, and flower early (Chaudhury et al., 1993). At least some of the *amp1* mutant phenotypes may be explained by the increased cytokinin levels measured in the *amp1* mutant resulting in the increased expression of the cell cycle regulator *CYCD3* (Chaudhury et al., 1993; Riou-Khamlichi et al., 1999). *AMP1* has homology to *N*-acetyl- α -linked acidic dipeptidases, and based on this homology, *AMP1* has been proposed to participate in the processing of small acidic peptides and folate polyglutamate (Helliwell et al., 2001). However, the postulated biochemical role of *AMP1* in protein processing as well as its role as a developmental regulator has not been defined yet.

To examine a possible link between *TGH* and *AMP1* function, we investigated *TGH* gene expression in the *amp1-1* mutant using RT-PCR. *amp1-1* is an ethyl methanesulfonate-induced loss-of-function allele with a base change mutation leading to an early stop codon mutation (Helliwell et al., 2001). In our studies, we consistently observed reduced *AMP1* expression in the *amp1-1* mutant allele, possibly a result of the destabilization of the mutant transcript (Figure 6). Consistent with previous reports, we found *CYCD3* expression to be elevated in the *amp1-1*

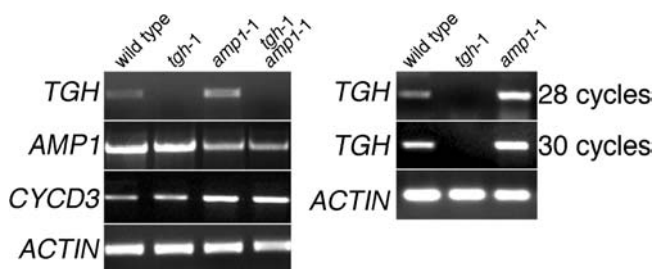


Figure 6. *TGH* Expression Is Elevated in the *amp1-1* Mutant.

Gene expression analysis of *TGH*, *AMP1*, and the G1 cell cycle phase marker *CYCD3* in 3-week-old wild-type, *tgh-1*, *amp1-1*, and *tgh-1 amp1-1* double mutants (28 PCR amplification cycles). *TGH* expression was reproducibly found to be elevated in the *amp1-1* mutant. Two additional independent experiments are shown in the right panel for comparison. *ACTIN* expression (28 cycles) was used as a control for all experiments.

mutant, indicative of increased cell cycle activity in the mutant (Riou-Khamlichi et al., 1999). Interestingly, our *TGH* gene expression analyses also revealed increased *TGH* expression in the *amp1-1* mutant compared with the wild type (Figure 6). We therefore went on to examine the genetic interaction between *AMP1* and *TGH* in *amp1-1 tgh-1* double mutants. In the progeny of *amp1-1 tgh-1/TGH* lines, we identified plants with a new phenotype that was not observed in the parental lines or in the single mutants. In seedlings, this phenotype is characterized by dramatic alterations of cotyledon shape, such as fused cotyledons and the impairment of leaf and shoot growth and differentiation (Figures 7A to 7E, 7L, and 7M). In 2-week-old adult plants, the rosette diameter of these mutants was reduced at least 10-fold (Figures 7N, 7O, inset in 7O, and 7X). By genotyping and gene expression analysis, we could show that these plants represented the *amp1-1 tgh-1* double mutant segregants of the *amp1-1 tgh-1/TGH* lines, and we therefore propose a genetic interaction between *TGH* and *AMP1*.

Since *amp1-1* and *tgh-1* single mutants have defects in vascular initiation, we also examined vascularization in these mutants. We found that vascular initiation is significantly more disturbed in the *amp1-1 tgh-1* double mutants than in the respective single mutants (Figures 7F to 7K, 7S, and 7W). For example, in cotyledons and leaves of the *amp1-1 tgh-1* double mutants, often only the primary vascular strand but no secondary or tertiary strands differentiated (Figures 7P to 7W). Furthermore, the lack of vascularization in these double mutant plants is accompanied by an inability to form normal leaf blades. We therefore propose that *TGH* and *AMP1* are required for the proper differentiation of the vascular network and normal leaf growth.

The *amp1-1* mutant has increased cytokinin levels and increased levels of the cytokinin-inducible G1 cell cycle regulator *CYCD3* (Riou-Khamlichi et al., 1999) (Figure 6). Since *CYCD3* expression has been proposed to be a direct consequence of the *amp1-1* mutant's increased cytokinin levels, we reasoned that the observed *amp1-1 tgh-1* double mutant phenotype may be a result of the combined effects of increased cytokinin levels and loss of *TGH* gene function. We therefore examined the effects of

cytokinin treatment on the *tgh-1* mutant seedlings. However, by treating *tgh-1* mutants with different cytokinins and different cytokinin concentrations, we failed to induce phenotypes in the *tgh-1* mutant comparable to those observed in the *amp1-1 tgh-1* double mutant (data not shown). At the same time, we found *CYCD3* expression to be elevated to the same extent in both the *amp1-1* and the *amp1-1 tgh-1* double mutant, suggesting that *TGH* does not influence *CYCD3* expression (Figure 6). We therefore conclude that the strong *amp1-1 tgh-1* double mutant phenotype is not the direct result of cytokinin overproduction or *CYCD3* overexpression in the *amp1-1 tgh-1* double mutants.

DISCUSSION

In this report, we describe the previously uncharacterized *TGH* protein and its role in *Arabidopsis* growth and development. *TGH* is an evolutionarily conserved regulator with a G-patch and a SWAP domain, and both domains are exclusively found in RNA binding and processing proteins (Figure 1) (Denhez and Lafyatis, 1994; Spikes et al., 1994; Aravind and Koonin, 1999). *TGH* colocalizes with the SR protein SRp34 to subnuclear particles and the enrichment of Ser and Arg residues in the KRDES domain of *TGH* is reminiscent of the Arg- and Ser-rich RS domains found in SR proteins (Figures 1 and 2). SR proteins play key roles in constitutive and alternative splicing either as essential splicing factors or as specific regulators that act during different stages of spliceosome assembly (Blencowe et al., 1999; Graveley, 2000). The only other data available on *TGH* function besides the studies reported here come from a *Drosophila* interactome study where the *Drosophila* *TGH* ortholog CG8833 was found to interact with CG6843 (Giot et al., 2003). CG6843 is an uncharacterized SR protein, which in turn interacts with splicing factors such as SWAP and SRp54. Taken together, the different findings strongly suggest that *TGH* functions as an RNA binding and processing protein that may act close to the splicing machinery. Another point that indirectly supports this hypothesis is the absence of a *TGH* ortholog from the budding yeast *S. cerevisiae*, an organism where splicing is not an important regulatory mechanism (Figure 1). On the other side, two large-scale purifications of spliceosomes have been reported, and none of these reports identified *TGH* orthologs as components of the spliceosome (Rappsilber et al., 2002; Zhou et al., 2002). It is therefore unlikely that *TGH* is an integral spliceosome subunit.

In our study, we observed a yeast two-hybrid interaction between *TGH* and TBP2, and we observed that *TGH* promotes gene expression when tethered to the promoter of a reporter gene (Figures 1E to 1G). Transcription and pre-mRNA processing are known to be intimately related processes, and alternative splicing can be determined by the identity of the promoter driving gene expression (Smith and Valcarcel, 2000; Fong and Zhou, 2001; Proudfoot et al., 2002). Multiple splicing regulators have been reported to interact with the C-terminal domain (CTD) of RNA polymerase II, and it is thought that CTD serves as an assembly platform for and a regulator of transcription and pre-mRNA processing machines (Maniatis and Reed, 2002). Interestingly, in addition to the clear sequence homologies described in this report, *TGH* has also limited similarity to the CTD-interacting protein 6, an interactor of the C terminus of RNA

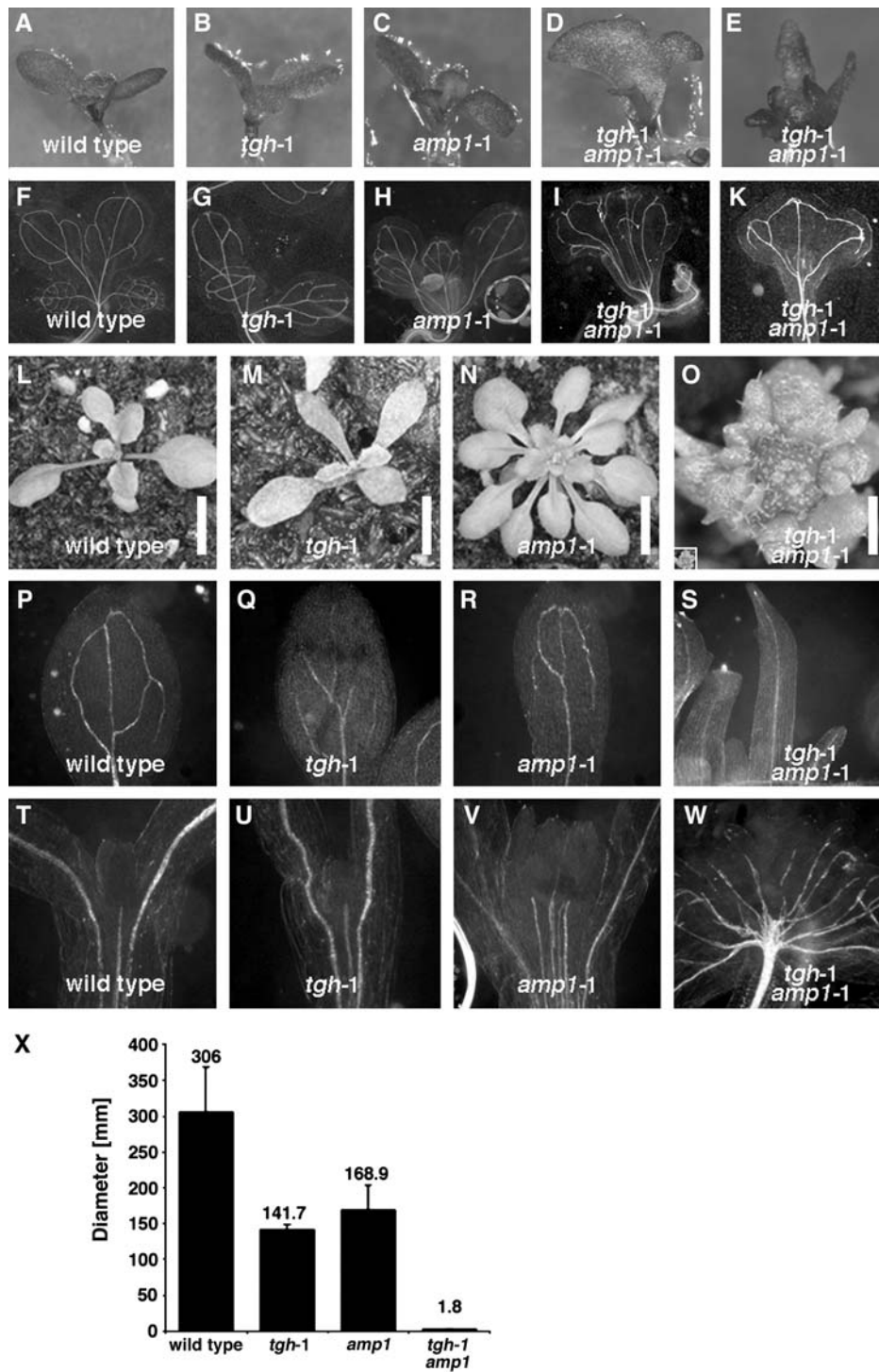


Figure 7. Genetic Interaction between *TGH* and *AMP1*.

(A) to (S) Development of 7-d-old seedlings [(A) to (E)] and 2-week-old adult plants [(L) to (O)] is severely affected in the *tgh-1 amp1-1* double mutants. Genotypes are as indicated in the panel. All pictures are taken at comparable magnification, except (O), which is 10 times magnified. See the inset in (O) for the original size of the adult *tgh-1 amp1-1* mutant in scale with the single mutants shown in (L) and (M). Growth impairment of the double mutant is reflected at the level of vascular development in seedlings [(F) to (K)] and cotyledons [(P) to (S)]. Bars = 5 mm in (L) to (N) and 1 mm in (O).

(T) to (W) Vascularization in the cotyledons and leaves of cleared 10-d-old dark-grown seedlings.

(X) Quantitative analysis of rosette diameters of adult wild-type plants, single mutants, and the *tgh-1 amp1-1* double mutant ($n \geq 10$; bars and error bars represent means and standard deviations).

polymerase II (data not shown). It may therefore be hypothesized that TGH is an RNA binding or processing protein that functions cotranscriptionally.

Our developmental analysis reveals that *TGH* is essential for proper plant development. Two independent mutant alleles show identical phenotypes, including reduced elongation growth, tricotyly, reduced vascularization, and reduced pollen formation (Figures 2 and 4). Altered cotyledon number in combination with reduced vascularization has been observed in a limited number of mutants that are defective in auxin transport and response as well as in mutants defective in AMP1, a putative *N*-acetyl- α -linked acidic dipeptidase (Helliwell et al., 2001). In our studies, we failed to establish a link between TGH function and the auxin transport and auxin response pathways (Figure 5). By contrast, however, we observed *TGH* gene expression to be elevated in an *amp1* mutant. This observation may suggest that a *TGH* expressing cell type is more abundant in the *amp1* mutant or that AMP1 represses *TGH* gene expression in the wild type (Figure 6). The latter explanation is unlikely based on the proposed biochemical function of AMP1 as a putative *N*-acetyl- α -linked acidic dipeptidase with a presumed role in protein or peptide processing. On the other side, *amp1* mutants have increased cell cycle activity and increased meristem size (Riou-Khamlichi et al., 1999). Since TGH:GUS data suggest that *TGH* is expressed in meristematic and young tissue, the increased *TGH* gene expression observed by RT-PCR may be a consequence of the *amp1* mutant's increased meristem size.

TGH shows a strong genetic interaction with *AMP1* (Figure 7). Double mutants defective in both gene functions initiate but fail to differentiate leaves. It may be postulated that the impaired and strongly reduced differentiation of leaves in the double mutant restricts proper vascularization, so that impaired cotyledon and leaf development may be the primary cause for reduced vascularization. Conversely, since both mutants are defective in vascularization and since this effect is strongly enhanced in the double mutant, it may also be postulated that reduced vascularization is the biological cause for the dramatic double mutant phenotype.

Although the strong genetic interaction between *TGH* and *AMP1* is very intriguing, the interaction of their gene products can at present not be explained based on the proposed biochemical function of TGH and AMP1. While we postulate TGH to act in RNA binding or processing, AMP1 is a putative *N*-acetyl- α -linked acidic dipeptidase with a presumed role in protein or peptide processing (Helliwell et al., 2001). To date, no substrates for AMP1's proposed peptidase activity have been identified nor has AMP1 been localized to any subcellular compartment. We can therefore at present not provide an explanation for the strong genetic interaction observed between the two genes based on the nature of their gene products.

In plants, RNA binding and processing proteins have so far only been implicated in floral transition and patterning, vegetative phase change, as well as abscisic acid signaling, stress responses, and circadian rhythms (Chen and Cheng, 2004). The putative RNA binding and processing protein TGH with its proposed role in vascularization adds a new biological function to this list. However, based on the large numbers of proteins with domains indicative for a role in RNA binding and processing and

based on the essential role of these proteins in gene expression, it can be expected that there are many novel developmental functions for these proteins that await to be identified (Lorkovic and Barta, 2002).

METHODS

Biological Material

The *TGH* T-DNA insertion lines SALK_053445 (Columbia background) and GABI_774H04 (Columbia background) were identified in the SIGNAL database (<http://signal.salk.edu/cgi-bin/tdnaexpress>) and obtained from the Nottingham Arabidopsis Stock Centre (NASC) and from GABI-KAT at the Max-Planck Institute for Plant Breeding Research (Cologne, Germany), respectively (Alonso et al., 2003; Rosso et al., 2003). To test for the presence of the *TGH* wild-type gene and the *TGH* T-DNA insertion, segregants of SALK_053445 were PCR genotyped using combinations of primers flanking the T-DNA insertion site, TGHFW 5'-ATGTTGAGGA-TGAAGATGTCTATGC-3' and TGHVRV 5'-AGATGAAGCTGATTTGGTG-AATGTG-3', or TGHFW and the T-DNA specific primer LBb1 5'-GCG-TGGACCGCTTGCTGCAACT-3'. Segregants of GABI_774H04 were genotyped with TGHFW and TGHVRV or TGHVRV in combination with the T-DNA-specific GABI primer 5'-ATATTGACCATCATACTCATTGC-3'.

The reporter line AtHB-8:GUS was obtained from Giorgio Morelli (Rome, Italy) and crossed to *tgh-1/TGH* lines. Tissue-specific GUS expression was analyzed in *TGH* wild-type and mutant segregants of the F2 and F3 progeny as described elsewhere (Baima et al., 1995; Weigel and Glazebrook, 2002). The *mp* allele was derived from the T-DNA insertion line SALK_023812 and was a gift from D. Weijers (Tübingen, Germany). *bdl* and *axr6-2* alleles were previously described (Hamann et al., 1999; Hobbie et al., 2000; Hellmann et al., 2003). *pin1-3/PIN1* mutant seed were a gift from N. Geldner (Tübingen University, Germany). *pin1-3/PIN1* were identified by a *Scal* cleaved-amplified polymorphic sequence marker and then crossed with *tgh-1/TGH*. The resulting F1 plants were genotyped to identify *pin1-3/PIN1 tgh-1/TGH* lines. The F2 progeny of these lines was then used for phenotype and genotype analyses. *amp1-1* (Columbia background) mutant seed were obtained from NASC and crossed to *tgh-1/TGH*. *amp1-1/amp1-1 tgh-1/TGH* plants were identified among the F2 progeny based on the *amp1-1* phenotype and the genotype of the *TGH* locus. The F3 progeny of these lines was subjected to phenotype analyses. Phenotypes were linked to the segregating genotypes using PCR analysis as described above. When different ecotypes were combined for genetic crosses, segregating wild-type plants were used as wild-type control.

Subcellular Localization Studies

Constructs expressing TGH:GFP fusions were prepared using the Gateway system (Invitrogen). To generate 35S:TGH:GFP, the *TGH* gene fragment was amplified by PCR using the primers 5'-attB1-TCATGG-GGTCAGACGAGGAAGATTTCTGTGTTTC-3' and 5'-attB2-CGTCTCGT-CGCCTTCTTCTCCCGCCTTGAC-5' and introduced into pDONR 201. One entry clone was fully sequenced and inserted into the vector 35S-GW-GFP(Kan), a gift from F. Turck (Max-Planck Institute for Plant Breeding Research, Cologne, Germany). To generate TGH:TGH:GFP, a 6.6-kb *TGH* genomic fragment was amplified by PCR using the primers 5'-attB1-CATGCTCAGGAGCAATCGTCCGTTTATC-3' and attB2-CGTCTCGTCTGCCTTCTTCTCCCGCCTTGAC-5'. The fragment was introduced into pDONR 201, and one clone was fully sequenced and then inserted into the vector pGWB8 (a gift from T. Nakagawa, Shimane University, Japan). Twenty stable transgenic lines expressing each TGH:GFP fusion construct were generated and propagated in *Arabidopsis thaliana* ecotype Columbia (Clough and Bent, 1998). For transient

expression, the 35S:TGH:GFP and TGH:TGH:GFP constructs were introduced alone or in combination with the constructs SRp34:DsRED and RSZ33:DsRED (a gift from Z. Lorkovic and A. Barta, Vienna Biocentre, Austria) into *Arabidopsis* var Columbia suspension culture cells using established procedures (Negrutiu et al., 1987; Lorkovic et al., 2004a). The DsRED constructs express the respective fusion proteins from the 35S promoter of *Cauliflower mosaic virus*. Protein fluorescence was analyzed using a Leica TCS SP2 confocal microscope.

Tissue Clearing

Tissue of 7-d-old *Arabidopsis* seedlings and 3-week-old *Arabidopsis* plants was fixed for 12 h in an ethanol:acetic acid (6:1) mixture followed by two 30-min washes with 100% ethanol and one wash with 70% ethanol. Tissues were finally cleared with chloral hydrate:glycerol:water (8 g:1 mL:2 mL) for several hours as previously described (Weigel and Glazebrook, 2002).

Yeast Two-Hybrid System

A previously described yeast two-hybrid system cDNA library was used to perform a library screen with pGBT9/pTBP expressing potato (*Solanum tuberosum*) TBP (Holdsworth et al., 1992; Kim et al., 1997; Schwechheimer and Deng, 2002). To this end, full-length pTBP was cloned in frame by ligating a blunt-ended *Bam*HI fragment to the blunt-ended *Sal*I site of the pGBT9 vector. The screen resulted in the isolation of pACT2-8/5 expressing the C-terminal 245 amino acids of TGH, including its KRDES domain. pACT/TGH was obtained by cloning a *Bam*HI linked full-length TGH cDNA fragment into pACT2. The interaction between full-length TGH and *Arabidopsis* TBP2 was then confirmed in the yeast two-hybrid system with pGBT9/AtTBP expressing the *Arabidopsis* TBP2 ortholog (At1g55520) cloned in an identical manner to construct pGBT9/pTBP.

Isolation of TGH Full-Length cDNA Clones

A size-fractionated *Arabidopsis* cDNA library provided by NASC was screened for full-length cDNAs using the TGH cDNA fragment isolated in the yeast two-hybrid system as a probe. Sequence analyses of several full-length cDNAs confirmed the exon-intron predictions for the TGH gene found in the databases and revealed that polyadenylation of TGH mRNAs occurs at two alternative positions 76 and 285 base pairs after the stop codon.

Transactivation Studies

pGBT9/TGH containing the full-length TGH gene and pGBT9/KRDES containing the TBP2-interacting TGH fragment originally identified in the yeast two-hybrid system library screen were tested for their ability to transactivate expression of the *LacZ* reporter gene in the yeast strain HF7C using Galacto-Star (Tropix). The TGH coding sequence and the KRDES fragment present in the original yeast two-hybrid clone were subcloned into the vector pGAL4 and tested as previously described for their ability to transactivate transcription from UAS_{4xGAL}LUC in tobacco (*Nicotiana tabacum*) mesophyll protoplasts (Negrutiu et al., 1987; Schwechheimer et al., 1998).

The TGH Promoter:GUS Fusion Construct

A 1021-bp TGH promoter fragment was amplified using 5'-attB1-CATGCTCAGGAGCAATCGTCCGTTTATC-3' and 5'-attB2-TGTCTTCA-CCACCGAGACCGAGAGGAGCAG-3'. The fragment was introduced into pDONR 201, fully sequenced, and subsequently cloned into the Gateway compatible pGWB3 vector (a gift from T. Nakagawa). Twenty

transgenic lines were established harboring the TGH:GUS transgene. Seedlings and plants were stained for GUS expression using standard procedures (Weigel and Glazebrook, 2002).

Gene Expression Analysis

Gene expression analyses were performed by RT-PCR. RNA was extracted from plant material using the RNeasy method (Qiagen). Two micrograms of total RNA were used for the reverse transcription reaction with an oligo(dT) primer and Platinum reverse transcriptase as previously described (Invitrogen) (Frohman et al., 1988). TGH gene expression was monitored using the gene-specific primers TGHFW and TGHRV, primers identical to those used for TGH genotyping. Gene expression of auxin-induced genes was monitored using GH3-FW 5'-ATGGAGGAGTCGTT-GAACTCTGTG-3' and GH3-RV 5'-AAGCTCCATTATTGGCGTGAAAC-CTC-3' for GH3 (At2g23170); IAA19-FW 5'-GTGATGTACCTTGGGG-GATGTTTC-3' and IAA19-RV 5'-AATGAACCAGCTCCTTGCTTCTTG-3' for IAA19 (At3g15540); SAUR10-FW 5'-CGAAGTCGGTACATCGTTCC-TATC-3' and SAUR10-RV 5'-CATGGAGATAAGAGACCTGAAGAAGA-3' for SAUR10 (At2g18010). Gene expression of AMP1 and CYCD3 was determined using the primers AMP1-FW 5'-ATGTCAACAACCTCTCAC-3' and AMP1-RV 5'-TCATGTGAAACCTCCTT-3' for AMP1 and CYCD3-FW 5'-ATGGCTTTAGAAGAGGAGGAAGA-3' and CYCD3-RV 5'-TTAGC-GAGGACTACTACTAAGCAC-3' for CYCD3 (At3g50070). ACTIN-FW 5'-ATTCAGATGCCAGAGTCTTGTTCC-3' and ACTIN-RV 5'-GCAAGT-GCTGTGATTTCTTTGCTCA-3' for ACTIN (At3g18780) were used as a loading control in all cases. All RT-PCR reactions were repeated using independent RNA preparations and reverse transcription reactions. Transcripts were amplified using 28 or 30 amplification cycles as indicated in the text. Each experiment was repeated at least twice with independent RNA preparations.

Accession Numbers

TGH sequence data from this article have been deposited with the GenBank data library under accession number AAR99647. TOUGH (TGH) is registered as a gene class symbol at www.arabidopsis.org. Arabidopsis Genome Initiative locus identifiers for the *Arabidopsis* genes used in this article are as follows: TGH (At5g23080), AtTBP2 (At1g55520), GH3 (At2g23170), IAA19 (At3g15540), SAUR10 (At2g18010), CYCD3 (At3g50070), and ACTIN (At3g18780). Accessions of the TGH orthologs listed in Figures 1B and 1C are as follows: rice (BAD37703.1), human (NP_060495.2), mouse (NP_080457.1), *Drosophila* (NP_648669.1), *C. elegans* (CAA83621.1), *N. crassa* (EAA31042.1), *S. pombe* (NP_593626.1), and *A. gambiae* (NP_593626.1). Accessions of the SWAP domain containing proteins listed in Figure 1D are as follows: rice (BAD37703.1), human (AAN77183.1), mouse (NP_613051.2), *Drosophila* (AAN77184.1), *A. gambiae* (EAA11741.1).

ACKNOWLEDGMENTS

We thank Dolf Weijers and Melina Zourelidou for helpful comments on the manuscript, Eike Rademacher for assistance during the initial characterization of the *tgh-1* mutant, Catarina Brancato for *Arabidopsis* protoplast transformations, colleagues in Tübingen for providing mutant seed, the Salk Institute Genomic Analysis Laboratory and NASC for generating and providing the sequence-indexed *Arabidopsis* T-DNA insertion mutant SALK_053445, B. Weisshaar and the GABI-KAT program (Max-Planck Institute for Plant Breeding Research) for the T-DNA mutant GABI774H04, Z.J. Lorkovic and A. Barta for providing the constructs SRp34:DsRED and RSZ33:DsRED, and Giovanni Spina for AtHB8:GUS seeds. The work in our laboratory was supported by funds from Tübingen University and by the Deutsche Forschungsgemeinschaft (SCHW 751/4).

Received January 31, 2005; revised June 17, 2005; accepted June 19, 2005; published July 15, 2005.

REFERENCES

- Alonso, J.M., et al. (2003). Genome-wide insertional mutagenesis of *Arabidopsis thaliana*. *Science* **301**, 633–657.
- Aravind, L., and Koonin, E.V. (1999). G-patch: A new conserved domain in eukaryotic RNA-processing proteins and type D retroviral polyproteins. *Trends Biochem. Sci.* **24**, 342–344.
- Baima, S., Nobili, F., Sessa, G., Lucchetti, S., Ruberti, I., and Morelli, G. (1995). The expression of the *ATHB-8* homeobox gene is restricted to provascular cells in *Arabidopsis thaliana*. *Development* **121**, 4171–4182.
- Blencowe, B.J., Bowmann, J.A.L., McCracken, S., and Rosonina, E. (1999). SR-related proteins and the processing of messenger RNA precursors. *Biochem. Cell Biol.* **77**, 277–291.
- Blilou, I., Fugier, F., Folmer, S., Serralbo, O., Willemsen, V., Wolkenfeldt, H., Eloy, N.B., Ferreira, P.C.G., Weisbeek, P.J., and Scheres, B. (2002). The *Arabidopsis* HOBBIT gene encodes a CDC27 homolog that links the plant cell cycle to progression of cell differentiation. *Genes Dev.* **16**, 2566–2575.
- Carland, F.M., Fujioka, S., Takatsuto, S., Yoshida, S., and Nelson, T. (2002). The identification of CVP1 reveals a role for sterols in vascular patterning. *Plant Cell* **14**, 2045–2058.
- Chaudhury, A.M., Letham, S., Craig, S., and Dennis, E.S. (1993). *amp1*: A mutant with high cytokinin levels and altered embryonic pattern, faster vegetative growth, constitutive photomorphogenesis and precocious flowering. *Plant J.* **4**, 907–916.
- Chen, X., and Cheng, Y. (2004). Posttranscriptional control of plant development. *Curr. Opin. Plant Biol.* **7**, 20–25.
- Christensen, S.K., Dagenais, N., Chory, J., and Weigel, D. (2000). Regulation of auxin response by the protein kinase PINOID. *Cell* **100**, 469–478.
- Clough, S.J., and Bent, A.F. (1998). Floral dip: A simplified method for Agrobacterium-mediated transformation of *Arabidopsis thaliana*. *Plant J.* **16**, 735–743.
- Conway, L.J., and Poethig, R.S. (1997). Mutations of *Arabidopsis thaliana* that transform leaves into cotyledons. *Proc. Natl. Acad. Sci. USA* **94**, 10209–10214.
- Denhez, F., and Lafyatis, R. (1994). Conservation of regulated alternative splicing and identification of functional domains in vertebrate homologs to the *Drosophila* splicing regulator, suppressor-of-white-apricot. *J. Biol. Chem.* **269**, 16170–16179.
- Dingwall, C., and Laskey, R.A. (1991). Nuclear targeting sequences: A consensus? *Trends Biochem. Sci.* **16**, 478–481.
- Dynlacht, B.D., Hoey, T., and Tjian, R. (1991). Isolation of coactivators associated with the TATA-binding protein that mediate transcriptional activation. *Cell* **66**, 563–576.
- Fong, Y.W., and Zhou, Q. (2001). Stimulatory effect of splicing factors on transcriptional elongation. *Nature* **414**, 929–933.
- Frohman, M.A., Dush, M.K., and Martin, G.R. (1988). Rapid production of full-length cDNAs from rare transcripts: Amplification using a single gene-specific oligonucleotide primer. *Proc. Natl. Acad. Sci. USA* **85**, 8998–9002.
- Fukuda, H. (2004). Signals that control plant vascular cell differentiation. *Nat. Rev. Mol. Cell Biol.* **5**, 379–391.
- Gälweiler, L., Guan, C., Müller, A.J., Wismann, E., Medgen, K., Yephremov, A., and Palme, K. (1998). Regulation of polar auxin transport by AtPIN1 in *Arabidopsis* vascular tissue. *Development* **282**, 2226–2230.
- Giot, L., et al. (2003). A protein interaction map of *Drosophila melanogaster*. *Science* **302**, 1727–1736.
- Goodrich, J.A., and Tjian, R. (1994). TBP-TAF complexes: Selectivity factors for eukaryotic transcription. *Curr. Biol.* **6**, 403–409.
- Graveley, B.R. (2000). Sorting out the complexity of SR protein functions. *RNA* **6**, 1197–1211.
- Hamann, T., Benkova, E., Bäurle, I., Kientz, M., and Jürgens, G. (2002). The *Arabidopsis* BODENLOS gene encodes an auxin response protein inhibiting MONOPTEROS-mediated embryo patterning. *Genes Dev.* **16**, 1610–1615.
- Hamann, T., Mayer, U., and Jürgens, G. (1999). The auxin-insensitive *bodenlos* mutation affects primary root formation and apical-basal patterning in the *Arabidopsis* embryo. *Development* **126**, 1387–1395.
- Hardtke, C.S., and Berleth, T. (1998). The *Arabidopsis* gene MONOPTEROS encodes a transcription factor mediating embryo axis formation and vascular development. *EMBO J.* **17**, 1405–1411.
- Helliwell, C.A., Chin-Atkins, A.N., Wilson, I.W., Chapple, R., Dennis, E.S., and Chaudhury, A. (2001). The *Arabidopsis* AMP1 gene encodes a putative glutamate carboxypeptidase. *Plant Cell* **13**, 2115–2125.
- Hellmann, H., Hobbie, L., Chapman, A., Dharmasiri, S., Dharmasiri, N., del Pozo, C., Reinhardt, D., and Estelle, M. (2003). *Arabidopsis* AXR6 encodes CUL1 implicating SCF E3 ligases in auxin regulation of embryogenesis. *EMBO J.* **22**, 3314–3325.
- Hobbie, L., McGovern, M., Hurwitz, L.R., Pierro, A., Liu, N.Y., Bandyopadhyay, A., and Estelle, M. (2000). The *axr6* mutants of *Arabidopsis thaliana* define a gene involved in auxin response and early development. *Development* **127**, 23–32.
- Holdsworth, M.J., Grierson, C., Schuch, W., and Bevan, M. (1992). DNA-binding properties of cloned TATA-binding protein from potato tubers. *Plant Mol. Biol.* **19**, 455–464.
- Hou, Y., von Arnim, A.G., and Deng, X.-W. (1993). A new class of *Arabidopsis* constitutive photomorphogenic genes involved in regulating cotyledon development. *Plant Cell* **5**, 329–339.
- Jürgens, G., Mayer, U., Torres Ruiz, R.A., Berleth, T., and Miséra, S. (1991). Genetic analysis of pattern formation in the *Arabidopsis* embryo. *Dev. Suppl.* **1**, 27–38.
- Kim, J., Harter, K., and Theologis, A. (1997). Protein-protein interactions among the Aux/IAA proteins. *Proc. Natl. Acad. Sci. USA* **94**, 11786–11791.
- Lieberman, P.M., and Berk, A.J. (1994). A mechanism for TAFs in transcriptional activation: Activation domain enhancement of TFIID-TFIIA-promoter DNA complex formation. *Genes Dev.* **8**, 995–1006.
- Lopato, S., Forstner, C., Kalyna, M., Hilscher, J., Langhammer, U., Indrapichate, K., Lorkovic, Z.J., and Barta, A. (2002). Network of interactions of a novel plant-specific Arg/Ser-rich protein, atRSZ33, with atSC35-like splicing factors. *J. Biol. Chem.* **277**, 39989–39998.
- Lopato, S., Kalyna, M., Dörner, S., Kobayashi, R., Krainer, A.R., and Barta, A. (1999). atSRp30, one of two SF2/ASF-like proteins from *Arabidopsis thaliana*, regulates splicing of specific plant genes. *Genes Dev.* **13**, 987–1001.
- Lorkovic, Z.J., and Barta, A. (2002). Genome analysis: RNA recognition motif (RRM) and K homology (KH) domain RNA-binding proteins from the flowering plant *Arabidopsis thaliana*. *Nucleic Acids Res.* **30**, 623–635.
- Lorkovic, Z.J., Hilscher, J., and Barta, A. (2004a). Use of fluorescent protein tags to study nuclear organization of the spliceosomal machinery in transiently transformed living plant cells. *Mol. Biol. Cell* **15**, 3233–3243.
- Lorkovic, Z.J., Lopato, S., Pexa, M., Lehner, R., and Barta, A. (2004b). Interactions of *Arabidopsis* RS domain containing cyclophilins with SR proteins and U1 and U11 small nuclear ribonucleoprotein-specific proteins suggest their involvement in pre-mRNA splicing. *J. Biol. Chem.* **279**, 33890–33898.

- Maniatis, T., and Reed, J.** (2002). An extensive network of coupling among gene expression machines. *Nature* **416**, 499–506.
- Mattsson, J., Ckurshumova, W., and Berleth, T.** (2003). Auxin signaling in *Arabidopsis* leaf vascular development. *Plant Physiol.* **131**, 1327–1339.
- Mattsson, J., Sung, Z.R., and Berleth, T.** (1999). Responses of plant vascular systems to auxin transport inhibition. *Development* **126**, 2979–2991.
- Murashige, T., and Skoog, F.** (1962). A revised medium for rapid growth and bio-assays with tobacco tissue cultures. *Plant Physiol.* **15**, 473–497.
- Negrutiu, I., Shillito, R., Potrykus, I., and Sala, F.** (1987). Hybrid genes in the analysis of transformation conditions. I. Setting up a simple method for direct gene transfer in plant protoplasts. *Plant Mol. Biol.* **8**, 363–373.
- Orphanides, G., and Reinberg, D.** (2002). A unified theory of gene expression. *Cell* **108**, 439–451.
- Proudfoot, N.J., Furger, A., and Dye, M.J.** (2002). Integrating mRNA processing with transcription. *Cell* **108**, 501–512.
- Rappsilber, J., Ryder, U., Lamond, A.I., and Mann, M.** (2002). Large-scale proteomic analysis of the human spliceosome. *Genome Res.* **12**, 1231–1245.
- Reinhardt, D.** (2003). Vascular patterning: More than just auxin? *Curr. Biol.* **13**, R485–R487.
- Riou-Khamlichi, C., Huntley, R., Jacqumard, A., and Murray, J.A.H.** (1999). Cytokinin activation of *Arabidopsis* cell division through a D-type cyclin. *Science* **283**, 1541–1544.
- Rosso, M.G., Li, Y.-F., Strizhov, N., Reiss, B., Dekker, K., and Weisshaar, B.** (2003). An *Arabidopsis thaliana* T-DNA mutagenized population (GABI-Kat) for flanking sequence tag-based reverse genetics. *Plant Mol. Biol.* **53**, 247–259.
- Sachs, T.** (1991). Cell polarity and tissue patterning in plants. *Dev. Suppl.* **1**, 83–93.
- Schwechheimer, C., and Deng, X.W.** (2002). Studying protein-protein interactions with the yeast two-hybrid system. In *Molecular Plant Biology*, P.M. Gilmartin and C. Bowler, eds (Oxford: Oxford University Press), pp. 173–198.
- Schwechheimer, C., Smith, C., and Bevan, M.** (1998). The activities of acidic and glutamine-rich transcriptional activation domains in plant cells: Design of modular transcription factors for high-level expression. *Plant Mol. Biol.* **36**, 195–204.
- Smith, C.W.J., and Valcarcel, J.** (2000). Alternative pre-mRNA splicing: The logic of combinatorial control. *Trends Biochem. Sci.* **25**, 381–388.
- Spikes, D.A., Kramer, J., Bingham, P.M., and van Doren, K.** (1994). SWAP pre-mRNA splicing regulators are a novel, ancient protein family sharing a highly conserved sequence motif with the *prp21* family of constitutive splicing proteins. *Nucleic Acids Res.* **22**, 4510–4519.
- Steinmann, T., Geldner, N., Grebe, M., Moangold, S., Jackson, C.L., Paris, S., Gälweiler, L., Palme, K., and Jürgens, G.** (1999). Co-ordinated polar localization of auxin efflux carrier PIN1 by GNOM ARF GEF. *Science* **286**, 316–318.
- Tansey, W.P., and Herr, W.** (1997). TAFs: Guilt by association? *Cell* **88**, 729–732.
- Tjian, R., and Maniatis, T.** (1994). Transcriptional activation: A complex puzzle with few easy pieces. *Cell* **77**, 5–8.
- Verrijzer, C.P., and Tjian, R.** (1996). TAFs mediate transcriptional activation and promoter selectivity. *Trends Biochem. Sci.* **21**, 338–342.
- Weigel, D., and Glazebrook, J.** (2002). *Arabidopsis: A Laboratory Manual*. (Cold Spring Harbor, NY: Cold Spring Harbor Laboratory Press).
- Willemsen, V., Friml, J., Grebe, M., van den Toorn, A., Palme, K., and Scheres, B.** (2003). Cell polarity and PIN protein positioning in *Arabidopsis* require STEROL METHYLTRANSFERASE1 function. *Plant Cell* **15**, 612–625.
- Willemsen, V., Wolkenfelt, H., de Vrieze, G., Weisbeek, P.J., and Scheres, B.** (1998). The *HOBBIT* gene is required for formation of the root meristem in the *Arabidopsis* embryo. *Development* **125**, 521–531.
- Wu, S.Y., and Chiang, C.M.** (2001). TATA-binding protein-associated factors enhance the recruitment of RNA polymerase II by transcriptional activators. *J. Biol. Chem.* **276**, 34235–34243.
- Zhou, Z., Licklider, L.J., Gygi, S.P., and Reed, R.** (2002). Comprehensive proteomics analysis of the human spliceosome. *Nature* **419**, 182–185.

III.V. Calderón Villalobos et al. (manuscript of a research article)

Luz Irina A. Calderón Villalobos, Carola Kuhnle, Hanbing Li,
Mario Rosso, Bernd Weisshaar, and Claus Schwechheimer

**LucTrap Vectors – a versatile tool for the analysis of
transcriptional and translational luciferase fusions**

(Under revision in *Plant Physiology*)

LucTrap Vectors – a versatile tool to generate transcriptional and translational luciferase fusions.

Luz Irina A. Calderon-Villalobos¹, Carola Kuhnle¹, Hanbing Li¹, Mario Rosso^{2,3}, Bernd Weisshaar^{2,3}, and Claus Schwechheimer^{1,4}

¹ Centre for Plant Molecular Biology, Developmental Genetics, Auf der Morgenstelle 5, 72076 Tübingen, Germany.

² GABI-Kat, Max Planck Institute for Plant Breeding Research, Carl-von-Linné-Weg 10, 50829 Cologne, Germany.

³ Institute for Genome Research, Centre for Biotechnologie, Bielefeld University, Universitätsstrasse 25, 33615 Bielefeld, Germany.

⁴ Author for correspondence: Centre for Plant Molecular Biology, Developmental Genetics, Auf der Morgenstelle 5, 72076 Tübingen. Phone: ++49 7071 2976669; fax: ++49 7071 295135; email: claus.schwechheimer@zmbp.uni-tuebingen.de.

¹ Research on the LucTrap vectors is funded by the Deutsche Forschungsgemeinschaft (SCHW751/4-1 and SCHW751/4-2 as part of the Arabidopsis Functional Genomics Network (AFGN) Schwerpunktprogramm.

² Corresponding author: Claus Schwechheimer,

claus.schwechheimer@zmbp.uni-tuebingen.de; fax: ++49 (0)7071 295135.

Abstract

Proper plant growth and development strongly relies on the ability of plants to respond to signals and cues from their extra- and intracellular environment in a highly dynamic manner. It is a commonly accepted fact that most of these responses require specific changes at the level of gene expression. It is however becoming increasingly clear that, at least in plants, many response pathways are also controlled by the proteolysis of regulatory proteins via the ubiquitin-proteasome system. It is a major challenge for signal transduction research to understand how specific and dynamic outputs are generated through the integration of distinct signalling inputs. This understanding cannot be obtained without tools that allow to visualize the dynamics of transcript and protein changes *in vivo*. In this article, we describe the LucTrap plant transformation vectors that allow to generate transcriptional and translational fusions with the fire fly luciferase reporter. We demonstrate that these vectors can be used (i) to monitor gene expression *in vivo*, (ii) to generate gene traps, (iii) to monitor protein degradation and (iv) to monitor the role of protein degradation in transcriptional regulation *in vivo* in a highly dynamic manner. We therefore propose that the LucTrap vectors are versatile tools to examine gene expression and protein dynamics *in vivo*.

INTRODUCTION

Plants are sessile organisms that need to respond to signals and cues from their intra- and extracellular environment in a highly dynamic manner. It is a widely accepted fact that these responses typically require the transcription of specific sets of response genes (Schwechheimer and Bevan, 1998; Schmid et al., 2005). At the level of the individual gene, the spatial and temporal control of gene expression is mediated by promoters and enhancers that serve to integrate multiple positive and negative inputs to produce the correct gene expression output. To understand the full complexity of transcriptional regulation is a major challenge for plant biology.

In recent years, the understanding of transcriptional regulation has been greatly advanced by the extensive analysis of data from microarrays and GeneChip studies that allow to examine the expression of thousands of genes in parallel (Hennig et al., 2003; Zhu, 2003; Schmid et al., 2005). Especially in *Arabidopsis thaliana*, these approaches have lead to the compilation of large data sets, and in combination these are now of great value to get a glimpse of the tissue-specific and developmental expression control of individual genes (Schmid et al., 2005; Zimmermann et al., 2005). Nevertheless, the comparatively high cost of microarray and GeneChip experiments adds restrictions to the number of experimental conditions that can be tested in such studies. Therefore, these techniques cannot be extensively used to understand the expression of a single gene of interest, its transcriptional regulation over time and its responses to complex signalling events. In these cases, transgenic plants expressing transcriptional or translational fusions between the promoter of the gene of interest and the reporter proteins β -glucuronidase (GUS), green fluorescent protein (GFP) and its derivatives, or luciferase (LUC) represent a more suitable option (for a review see e.g. (de Ruijter et al., 2003)). The goal of the specific experiment generally determines, which of these three reporters will be chosen. Rather

than discussing the advantages and disadvantages of the individual reporters, we would like to emphasize here that LUC has at least two specific advantages that render this protein an excellent reporter to determine gene expression dynamics over time: (i) luciferase activity can be measured and quantified *in planta* in non-destructive assays, and (ii) luciferase enzyme activity is consumed after the luciferase reaction and therefore only reveals *de novo* synthesized protein rather than protein that has accumulated over time (de Ruijter et al., 2003).

While in many cases it is already known how specific transcriptional regulators and gene expression cascades are activated or repressed, it is largely unknown how this activation or repression is consequently turned off. In recent years, it has become increasingly clear that many transcriptional regulators are controlled by degradation via the ubiquitin-proteasome system (Schwechheimer and Calderon-Villalobos, 2004). This is best illustrated using the well understood auxin response pathway. Genetic and biochemical studies from *Arabidopsis* have identified the AUXIN/INDOLE ACETIC ACID (AUX/IAA) proteins as transcriptional repressors that repress gene expression in the absence of auxin (Gray et al., 2001; Tiwari et al., 2001). In response to auxin, these AUX/IAA repressors are degraded and their proteolysis frees the activity of the AUXIN RESPONSE FACTOR (ARF) proteins that function as activators of auxin-induced gene expression (Dharmasiri et al., 2005; Kepinski and Leyser, 2005). It is thought that auxin-induced gene expression is consequently turned off by *de novo* synthesized AUX/IAAs since their expression is also under the control of the AUX/IAA and ARF proteins (Abel et al., 1994; Abel et al., 1995; Tian and Reed, 1999). Through this negative feedback mechanism, auxin-induced gene expression seems to keep itself in check. While auxin-induced gene expression is currently the best understood proteolysis-dependent gene expression system, it can be expected that also other pathways such as the signalling events that are controlled by the unstable regulator of the gibberellic acid

signalling pathway REPRESSOR-OF-GA1-3 (RGA) are regulated in a similar manner (Dill et al., 2004; Fu et al., 2004).

The detection of changes in protein abundance, e.g. as a result of protein degradation by the ubiquitin-proteasome pathway, demands sensitive ways for the detection of these unstable proteins *in planta*. Since these proteins are - almost by definition - not abundant, translational reporter protein fusions are most appropriate to visualize these proteins. In the case of the AUX/IAAs, protein fusions to GUS and LUC have been used so far to detect and study the degradation of these proteins *in planta* (Worley et al., 2000; Gray et al., 2001; Ramos et al., 2001; Schwechheimer et al., 2001; Zenser et al., 2001; Zenser et al., 2003). Due to the fact that the LUC reporter has a comparatively short half-life, LUC turned out to be the best reporter to determine AUX/IAA degradation in response to auxin in a highly dynamic and authentic manner. Therefore, it can be proposed that LUC should be the reporter of choice for translational fusions that aim at the detection of protein abundance and degradation.

Promoter, enhancer, or gene traps are genomic approaches to generate and screen for untargeted reporter gene fusions (Evans et al., 1997; Durick et al., 1999; Springer, 2000). Promoter, enhancer, or gene traps are designed in a way that the insertion of a promoterless reporter gene in a gene (gene trap) or in the proximity of a promoter or enhancer element (promoter or enhancer trap) will lead to the detectable expression of the reporter either as a result of a transcriptional (enhancer or promoter trap) or of a translational fusion (gene trap). In Arabidopsis, such unbiased trapping approaches have been successfully used for the discovery of genes and reporter lines that show expression in specific tissues, in specific developmental stages or in response to specific signals, as well as for the discovery of proteins that localize to specific subcellular structures (Kertbundit et al., 1991; Sundaresan et al., 1995; Campisi et al., 1999; Parinov et al., 1999; Geisler et al., 2002; Birnbaum et al., 2003; Tian et al., 2004; Nakayama et al., 2005). When comparing all these different

approaches, gene and promoter traps using the LUC reporter turned out to be best suited for the identification and characterization of genes and reporter lines that are responsive to stress, light, and circadian rhythms (Yamamoto et al., 2003; Alvarado et al., 2004).

In this paper, we report on the LucTrap vector series and describe their use for the analysis of transcriptional responses and protein dynamics. The LucTrap and LucTrap-3(GW) vectors are designed for the convenient cloning of transcriptional and translational LUC fusions. Using selected examples, we demonstrate that these vectors serve to monitor and quantify gene and protein expression in a dynamic manner *in planta*. We also describe and characterize a small collection of gene trap lines that we generated using LucTrap-2. Finally, we demonstrate that these lines can serve to uncover novel regulatory mechanisms that are dependent on ubiquitin-proteasome mediated protein degradation.

RESULTS

The LucTrap vector for *in vivo* gene expression analyses: In order to obtain a luciferase reporter vector suitable for transcriptional and translational fusions, we generated the plant transformation vector LucTrap (Fig. 1A). LucTrap is derived from the previously published plant transformation vector pGREEN0029-II, and it contains the modified fire fly *LUCIFERASE* (*LUC+*) gene flanked by a multiple cloning site (MCS) with six unique restriction sites and the 35S cauliflower mosaic virus (CaMV) terminator (Hellens et al., 1999). Since the *Nco*I restriction site of the LucTrap MCS overlaps with the ATG start codon of *LUC+*, the *Nco*I site can be conveniently used to generate transcriptional and translational luciferase fusions.

In order to assess the performance of LucTrap as a vector to report gene expression, we inserted a *GH3-2* (At4g37390) gene fragment into LucTrap that corresponds to the 800 base pairs upstream of the *GH3-2* start codon (Fig. 1B). We subsequently generated transgenic *Arabidopsis thaliana*

lines harboring the resulting GH3-2:LucTrap construct. Since *GH3-2* expression has previously been shown to be induced by auxin, we tested auxin-induced luciferase expression in 5 day-old light-grown seedlings of these transgenic lines (Tian et al., 2003). As expected, increased luciferase activity was detected as early as 50 min following induction with the synthetic auxin 2,4-dichlorophenoxyacetic acid (2,4D) in 18 out of 20 lines tested, while no significant luciferase activity was detected in the absence of auxin (Fig. 1C). To confirm that *GH3-2* gene expression mirrors the expression of the endogenous *GH3-2* gene, we analysed *GH3-2* mRNA accumulation by semi-quantitative reverse transcription followed by polymerase chain reaction (RT-PCR; Figs. 1D and 1E). In this experiment, we found a strong correlation between *GH3-2* induction as reported by luciferase activity measurements and the transcription of the *GH3-2* gene *in vivo* (Fig. 1C – E). The comparatively earlier onset of *GH3-2* transcript accumulation in these experiments may be attributed to the time required for the translation of the LUC+ reporter. In summary, we suggest that transcriptional fusions using the LucTrap vector can be used to monitor gene expression *in vivo* in a dynamic and authentic manner.

The LucTrap-1 and LucTrap-2 vectors for promoter and gene trapping:

Random insertions of the luciferase reporter as a promoter or gene trap may allow to follow the expression of a trapped promoter or gene over time or to identify genes that are expressed in response to a specific stimulus. We generated LucTrap-1 as a vector for promoter and gene trapping in plants. LucTrap-1 contains a modified intron of the *Arabidopsis thaliana* *G PROTEIN* α subunit gene ($G\alpha$; At2g26300) that was inserted between the T-DNA right border and the *LUC+* open reading frame (Fig. 2A). In the context of a similar arrangement, this $G\alpha$ intron had previously been used successfully for promoter and gene trapping in *Arabidopsis* with the *GUS* reporter (Sundaresan et al., 1995). The rationale of LucTrap-1 is such that in the case of a successful promoter trap, the insertion of the the LucTrap-1 T-DNA will

result in *LUC+* expression under the spatial and temporal control of the trapped promoter (Fig. 2C).

LucTrap-1 also serves as a gene trap since the $G\alpha$ intron contains one splice donor site (D) located directly adjacent to the T-DNA right border as well as three splice acceptor sites (A1, A2, A3) located upstream of the *LUC+* gene (Fig. 2A). The acceptor sites are spaced in the three forward reading frames and this spacing should result in the formation of alternatively spliced transcripts either between a splice donor site of the trapped gene and the LucTrap-1 acceptors A1, A2, and A3, or the formation of alternatively spliced transcripts between the LucTrap-1 donor site and its acceptors. Taken together, this arrangement should guarantee the formation of alternatively spliced variants, one of which is expected to be in frame with *LUC+* to give rise to productive *LUC+* fusions (Fig. 2C).

Since the *LUC+* gene in LucTrap-1 still contains the *LUC+* gene's ATG start codon, luciferase activity detected in LucTrap-1 gene trap lines may not necessarily originate from a fusion between the trapped gene and luciferase, but may be solely the result of *LUC+* expression controlled by the trapped gene's promoter. We therefore generated LucTrap-2 that lacks the *LUC+* ATG start codon and reasoned that such a vector should only express *LUC+* when the trapped gene provides the ATG start codon, thereby assuring the formation of translational fusions between the trapped gene and *LUC+*.

Characterization of a gene trap collection: To test the performance of LucTrap-2 as a gene trap vector, we generated and analysed a collection of 700 transgenic Arabidopsis lines carrying LucTrap-2. The segregation of the Kanamycin resistance trait in the T2 progeny of these lines indicated that the vast majority of lines has single locus insertions. We then tested 5 day-old light grown progeny seedlings for *LUC+* expression. In this analysis, we found 90 lines (12.8%) to express *LUC+* at levels that are at least two-fold above the levels detected in non-transgenic control plants (Fig. 3A). This group included 46 lines (6.6%) lines that expressed *LUC+* at levels at least

10 times that detected in non-transgenic seedlings (Fig. 3A and 3B). This shows that the *LUC+* gene of LucTrap-2 is functional in Arabidopsis in the context of genomic insertions.

We then adopted previously established strategies for the amplification of LucTrap-2 flanking sequence tags (FSTs) (Devon et al., 1995; Strizhov et al., 2003). A complete list of primers that can be used for LucTrap-2 (FST) amplification is provided in Table I. Since the *LUC+* gene is located adjacent to the T-DNA right border, we used preferentially the LucR3 primer for amplification of sequences that may be fused to the *LUC+* gene. Since our main interest was to identify FSTs from *LUC+* expressing lines, the sample provided here is not representative for the entire LucTrap-2 collection but has a bias towards the luciferase expressors.

A total of 49 LucTrap-2 FSTs were identified (Table II). FSTs were analysed using BLASTN searches and, based on T-DNA insertion position and orientation, 27 lines are predicted to give rise to productive fusions between the trapped gene and *LUC+* (Table IIA). The remaining 22 lines are predicted to produce non-productive fusions (Table IIB). The lines predicted to produce *LUC+* fusions include 12 lines that also express luciferase, suggesting that the trapped genes are expressed during the seedling stage. In the remaining cases, we assume that the trapped gene is not expressed during the seedling stage, that the luciferase expression levels are too low to be detected in our experiments, or that the fusion protein or mRNA is unstable.

Interestingly, we also identified luciferase expressing lines with non-productive insertions. This may indicate that the expression of *LUC+* can also be driven from cryptic promoters and cryptic open reading frames, or, alternatively, that our FST analysis did not identify the correct gene. Since the latter explanation implies that multiple T-DNA insertions are present in the genome of a specific line and since our genetic analysis had shown that these events are rare in the LucTrap-2 collection, we tend to exclude this explanation. An additional alternative explanation may be that a second

LucTrap-2 T-DNA is inserted in the specific locus with its right border located to give rise to productive fusions. Such more complex T-DNA insertion events are frequently found in populations of T-DNA tagged lines (De Neve et al., 1997; Forsbach et al., 2003; Lechtenberg et al., 2003; Windels et al., 2003). In summary, we suggest that LucTrap-2 can be used as a gene trap vector and that our method for the identification of FSTs can be successfully employed for the identification of tagged genes.

The LucTrap-3(GW) vector for Gateway™-compatible luciferase fusions: To generate a vector that is compatible with the Gateway™ cloning technology, we inserted the Gateway cassette (rfB) upstream of the *LUC+* open reading frame of LucTrap and obtained LucTrap-3(GW). This vector is compatible with the Gateway™ cloning system and can be used to generate transcriptional and translational fusions (Fig. 4). We tested LucTrap-3(GW) with five different Gateway™ system compatible entry clones and achieved full cloning efficiency in all cases, suggesting that LucTrap-3(GW) is a fully functional Gateway™ vector.

We examined in more detail transgenic Arabidopsis lines that carry the construct RGA:RGA:LUC. REPRESSOR-OF-GA1-3 (RGA) is a predominantly nuclear localized downstream regulator of the gibberellic acid (GA) signalling pathway that is degraded in response to GA (Silverstone et al., 2001). RGA degradation is mediated by the 26S proteasome and requires the activity of the E3 ubiquitin ligase SCF^{SLY1} (Dill et al., 2004). RGA:RGA:LUC expresses a fusion protein between Arabidopsis RGA and LUC+ under control of a 2 kb RGA promoter fragment. RGA:RGA:LUC lines show a moderate expression of the fusion protein in light-grown seedlings (Figure 5A). Application of the GA biosynthesis inhibitor Paclobutrazol (PAC), however, resulted in the stabilization of the fusion protein as indicated by increased luciferase activity, an effect that we attribute to a reduction of endogenous GA levels. In turn this reduction in endogenous GA levels was overcome by the concomitant application of exogenous GA that resulted in

the degradation of the protein in response to the exogenously applied GA. The fact that the RGA:LUC protein was also stabilized after application of the 26S proteasome inhibitor MG132 confirms the notion that RGA:LUC degradation is 26S proteasome dependent (Figure 5A).

So far, RGA protein abundance has almost exclusively been studied using transgenic lines that express a fusion protein between RGA and the reporter green fluorescent protein (GFP) under control of a *RGA* promoter fragment from a construct designated RGA:GFP:RGA (Silverstone et al., 2001). As a control experiment, we therefore subjected transgenic seedlings GFP:RGA to the same treatments that had been applied to the RGA:RGA:LUC lines. In these lines, we found the GFP:RGA fusion protein to respond to the different treatments in a similar manner as observed with the RGA:LUC fusion, thus stabilization by PAC or MG132 treatments and destabilization by GA treatment (Figure 5B). In summary, we therefore propose that the LucTrap-3(GW) vector can be used to generate LUC+ fusion proteins and to examine protein abundance and dynamics as exemplified here using the unstable repressor protein RGA.

Unstable negative and positive regulators control auxin-induced gene expression: During our analysis of the LucTrap-2 gene trap collection, we also examined the effect of the synthetic auxin 2,4D on luciferase gene expression. We identified three LucTrap-2 lines, namely LT028, LT032, and LT095, that showed increased luciferase expression in response to 2,4D and other auxins. Since it is known that auxin induced gene expression requires the proteasomal degradation of the unstable AUX/IAA transcriptional repressors, we went on to study the effects of the proteasome inhibitor MG132 in these lines as well as in the GH3-2:LucTrap lines that were introduced above (Fig. 1B and 1C). Consistent with the role of unstable repressors acting in auxin-induced gene expression, we found that auxin induction was severely impaired when MG132 was applied together with auxin in the case of GH3-2:LucTrap, LT028, and LT095 (Fig. 6A - 6C).

Therefore, these findings are in agreement with the current model of auxin-induced gene expression.

In contrast, our studies of LT032 indicate that auxin-induced gene expression may also be governed by another mechanism (Fig. 6D). While MG132 treatments alone did not have an effect on luciferase expression in GH3-2:LucTrap, LT028, and LT095, we found that MG132 treatments were sufficient to induce gene expression in line LT032 (Fig. 6A - 6D). Furthermore, auxin-induced gene expression in this line was enhanced rather than reduced by the concomitant application of MG132 (Fig. 6D). This result cannot be explained by the activity of repressors but it rather suggests that an unstable transcriptional activator regulates the expression of the gene trapped in LT032. Such an unstable activator could be stabilized by auxin and by inhibition of proteasomal activity. Concomitant application of both stabilizing agents may therefore result in the superinduction observed in our experiments.

In all cases examined, auxin-induced reporter gene expression was followed by its downregulation (Fig. 6A – D). This negative feedback mechanism may be explained by the well established fact that the genes encoding the AUX/IAA repressors are themselves induced by auxin (Abel et al., 1994; Abel et al., 1995; Tian and Reed, 1999). In this way, *de novo* synthesized AUX/IAA repressors mediate the negative feedback after auxin induction. Interestingly, also the auxin induced gene expression observed in line LT032, which we propose to be under the control of an unstable activator, is subject to negative feedback regulation. Therefore, also this gene expression mechanism may be negatively controlled by AUX/IAAs or other repressors, or alternatively it may be that the expression of the putative and as yet unidentified activator is downregulated in response to auxin. Regardless of the underlying molecular mechanism, one major apparent strength of the luciferase-based reporter system lies in the fact that, unlike other reporter systems, it is able to visualize this feedback regulation in a highly dynamic manner.

DISCUSSION

Dynamic detection of transcript and protein abundance using the LucTrap vectors: In this paper, we introduce the LucTrap vectors that make use of fire fly luciferase (LUC) as a reporter for the detection of transcriptional activities and fusion protein abundance. Using transgenic Arabidopsis lines that express a promoter fragment of the auxin-inducible *GH3-2* gene, we demonstrate that these vectors, and here specifically LucTrap, are well suited to follow gene expression patterns in a highly dynamic manner (Fig. 1). Using transgenic plants that express translational fusions between LUC and the gibberellic acid (GA) pathway regulator RGA from the Gateway™ vector LucTrap-3(GW), we show that the fusion protein responds to intracellular GA levels in the same way as previously reported for a similar fusion protein between RGA and GFP (Figure 5) (Dill et al., 2001).

Furthermore, the analysis of a collection of 700 transgenic Arabidopsis lines harboring the vector LucTrap-2 revealed that random LUC fusions may be generated using an unbiased gene trapping approach (Fig. 2 and 3). In 27 cases, we were able to provide evidence for LucTrap-2 insertions that would be predicted to give rise to productive LUC fusions as judged by the T-DNA insertion position and orientation (Table IIA). This prediction is confirmed by the fact that we were able to detect significant luciferase activity in 12 of these lines. Luciferase activity measurements in another 10 lines where no functional LUC fusions are predicted, may be explained by complex T-DNA insertions with more than one T-DNA present at the insertion locus (Table IIB) (Forsbach et al., 2003; Lechtenberg et al., 2003). Taken together we propose that the LucTrap vectors are versatile vectors that can be used to monitor gene expression dynamics as well as protein abundance and degradation in a highly sensitive manner *in vivo*.

Protein degradation as a regulatory mechanism: In plants, the degradation of regulatory proteins is seemingly a predominant mechanism for the control of growth and development (Schwechheimer and Calderon-Villalobos, 2004). The transcriptional regulation in response to auxin is one of the best understood plant signalling processes, and auxin response has been shown to be strictly dependent on the degradation of the AUX/IAA transcriptional repressors (Gray et al., 2001; Dharmasiri et al., 2005). Through the application of the 26S proteasome inhibitor MG132, we demonstrate that auxin-inducible gene expression in GH3-2:LucTrap as well as two LucTrap-2 gene trap lines is protein degradation dependent (Fig. 6A – 6C). Based on the current model for auxin-inducible gene expression, we would postulate that the stabilization of AUX/IAAs in response to MG132 treatment is responsible for this impaired induction (Worley et al., 2000; Ramos et al., 2001; Kepinski and Leyser, 2005). In fact, in the case of GH3-2 this is supported by the observation that its expression is negatively regulated in the *Arabidopsis shy2* mutant, which expresses a stabilized form of the AUX/IAA protein IAA7, as well as in mutants of the COP9 signalosome, a protein complex required for proper AUX/IAA degradation (Schwechheimer et al., 2001; Tian et al., 2003; Dohmann et al., 2005).

Interestingly, we discovered also one LucTrap-2 line, LT032, where the inhibition of proteasomal activity resulted in a superinduction of auxin-induced gene expression (Fig. 6D). Furthermore, the inhibition of proteasomal activity was sufficient to induce gene expression in the absence of auxin. The relative speed of induction and the overlap of their induction kinetics suggest that the induction is direct and that auxin-induction and proteolysis are coupled mechanisms. Such induction kinetics cannot be explained through the activity of an unstable repressor but may best be explained through the activity of an unstable activator. As far as we are aware, such a regulatory mechanism has not been described as yet for auxin-induced gene expression and LT032 may therefore represent a good

starting point for the isolation of factors that are involved in this novel type of regulation.

Conclusion: In summary, we have provided evidence that transcriptional and translational LUC fusions expressed from the LucTrap plant transformation vectors can be used to monitor gene expression and protein abundance *in vivo* in a highly dynamic manner. The fact that the Arabidopsis genome encodes for hundreds of proteins with clear homology to known components of the ubiquitin-proteasome pathway suggests that future research will identify many as yet unknown proteolysis-dependent pathways (Bachmair et al., 2001; Gagne et al., 2002). In order to understand signalling events at their highest complexity, the analysis of the respective degradation targets will require sensitive tools to study these degradation events and protein abundance *in vivo*. We propose that the LucTrap vectors will be an essential part of this tool kit.

MATERIALS AND METHODS

Biological material: *Arabidopsis thaliana* ecotype Columbia was used for all plant transformations described in this study. Arabidopsis transformation was performed using the floral dip method (Desfeux et al., 2000).

LucTrap vector cloning: To generate LucTrap-1, the intron sequence of the *G-PROTEIN* α subunit gene (*G α* , At2g26300) was PCR amplified from the previously published CD126 vector using the primers INTRON-FW 5'-AGATCTAGGCCTGTCTCGAAATCGGACGG-3' and INTRON-RV 5'-CCATGGACCTGCATATAACCTG-3' (Sundaresan et al., 1995). The intron fragment was cloned into pGEM-T (Promega, Madison, Wisconsin), sequence verified, and inserted as *Bgl*III/*Nco*I fragment upstream of the *LUC+* gene in pSP-LUC+ (Promega, Madison, Wisconsin). Subsequently, the 35S cauliflower mosaic virus (CaMV) terminator sequence was obtained by

PCR from the vector pCAMBIA-1391Z with the primers CaMV TER FW 5'-GAATTCCAGATAA GGAATTAG-3' and CaMV TER RV 5'-CCATGGCAACCACTTTGTACAAGA-3', cloned into pGEM-T (Promega, Madison, Wisconsin), sequence verified and subcloned as *Xba*1/*Eco*R1 fragment into the G α intron-containing pSP-LUC+. The resulting *LUC*+ gene cassette was then inserted as a *Stu*1/*Eco*R1 fragment adjacent to the T-DNA right border of previously published plant transformation vector pGREEN0029 (Hellens et al., 1999). The resulting vector was designated LucTrap-1 (GenBank accession AY944581).

LucTrap-2 (GenBank accession AY944582) is derived from LucTrap-1 and was obtained by religation of the *Nco*1 and subsequently S1 nuclease digested LucTrap-1 vector. The identity of the desired LucTrap-2 vector with a four base pair deletion including the ATG start codon of *LUC*+ was confirmed by DNA sequencing.

LucTrap (GenBank accession DQ073044) is derived from LucTrap-1 and was obtained by insertion of the phosphorylated and annealed oligonucleotides LucTrap-MCS-FW 5'-CCTGGATCCTGCAGAGCTCACTAGTC-3' and LucTrap-MCS-RV 5'-CATGGACTAGTGAGCTCTGCAGGATCCAGG-3' into the *Stu*1/*Nco*1 digested LucTrap-1 vector.

LucTrap-3(GW) (GenBank accession AY968054) was obtained by insertion of the *rfB* Gateway™ selection cassette (Invitrogen, Carlsbad, CA) into LucTrap-1. To this end, the Gateway™ *rfB* cassette was PCR-amplified using the primers attR1-*Stu*1 5'-AGGCCTATCAACAAGTTTGTACAAAAAAG-3' and attR2-*Nco*1 5'-CCATGGCAA CCACTTTGTACAAGA-3', cloned into pCR-TOPO (Invitrogen, Karlsruhe, Germany), sequence verified, and subsequently subcloned as a *Stu*1/*Nco*1 fragment into LucTrap-1. LucTrap-3(GW) confers resistance to Kanamycin in *Escherichia coli*, and therefore LucTrap-3(GW) works best in combination with the Gentamycin-resistant donor vector pDONR207 (Invitrogen, Carlsbad, CA).

Since all LucTrap vectors are based on the previously published pGreen0029-II vector, agrobacterium and plant transformation require the presence of the helper plasmid pSOUP (Hellens et al., 1999).

LucTrap-derived constructs: To generate GH3-2:LucTrap, an 800 base pair *GH3-2* (At4g37390) fragment was PCR-amplified from *Arabidopsis thaliana* genomic DNA using the primers GH3-1 5'-CCATGGTTGTTTTTTTTCTAAAAGAAAAAGTG-3' and GH3-2 5'-AGATCTGTCGACATGCTATAGATTGATATAAGAAAAAAG-3'. The resulting PCR fragment was cloned into pGEM-T (Promega, Madison, WI), sequence verified, and subcloned as a *Nco* I/*Stu* I fragment into LucTrap-1. 20 independent transgenic lines that harbor GH3-2:LucTrap were generated and analysed.

For RGA:RGA:LUC, a 3600 base pair genomic fragment that comprises the *RGA* (At2g01570) open reading frame and a 2000 base pair promoter fragment was amplified from genomic DNA of *Arabidopsis thaliana* ecotype Columbia with the primers RGA-FW 5'-AGGCCTTTTATGTTTTTCGATGGCTGAGCTTC-3' and RGA-RV 5'-CCATGGGCGCCGCGTCGAGAGTTTCCAAGCGGA-3'. The resulting fragment was inserted into pENTR/D-TOPO (Invitrogen), sequence verified and from there transferred into LucTrap-3(GW). 10 transgenic lines that harbor RGA:RGA:LUC were generated and analysed.

Luciferase activity measurements: Luciferase activity was measured using 5 day-old seedlings that had been grown in continuous light on moist filter paper in 96 well microtiter plates (Thermo LabSystems, Vantaa, Finland). Seedlings were assayed in a Berthold Mithras LB940 luminometer in the presence of 80 μ l MS medium (Duchefa, Haarlem, The Netherlands) supplemented with 5 mM D-luciferin (PJK, Kleinblittersdorf, Germany) and plant hormones (Duchefa) or inhibitors (paclobutrazol, Duchefa; MG132, Sigma) as indicated.

Fluorescence microscopy: Transgenic seedlings expressing RGA:GFP:RGA were treated for 12 hours with gibberellic acid 3, paclobutrazol (Duchefa) and MG132 (Sigma) as indicated and then imaged with constant settings using a Leica TCS SP2 confocal microscope.

Identification of LucTrap-2 flanking sequences: For the determination of flanking sequences from LucTrap-2 transgenic lines, procedures were adapted from (Devon et al., 1995; Strizhov et al., 2003). In brief, genomic DNA was digested using the restriction enzymes *Bam*HI, *Bgl*II, or *Bcl*I. Subsequently, an asymmetrical adaptor, obtained by annealing the TopL and phosphorylated BamHI primers, was ligated to the digested genomic DNA (Devon et al., 1995). LucTrap-2 specific fragments were amplified in two or three PCR rounds with the nested vectorette primers VEC1 and VEC2 in combination with LucTrap-2 specific primers. Amplification products were sequenced using LucR3 or LucL3. Sequence reads were analysed using the BLASTN algorithm at <http://www.arabidopsis.org/blast>. All primer sequences are provided in Table I.

RT-PCR Analysis: Auxin-induced *GH3-2* (At4g37390) gene expression was examined by semi-quantitative reverse transcription and polymerase chain reaction (RT-PCR). Total RNA was prepared using the RNeasy Kit (Qiagen, Hilden, Germany) from 5 day-old seedlings that had been treated with 5 μ M 2,4D. 1 μ g total RNA was used in combination with the oligo-dT adaptor primer 5'-GACTCGAGTCGACATCGA(17xT)-3' for reverse transcription as previously described and *GH3-2* transcription was examined by PCR (28 cycles) using the *GH3-2* gene specific primers GH3-2FW 5'-GTTTCAGCGACGACTTCTGAGAAAGATGT-3' and GH3-2RV 5'-TCTTCGCTCATAAGAGCATTGCT-3' (Frohman et al., 1988). RT-PCR results were quantified using ImageJ software.

ACKNOWLEDGMENTS: The authors wish to thank Esther M.N. Dohmann and Dr. Melina Zourelidou for comments on the manuscript. Wolfdieter Braun is thanked for his contributions during the initial stages of this project. We thank Tai-ping Sun for providing the RGA:GFP:RGA lines and the Nottingham Arabidopsis Stock Centre for providing the CD126 gene trap construct.

LITERATURE CITED

- Abel S, Nguyen MD, Theologis A (1995) The PS-IAA4/5-like family of early auxin-inducible mRNAs in *Arabidopsis thaliana*. *J Mol Biol* 251: 533-549
- Abel S, Oeller PW, Theologis A (1994) Early auxin-induced genes encode short-lived nuclear proteins. *Proc Natl Acad Sci USA*. 91: 326-330
- Alvarado MC, Zsigmond LM, Kovacs I, Cseplo A, Koncz C, Szabados LM (2004) Gene trapping with firefly luciferase in *Arabidopsis*. Tagging of stress-responsive genes. *Plant Phys* 134: 18-27
- Bachmair A, Novatchkova M, Potuschak T, Eisenhaber F (2001) Ubiquitylation in plants: a post-genomic look at a post-translational modification. *Trends Plant Sci* 6: 463 - 470
- Birnbaum K, Shasha DE, Wang JY, Jung JW, Lambert GM, Galbraith DW, Benfey PN (2003) A gene expression map of the *Arabidopsis* root. *Science* 302: 1956-1960
- Campisi L, Yang Y, Yi Y, Heilig E, Herman B, Cassista AJ, Allen DW, Xiang H, Jack T (1999) Generation of enhancer trap lines in *Arabidopsis* and characterization of expression patterns in the inflorescence. *Plant J* 17: 699-707
- De Neve M, De Buck S, Jacobs A, Van Montagu M, Depicker A (1997) T-DNA integration patterns in co-transformed plant cells suggest that T-DNA repeats originate from co-integration of separate T-DNAs. *Plant J* 11: 15-29
- de Ruijter NCA, Verhees J, van Leeuwen W, van der Krol AR (2003) Evaluation and comparison of the GUS, LUC and GFP reporter system for gene expression studies in plants. *Plant Biol* 5: 103 - 115
- Desfeux C, Clough SJ, Bent AF (2000) Female reproductive tissues are the primary target of *Agrobacterium*-mediated transformation by the *Arabidopsis* floral dip method. *Plant Phys* 123: 895 - 904
- Devon RS, Porteous DJ, Brookes AJ (1995) Splinkerettes - improved vectorettes for greater efficiency in PCR walking. *Nucl Acids Res* 23: 1644 - 1645
- Dharmasiri N, Dharmasiri S, Estelle M (2005) The F-box protein TIR1 is an auxin receptor. *Nature* 435: 441-445
- Dill A, Jung H-S, Sun T-p (2001) The DELLA motif is essential for gibberellin-induced degradation of RGA. *Proc Natl Acad Sci USA* 98: 14162 - 14167

- Dill A, Thomas SG, Hu J, Steber CM, Sun T-p (2004) The Arabidopsis F-box protein SLEEPY1 targets gibberellin signaling repressors for gibberellin-induced degradation. *Plant Cell* 16: 1392 - 1405
- Dohmann EM, Kuhnle C, Schwechheimer C (2005) Loss of the CONSTITUTIVE PHOTOMORPHOGENIC9 signalosome subunit 5 is sufficient to cause the cop/det/fus mutant phenotype in Arabidopsis. *Plant Cell* 17: 1967-1978
- Durick K, Mendlein J, Xanthopoulos KG (1999) Hunting with traps: genome-wide strategies for gene discovery and functional analysis. *Genome Res* 9: 1019-1025
- Evans MJ, Carlton MB, Russ AP (1997) Gene trapping and functional genomics. *Trends Genet* 13: 370-374
- Forsbach A, Schubert D, Lechtenberg B, Gils M, Schmidt R (2003) A comprehensive characterization of single-copy T-DNA insertions in the Arabidopsis thaliana genome. *Plant Mol Biol* 52: 161-176
- Frohman MA, Dush MK, Martin GR (1988) Rapid production of full-length cDNAs from rare transcripts: amplification using a single gene-specific oligonucleotide primer. *Proc Natl Acad Sci USA* 85: 8998-9002
- Fu X, Richards DE, Fleck B, Xie D, Burton N, Harberd NP (2004) The Arabidopsis mutant sleepy1^{gar2-1} protein promotes plant growth by increasing the affinity of the SCF^{SLY1} E3 ubiquitin ligase for DELLA protein substrates. *Plant Cell* 16: 1406 - 1418
- Gagne JM, Downes BP, Shiu SH, Durski AM, Vierstra RD (2002) The F-box subunit of the SCF E3 complex is encoded by a diverse superfamily of genes in Arabidopsis. *Proc Natl Acad Sci USA* 99: 11519 - 11524
- Geisler M, Jablonska B, Springer PS (2002) Enhancer Trap Expression Patterns Provide a Novel Teaching Resource. *Plant Phys* 130: 1747 - 1753
- Gray WM, Kepinski S, Rouse D, Leyser O, Estelle M (2001) Auxin regulates SCF^{TIR1}-dependent degradation of AUX/IAA proteins. *Nature* 414: 271 - 276
- Hellens R, Joyce N, Mullineaux P (1999) A new and versatile Agrobacterium-based plant transformation vector. *In A Altman, M Ziv, S Izhar, eds, Plant Biotechnology and In Vitro Biology in the 21st Century. Kluwer Academic Press, Dordrechts, Netherlands., pp 155-158*
- Hennig L, Menges M, Murray JA, Grissem W (2003) Arabidopsis transcript profiling on Affymetrix GeneChip arrays. *Plant Mol Biol* 53: 457-465
- Kepinski S, Leyser O (2005) The Arabidopsis F-box protein TIR1 is an auxin receptor. *Nature* 435: 446-451
- Kertbundit S, De Greve H, Deboeck F, Van Montagu M, Hernalsteens JP (1991) In vivo random beta-glucuronidase gene fusions in Arabidopsis thaliana. *Proc Natl Acad Sci USA* 88: 5212-5216
- Lechtenberg B, Schubert D, Forsbach A, Gils M, Schmidt R (2003) Neither inverted repeat T-DNA configurations nor arrangements of tandemly repeated transgenes are sufficient to trigger transgene silencing. *Plant J* 34: 507-517

- Nakayama N, Arroyo JM, Simorowski J, May B, Martienssen R, Irish VF (2005) Gene trap lines define domains of gene regulation in Arabidopsis petals and stamens. *Plant Cell* 17: 2486-2506
- Parinov S, Sevugan M, Ye D, Yang W-C, Kumaran M, Sundaresan V (1999) Analysis of flanking sequences from Dissocation insertion lines: A database for reverse genetics in Arabidopsis. *Plant Cell* 11: 2263 - 2270
- Ramos JA, Zenser N, Leyser O, Callis J (2001) Rapid degradation of auxin/indoleacetic acid proteins requires conserved amino acids of domain II and is proteasome dependent. *Plant Cell* 13: 2349-2360.
- Schmid M, Davison TS, Henz SR, Pape UJ, Demar M, Vingron M, Scholkopf B, Weigel D, Lohmann JU (2005) A gene expression map of Arabidopsis thaliana development. *Nature Genet* 37: 501 - 506
- Schwechheimer C, Bevan M (1998) Transcriptional regulation of plant gene expression. *Trends Plant Sci* 3: 378-383
- Schwechheimer C, Calderon-Villalobos LI (2004) Cullin-containing E3 ubiquitin ligases in plant development. *Curr Opin Plant Biol* 7: 677-686
- Schwechheimer C, Serino G, Callis J, Crosby WL, Lyapina S, Deshaies RJ, Gray WM, Estelle M, Deng X-W (2001) Interactions of the COP9 signalosome with the E3 ubiquitin ligase SCF^{TIR1} in mediating auxin response. *Science* 292: 1379 - 1382
- Silverstone AL, Jung H-S, Dill A, Kawaide H, Kamiya Y, Sun T-p (2001) Repressing a repressor: gibberellin-induced rapid reduction of the RGA protein in Arabidopsis. *Plant Cell* 13: 1555 - 1565
- Springer PS (2000) Gene traps: Tools for Plant Development and Genomics. *Plant Cell* 12: 1007 - 1020
- Strizhov N, Li Y-F, Rosso MG, Viehoveer P, Dekker KA, Weisshaar B (2003) High-throughput generation of sequence indexes from T-DNA mutagenized Arabidopsis thaliana lines. *BioTechniques* 35: 1164 - 1168
- Sundaresan V, Springer P, Volpe T, Haward S, Jones JDG, Dean C, Ma H, Martienssen R (1995) Patterns of gene action in plant development by enhancer trap and gene trap transposable elements. *Genes & Dev.* 8: 1787 - 1810
- Tian G-W, Mohanty A, Chary SN, Li S, Pappa B, Drakakaki G, Kopec CD, Li J, Ehrhardt DW, Jackson D, Rhee SY, Raikhel NV, Citovsky V (2004) High-throughput fluorescent tagging of full-length Arabidopsis gene products in planta. *Plant Phys.* 135: 25 - 38
- Tian Q, Nagpal P, Reed JW (2003) Regulation of Arabidopsis SHY2/IAA3 protein turnover. *Plant J.* 36: 643 - 651
- Tian Q, Reed JW (1999) Control of auxin-regulated root development by the Arabidopsis thaliana SHY2/IAA3 gene. *Development* 126: 711-721
- Tiwari SB, Wang X-J, Hagen G, Guilfoyle TJ (2001) AUX/IAA proteins are active repressors, and their stability and activity are modulated by auxin. *Plant Cell* 13: 2809 - 2822
- Windels P, De Buck S, Van Bockstaele E, De Loose M, Depicker A (2003) T-DNA integration in Arabidopsis chromosomes. Presence and origin of filler DNA sequences. *Plant Physiol* 133: 2061-2068

- Worley CK, Zenser N, Ramos J, Rouse D, Leyser O, Theologis A, Callis J (2000) Degradation of Aux/IAA proteins is essential for normal auxin signalling. *Plant Journal* 21: 553-562
- Yamamoto YY, Tsuchida Y, Gohda K, Suzuki K, Matsui M (2003) Gene trapping of the Arabidopsis genome with a firefly luciferase reporter. *Plant J.* 35: 273 - 283
- Zenser N, Dreher KA, Edwards SR, Callis J (2003) Acceleration of Aux/IAA proteolysis is specific for auxin and independent of AXR1. *Plant J.* 35: 285 - 294
- Zenser N, Ellsmore A, Leasure C, Callis J (2001) Auxin modulates the degradation rate of Aux/IAA proteins. *Proc Natl Acad Sci U S A* 98: 11795-11800.
- Zhu T (2003) Global analysis of gene expression using GeneChip microarrays. *Curr Opin Plant Biol* 6: 418-425
- Zimmermann P, Hennig L, Grissem W (2005) Gene-expression analysis and network discovery using Genevestigator. *Trends Plant Sci* 10: 407-409

Table I. Primers for the amplification of LucTrap-2 T-DNA flanking sequences.

A. Vectorette primers

Name	Sequence
TopL	5'-CGAATCGTAACCGTTTCGTACGAGAATTCGTACGAGAATCGCT -GTCCTCTCCAACGAGCCAAGG-3'
BamHI	5'-GATCCCTTGGCTCGTTTTTTTTTGCAAAA-3'
VEC1	5'-CGAATCGTAACCGTTTCGTACGAGAA-3'
VEC2	5'-TCGTACGAGAATCGCTGTCCTCTCC-3'

B. LucTrap-2 Right border primers

Name	Sequence
LucR1	5'-CAATCAATTTTCCTTGTGGACTTGG-3'
LucR2	5'-GTTTTCATGTGTGATTTTACCGAAC-3'
LucR3	5'-GGTCCCAGTCCGATTTGACAGG-3'

C. LucTrap-2 Left border primers

Name	Sequence
LucL1	5'-CGATAGAAAACAAAATATAGCGCGC-3'
LucL2	5'-CTAGGATAAATTATCGCGCGCGG-3'
LucL3	5'-CTAGATCGACCGGCATGCAAGC-3'

Table II. Insertion sites identified in LucTrap-2 lines.

LucTrap-2 (LT) lines with flanking sequence tags (FSTs) identify genomic insertions. The E-values obtained in BLASTN searches using FST reads and primers used for FST identification are indicated. Productive luciferase fusions are expected in 27 lines (A), non-productive luciferase fusions are predicted in 22 lines (B). Relative light units (RLUs) and standard deviations as detected in 5 day-old seedlings are indicated; bg signifies background activity; $n \geq 4$.

A. LucTrap-2 lines expected to give rise to LUC+ fusions.

LT#	Locus	Position	E-value	Primer	Fusion
	RLUs				
LT001	At4g21750 (ML1-specific homeobox gene) 4368+/-1170	1st intron	3.00E-73	LUCR3	Yes
LT005	At5g40730 (Arabinogalactan-protein AGP24)	3' UTR	0	LUCR3	Yes bg
LT033	At5g45775 (60S ribosomal protein L11) 150+/-42	3rd intron	0	LUCR3	Yes
LT042	At3g08810 (F-box family protein)	3' UTR	1.00E-105	LUCR3	Yes bg
LT055	At4g32450 (Pentatricopeptide repeat-containing protein)	Unique exon	0	LUCR3	Yes bg
LT134	At3g23260 (F-box family protein)	Unique exon	1.00E-18	LUCR3	Yes bg
LT136	At2g44260 (Expressed protein)	2nd exon	8.00E-26	LUCR3	Yes bg
LT140	At1g77440 (20S proteasome beta subunit PBC2)	5th intron	3.00E-26	LUCR3	Yes bg
LT155	At5g57399 (UbiE/COq5 methyl transferase) 105+/-39	3rd exon	3.00E-15	LUCL3	Yes
LT171	At4g18570 (Proline-rich family protein) 221+/-70	1st intron	2.00E-68	LUCL3	Yes
LT174	At3g19510 (Homeobox protein HAT3.1)	6th intron	1.00E-102	LUCR3	Yes bg
LT179	At3g02820 (Zinc knuckle (CCHC-type) family protein)	4th exon	1.00E-139	LUCR3	Yes bg
LT184	At3g11580 (B3 domain transcription factor) 240+/-0	1st exon	1.00E-21	LUCR3	Yes
LT186	At1g05630 (At5PTase 13 inositol 5-phosphatase)	5th intron	3.00E-126	LUCR3	Yes bg
LT188	At1g65365 (Putative protein kinase, pseudogene)	Unique exon	0	LUCR3	Yes bg
LT189	At5g10520 (Protein kinase)	7th intron	2.00E-78	LUCR3	Yes bg
LT200	At5g67420 (LOB domain protein 37)	3rd exon	1.00E-48	LUCR3	Yes bg
LT206	At1g75840 (Rac-like GTP-binding protein ARAC5)	3'-UTR	4.00E-43	LUCR3	Yes bg
LT210	At1g73230 (NPAC BTF3 transcription factor)	3'-UTR	1.00E-109	LUCR3	Yes bg
LT301	At5g65110 (Acyl-CoA oxidase ACX2) 467+/-195	5' UTR	4.00E-32	LUCL3	Yes
LT316	At4g33620 (Ulp1 protease family SUMO protease)	17nd exon	1.00E-124	LUCR3	Yes bg
LT332	At1g48900 (SRP-54C signal recognition particle) 241+/-58	7th exon	1.00E-101	LUCR3	Yes
LT334	At3g02470 (S-adenosylmethionine decarboxylase) 26391+/-6355	1st intron	7.00E-57	LUCR3	Yes
LT348	At1g21065 (Expressed protein) 490+/-122	1st intron	6.00E-22	LUCL3	Yes
LT368	At1g49880 (Erv1/Air family protein) 225+/-48	4th exon	8.00E-40	LUCL3	Yes
LT430	At4g20410 (Gamma-SNAP) 940+/-382	1st intron	3.00E-83	LUCR3	Yes
LT649	At5g48560 (Basic helix-loop-helix transcription factor) 72+/-26	5th exon	3.00E-70	LUCR3	Yes

B. LucTrap-2 lines that are not expected to give rise to LUC+ fusions

LT#	Locus	Position	E-value	Primer	Fusion RLUs
LT004	At2g18700 and At2g18690	Intergenic region	1.00E-21	LUCR3	No bg
LT037	At2g44260 (Expressed protein)	2nd exon	1.00E-34	LUCR3	No bg
LT042	At3g08810 (F-box family protein)	3' UTR	1.00E-105	LUCR3	No bg
LT046	At5g10980 (Expressed protein)	5' UTR	1.00E-167	LUCR3	No bg
LT062	At5g40270 and At5g40260	Intergenic region	0	LUCR3	No bg
LT104	At3g58500 (serine/threonine protein phosphatase subunit)	7th intron	4.00E-71	LUCR3	No bg
LT117	At5g38200 and unannotated open reading frame	Intergenic region	6.00E-69	LUCR3	No bg
LT173	At5g40260 and At5g40270	Intergenic region	6.00E-67	LUCR3	No bg
LT178	At1g47600 (Thioglucosidase) 3270+/-951	13th exon	9.00E-61	LUCL3	No
LT190	At3g23900 (RNA recognition motif-containing protein)	6th intron	2.00E-45	LUCR3	No bg
LT196	At1g04830 and At1g04840	Intergenic region	6.00E-101	LUCR3	No bg
LT221	At3g53450 (Decarboxylase) 25	4th intron	2.00E-06	LUCL3	No 51+/-
LT224	At1g13260 (DNA binding protein RAV1)	5'-UTR	1.00E-93	LUCR3	No bg
LT263	At4g25620 and At4g25630 75	Intergenic region	6.00E-56	LUCR3	No 200+/-
LT278	At5g15460 (Expressed protein with ubiquitin domain) 30	2nd exon	2.00E-14	LUCR3	No 61+/-
LT297	At5g34960 and At5g34965 59	Intergenic region	3.00E-10	LUCL3	No 154+/-
LT303	At5g53570 (RabGAP/TBC domain-containing protein)	5th exon	2.00E-28	LUCR3	No bg
LT322	At4g33520 (Metal-transporting P-type ATPase) 46	15th exon	0.002	LUCR3	No 112+/-
LT340	At4g38730 and At4g38740 50	Intergenic region	4.00E-11	LUCR3	No 70+/-
LT414	At4g38710 (Glycine-rich protein cylicin II) 9730+/-3000	1st exon	6.00E-05	LUCR3	No
LT510	At1g79430 and At1g79440 29	Intergenic region	6.00E-43	LUCR3	No 122+/-
LT516	At3g03700 (Expressed protein) 16	3' UTR	5.00E-83	LUCR3	No 42+/-

Figures and Legends

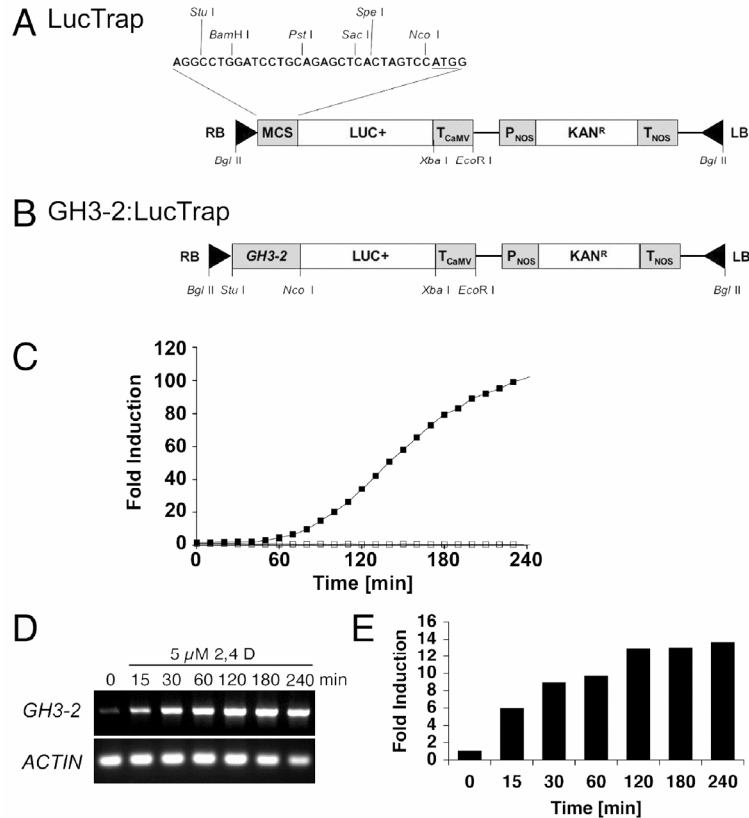


Figure 1

Figure 1. The plant transformation vector LucTrap allows to generate transcriptional and translational luciferase reporter fusions. **A**, Schematic representation of the LucTrap vector T-DNA. Black triangles mark the T-DNA right (RB) and left (LB) borders, respectively. The *Nco*I site of the LucTrap multiple cloning site (MCS) overlaps with the ATG start codon of the modified fire fly *LUCIFERASE* gene (*LUC+*). 35S cauliflower mosaic virus (CaMV) terminator, T_{CaMV} ; nopaline synthase (NOS) promoter, P_{NOS} ; NOS terminator, T_{NOS} ; neomycin phosphotransferase II/Kanamycin resistance gene (KAN^R). The GenBank accession of LucTrap is DQ073044. **B**, GH3-2:LucTrap carries a *GH3-2* (*At4g37390*) gene fragment corresponding to the 800 base pairs upstream of the predicted *GH3-2* start codon. **C**, Typical result of an auxin induction experiment with 5 day-old seedlings of a selected transgenic Arabidopsis GH3-2:LucTrap line. Open squares, luciferase expression without induction, black squares, luciferase expression following induction with 5 μ M 2,4D. Luciferase activity at time = 0 min of the untreated sample was set as 1. **D**, *GH3-2* gene expression following 5 μ M 2,4D induction as monitored by semi-quantitative reverse transcription and polymerase chain reaction (RT-PCR). *ACTIN* was used as an internal standard for cDNA amounts used in the experiment. **E**, Quantification of the RT-PCR results. *GH3-2* expression at t = 0 min was set as 1.

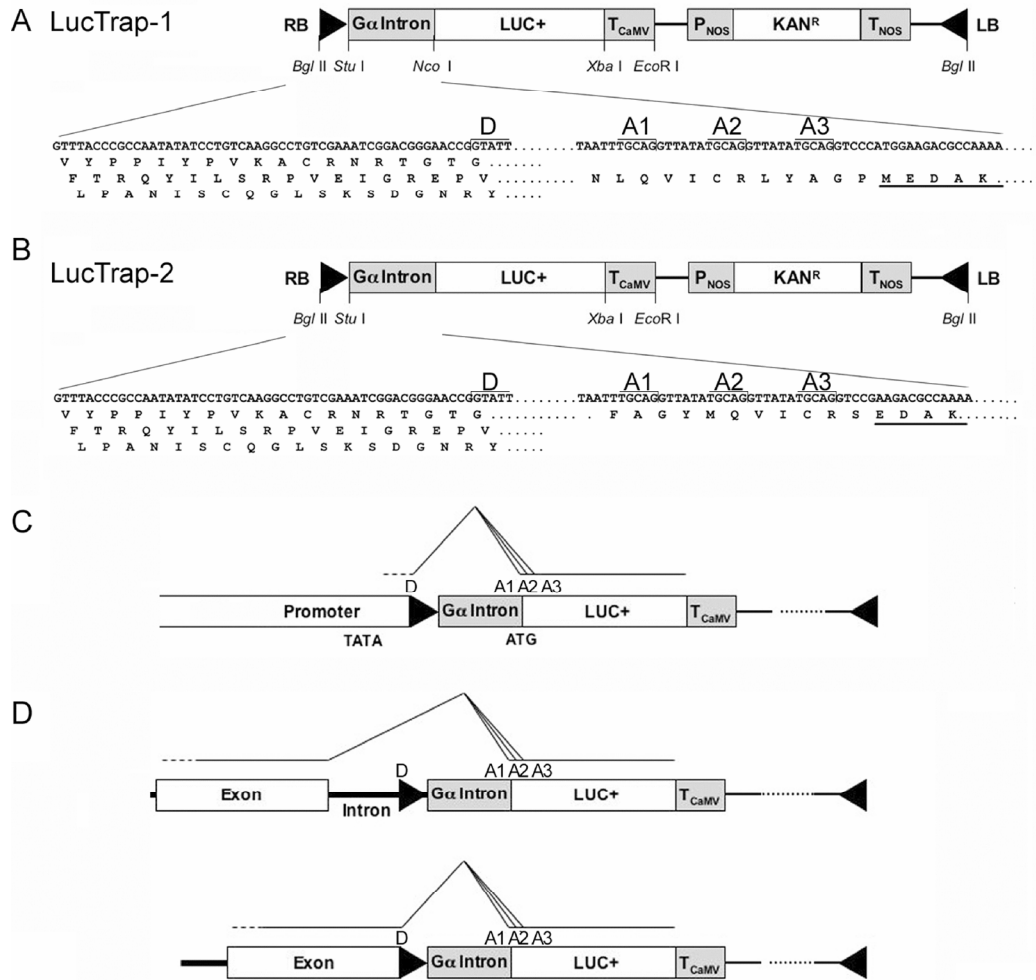


Figure 2

Figure 2. LucTrap-1 and LucTrap-2 plant transformation vectors for promoter and gene trapping. **A**, Schematic representation of the LucTrap-1 T-DNA. The intron of the *G-PROTEIN* α subunit gene ($G\alpha$; At2g26300) was placed between the T-DNA RB and the *LUC+* gene. The artificial splice donor (D) and three splice acceptor sites (A1, A2, A3) flanking the $G\alpha$ intron are indicated. The A1, A2, and A3 sites are spaced in a manner that will allow the formation of three alternatively spliced products, one of which will be in frame with the *LUC+* reporter and will therefore generate productive *LUC+* fusions. The first amino acids of the *LUC+* protein are underlined. The GenBank accession of LucTrap-1 is AY944581. **B**, Schematic representation of the LucTrap-2 T-DNA. The vector is identical to LucTrap-1 except that the *LUC+* start codon was eliminated. The initial amino acids of the *LUC+* protein are underlined. The RB sequence and the adjacent $G\alpha$ intron sequence lack stop codons in any of the three reading frames to avoid premature chain termination during translation. The GenBank accession of LucTrap-2 is AY944582. **C**, Rational of the LucTrap-1 promoter trap vector where LucTrap-1 T-DNA insertions in transcriptionally active regions will result in the formation of *LUC+* fusion mRNAs. **D**, Rational of the LucTrap-2 gene trap vector where forward LucTrap-2 T-DNA insertions in an exon (upper panel) or intron (lower panel) will result in the formation of productive *LUC+* fusions as indicated by the line drawing.

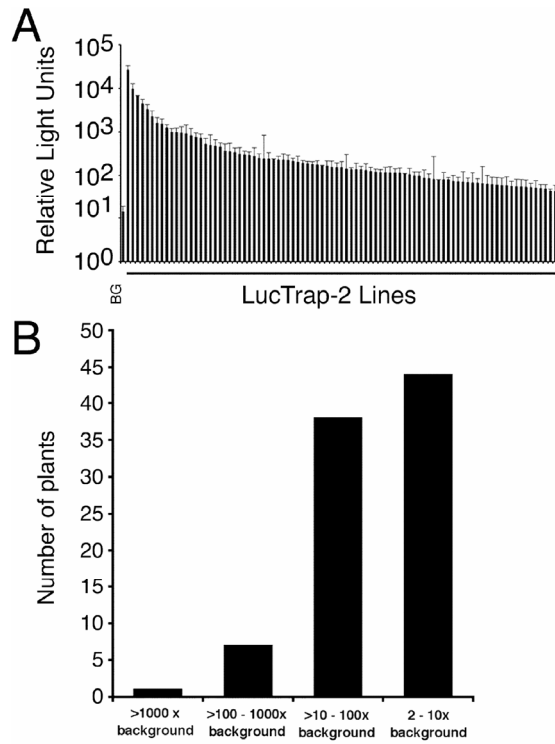


Figure 3

Figure 3. Quantitative analysis of 700 *Arabidopsis thaliana* LucTrap-2 gene trap lines identifies 90 luciferase expressing lines. **A**, Distribution of luciferase activity in the 90 luciferase expressing LucTrap-2 lines. The average and standard deviation of four replicate measurements is shown. Background activity (BG) in this particular experiment was 14 relative light units (RLUs). Please note the logarithmic scale of the representation. **B**, Absolute number of LucTrap-2 lines with luciferase expression levels above specified background activities.

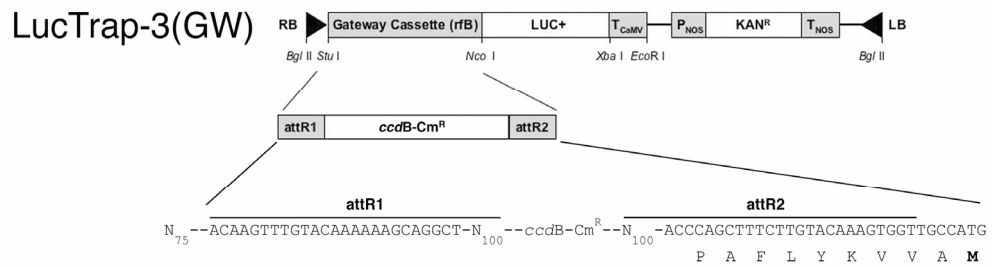


Figure 4

Figure 4. The Gateway™ destination vector LucTrap-3(GW) for plant transformation. Scheme of the LucTrap-3(GW) T-DNA with the *attR1* and *attR2* recombination sites of the Gateway™ rfB cassette. *ccdB*, *Escherichia coli* DNA gyrase for negative selection; Cm^R, chloramphenicol resistance gene for positive selection. The first amino acid of LUC+ is underlined. For other abbreviations please refer to the legend of Figure 1. The GenBank accession of LucTrap-3(GW) is AY968054.

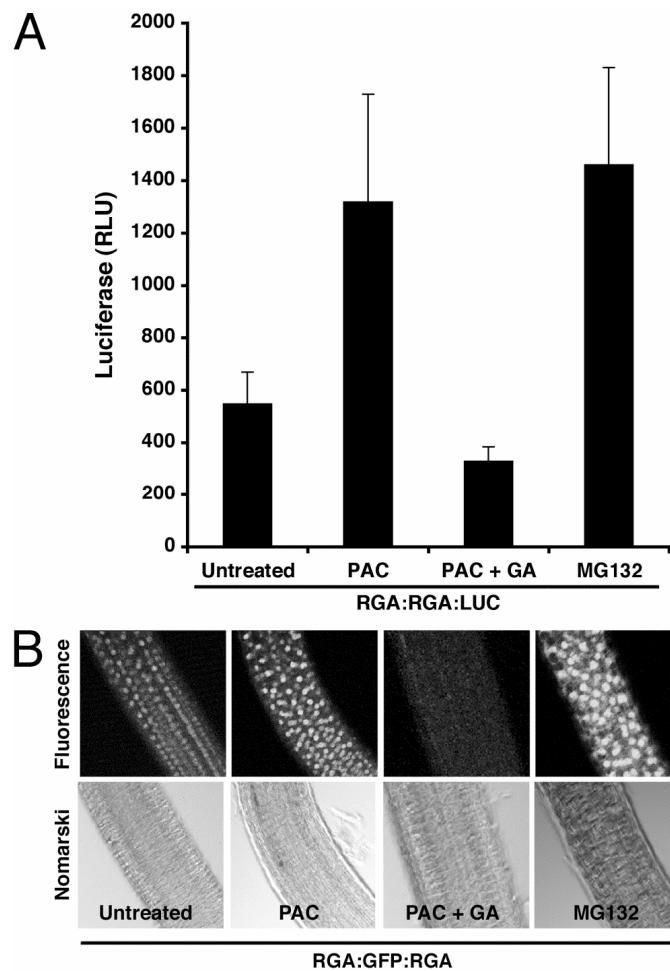


Figure 5

Figure 5. Translational LUC+ fusions with the REPRESSOR OF GA1-3 (RGA) protein allow to detect protein degradation events. **A**, Representative result of a transgenic line expressing the luciferase gene fused to the *RGA* open reading frame under control of a 2 kb *RGA* promoter fragment (RGA:RGA:LUC). Luciferase activity was measured in 5 day-old seedlings (untreated) and after 12 hour treatment with 100 μ M of the gibberellic acid biosynthesis inhibitor paclobutrazol (PAC), 100 μ M PAC and 100 μ M gibberellic acid 3 (PAC + GA), as well as 100 μ M of the 26S proteasome inhibitor MG132 (MG132) as indicated. $n = 4$. **B**, Fluorescence microscopy and Nomarski images of root cells of 5 day-old *Arabidopsis* seedlings expressing the RGA:GFP:RGA fusion protein. Treatments were as described in A.

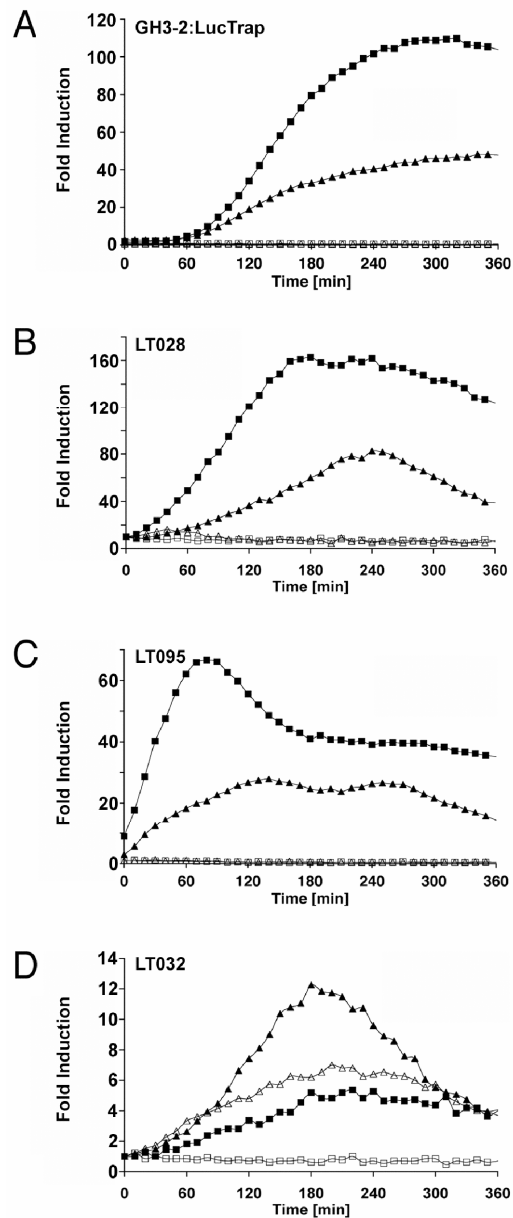


Figure 6

Figure 6. MG132 proteasome inhibitor treatments reveal the role of unstable repressors and activators in controlling auxin-induced gene expression. Relative luciferase expression of GH3-2:LucTrap (**A**), LT028 (**B**), LT095 (**C**) and LT032 (**D**) as detected over time in 5 day-old seedlings (open squares), after auxin induction (5 μ M 2,4D, black squares), after proteasomal inhibition (100 μ M MG132, open triangles), and after auxin induction (5 μ M 2,4D) with concomitant proteasomal inhibition (100 μ M MG132) (black triangles). The result of a typical induction experiment is shown. The data for GH3-2:LucTrap uninduced and auxin treated were derived from the same experiment as shown in Figure 1C. Luciferase activity at time = 0 min of the untreated sample was set as 1.

IV. Zusammenfassung

Ubiquitin (Ub)-vermittelte Proteolyse ist ein wichtiger regulatorischer Mechanismus in eukaryotischen Organismen. Hierbei binden E3 Ubiquitinligasen spezifisch an für den Abbau vorgesehene Substrate und vermitteln deren Ubiquitylierung. Diese ist eine notwendige Voraussetzung für den Abbau durch das 26S Proteasom. In Hefe- und Säugerzellen regulieren die E3 Ubiquitinligasen des SCF-Typs essentielle Prozesse durch Wachstum und Entwicklung wie den Zellzyklus. Arabidopsis weist eine erstaunlich hohe Zahl (694, ~ 2,5% des Proteoms) an F-box Proteinen (FBPs) auf, die die substratbindenden Komponenten der SCF Komplexe darstellen. Dies legt die Vermutung nahe, dass SCF Komplexe in Pflanzen für zahlreiche zelluläre und entwicklungsbiologische Prozesse von Bedeutung sind. Trotz dieser offensichtlich zentralen Rolle ist bisher die biologische Funktion von nur wenigen FBPs bzw. SCF-Komplexen verstanden.

Die vorgelegte Arbeit lässt sich in drei Bereiche aufteilen (i) die Charakterisierung des FBPs AtFBP7 und der VIER F-Box PROTEINE (VFB) Familie als neue, bisher nicht untersuchte, FBPs von Arabidopsis, (ii) die Untersuchung des TOUGH Proteins, einem vermeintlichen Proteinabbausubstrat, (iii) und die Einführung der LucTrap Vektoren mit deren Hilfe neue instabile Proteine identifiziert und untersucht werden können. Ergänzender Bestandteil der Dissertation ist ein Übersichtsartikel, welcher anhand spezifischer relevanter Beispiele das bisherige Wissen über den Ubiquitin-Proteasom-abhängigen Proteinabbau bei Pflanzen gibt.

Das evolutionär konservierte F-Box Protein AtFBP7 konnte als essentiell für die Proteinsynthese nach Temperaturstress nachgewiesen werden. Dieses Ergebnis bestätigt die Vermutung nach einer ursprünglichen Funktion in einem konservierten biologischen Prozess.

Die pflanzenspezifischen VFBs gehören zu der bisher am besten charakterisierten C3 Subfamilie der FBP Superfamilie bei Arabidopsis. Es wurde gezeigt, dass der Verlust der VFB Funktion zu verzögertem Wachstum und verminderter Seitenwurzelbildung führt und mit einer Expressionsreduktion Auxin-responsiver Gene einhergeht. Die fortlaufende Forschung in unserem Labor zu den VFBs wird neues Licht auf die Mechanismen werfen, die durch VFBs reguliert sind.

Die Identifizierung der durch das Ubiquitin-Proteasomsystem abgebauten Proteine stellt eine grosse Herausforderung dar. Das Problem liegt darin, dass diese aufgrund ihres schnellen Umsatzes und weil sie keine charakterisierten Erkennungssequenzen tragen, nur schwer zu identifizieren sind. Das Protein TOUGH ist eines dieser putativen Abbau-Substrate, für das man zeigen konnte, dass es eine wichtige Rolle während der pflanzlichen Entwicklung besonders bei der Differenzierung der Leitbündel spielt. Weitere Proteinabbau-substrate können in Zukunft mit Hilfe der ebenfalls in dieser Dissertation beschriebenen LucTrap Technologie identifiziert werden.

V. Curriculum vitae

Name:	Luz Irina Alejandrogna Calderón Villalobos
Date and place of birth:	19th of June 1975 in Bogotá, Colombia
Nationality:	Colombian
Education and Training:	
Since Nov. 2001	PhD studies in the laboratory of Claus Schwechheimer at the ZMBP, University of Tübingen, Developmental Genetics Department (Prof. G. Jürgens). Tübingen, Germany
Nov. 2000 - Nov. 2001	Trainee in the Department of Pulmonary Research Boehringer Ingelheim. Studies on the Role of Cytokines on Mucus Production in Various Cell Culture Systems. Ingelheim, Germany
May 2001 - July 2001	Research stay in the Group of Prof. H. Beug at the IMP, Research Institute of Molecular Pathology. Scientific project conducted with Boehringer Ingelheim. <i>Developmental Plasticity: Deregulation in Oncogenesis and TGFβ response.</i> Vienna, Austria
Mar. 1999 - Feb. 2000	German Studies, Essenheim, Germany.
Sept.1997 - Feb. 1999	Young Investigator at the Centro Internacional de Entrenamiento e Investigaciones Medicas (CIDEIM, International Centre of Medical Science and Training) Studentship Program from COLCIENCIAS, Colombia. <i>Molecular Epidemiology of Multidrug Resistant Tuberculosis.</i> <i>In vivo Expression of DNA Vaccines against American Leishmaniasis.</i> Cali, Colombia
Jan.1992 - Jul. 1997	Master in Microbiology at the Universidad de Los Andes, Bogotá, Colombia
Jan. 1980-Dec. 1991	School and High school, Bogotá, Colombia